

THE ROLE OF PARKIN IN THE RECOVERY OF CENTRAL DOPAMINE NEURONS
FROM ACUTE NEUROTOXICANT EXPOSURE

By

Matthew John Benskey

A DISSERTATION

Submitted to
Michigan State University
in partial fulfillment of the requirements
for the degree of

Neuroscience-Doctor of Philosophy

2013

ABSTRACT

THE ROLE OF PARKIN IN THE RECOVERY OF CENTRAL DOPAMINE NEURONS FROM ACUTE NEUROTOXICANT EXPOSURE

By

Matthew John Benskey

Parkinson Disease (PD) pathology is associated with the selective degeneration of nigrostriatal dopamine (NSDA) neurons, while the tuberoinfundibular DA (TIDA) neurons of the hypothalamus remain intact. The same pattern of selective degeneration has been observed following exposure to 1-methyl-4-phenyl-1, 2, 3, 6-tetrahydropyridine (MPTP), a mitochondrial complex I inhibitor which recapitulates many of the molecular pathologies associated with PD. The purpose of this dissertation is to identify early molecular events that underlie TIDA neuron recovery from toxicant exposure and adapt these mechanisms in an attempt to rescue NSDA neurons from toxicity. NSDA neurons show loss of axon terminal DA concentrations following acute (20mg/kg; s.c.) and chronic (10 x 20mg/kg; s.c. over 35 days) MPTP administration and exhibit cell death following chronic MPTP administration. In contrast, TIDA neurons show no loss of axon terminal DA concentrations or cell death following acute or chronic MPTP exposure. The recovery of TIDA neurons is independent of extrinsic factors such as decreased toxicant exposure or hormonal activation. TIDA neuron recovery is associated with an increase in the PD-associated proteins, parkin and ubiquitin carboxy-terminal hydrolase L-1 (UCHL-1) within the arcuate nucleus (ARC) 24 h following MPTP. Additionally, parkin protein concentrations remain elevated in the ARC for up to 22 days following chronic MPTP administration. In contrast, the susceptibility of NSDA neurons is associated with decreased expression of both parkin and UCH-L1. The high correlation between the presence of the parkin protein and the recovery of DA neurons from MPTP toxicity is consistent with a role of parkin in

DA neuron survival. In order to determine if parkin is necessary and sufficient in the recovery of TIDA neurons following MPTP, recombinant adeno-associated viral (rAAV) vectors containing parkin shRNA or a scrambled shRNA were created. Mice received stereotaxic ARC injections of rAAV containing either parkin shRNA or scrambled shRNA (250nl/side; 3.5×10^{13} vg/ml), or remained naïve to surgery, and were administered a single injection of MPTP (20mg/kg; s.c.) 30 days following rAAV surgery. Twenty-four h post-MPTP, TIDA neurons were able to recover axon terminal DA concentrations following MPTP in control and scrambled shRNA treated animals. However, axon terminal DA was significantly reduced 24 hr following MPTP exposure following knockdown of parkin in TIDA neurons. To determine if parkin overexpression would protect NSDA neurons from MPTP toxicity, mice received unilateral stereotaxic injection of rAAV containing parkin into the substantia nigra (SN) (500nl; 3.4×10^{13} vg/ml) and were administered a single injection of MPTP (20mg/kg; s.c.) 30 days following rAAV surgery. Twenty-four hours post-MPTP, parkin overexpression was unable to rescue MPTP-induced loss of DA in the striatum (ST), but did rescue MPTP-induced loss of tyrosine hydroxylase (TH) in the SN and ST. These findings are consistent with the following conclusions: 1) TIDA neuronal recovery from acute MPTP exposure is independent of extrinsic factors and is mediated by an intrinsic ability to increase expression of neuroprotective proteins, 2) The ability of TIDA neurons to up-regulate parkin is at least partially responsible for recovery of axon terminal DA following MPTP, 3) toxicant-induced loss of parkin contributes to MPTP toxicity within NSDA neurons.

ACKNOWLEDGEMENTS

This dissertation represents the culmination of many years of hard work that would not have been possible but for the support and contribution of many people. I would first like to thank my advisors Drs. Keith Lookingland and John Goudreau. The work I completed in your lab laid the groundwork for my continual growth as a scientist. Keith, I would like to thank you for all your dedication to the laboratory. You are truly a natural teacher and a great mentor. You were able to strike the perfect balance of training when I needed help and giving me freedom to pursue my own ideas and innovations. Without the autonomy you granted me in the lab I would have struggled throughout my graduate career. John, I would like to thank you for showing me how to think critically and creatively about scientific problems as well as showing me that sometimes science is about who you know.

I would also like to thank my GoudLooking labmates. The unique and friendly dynamic that was deep rooted in the lab is why I joined the lab and why I was happy to come into work for 5 years. I would like to send special thanks to Dr. Sam Pappas, Tyrell Simkins and Dr. Chelsea Tiernan. I will never forget the many adventures we shared both in and out of the lab.

Most importantly I would like to thank my friends and family. Your constant love and support allowed me to endure when the trials and tribulations of graduate school seemed insurmountable. To the love of my life Chelsea Tiernan, I can never thank you enough. Beyond being the best office mate ever, you are my rock. Thank you for supporting me when I am weak, for loving me for who I am, and for growing with me as both a person and a scientist. I can't wait for all the adventures to come. To my sister Rachel, you have always been and will always be my role model. Your strength, intensity and love have encouraged me to always stand up for

myself. To my brother Mikey, you are sunshine on a cloudy day. Your compassion and sense of humor can always save me from the depths of despair. To my dad, thank you for being there when I need some help in a pinch. Finally and most importantly I would like to thank my mother. Mom, you are one of the most beautiful people I have ever known. You have always been there for me no matter what disastrous situation I managed to get myself into. You have been a sympathetic ear, a friend to chat with, a stern hand, but most importantly you have been the paragon of a loving mother. Your patience, grace and eternal love laid the foundation for my entire life and are now the source of inspiration to grow into the best person I can be. You are the reason I am the person I am today and I will always love you with all my heart. Thank you.

TABLE OF CONTENTS

LIST OF TABLES.....	x
LIST OF FIGURES.....	xi
KEY TO ABBREVIATIONS.....	xv
Chapter 1. General Introduction.....	1
Statement of Purpose.....	1
Introduction.....	3
Parkinson Disease.....	3
Pathophysiology of PD.....	5
NSDA Neuronal Physiology.....	5
NSDA Neurons and the Basal Ganglia.....	9
Etiology of PD.....	13
Environmental Risk Factors in PD.....	13
Genetic Risk Factors in PD.....	14
Molecular Pathology Associated with PD.....	15
Mitochondrial Dysfunction.....	16
UPP Impairment.....	20
Abnormal DA Catabolism.....	24
Overlapping Molecular Pathologies of PD.....	25
MPTP Neurotoxicity and PD.....	28
MPTP metabolism and molecular pathology.....	28
MPTP and Mitochondrial Dysfunction.....	31
MPTP and UPP Dysfunction.....	31
MPTP and DA Toxicity.....	32
MPTP Dosing Regimens.....	33
Differential Susceptibility of Central DA Neurons.....	35
UCH-L1.....	39
Parkin.....	39
Experimental Paradigm and Goal of Dissertation.....	43
Summary.....	44
Thesis Objective.....	46
Chapter 2. Materials and Methods.....	48
Animals.....	48
Drugs and Administration.....	48
Single Acute MPTP.....	48

Chronic + Single Acute MPTP.....	48
NSD-1015.....	49
Bromocriptine.....	49
Tissue Preparation	49
Neurochemical Analyses.....	53
Western Blot Analyses.....	54
Immunohistochemistry.....	55
Brightfield Immunohistochemistry.....	55
Fluorescence Immunohistochemistry.....	55
Unbiased Stereological Cell Counting.....	58
Stereotaxic Surgery.....	59
Statistical Analysis.....	61

Chapter 3. Characterization of the differential susceptibility of TIDA and NSDA neurons to single-acute MPTP exposure.....	62
Introduction.....	62
Results	64
Time Course of the Neurochemical Responses of TIDA and NSDA Neurons to a Single injection of MPTP.....	64
Time course of TH protein expression following a single injection of MPTP	66
Changes in UCH-L1 and Parkin Protein Expression in TIDA and NSDA Neurons Following a Single Injection of MPTP.....	68
Discussion.....	73
Conclusions.....	77

Chapter 4. The role of toxicant exposure, prolactin activation and DA synthesis in the differential susceptibility of TIDA and NSDA neurons to single-acute MPTP toxicity.....	78
Introduction.....	78
Decreased Toxicant Exposure in the Recovery of TIDA Neurons from MPTP...	78
PRL Activation in the Recovery of TIDA Neurons from MPTP.....	79
DA Synthesis in the Recovery of TIDA Neurons from MPTP.....	81
Results.....	82
Time Course of MPP+ Accumulation in the Median Eminence and Striatum Following Single-Acute MPTP Administration.....	82
The Effects of Bromocriptine-induced Suppression of PRL Secretion on the Ability of TIDA Neurons to Recover from Single-Acute MPTP Exposure.....	86
The Role of DA Synthesis in the Differential Susceptibility of TIDA and NSDA Neurons to Single-Acute MPTP Toxicity.....	89
Discussion.....	92
Decreased Toxicant Exposure in the Recovery of TIDA Neurons from MPTP Toxicity.....	92
PRL Activation in the Recovery of TIDA Neurons from MPTP Toxicity.....	94
DA Synthesis in the Recovery of TIDA Neurons from MPTP Toxicity.....	95
Conclusion.....	98

Chapter 5. Characterization of the differential susceptibility of TIDA and NSDA neurons to chronic MPTP exposure	100
Introduction.....	100
Results.....	102
The effects of MPTP on TH and DAT concentrations in the striatum: confirmation of successful neurotoxicant administration.....	102
The effects of MPTP on DA concentrations, DA metabolism and DA turnover in axon terminals of NSDA and TIDA neurons.....	105
The effects of MPTP on TH-ir cell numbers in the SN and ARC.....	109
Changes in protein concentrations in the SN and ARC following MPTP administration.....	112
Discussion.....	118
Conclusion.....	124
Chapter 6. The role of parkin in the differential susceptibility of TIDA and NSDA neurons to single-acute toxicant exposure	125
Introduction.....	125
Results.....	127
Characterization of rAAV Parkin-shRNA Vector Expression and Knockdown of Endogenous Parkin in the Medial Basal Hypothalamus.....	127
The Ability of TIDA Neurons to Recover from Single-Acute MPTP Toxicity following Knockdown of Parkin in the ARC.....	131
Characterization of rAAV Vector Expression and F-hParkin Protein Expression in the SN.....	137
The ability of NSDA neurons to Recover from Single-Acute MPTP Toxicity Following Overexpression of Parkin in the SN.....	140
Discussion.....	144
Conclusion.....	152
Chapter 7. General Discussion and Concluding Remarks	153
The Single-Acute MPTP Paradigm.....	153
The Role of DA Clearance in the Endogenous Neuroprotective Capability of TIDA Neurons.....	155
The Role of Protein Synthesis in the Endogenous Neuroprotective Capability of TIDA Neurons.....	158
The Role of Decreased Parkin in the Degeneration of DA Neurons.....	160
Mechanisms of Parkin Neuroprotection.....	163
Concluding Remarks.....	166
APPENDIX	168

REFERENCES	204
-------------------------	-----

LIST OF TABLES

Table 2-1. Description of primary antibodies.....	56
Table 2-2. Description of secondary antibodies.....	57
Table 4-1. Half-lives and elimination constants of MPP ⁺ in the terminal regions of TIDA and NSDA neurons following a single injection of MPTP.....	85
Table A-1. Experimental design used for the dual luciferase assay.....	191

LIST OF FIGURES

Figure 1-1. Location of NSDA neurons in the brain and DA metabolism within the NSDA nerve terminal.....	8
Figure 1-2. The Basal Ganglia in the normal brain.....	11
Figure 1-3. The Basal Ganglia in the PD brain.....	12
Figure 1-4. The electron transport chain and oxidative phosphorylation.....	18
Figure 1-5. The Ubiquitin Proteasome Pathway.....	23
Figure 1-6. Cycle of molecular pathology associated with PD.....	27
Figure 1-7. MPTP metabolism.....	30
Figure 1-8. Location of TIDA neurons in the brain and DA metabolism within the TIDA axon terminal.....	38
Figure 1-9. The structure of the parkin protein.....	42
Figure 2-1. Diagram of coronal brain sections showing localization of micropunches used to dissect the ST and SN.....	51
Figure 2-2. Diagram of coronal brain sections showing localization of micropunches used to dissect the ARC.....	52
Figure 2-3. Localization of stereotaxic injections into the ARC and the SN.....	60
Figure 3-1. The time course of effects of a single injection of MPTP on DA concentrations in ME and ST.....	65
Figure 3-2. The time course of effects of a single injection of MPTP on total TH protein concentrations in the ME and ST.....	68
Figure 3-3. The time course of effects of a single injection of MPTP on UCH-L1 protein expression in the ARC and SN.....	69
Figure 3-4. The time course of effects of a single injection of MPTP on parkin protein expression in the ARC and SN.....	70

Figure 3-5. Dose–response changes in parkin expression in the ARC.....	71
Figure 3-6. Dose-response changes of parkin expression in the SN.....	72
Figure 4-1. Time course of the effects of a single injection of MPTP on DA and MPP ⁺ concentrations in the ME (Panel A) and ST (Panel B).....	84
Figure 4-2. Effects of bromocriptine and MPTP on plasma PRL concentrations.....	87
Figure 4-3. Effects of bromocriptine and MPTP on ME DA concentrations.....	88
Figure 4-4. Effects of MPTP on DOPA accumulation in the ST and ME.....	90
Figure 4-5. The effects of MPTP on total TH protein concentrations in the ST and ME.....	91
Figure 5-1. The effects of MPTP on TH concentrations in the ST: confirmation of successful neurotoxicant administration.....	103
Figure 5-2. The effects of MPTP on DAT concentrations in the ST: confirmation of successful neurotoxicant administration.....	104
Figure 5-3. The effects of single-acute MPTP administration on DA concentrations in axon terminals of NSDA and TIDA neurons in mice chronically treated with MPTP.....	106
Figure 5-4. The effects of single-acute MPTP administration on DA metabolism and turnover in axon terminals of NSDA neurons in mice chronically treated with MPTP.....	107
Figure 5-5. Lack of effects of single-acute MPTP administration on DA metabolism and turnover in axon terminals of TIDA neurons in mice chronically treated with MPTP.....	108
Figure 5-6. Representative photomicrographs of TH-ir cells in the SN and ARC following single acute and chronic MPTP administration.....	110
Figure 5-7. The effects of single-acute MPTP administration on TH-ir cell numbers in the SN and ARC in mice chronically treated with MPTP.....	111
Figure 5-8. Changes in UCH-L1 protein concentrations in the SN following single-acute MPTP administration in mice chronically treated with MPTP.....	114
Figure 5-9. Changes in UCH-L1 protein concentrations in the ARC following single acute MPTP administration in mice chronically treated with MPTP.....	115
Figure 5-10. Changes in parkin protein concentrations in the SN following single-acute MPTP administration in mice chronically treated with MPTP.....	116

Figure 5-11. Changes in parkin protein concentrations in the ARC following single-acute MPTP administration in mice chronically treated with MPTP.....	117
Figure 6-1. Immunohistochemical characterization of rAAV expression in the ARC.....	129
Figure 6-2. The effects of rAAV-parkin shRNA on endogenous parkin expression in the ARC.....	130
Figure 6-3. Parkin protein concentrations in the ARC following administration of scrambled or parkin shRNA in saline and MPTP treated mice.....	133
Figure 6-4. The effects of parkin knockdown on TIDA axon terminal DA concentrations following single-acute MPTP exposure.....	134
Figure 6-5. The effects of parkin knockdown on TIDA axon terminal TH concentrations following single-acute MPTP exposure.....	135
Figure 6-6. The effects of rAAV administration on neuroinflammation in the ARC.....	136
Figure 6-7. Immunohistochemical characterization of rAAV expression in the SN.....	138
Figure 6-8. Confirmation of F-hParkin expression within the SN and ST.....	139
Figure 6-9. The effects of parkin overexpression on NSDA axon terminal DA concentrations following single-acute MPTP exposure.....	141
Figure 6-10. The effects of parkin overexpression on NSDA axon terminal TH concentrations following single-acute MPTP exposure.....	142
Figure 6-11. The effects of parkin overexpression on NSDA cell body TH concentrations following single-acute MPTP exposure.....	143
Figure A-1. Structure of wild-type and recombinant AAV genome.....	171
Figure A-2. The sequence of parkin shRNA constructs.....	175
Figure A-3. Confirmation of parkin PCR product.....	179
Figure A-4. Diagrammatic representation of PCR product subcloning using the TOPO TA cloning system.....	183
Figure A-5. Confirmation of successful insertion of parkin clone into TOPO vector.....	186
Figure A-6. Confirmation of successful insertion of parkin clone into psiCHECK plasmid.....	189
Figure A-7. shRNA mediated knockdown of parkin expression in HEK 293 cells.....	192

Figure A-8. Site Map of the recombinant AAV genome pTR UF11 expressing shRNA.....196

Figure A-9. pTRUF11 plasmid digested with Sma1 demonstrating the presence of both intact and damaged ITR.....197

Figure A-10. Final insert and terminal repeat confirmation of shRNA-AAV constructs.....198

Figure A-11. Site map of parkin protein isoforms.....201

Figure A-12. FLAG-hParkin PCR products.....202

Figure A-13. Final insert and terminal repeat confirmation of WT FLAG-hParkin-AAV constructs.....203

KEY TO ABBREVIATIONS

AADC	Aromatic amino acid decarboxylase
AAV	Adeno-associated virus
AC	Adenylate cyclase
ADP	Adenine diphosphate
AIMP2	Aminoacyl-tRNA synthetase interacting multifunctional protein type 2
ALDH	Aldehyde dehydrogenase
ANOVA	Analysis of variance
ARC	Arcuate nucleus
ARJP	Autosomal recessive juvenile parkinsonism
ATP	Adenosine triphosphate
ATP Syn	Adenine triphosphate synthase
CHIP	C-terminus of HSC-70 interacting protein
Cyt C	Cytochrome C
CNS	Central nervous system
DAT	Dopamine transporter
DBS	Deep brain stimulation
DOPAC	3, 4-Dihydroxyphenylacetic acid
DOPAL	3, 4-Dihydroxyphenylacetaldehyde
ETC	Electron transport chain
FADH ₂	Flavin adenine dinucleotide

FBP-1	Far upstream element-binding protein 1
FhParkin	FLAG tagged-human parkin
GAPDH	Glyceraldehyde phosphate dehydrogenase
GPI	Globus Pallidus interna
hParkin	Human parkin
hluc+	firefly luciferase gene
hRluc	Renilla luciferase gene
HSP-70	Heat shock protein 70kDa
HTRA2	High temperature requirement protein A2
IBA1	Inonized calcium-binding adapter molecule 1
IBR	In between RING
IHC	Imunohistochemical
ITR	Inverted terminal repeat
Kb	kilobase
LAT	Large neutral amino acid transporter
L-DOPA	Levo-dihydroxyphenylalanine
LRRK2	Leucine-rich repeat kinase 2
MAO-B	Monoamine oxidase-B
ME	Median eminence
MPDP	1-Methyl-4-phenyl-2,3-dihydropyridine
MPP ⁺	1-Methyl-4-phenylpyridinium
MPPP	1-Methyl-4-phenyl-4-propionoxypiperidine
MPTP	1-Methyl-4-phenyl-1, 2, 3, 6-tetrahydropyridine

MSN	Medium spiny neurons
MT	Microtubule
NADH	Nicotinamide adenine dinucleotide
NS	Nigrostriatal
NSD-1015	3-Hydroxybenzylhydrazine
NSDA	Nigrostriatal dopamine
OCT	Organic cation transporter
P _i	Inorganic phosphate
PD	Parkinson Disease
PINK1	PTEN putative induced kinase
PGC-1 α	peroxisome proliferator-activated receptor- γ -coactivator-1 α
PRL	Prolactin
rAAV	Recombinant adeno-associated virus
RING	Really interesting new gene
RISC	RNA-induced silencing complex
ROS	Reactive oxygen species
shRNA	Short hairpin RNA
SN	Substantia nigra
SNpc	Substantia nigra <i>pars compacta</i>
SOD	Superoxide dismutase
<i>ST</i>	Striatum
TH	Tyrosine hydroxylase
TH-ir	Tyrosine hydroxylase-immunoreactive

TI	Tuberoinfundibular
TIDA	Tuberoinfundibular dopamine
Ub	Ubiquitin
UCH-L1	Ubiquitin-carboxy terminal hydrolase L1
UPP	Ubiquitin proteasome pathway
VMAT	Vesicular monoamine transporter

Chapter 1. General Introduction

Statement of Purpose

Parkinson Disease (PD) pathology is associated with the selective degeneration of central dopaminergic neurons. However, PD does not affect all dopaminergic subpopulations to the same extent, with nigrostriatal dopamine (NSDA) neurons showing severe degeneration and the tuberoinfundibular DA (TIDA) neurons of the hypothalamus remaining intact. The same pattern of selective degeneration has been observed following exposure to 1-methyl-4-phenyl-1, 2, 3, 6-tetrahydropyridine (MPTP), a neurotoxicant that recapitulates many of the molecular pathologies associated with PD

By examining the early changes in DA phenotypic markers that occur in susceptible NSDA neurons following toxicant administration and comparing these to early events within resistant TIDA neurons, it may be possible to identify cell-autonomous, phenotypic variations, which underlie the increased susceptibility of NSDA neurons to PD pathology. Further, it may also be possible to identify mechanisms specific to TIDA neurons that render these neurons resistant to MPTP and PD, and use these as targets for translational therapeutics. It is presently unclear why TIDA neurons are resistant to the same toxicity that affects NSDA neurons, however, TIDA resistance has been found to be protein synthesis dependent and associated with the up-regulation of the PD-associated gene parkin.

The overall aim of the research described in this dissertation is two-fold: 1) to characterize the differential susceptibility of TIDA and NSDA neurons to MPTP toxicity, 2) to determine the role parkin plays in the differential susceptibility of TIDA and NSDA neurons to acute MPTP toxicity. The overarching hypothesis guiding the experiments described herein is

that TIDA neuronal resistance to acute MPTP toxicity is mediated by a cell-autonomous ability to up-regulate parkin protein expression under conditions of cellular stress, whereas NSDA neuronal susceptibility to acute MPTP toxicity is due to an inability to increase parkin expression.

Introduction

Parkinson Disease

Dr. James Parkinson provided the original clinical description of Parkinson Disease (PD) in 1817 within his work “An Essay On the Shaking Palsy”. In this seminal essay Parkinson described the clinical manifestation of what he dubbed “*paralysis agitans*” as; “Involuntary tremulous motion, with lessened muscular power, in parts not in action and even when supported; with a propensity to bend the trunk forward, and to pass from a walking to a running pace.” This relatively accurate description of the disorder we now know as PD has been augmented and corrected over the years to be clinically defined as a progressive neurodegenerative disorder whose cardinal symptoms include: bradykinesia (hypokinesia or akinesia) rigidity, resting tremor, flexed posture of neck, trunk and limbs, loss of postural reflexes and freezing phenomenon (Fahn, 2003). Other non-motor symptoms may also include sleep disturbances, gastrointestinal immotility, dysphagia, dysarthria, hyposmia and cognitive impairment.

PD is a complex disorder that affects approximately seven million people worldwide (de Lau & Breteler, 2006). Although PD can occur at any age, the mean age of onset is 60 years. Further, age is the primary risk factor associated with PD, with prevalence increasing from 1% of the population at age 60 to 4% of the population by age 80 (de Lau & Breteler, 2006). A definitive diagnosis of PD is only possible through post mortem confirmation of loss of dopamine (DA) neurons of the substantia nigra pars compacta (SNpc) and proteinacious intraneuronal inclusions known as Lewy bodies.

Despite the severity and prevalence of PD, current therapies available to treat PD are conspicuously lacking. The loss of nigrostriatal (NS) DA neurons of the SNpc results in a

corresponding loss of DA innervation to the striatum (ST). The early symptoms observed in PD, such as resting tremor, bradykinesia and rigidity result from the loss of DA in the ST. Thus, although loss of NSDA cell bodies is used as a postmortem confirmation of the disease, the actual effector of PD symptomatology is NSDA terminal dysfunction and the corresponding loss of DA neurotransmission. As such, the primary therapies available for PD focus on DA replacement strategies.

Currently, the most common and successful DA replacement therapy is the DA precursor levo-dihydroxyphenylalanine (L-DOPA). When administered in combination with a peripheral decarboxylase inhibitor, L-DOPA will enter the brain and subsequently be decarboxylated to form DA, compensating for the lack of presynaptic DA in the ST and restoring DA neurotransmission. Alternatively, DA agonists such as apomorphine, pergolide, pramipexole and ropinirole have also shown to be successful in ameliorating the motor abnormalities of PD. However, both L-DOPA and DA agonists lose their efficacy as PD progresses and are thus only temporarily successful in treating the motor symptoms of PD. In addition, there are unwanted sides effects associated with both therapies such as dyskinesias produced from long term use of L-DOPA or hallucinations, confusion and psychosis associated with DA agonists (Fahn, 2003; Holloway, 2000). Other lesser-used DA replacement therapies include drugs such as amantadine, which will act to release as well as block reuptake of DA from presynaptic terminals, or monoamine oxidase B (MAO-B) inhibitors used to stop the breakdown of DA. Unfortunately, clinical studies have determined these therapies to be only minimally effective (RS, AG, Pskkanzer, & Young, 1969; Youdim & Bakhle, 2009).

As an alternative to DA replacement strategies the use of deep brain stimulation (DBS) has recently shown to be effective in rectifying the abnormal physiology produced downstream

of degenerating NSDA neurons. However, DBS has the drawbacks of being expensive as well as very invasive. The common denominator associated with all aforementioned therapies is that they are only partially effective and usually for a limited time. Further, these treatments focus on the symptoms of PD while ignoring the underlying cause of the motor abnormalities. As such, it is necessary to develop treatments that target the root of the problem, which is the progressive degeneration of NSDA neurons and corresponding loss of normal DA neurotransmission in the ST.

Pathophysiology of PD

NSDA neurons contain cell bodies in the SNpc and send long projecting axons along the medial forebrain bundle to terminate in the ST (Figure 1-1, A). DA released from NSDA neurons in the ST is a critical component in the modulation of the extrapyramidal motor system. Thus, degeneration of NSDA neurons and loss of the neuromodulatory effects of striatal DA result in the motor abnormalities observed in PD. However, in order to fully understand the consequence of decreased NSDA neurotransmission, it is necessary to first understand the normal physiology of NSDA neurons as well as the basal ganglia.

NSDA Neuronal Physiology

The primary function of NSDA neurons is the production and release of the neurotransmitter DA into the ST. Within the NSDA nerve terminal, DA synthesis, release, reuptake and metabolism is a tightly controlled process (Figure 1-1, B). DA synthesis begins with transport of the dietary amino acid tyrosine across the blood brain barrier into the NSDA cytosol by the large neutral amino acid transporter (LAT) (2003; J. D. Fernstrom & Fernstrom,

2007). Tyrosine is then hydroxylated to form DOPA by the rate limiting enzyme in catecholamine synthesis, tyrosine hydroxylase (TH) (Levitt, Spector, Sjoerdsma, & Udenfriend, 1965). Following this, DOPA is rapidly decarboxylated by L-aromatic amino acid decarboxylase (AADC) to form DA, which is transported into synaptic vesicles by action of the vesicular monoamine transporter (VMAT) (Chen, Wei, Fowler, & Wu, 2003; Lovenberg, Weissbach, & Udenfriend, 1962; Weihe, Schäfer, Erickson, & Eiden, 1994).

Upon arrival of an action potential in the NSDA axon terminal, synaptic vesicles will fuse to the presynaptic membrane and exocytose DA into the synaptic cleft, where it can bind to post-synaptic D1- or D2-like DA receptors. Binding of DA to D1-like receptors will increase postsynaptic neuronal excitability through activation of adenylate cyclase (AC) and the resultant downstream pathway. Alternatively, DA bound to postsynaptic D2-like receptors will decrease neuronal excitability through an inhibition of AC and activation of K^+ channels (Kebabian & Calne, 1979; Niznik, 1987). DA may also bind to presynaptic D2 autoreceptors, which will act as a negative feedback mechanism to decrease DA synthesis and release from the NSDA terminal (Christiansen & Squires, 1974; Tang, Todd, & O'Malley, 1994; Usiello et al., 2000). Any DA remaining in the synaptic cleft will be scavenged and transported back into the presynaptic NSDA axon terminal by the high affinity DA transporter (DAT) (Shimada et al., 1991). Recently transported or newly synthesized cytosolic DA will act as another negative feedback to inhibit TH activity through end product inhibition (Okuno & Fujisawa, 1985).

Cytosolic DA will either be repackaged into vesicles or degraded in a two-step process by the mitochondrial associated enzymes MAO-B and aldehyde dehydrogenase (ALDH). First, DA will undergo oxidative deamination by MAO-B to form the highly reactive intermediate 3, 4-dihydroxyphenylacetaldehyde (DOPAL) (Hafer, Agarwal, & Goedde, 1987; O'Carroll, Fowler,

Phillips, Tobbia, & Tipton, 1983). DOPAL will then be degraded to 3, 4-dihydroxyphenylacetic acid (DOPAC), which can freely diffuse out of the nerve terminal.

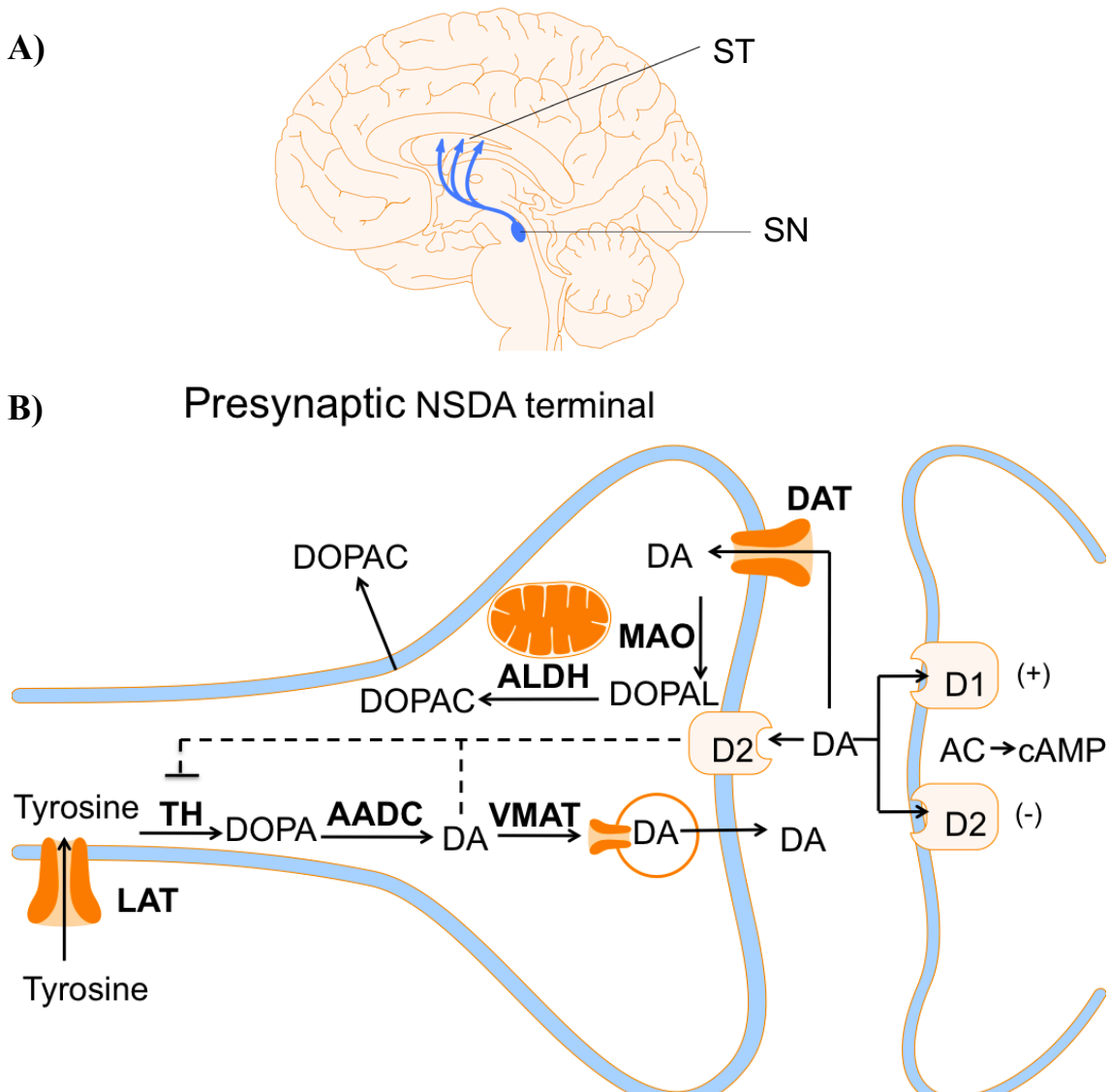


Figure 1-1. Location of NSDA neurons in the brain and DA metabolism within the NSDA nerve terminal. **Panel A**, NSDA neurons have soma in the SNpc and terminate in the ST. **Panel B**, Dietary tyrosine is hydroxylated by TH to form DOPA. DOPA is decarboxylated by AADC to form DA which is packaged into vesicles by VMAT. Upon arrival of an action potential DA is released into the synapse and binds to D1- or D2-like DA receptors. Synaptic DA is recaptured by DAT and can either be repackaged into vesicles or metabolized. DA metabolism begins with deamination by MAO-B to form DOPAL followed by oxidation by ALDH to form DOPAC. Abbreviations: ST, striatum; SN, substantia nigra; DA, dopamine; LAT, large neutral amino acid transporter; TH, Tyrosine hydroxylase; DOPA, dihydroxyphenylalanine; AADC, aromatic amino acid decarboxylase; VMAT, vesicular monoamine transporter; D1, excitatory D1-like DA receptor; D2, inhibitory D2-like DA receptor; AC, adenylate cyclase; cAMP, cyclic adenosine monophosphate; DAT, DA transporter; MAO, monoamine oxidase; DOPAL, dihydroxyphenylacetylaldehyde; ALDH, aldehyde dehydrogenase; DOPAC, dihydroxyphenylacetic acid. For interpretation of the references to color in this and all other figures, the reader is referred to the electronic version of this dissertation.

NSDA Neurons and the Basal Ganglia

The basal ganglia are a group of interconnected subcortical nuclei that form a reentrant circuit with the cerebral cortex, the thalamus, the midbrain and certain brainstem nuclei. Currently, it is believed that the major function of the basal ganglia is the smooth initiation and execution of motor control. The major nuclei that make up the basal ganglia are the striatum (caudate and putamen), the globus pallidus (internal and external segments), the substantia nigra (reticulata and pars compacta segments) and the subthalamic nucleus. Within the basal ganglia, the ST serves as the major input nuclei while the globus pallidus interna (GPi) and the SN pars reticulata serve as the major output nuclei. These two major output nuclei tonically inhibit their target in the thalamus, thus decreasing excitation of the motor cortex and the propensity for movement. However, two parallel pathways within the basal ganglia, known as the direct and indirect pathway, modulate this tonic inhibition. Activation of the direct pathway disinhibits the thalamus while activation of the indirect pathway further inhibits the thalamocortical output neurons (Figure 1-2, A). Thus, activation of the direct pathway facilitates movement, while activation of the indirect pathway inhibits movement.

NSDA neurons synapse on medium spiny neurons (MSN) within the ST that comprise both the direct and indirect pathways. However, DA released from NSDA neurons modulates MSN of these different pathways in opposing manners. MSN within the direct pathway express D₁-like DA receptors and are excited by DA, while MSN in the indirect pathways express D₂-like DA receptors and are inhibited by DA (Surmeier, Ding, Day, Wang, & Shen, 2007). DA released from NSDA neurons into the ST will activate the direct pathway and facilitate movement while at the same time inhibiting the neurons of the indirect pathway, again facilitating movement. Thus, through opposing mechanism, DA in the ST works toward the

ultimate goal of disinhibiting the output of the basal ganglia and promoting movement. Due to the critical role of DA neuromodulation in the facilitation of motor control it essential to maintain proper NSDA axon terminal homeostasis and neurotransmission.

As previously mentioned the loss of NSDA neurons in PD results in loss of DA innervation to the ST. The lack of DA in the ST will result in a loss of activation of the direct pathway as well as decreased disinhibition of the indirect pathway (Figure 1-2, B). The net outcome of decreased DA in the ST is an increased firing of the inhibitory output nuclei of the basal ganglia, causing lower firing rates of the thalamocortical neurons and decreased activation of neurons of the primary motor cortex. This aberrant extrapyramidal signaling manifests in the symptoms observed in PD. Though it is clear that the loss of NSDA neurons and the modulatory influence of DA within the basal ganglia result in the motor impairment seen in PD, the underlying cause of NSDA neuronal degeneration is still unknown.

Normal Basal Ganglia

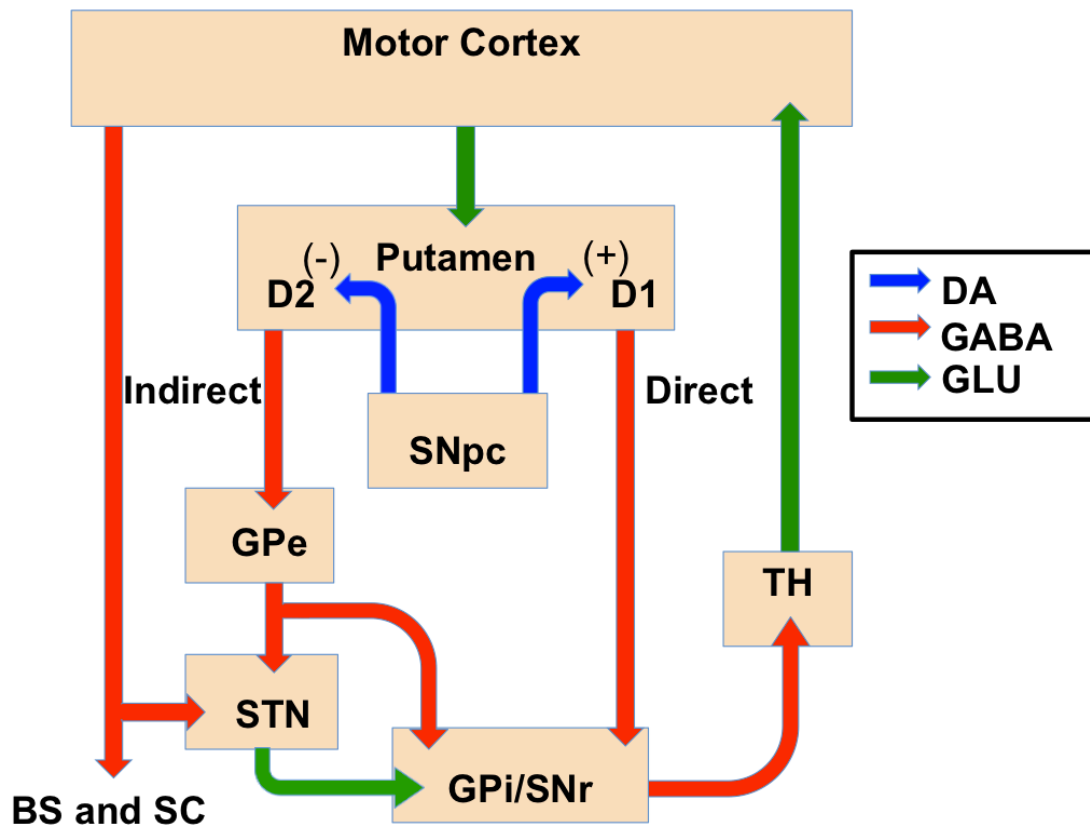


Figure 1-2. The Basal Ganglia in the normal brain. DA released from NSDA neurons activates the direct pathway and inhibits the indirect pathway, leading to disinhibition of the thalamus and initiation of movement. Abbreviations: SNpc, Substantia nigra pars compacta; D1, excitatory D1-like DA receptor; D2, inhibitory D2-like DA receptor; GPe, globus pallidus externa; GPi, globus pallidus interna; STN, subthalamic nucleus; SNr, substantia nigra pars reticulata; TH, thalamus; BS, brainstem; SC, spinal cord.

Basal Ganglia in PD

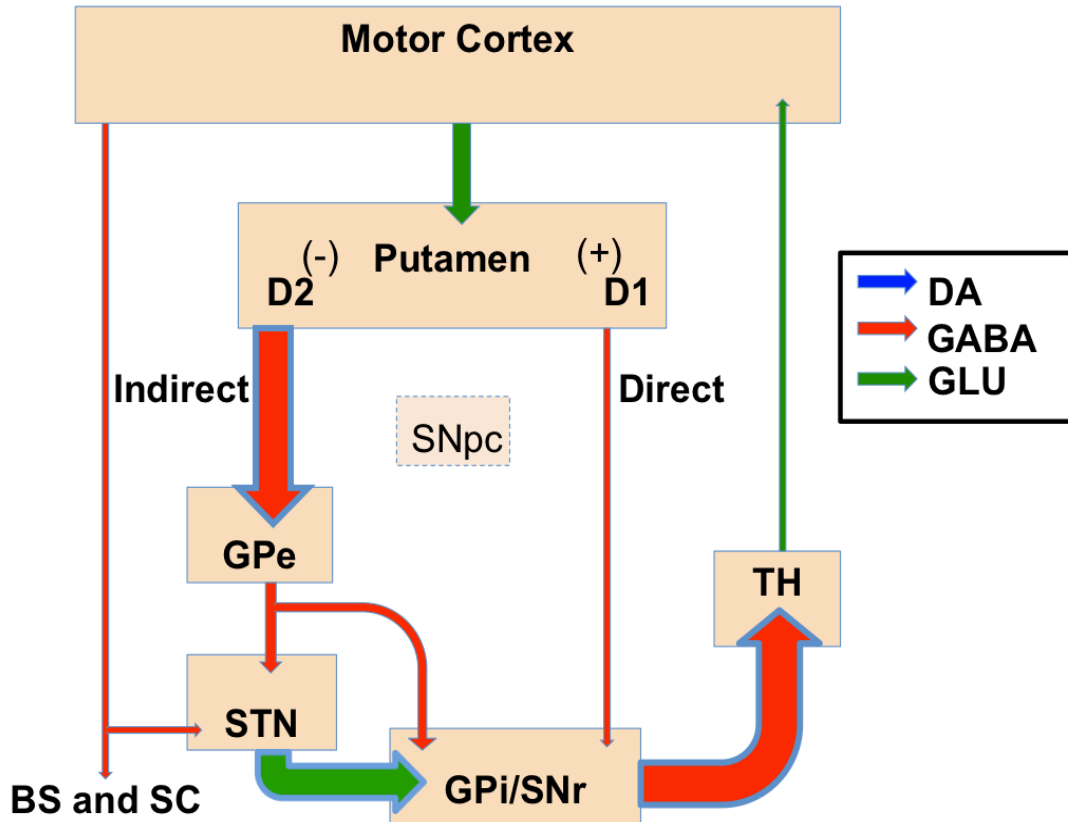


Figure 1-3. The Basal Ganglia in the PD brain. In PD, loss of DA innervation to the ST causes decreased activation of the direct and increased activation of the indirect pathway, leading to inhibition of the thalamus and a corresponding inability to initiate movement. Abbreviations: SNpc, Substantia nigra pars compacta; D1, excitatory D1-like DA receptor; D2, inhibitory D2-like DA receptor; GPe, globus pallidus externa; GPi, globus pallidus interna; STN, subthalamic nucleus; SNr, substantia nigra pars reticulata; TH, thalamus; BS, brainstem; SC, spinal cord.

Etiology of PD

Currently the cause of PD is unknown, however, a growing body of evidence suggests that both environmental and genetic factors play a role in the etiology of the disease.

Environmental Risk Factors in PD

Rural living, drinking well water, farming, living in close contact with farm animals and exposure to pesticides are all environmental risk factors that are thought to play a role in the etiology of PD. Although epidemiological studies normally treat these as separate risk factors, it is likely that rural living, farming, and drinking well water are merely proximate mediators of an ultimate underlying environmental risk factor, which is exposure to pesticides and other toxic chemicals involved in agricultural industry. Rural living is normally supported by farming, which inherently exposes farmers to herbicides and pesticides. Further, farmers who live in rural areas normally have shallow drinking wells when compared to large municipal wells and it is thought that herbicides and pesticides can build up in ground water and shallow drinking wells, which can increase the concentrations of these toxic chemicals. In support of this view, organochloride pesticides have been found in the brains of PD patients living in rural Germany (Semchuck, Love, & Lee, 1991). Additionally, a commonly used pesticide, rotenone, is a potent mitochondrial complex I inhibitor that has been shown to cause relatively selective NSDA neuronal degeneration and the presence of proteinacious inclusions resembling Lewy bodies in rodents (Betarbet et al., 2000).

Drug use has also been listed as a potential environmental risk factor associated with the development of PD. This is primarily due to the discovery that a group of young drug addicts developed severe parkinsonism following the intravenous administration of a meperidine analog,

1-methyl-4-phenyl-4-propionoxypiperidine (MPPP). It was later discovered that the MPPP was tainted with another complex I inhibitor, 1-methyl, 4-phenyl, 1, 2, 3, 6-tetrahydropyridine (MPTP) (P. A. Ballard, Tetrad, & Langston, 1985; Langston et al., 1999). This inadvertent exposure to MPTP provided one of the first pieces of solid evidence that an environmental toxicant could cause selective degeneration of NSDA neurons resulting in a parkinsonian state.

Genetic Risk Factors in PD

Although the vast majority of cases of PD are idiopathic and of unknown origin, there is now emerging data that suggests that there may be some genetic component to the disease. From early on in the study of PD, it was suspected that an increased number of PD patients had affected family members when compared to non-PD patients. A very early account indicated that 15% of PD patients reported a family member who also suffered from PD (Gowers, 1896). However, reports were heavily scrutinized and many family clusters of PD were dismissed due to shared environmental risk factors. Yet, these early accounts may have not have been completely unfounded, with recent reports finding a positive family history in 10-15% of PD patients (T. Gasser, 2007). Conversely, the concordance rates of PD within monozygotic versus dizygotic twins is less consistent. Some reports show concordance of PD is significantly higher in monozygotic as compared to dizygotic twins {Piccini:1999de}, while alternative studies have found no difference {Marttila:1988um}. As such, the role that inheritance plays in idiopathic PD is currently tenuous, however, there are known genetic mutations that irrevocably cause rare forms of familial PD.

Currently there are sixteen genetic loci that are associated with familial PD (T. Gasser, 2007). PD-linked mutations result in both autosomal recessive and autosomal dominant forms of

the disease. Of the more prominent forms of familial PD, mutations in genes coding for α -synuclein (PARK1), ubiquitin-carboxy terminal hydrolase L1 (UCH-L1; PARK5) and leucine rich repeat kinase 2 (LRRK2; PARK8) cause an autosomal dominant form of PD, while mutations in parkin (PARK2), PTEN putative induced kinase (PINK1; PARK6) and DJ-1, (PARK7) cause a recessive form of PD. The age of onset is normally younger in familial forms of the disease and there are some pathological differences between the many familial forms of PD.

Although monogenic forms of PD are exceedingly rare, it is now clear that the molecular pathologies associated with these mutations encompass many overlapping cellular pathways. Many of these molecular pathologies associated with familial PD have also been identified in the idiopathic form of the disease. This information has led to the understanding that PD is not necessarily a disease with one etiology but more accurately a syndrome with multiple heterogeneous pathologies, resulting in a distinct clinicopathological description. As such, research into molecular pathologies associated with PD-linked mutations may yield insight into common pathways underlying NSDA neuronal degeneration.

Molecular Pathology Associated with PD

Although the etiology of PD is still unknown, research investigating the complex interactions between genetics and environment has shed light on several molecular mechanisms that are consistently implicated in PD pathogenesis. Mitochondrial dysfunction, dysfunction of the ubiquitin proteasome pathway (UPP), aberrant DA metabolism and the synergistic interactions between these pathways are all thought to contribute to NSDA neuronal degeneration.

Mitochondrial Dysfunction

The first piece of evidence implicating mitochondrial dysfunction in PD was the discovery of the MPTP-induced parkinsonian state observed in drug users from California. After presenting the cardinal symptoms of PD, post mortem analysis of the brains of these patients revealed significant nigral degeneration and the presence of Lewy bodies, confirming parkinsonism (Langston et al., 1999). Upon discovery that MPTP was a mitochondrial complex I inhibitor, the contribution of mitochondrial dysfunction in the pathogenesis of PD came into question. Since then a large body of evidence has consistently shown mitochondrial dysfunction in both sporadic and monogenic PD.

The main function of mitochondria is to provide energy in the form of adenosine triphosphate (ATP) to the cell. However, mitochondria are incredibly complex and multifaceted organelles that are integral in various cellular processes such as regulation of calcium homeostasis, stress response and cell death pathways. Mitochondria produce ATP through the process of oxidative phosphorylation, which involves the coupling of several redox reactions within the electron transport chain (ETC) (Figure 1-4). The first step in oxidative phosphorylation is the oxidation of either nicotinamide adenine dinucleotide (NADH) or flavin adenine dinucleotide (FADH₂). The electrons obtained from these co-factors are transferred to a series of multiprotein complexes (termed complexes I, II, III and IV) located within the inner membrane of the mitochondrial matrix. The mitochondrial complexes act as both electron donors and acceptors but are arranged such that each complex has a sequentially greater reduction potential than the complex preceding it. This allows electrons to flow “downhill” from complex I to complex IV in a series of exergonic reactions to the final electron acceptor, which is

normally oxygen. The free energy produced from this electron transfer is used to transport protons across the inner mitochondrial membrane. The movement of protons into the mitochondrial intermembrane space creates an electrochemical gradient known as the proton motive force. Mitochondria use this proton motive force to physically power complex V, or ATP synthase, in order to phosphorylate adenosine diphosphate to create ATP.

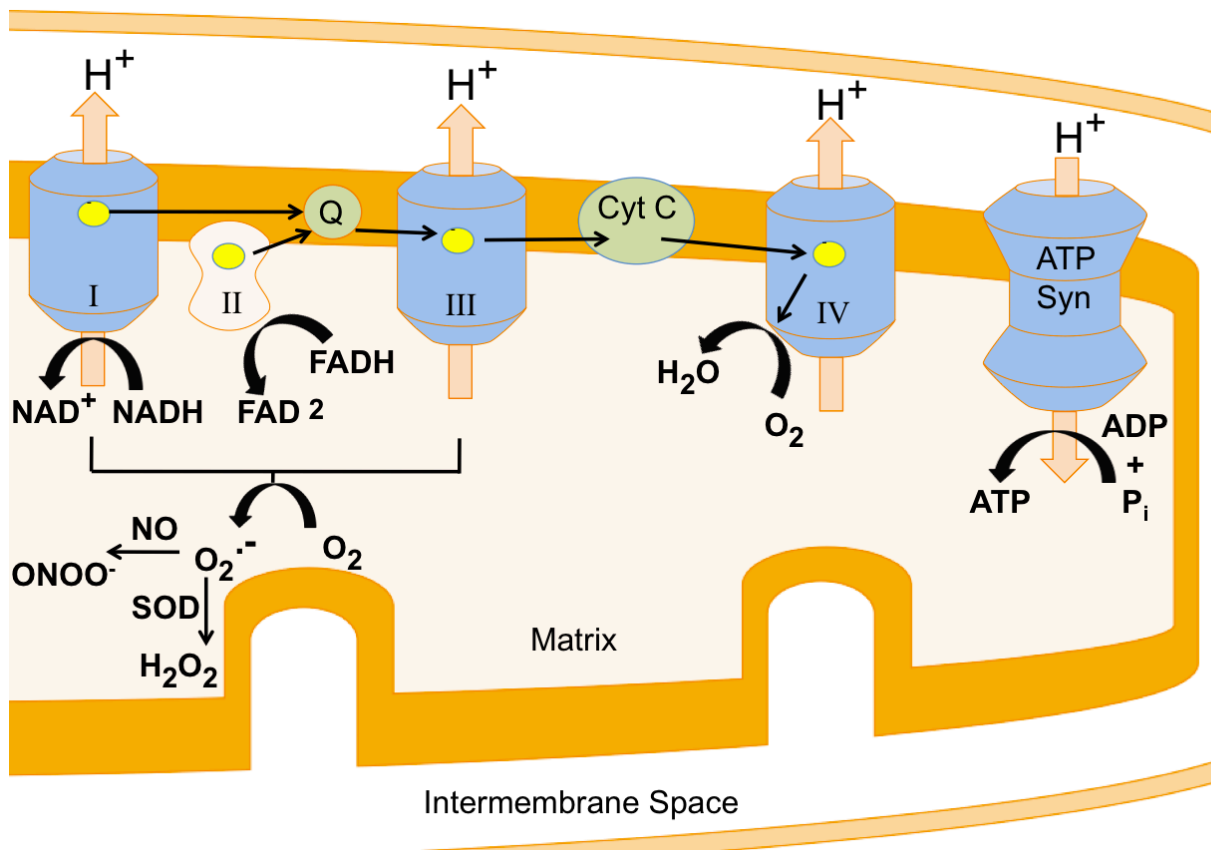


Figure 1-4. The electron transport chain and oxidative phosphorylation. To produce ATP mitochondria oxidize the cofactors NADH (complex I) or FADH₂ (complex II). Electrons gained from oxidation are passed down the mitochondrial complexes in a series of exergonic redox reactions. The free energy gained from redox reactions is used to pump protons into the intermembrane space at complexes I, III and IV. This proton motive force is used to power ATP synthase, which phosphorylates ADP to create ATP. Oxygen is used as the final electron acceptor in the ETC and is reduced to water. Dysfunction of the ETC can result in single electron transfers to oxygen to produce the superoxide radical, which can react with NO to produce peroxynitrite or be converted to hydrogen peroxide by the enzyme superoxide dismutase. Abbreviations: ATP, adenosine triphosphate; ADP, adenosine diphosphate; NADH, nicotinamide adenine dinucleotide; FADH₂, flavin adenine dinucleotide; Q, coenzyme Q; Cyt C, cytochrome C; ATP Syn, ATP synthase, P_i, inorganic phosphate; SOD, superoxide dismutase.

Due to the high amount of redox reactions as well as the use of oxygen as an electron acceptor, mitochondria inherently produce reactive oxygen species (ROS). The main ROS generated by mitochondria is superoxide, which is generated by a single electron transfer to oxygen. It is thought that complex I, and to a lesser extent complex III, are the main sources of superoxide formation (Winklhofer & Haass, 2010). Healthy mitochondria are normally able to use the enzyme superoxide dismutase to convert superoxide to hydrogen peroxide, which is then converted to water and molecular oxygen by the enzyme catalase. However, under pathological conditions, or in the presence of transition metals such as iron, superoxide can be converted to the highly reactive hydroxy radical through the Fenton reaction. High concentrations of ROS in a cell can cause severe damage to lipids, proteins and nucleic acids, and are believed to play a role in NSDA neuron degeneration. Factors which favor ROS production by mitochondria include conditions of low ATP production, decreased coenzyme Q concentrations or following inhibition of the mitochondrial complexes and subsequent electron transport inhibition or reversal (Winklhofer & Haass, 2010).

Many of the mitochondrial pathologies that can cause cytotoxicity have been linked to PD. Mitochondrial complex I activity is decreased in the SN and ST of patients with idiopathic PD (Mizuno et al., 1989; Schapira, Cooper, Dexter, Clark, & Jenner, 1990). Further, complex I activity is found to be impaired in the frontal cortex, fibroblasts, blood platelets, lymphocytes and skeletal muscle of PD patients, suggesting, that at least in some cases, mitochondrial dysfunction may be a systemic pathology (Blin et al., 1994; Haas et al., 1995; Mytilineou et al., 1994; Parker, Parks, & Swerdlow, 2008; Subramaniam & Chesselet, 2013). Other studies have also found oxidative damage to several of the protein complexes of the electron transport chain in the PD brain (Isobe, Abe, & Terayama, 2010; Keeney, Xie, Capaldi, & Bennett, 2006).

Further evidence for role of mitochondrial dysfunction in PD comes from familial forms of the disease. Genes associated with recessive forms of PD have been directly linked to normal mitochondrial homeostasis. Specifically, PINK1 and parkin physically interact with mitochondria and are crucial in the regulation of mitochondrial fission/fusion events and the maintenance of mitochondrial integrity and function (Deng, Dodson, Huang, & Guo, 2008; Dodson & Guo, 2007; Exner et al., 2007). Finally, mitochondrial inhibitors such as rotenone, paraquat and the aforementioned MPTP are shown to result in a parkinsonian state (Betarbet et al., 2000; Langston et al., 1999; McCormack et al., 2002). Taken together the large body of evidence implicating mitochondrial dysfunction in NSDA pathology has made mitochondria a major focus of research into the etiology of PD.

UPP Impairment

Dysfunction of the UPP has also long been implicated in PD pathogenesis. The UPP is responsible for the selective proteolysis of proteins, particularly regulatory proteins and proteins with abnormal conformations or post-translational modifications. Proteins destined for degradation are bound with multiple ubiquitin (Ub) peptides, flagging them for transport to the 26s proteasome where they are degraded. Ubiquitination is a tightly regulated process involving the coordinated actions of three separate enzymes including the E1 activating, E2 conjugating and E3 ligase enzymes (Figure 1-5). Following the ATP dependent activation of Ub by the E1 enzyme, the E2 conjugating enzyme will shuttle the activated Ub to the E3 enzyme. Finally the E3 ligase is responsible for the physical attachment of the Ub molecule to the targeted protein, providing substrate specificity to ubiquitination. Dysfunction of any step within this pathway can cause aggregation of abnormal proteins and subsequent disruption of cellular homeostasis.

Dysfunction of the UPP and abnormal protein degradation was first implicated in PD pathogenesis by the presence of Lewy bodies. Lewy bodies are intracellular cytoplasmic protein aggregates, composed mainly of α -synuclein, synphilin-1, Ub and other components of the UPP (Sharma, McLean, Kawamata, Irizarry, & Hyman, 2001; Wakabayashi et al., 2000; Wirdefeldt et al., 2001). Although it is presently unclear whether Lewy bodies represent a primary pathogenic or secondary protective mechanism, the presence of these cytosolic aggregates implicates a dysfunction in normal homeostatic proteolysis in PD, most likely due to impaired proteasomal function. Consistent with the role of UPP dysfunction in PD pathogenesis, recent studies have found both functional and structural deficits in the 20/26s proteasome in the SN of PD patients (McNaught, Belizaire, Jenner, Olanow, & Isacson, 2002; McNaught, Belizaire, Isacson, Jenner, & Olanow, 2003). Additionally, animal studies have shown that chronic exposure of rats to proteasome inhibitors results in motor abnormalities, progressive NSDA degeneration and the formation of Lewy body-like protein aggregates containing α -synuclein and Ub (McNaught, Perl, Brownell, & Olanow, 2004).

Further evidence supporting UPP dysfunction in PD pathogenesis comes from PD-linked mutations in parkin, UCHL-1 and α -synuclein. Mutations in α -synuclein result in an aggregation prone form of the protein, which has been shown to directly inhibit the proteasome and result in the formation of Lewy bodies (Bence, Sampat, & Kopito, 2001; H. Snyder et al., 2003). Parkin is an E3 ligase and UCH-L1 is a deubiquinating enzyme, both essential components of the UPP. Mutations in either of these genes result in familial forms of PD, and both parkin and UCH-L1 have been identified in Lewy bodies, directly linking the UPP to PD pathogenesis (Kitada, Tong, Gautier, & Shen, 2009; Leroy et al., 1998). Parkin is of particular interest as most familial associated mutations in the parkin gene result in defective E3 ligase activity of the corresponding

protein (Zhang et al., 2000). Lewy body pathology is not present in the brains of patients with recessive forms of PD caused by parkin mutations. The early age of onset and the lack of Lewy pathology characteristic of parkin associated PD has initiated the search for parkin substrates, which could result in toxicity if not properly sequestered or degraded. Although α -synuclein is not a parkin substrate itself, the α -synuclein interacting protein synphilin-1 as well as an o-glycosylated form of α -synuclein are potential parkin substrates and both are present in Lewy bodies (Chung et al., 2001; Shimura et al., 2001).

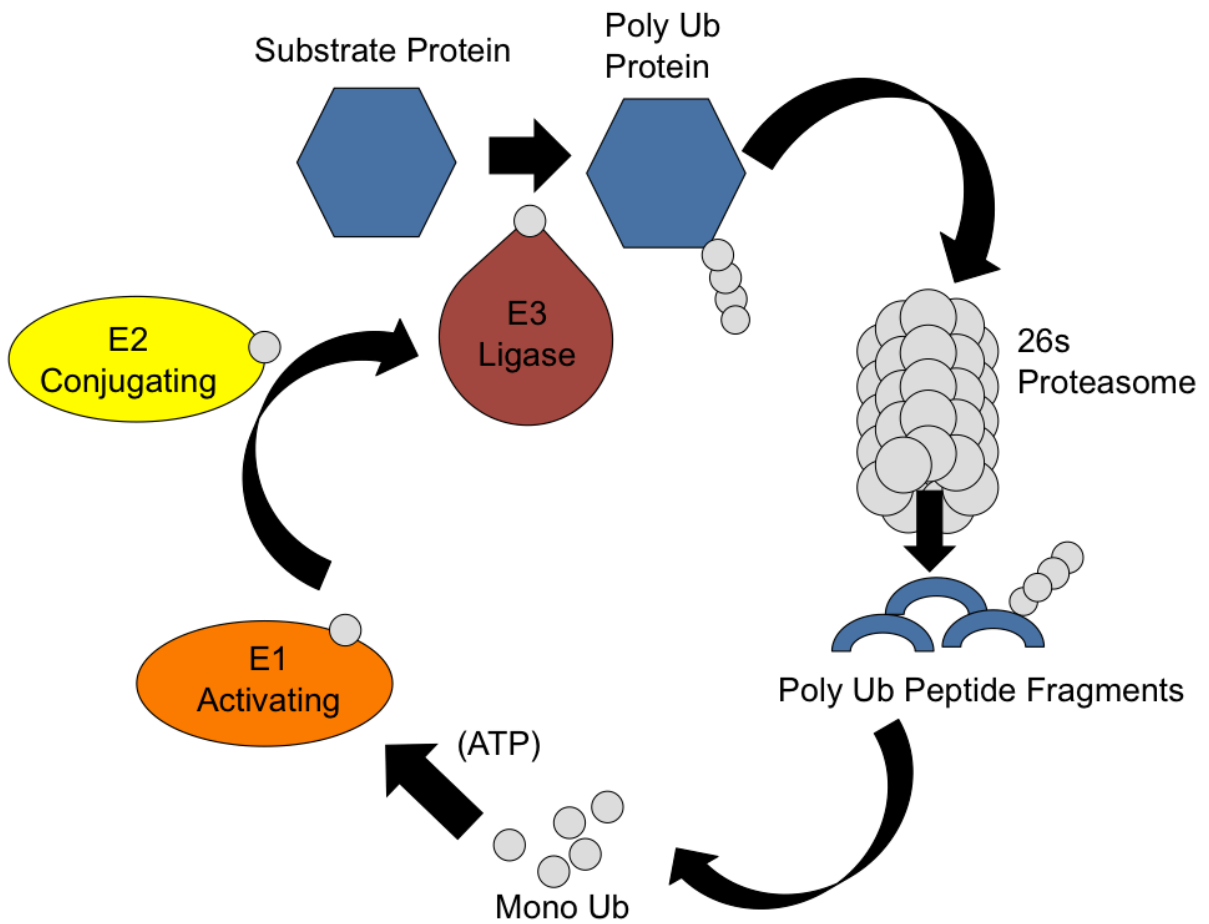


Figure 1-5. The Ubiquitin Proteasome Pathway. Following the ATP dependent activation of Ub by the E1 enzyme, the E2 conjugating enzyme will shuttle the activated Ub to the E3 enzyme. The E3 ligase is responsible for the physical attachment of the Ub molecule to the targeted protein. Polyubiquitinated proteins are degraded by the proteasome or the autophagic lysosomal pathway. The proteasome consists of a 19s regulatory cap and the 20s core particle which performs proteolysis. Following degradation polymeric Ub chains are recycled to mono Ub by deubiquitinating enzymes. Abbreviations: Ub, ubiquitin; ATP, adenosine triphosphate.

Abnormal DA Catabolism

Due to the relatively selective loss of DA containing neurons in PD, abnormal DA homeostasis has long been suspected in the pathogenesis of the disease. As many of the enzymatic reactions involved in DA metabolism, as well as DA and its metabolites themselves, are highly reactive and potentially toxic, it is crucial for DA neurons to maintain a tight coupling and control of DA synthesis, release, reuptake and catabolism. DA metabolism and neurotransmission processes are highly concentrated within the microenvironment of the DA axon terminal and as such renders these terminal regions highly vulnerable, due to increased exposure to oxidative stress. In support of this notion, evidence is beginning to accumulate showing that axon terminal degeneration precedes actual NSDA cell loss in PD and associated animal models (Innis et al., 1993; Ouchi et al., 2005; Petroske, Meredith, Callen, Totterdell, & Lau, 2001).

Under normal conditions the enzyme MAO-B oxidizes cytosolic DA to the transient intermediate DOPAL. DOPAL is quickly converted to DOPAC, which readily diffuses out of nerve terminals (Marchitti, Deitrich, & Vasiliou, 2007). DA oxidation by MAO is potentially toxic as it can result in both mitochondrial inhibition and the production of hydrogen peroxide (Cohen & Kesler, 1999). In addition, DOPAL itself is cytotoxic due to its highly reactive nature, readily forming adducts with many cellular components (Burke, Li, Williams, Nonneman, & Zahm, 2003; Marchitti et al., 2007). Furthermore, the conversion of DOPAL to DOPAC by ALDH can damage cells by producing hydrogen peroxide (Marchitti et al., 2007). Thus, even under normal conditions DA metabolism produces a high amount of cellular stress.

Alternatively, if normal DA metabolism is impaired, cytosolic DA is rendered vulnerable to autooxidation, resulting in the formation of DA quinones and the ROS superoxide and

hydrogen peroxide (Graham, Tiffany, Bell, & Gutknecht, 1978; LaVoie & Hastings, 1999). Hydrogen peroxide can react with transition metals to ultimately produce the highly reactive hydroxyl radical. DA neurons utilize the transition metal iron within the catalytic core of the enzyme TH. Accordingly, iron is found in high abundance in DA neurons and as such DA neurons are inherently predisposed to the production of ROS (Barzilai, Melamed, & Shirvan, 2001). Additionally, the ROS superoxide can react with nitric oxide to produce the toxic peroxynitrite species (Barzilai et al., 2001). If not properly handled by endogenous antioxidant systems, increases in ROS and reactive nitrogen species can interact with and cause damage to lipids, proteins and nucleic acids, resulting in significant cytotoxicity.

Further cellular damage can be caused by the auto-oxidation of DA and the resultant production of DA quinones. DA-quinones bind to cysteine residues on proteins forming cysteinyl DA adducts, resulting in loss of protein function (Graham et al., 1978; LaVoie & Hastings, 1999). As many antioxidants utilize free thiol groups as electron acceptors, antioxidants are especially vulnerable to DA-quinone modification, creating the potential to further exacerbate ROS damage. Thus under normal or aberrant conditions DA and the events involved its metabolism and transmission can produce cytotoxic by-products, which if not properly handled can severely damage the cell.

Overlapping Molecular Pathologies of PD

Mitochondrial respiration, protein degradation by the UPP, and DA metabolism are molecular pathways that intersect on many different levels. Accordingly, dysfunction in one of these paths has the potential to elicit a vicious cycle of pathology with the other two pathways (Figure 1-6). Both ROS and DA quinones have been shown to inhibit mitochondrial respiration,

resulting in decreases in cellular ATP and further ROS production (Berman & Hastings, 1999). Decreased mitochondrial output can subsequently result in a decrease in VMAT activity as well as decreases in the mitochondrial enzyme ALDH (Lamensdorf et al., 2000; Watabe & Nakaki, 2008), ultimately leading to increased levels of cytosolic DA and DOPAL, increased potential for DA auto-oxidation and consequent elevated toxic DA metabolites, quinones and ROS. Finally, decreased energy stores and the synergistic increases in ROS and damaged proteins caused by DA oxidation and mitochondrial dysfunction, can result in proteasome inhibition and protein aggregation (Betarbet et al., 2000; Shamoto-Nagai et al., 2003). Further, DA itself can directly inhibit the proteasome (Caneda-Ferrón et al., 2008), which in turn can cause further mitochondrial dysfunction and further increases in oxidatively damaged proteins (Höglinger et al., 2003; Qiu et al., 2000; Y. Tanaka et al., 2001).

As can be seen there is a significant interplay between these molecular pathways, and any initial dysfunction in one pathway has the potential to initiate a self-perpetuating cycle of toxicity. It is likely that this cycle of toxicity would initiate in the DA nerve terminal, as this is the major site of DA metabolism and neurotransmission, and thus requires a high metabolic demand and protein turnover. Within the PD brain, it is likely that this initial terminal dysfunction could overwhelm the endogenous cellular protective mechanisms, ultimately resulting in the death of NSDA neurons.

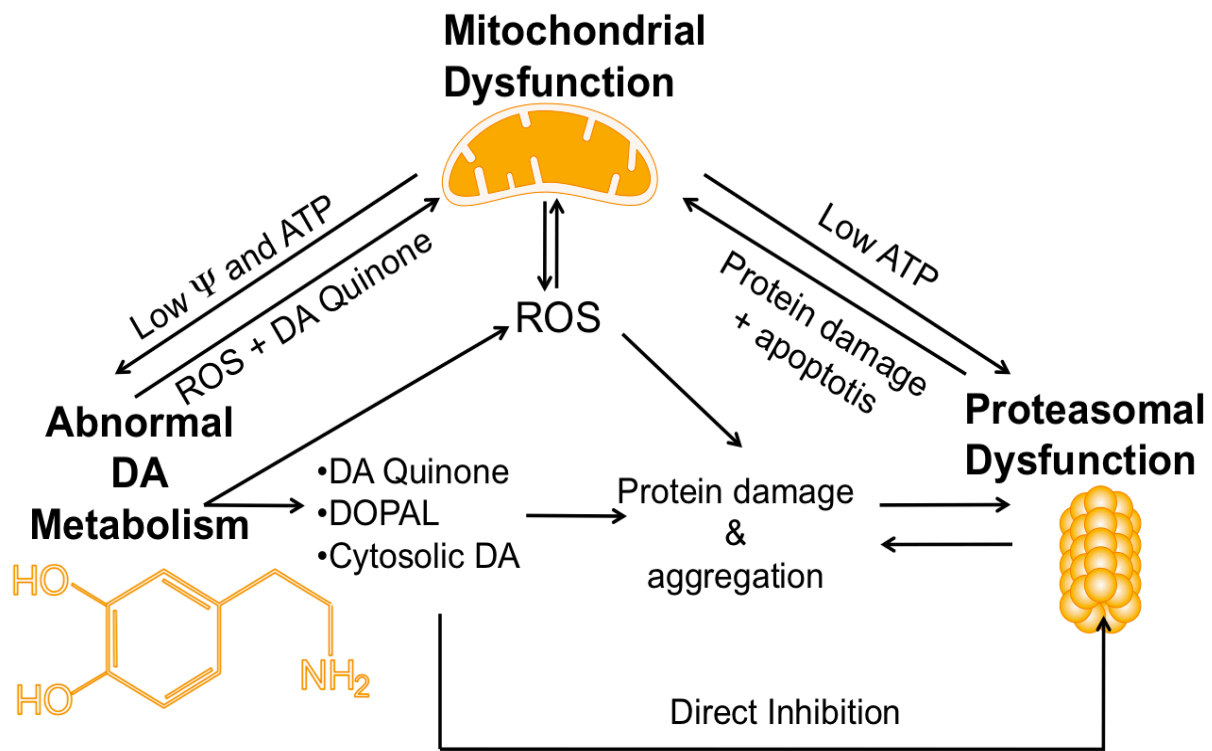


Figure 1-6. Cycle of molecular pathology associated with PD. Initial dysfunction of the UPP or mitochondria, or alterations in DA metabolism can initiate a pathological cascade involving all cellular systems. Abnormal DA metabolism causes increased production of ROS, DA quinones, DOPAL and cytosolic DA. ROS and DA quinones can directly inhibit mitochondria, while DA and its toxic metabolites can also inhibit the proteasome. Alternatively, DA, DA quinones, DOPAL and ROS can all indirectly inhibit the proteasome through protein damage and subsequent protein aggregation. In turn proteasomal dysfunction leads to mitochondrial impairment and initiation of the apoptotic cascade. Finally, mitochondrial dysfunction can lead to increases in cytosolic DA and DA toxicity as well as further proteasomal inhibition. Dysfunctions in DA metabolism, mitochondrial function and the UPP are all implicated in PD pathogenesis. Abbreviations: DA, dopamine; DOPAL; dihydroxyphenylacetaldehyde; ROS, reactive oxygen species; Ψ , mitochondrial membrane potential; ATP, adenosine triphosphate.

MPTP Neurotoxicity and PD

Since the original discovery of the MPTP-induced parkinsonian state observed in humans, MPTP has become the most commonly used neurotoxicant to study the cellular and molecular pathology associated with PD. Of the many neurotoxicants used to study dopaminergic toxicity, MPTP is the only toxicant that consistently produces a parkinsonian state clinically indistinguishable from PD in humans and monkeys (Jackson-Lewis & Przedborski, 2007; Langston, Ballard, Tetrud, & Irwin, 1983). Further, MPTP has been found to cause nigral degeneration and PD like symptoms in other species including; dogs, cats and mice (Jackson-Lewis & Przedborski, 2007; Petroske et al., 2001; Rapisardi, Warrington, & Wilson, 1990; Schneider, Yuwiler, & Markham, 1986). However, it must be noted that although MPTP replicates many aspects of PD, it does not mimic every aspect of the disease, most notably the progressive nature of cell loss observed in PD. Accordingly, MPTP is not truly a model of PD but rather an invaluable platform for studying the molecular underpinnings of the disease *in vivo*.

MPTP metabolism and molecular pathology

Following peripheral administration, the highly lipophilic MPTP will rapidly cross the blood-brain barrier. Once inside the central nervous system the pro-toxicant MPTP is oxidized by the enzyme MAO-B, to the intermediate 1-methyl-4-phenyl-2,3-dihydropyridine (MPDP), which is then converted to the active toxicant 1-methyl-4-phenylpyridinium (MPP^+), most likely through spontaneous oxidation (Jackson-Lewis & Przedborski, 2007). Due to simple mass action, the majority of this MPTP metabolism occurs in non-neuronal glia, and thereafter MPP^+ is released into the extracellular space through an unknown process. Unlike its pro-form, MPP^+

is a charged molecule and thus needs transporter facilitation to gain entry to cells. MPP^+ shows high affinity for DAT as well as some affinity for the norepinephrine and serotonin transporters (**Figure 1-7**) (Javitch, D'Amato, Strittmatter, & Snyder, 1985). The high affinity of MPP^+ for DAT explains the selective entry and subsequent toxicity to DA neurons. Once inside a DA neuron, MPTP recapitulates most, if not all of the molecular pathologies associated with PD, including mitochondrial dysfunction, proteasomal dysfunction and DA toxicity.

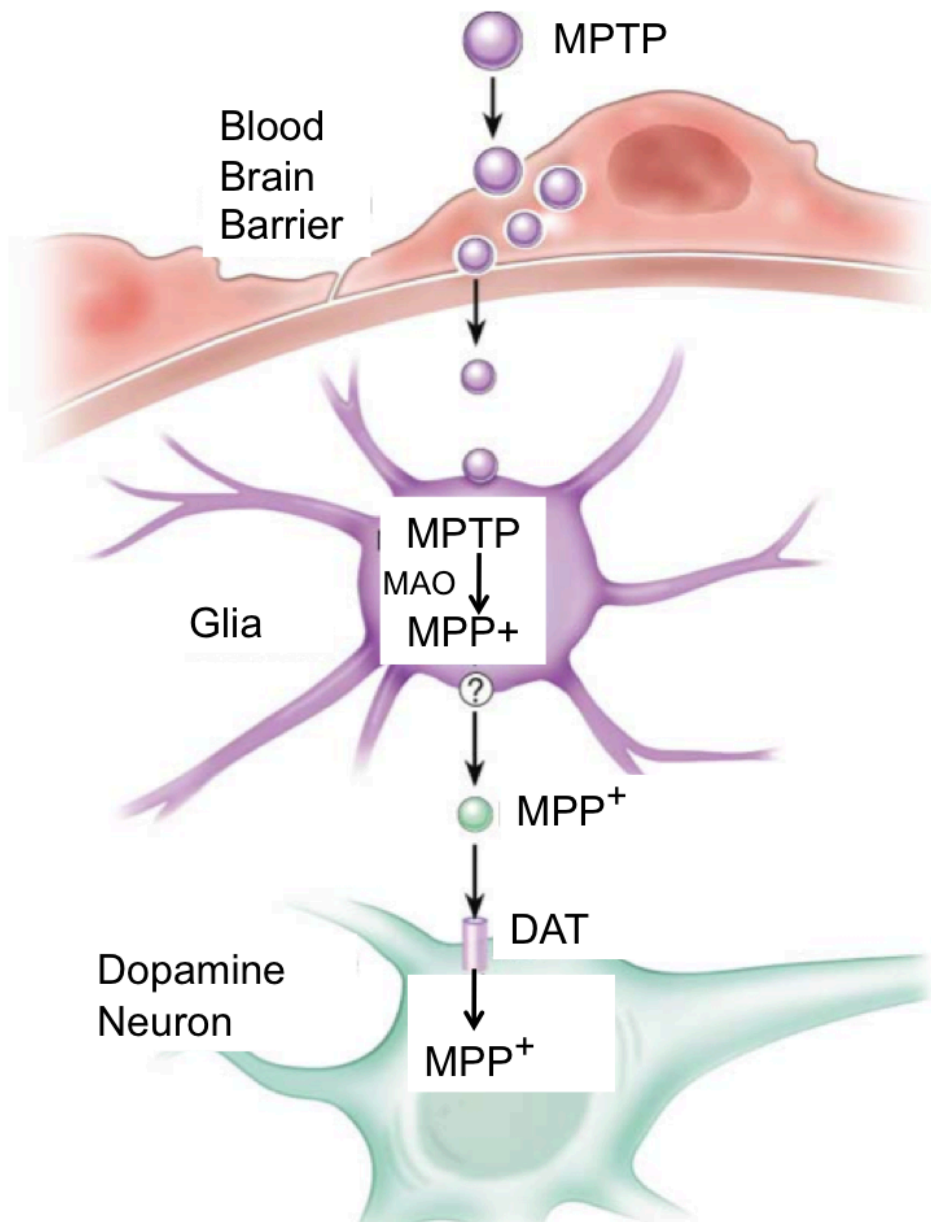


Figure 1-7. MPTP metabolism. Following peripheral administration, MPTP will cross the blood-brain barrier. Once inside the central nervous system MPTP is oxidized by the enzyme MAO-B, to the intermediate 1-methyl-4-phenyl-2,3-dihydropyridine (MPDP; not shown), which then spontaneously oxidizes to the active toxicant MPP⁺. The majority of MPTP metabolism occurs in glia, and thereafter MPP⁺ is released into the extracellular space. MPP⁺ enters the DA terminal through the dopamine transporter. Once inside the DA terminal, the majority of MPP⁺ will either enter the mitochondria or be sequestered into vesicle by the vesicular monoamine transporter. Abbreviations: MPTP, 1-methyl-4-phenyl-1, 2, 3, 6-tetrahydropyridine; MPP⁺, 1-methyl-4-phenylpyridinium; DA, dopamine; MAO-B, monoamine oxidase-B.

MPTP and Mitochondrial Dysfunction

Following entry into the cell, the majority of MPP^+ will be concentrated into the mitochondria. The transport of MPP^+ into mitochondria is an active transport against a concentration gradient, and thus relies upon an intact mitochondrial transmembrane potential for energy to support this gradient (Ramsay & Singer, 1986). The best-described action of MPP^+ is the inhibition of mitochondrial complex I of the ETC (Nicklas, Youngster, Kindt, & Heikkila, 1987). Recent studies have shown the IC_{50} for complex I inhibition to be somewhere in the range of 2.6 μ M (Höllerhage et al., 2009). Through the active transport of MPP^+ into mitochondria, concentrations can reach up to 20mM, well beyond the IC_{50} necessary for complex I inhibition (Ramsay & Singer, 1986). MPP^+ induced inhibition of complex I causes severe dysfunction of the ETC, resulting in loss of mitochondrial membrane potential, decreased cellular ATP levels, disruption of calcium homeostasis and increased free radical and ROS production (Cassarino et al., 1997; Di Monte, Jewell, Ekström, & Sandy, 1986; Schulz, Henshaw, Matthews, & Beal, 1995; Sheehan et al., 1997; Smith & Bennett, 1997). In a very similar mechanism to that found within NSDA neurons in PD, it is thought that the inhibition of mitochondrial function and subsequent decreases in ATP and increases in ROS play a major role in MPTP-induced cellular dysfunction, which could potentially lead to cell death.

MPTP and UPP Dysfunction

MPTP administration has also been found to result in impairment of the UPP and accumulation of damaged protein that is strikingly similar to that found in the SN of the PD

brain. Acute administration of MPTP has been shown to result in a transient inhibition of the UPP, while continuous MPTP exposure results in long-lasting proteasomal inhibition and the formation of protein inclusions closely resembling Lewy bodies (Fornai et al., 2005). MPTP treatment in marmosets results in a reduction of the catalytic β -subunits as well as a corresponding decrease in all enzymatic (trypsin-like, chymotrypsin-like and peptidyl-glutamyl peptide-hydrolyzing) activities of the 20S proteasome (Zeng et al., 2006). Finally, MPP^+ and to a lesser extent MPTP have been shown to directly inhibit the proteasome *in vitro*, most likely through oxidative modification to the 20s catalytic subunits (Caneda-Ferrón et al., 2008).

MPTP and DA Toxicity

MPTP has also been shown to result in severe DA associated toxicity via mechanisms independent of any direct action on mitochondria or the UPP. Following entry to the cell MPP^+ can be sequestered into DA containing synaptic vesicles through the action of VMAT (Y. Liu, Roghani, & Edwards, 1992). As MPP^+ is transported into vesicles, it will purge DA into the cytosol in the process. This massive efflux of DA into the cytosol causes a large increase in DA auto-oxidation, the formation of DA quinones and the aforementioned cascade of DA mediated toxicity. MPTP oxidation by MAO-B results in the production of hydrogen peroxide and superoxide (Zang & Misra, 1993). Further, as MPTP is a substrate for MAO-B, it will act as a competitive inhibitor of the enzyme (Chiba, Trevor, & Castagnoli, 1984; Salach, Singer, Castagnoli, & Trevor, 1984), resulting in a decreased ability of the cell to safely metabolize cytosolic DA, further exacerbating the propensity for DA auto-oxidation and cytotoxicity.

In summary, systemic administration of MPTP results in a nearly identical pattern of molecular dysfunction to that found in PD. This ability of MPTP to initiate the same cycle of molecular pathology within NSDA neurons makes MPTP an appropriate tool for studying the early molecular events involved in PD.

MPTP Dosing Regimens

The majority of the key cellular dysfunctions thought to contribute to NSDA cell death in PD are recapitulated by MPTP, however the specific mechanism and severity of toxicity are dependent upon the dosing paradigm used. In studies utilizing mice, MPTP is normally administered in one of several different dosing regimens, termed acute, sub-acute or chronic paradigms.

Acute MPTP administration may refer to a single MPTP injection or a regimen consisting of 4 MPTP injections within one day. For clarity these different dosing paradigms will now be referred to as the single-acute and acute MPTP paradigms, respectively. The small dose and short time course associated with the single-acute MPTP regimen results in transient decreases in striatal DA and TH-immunoreactivity (ir), ATP depletion and subsequent ROS formation (Chan, DeLanney, Irwin, Langston, & Di Monte, 1991; Chiba et al., 1984; Jackson Lewis, Jakowec, Burke, & Przedborski, 1995; Lotharius & O'Malley, 2000).

Alternatively the acute MPTP regimen consisting of 4 MPTP injections every 2 h within one day, results in far more severe toxicity. Depending on the doses used, this regimen results in anywhere from a 40%-90% depletion of ST DA and metabolites, loss of TH-ir in NSDA terminals and soma, and non-apoptotic (most likely necrotic) cell death (Jackson-Lewis & Przedborski, 2007; Petroske et al., 2001). The harsh nature of this dosing paradigm results in a

considerable amount of mortality, mostly resulting from peripheral toxicity, and as such this regimen is less relevant to the insidious pathology associated with PD (Petroske et al., 2001).

The sub-acute MPTP dosing regimen consists of one injection of MPTP daily for five consecutive days. This regimen results in 40%-50% loss of ST DA and metabolites, decreases in DA uptake in ST synaptosomes, and loss of TH-ir in NSDA axon terminals and dendritic processes (Petroske et al., 2001). Further, using the sub-acute regimen, some studies have found apoptotic like cell death in the SNpc and corresponding loss of NSDA cell numbers, while others studies have found no cell loss (Jackson-Lewis & Przedborski, 2007; Petroske et al., 2001). Experimental variation and differential timing in the termination of the experiment most likely explain the cause of this discrepancy.

Finally, the chronic MPTP regimen consists of 10 injections of MPTP combined with the organic cation transporter inhibitor probenecid, every 3.5 days. This regimen results in a severe 95%-98% loss of ST DA and metabolites, reduction of functional DA uptake in ST synaptosomes, loss of cells of the SN, impaired motor activity, and the accumulation of α -synuclein and ubiquitin proteins in the SN. Further, unlike the other MPTP dosing regimens, the pathology associated with the chronic MPTP regimen is shown to be relatively progressive and sustained for up to 6 months (Meredith, Totterdell, Potashkin, & Surmeier, 2008; Petroske et al., 2001).

As indicated above, the severity and mechanism of MPTP toxicity is variable and dependent upon the dose and timing of administration. As such it is imperative to choose an MPTP dosing paradigm that is appropriate for the hypotheses being tested and end points being measured. The majority of the studies detailed herein will utilize the single-acute MPTP

paradigm in order to determine early events in the cytotoxic cascade, which render some sets of DA neurons vulnerable to MPTP toxicity while others are resistant.

Differential Susceptibility of Central DA Neurons

Although many cell types are affected in PD, central DA neurons show the most profound degree of cell loss (Ahlskog, 2005; Braak et al., 2003; Sulzer, 2007). However, PD does not affect all DA neuronal systems to the same extent. For example, while NSDA neurons show severe degeneration in PD, mesolimbic DA neurons are only partially affected by PD. Further, even NSDA neurons within different anatomical subdivisions of the SN are differentially affected {Gibb:1991wl, Braak:2003ws}. Currently, the mechanism underlying the differential susceptibility of relatively similar DA neurons remains unknown. However, increased trophic support or gene expression is hypothesized to contribute to resistance {Hung:1996vv, Greene:2005ch}. Even more intriguing than the partial resistance of mesolimbic DA neurons is the near complete resistance of the tuberoinfundibular (TI) DA neurons of the hypothalamus.

Specifically, TIDA neurons are resistant to the loss of axon terminal DA concentrations and inclusion body formation that is the hallmark of NSDA degeneration in PD. (Ahlskog, 2005; Braak et al., 2003; Langston & Forno, 1978; Matzuk & Saper, 1985). TIDA neurons originate in the arcuate nucleus (ARC) of the mediobasal hypothalamus (MBH) and terminate adjacent to the hypophysial portal vessels in the median eminence (ME) (Figure 1-8; A). DA released from TIDA neurons is transported to the anterior pituitary where it acts to tonically inhibit prolactin secretion. Reuptake of DA in TIDA neurons is mediated by low affinity, high volume transport as well as by DAT, albeit to a lesser extent than NSDA neurons (Annunziato, Leblanc, Kordon,

& Weiner, 1980; Demarest & Moore, 1979a; Demaria et al., 2000; Lookingland & Moore, 2005; Revay, Vaughan, Grant, & Kuhar, 1996). Despite these differences in DA reuptake mechanisms, the cellular machinery responsible for DA synthesis, storage, release and catabolism are similar in both NSDA and TIDA neurons (Figure 1-8; B). As such, investigation into the mechanisms underlying the differential susceptibility of these two central DA subpopulations could potentially shed light onto the molecular pathogenesis of the disease.

The differential susceptibility of TIDA and NSDA neurons to PD-associated cellular pathology has also been observed in neurotoxicant-based animal models of PD. Again, while NSDA neurons show large depletions in axon terminal DA concentrations, TH-ir, and cell loss, TIDA neurons are completely spared (Behrouz, Drolet, Sayed, Lookingland, & Goudreau, 2007; Mogi, Harada, Kojima, Kiuchi, & Nagatsu, 1988; Willis & Donnan, 1987). Originally, the mechanism responsible for resistance of TIDA neurons to MPTP toxicity was thought to be lower levels of DAT expression and thus a decreased exposure to MPP^+ . However, TIDA neurons are also resistant to an alternative complex I inhibitor, rotenone, which does not require transporter facilitation to gain entry to the cell. Further, TIDA neurons show an initial depletion of axon terminal DA concentrations 4h post-MPTP but are able to fully recover terminal DA concentrations by 24h post-MPTP (Behrouz et al., 2007). These results indicate the MPP^+ does gain entry into TIDA neurons and causes some initial toxicity, yet through an unknown mechanism these neurons are able to recover and remain unaffected by MPTP toxicity.

Preliminary insights into the mechanisms that may render TIDA neurons resistant to MPTP toxicity have been made. The resistance of TIDA neurons to MPTP toxicity has been found to be protein synthesis dependent. Further, following MPTP administration, TIDA neurons are shown to up-regulate mRNA of the PD associated genes parkin and UCH-L1

(Benskey et al., 2012). Since mutations in both parkin and UCH-L1 have been shown to result in rare genetic forms of PD (Kitada et al., 2009; Leroy et al., 1998), this ability of MPTP-resistant, THDA neurons to up-regulate two genes following administration of a toxicant that mimics PD pathology, supports a role for parkin and UCH-L1 in dopaminergic neuronal homeostasis and neuroprotection. Toxicant-induced up-regulation of UCH-L1 and parkin and its role in the differential susceptibility of DA neurons to MPTP will be the focus of the current thesis. Accordingly it is necessary to understand the normal physiology of parkin and UCH-L1 as well as the pathophysiology of these proteins, which can lead to NSDA degeneration in PD.

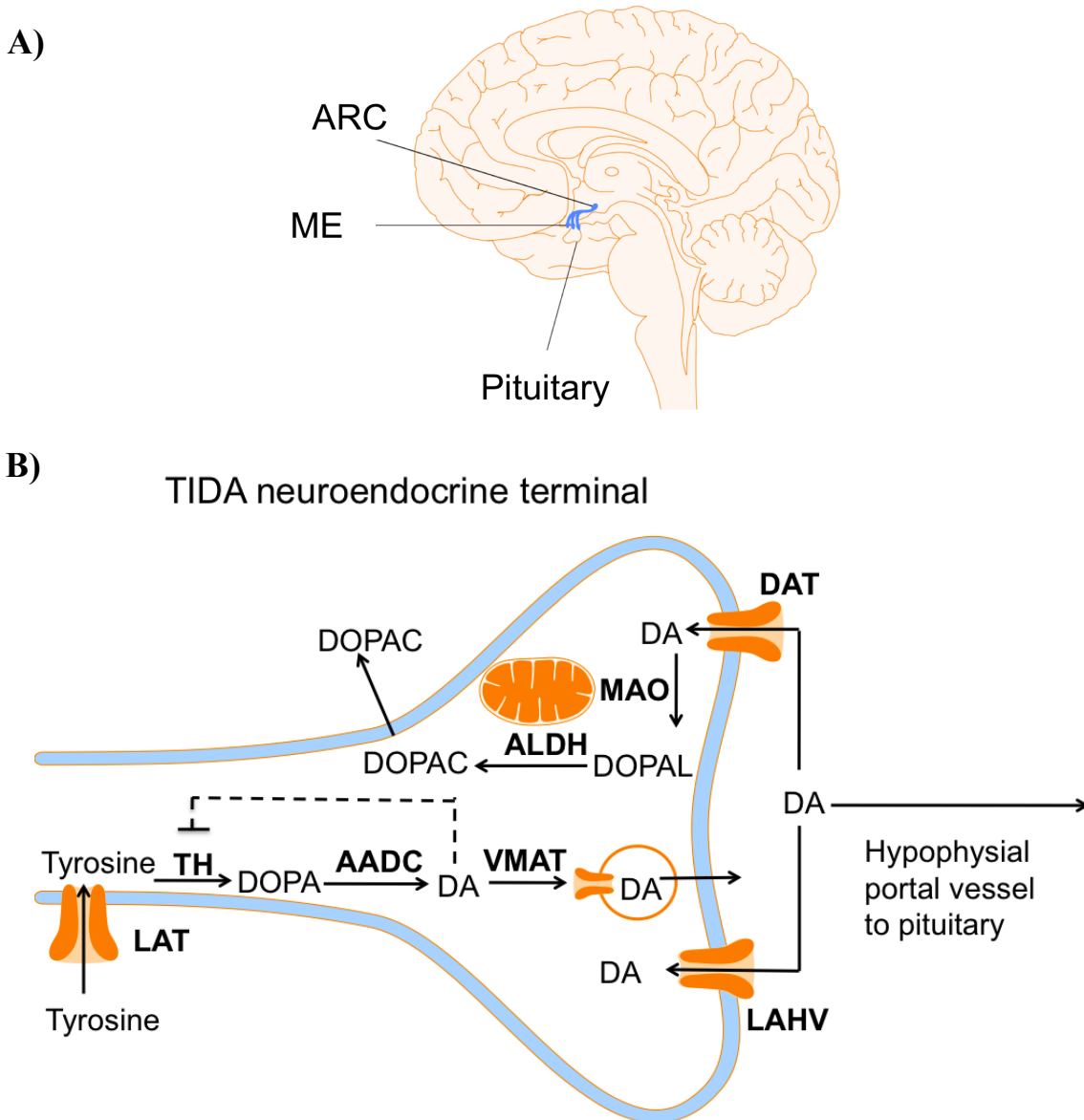


Figure 1-8. Location of TIDA neurons in the brain and DA metabolism within the TIDA axon terminal. Panel A, TIDA neurons have soma in the ARC and axons that terminate in the ME. Panel B, Dietary tyrosine is hydroxylated by TH to form DOPA. DOPA is decarboxylated by DDC to form DA which is packaged into vesicles by VMAT. Upon arrival of an action potential DA is released into the hypophysial portal and travels to the pituitary. Extracellular DA is recaptured by LAHV transporters or DAT and then can be repackaged into vesicles or metabolized. DA metabolism begins with deamination by MAO-B to form DOPAL followed by oxidation by ALDH to form DOPAC. Abbreviations: ARC, arcuate nucleus; ME, median eminence; DA, dopamine; LAT, large neutral amino acid transporter; TH, tyrosine hydroxylase; DOPA, 3,4-dihydroxyphenylalanine; AADC, aromatic amino acid decarboxylase; VMAT, vesicular monoamine transporter; D1, excitatory D1-like DA receptor; D2, inhibitory D2-like DA receptor; AC, adenylate cyclase; cAMP, cyclic adenosine monophosphate; DAT, DA transporter; LAHV, low affinity high volume transporter; MAO, monoamine oxidase; DOPAL, dihydroxyphenylacetylaldehyde; ALDH, aldehyde dehydrogenase; DOPAC, dihydroxyphenylacetic acid.

UCH-L1

UCH-L1 was originally discovered when a missense mutation in exon 4 of the gene was shown to be the proximate cause of a dominant form of familial PD (Leroy et al., 1998). UCH-L1 is one of the most abundant proteins in the human brain and is thought to be responsible for the cleavage of polymeric Ub to Ub monomers or to hydrolyse bonds between Ub and small adducts such as glutathione (Leroy et al., 1998; Wilkinson et al., 1989). Recent studies have shown UCH-L1 to also have Ub ligase activity (Y. Y. Liu, Fallon, Lashuel, Liu, & Lansbury, 2002). PD associated mutations in UCH-L1 lead to reductions in the catalytic activity of UCH-L1 (Leroy et al., 1998; Y. Y. Liu et al., 2002). It is thought that UCH-L1 mutations lead to decreased cleavage and turnover of Ub and other unknown UCH-L1 substrates, and eventual protein aggregation. Alternatively, mutations may also render UCH-L1 aggregate prone itself. This latter hypothesis is supported by the identification of UCH-L1 in Lewy bodies. Regardless of the mechanism, UCH-L1 mutations cause UPP deficits leading to abnormal protein aggregation and DA neuron degeneration (Leroy et al., 1998; Y. Y. Liu et al., 2002).

Parkin

Mutations in the parkin gene constitute the most common form of familial PD (Coelln et al., 2004). Specifically, parkin mutations cause autosomal recessive juvenile parkinsonism (ARJP). The association of AR-JP with large homozygous exon deletions of a gene on chromosome 6, led to the original discovery of the parkin gene (Kitada et al., 1998). Since then, a multitude of PD causing parkin mutations have been identified including; missense and nonsense point mutations, duplications and triplications of entire exons, deletions of single or entire exons and frameshift mutations (Coelln et al., 2004).

The parkin gene encodes an evolutionarily conserved 465 amino acid protein that consists of an N-terminal Ub-like domain, a linker region, and a C-terminal domain containing 2 really interesting new gene (RING) domains separated by an in-between RING (IBR) domain (Figure 1-9). The majority of PD-associated parkin mutations have been localized to the RING-IBR-RING domain, implying that this portion of the protein is essential to its function. Interestingly, there have been several cases of ARJP in which clinical manifestations of PD are present with only one parkin allele being affected, which would be unexpected in a recessively inherited disease. These anomalies seem to suggest that haploinsufficiency of the parkin protein may be a risk factor of PD (Farrer et al., 2001). In support of this notion parkin has also been shown to be s-nitrosylated in the brains of patients with idiopathic PD (Chung, 2004). S-nitrosylation impairs parkin's normal function and it is thought that loss of parkin function (through haploinsufficiency or nitrosative inactivation) is a risk factor for PD.

As was mentioned above, parkin acts as an E3 ligase in the UPP and has been shown to mediate classical K48 linked polyubiquitination, leading to proteasomal degradation. In addition, parkin can mediate K63 linked polyubiquitination and monoubiquitination, leading to autophagic degradation or post-translation modification of target proteins (Lim, 2005; Lim, Dawson, & Dawson, 2006). As the majority of parkin mutations inhibit the E3 ligase activity of parkin, it is speculated that loss of functional parkin causes aberrant or decreased ubiquitination, leading to corresponding deficits in the UPP or mitochondrial homeostatic pathways parkin is so integrally involved in.

Accordingly, loss of parkin function could lead to cytotoxicity on many different levels. Moreover, parkin appears to play a pivotal role, specifically in dopaminergic homeostasis, displaying an impressively wide range of neuroprotective benefits including protection against

DA associated oxidative stress, proteosomal dysfunction, and regulation of mitochondrial quality control (H. H. Jiang, Ren, Zhao, & Feng, 2004; Narendra, Kane, Hauser, Fearnley, & Youle, 2010; Petrucelli et al., 2002). Parkin thus seems to be at a nexus where many of the proposed molecular pathologies associated with both PD and MPTP toxicity meet. As such, parkin is a very interesting focus of investigation into possible mechanisms that may render TIDA neurons resistant to PD and MPTP.

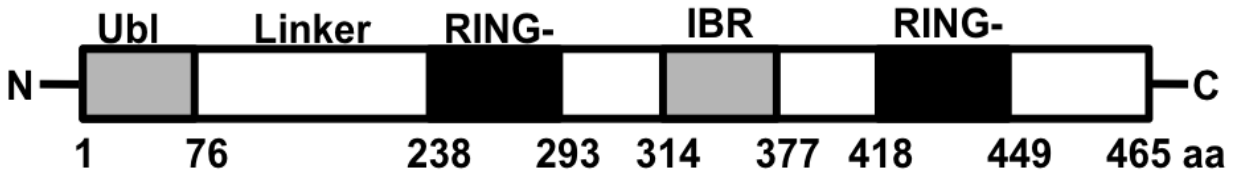


Figure 1-9. The structure of the parkin protein. The parkin protein is a 465 amino acid protein consisting of an N-terminal UBL domain, a linker region, and a C-terminal domain containing two RING finger domains separated by IBR domain. The majority of the PD-associated mutations in the parkin gene affect the c-terminal RIR motif and lead to decreased E3 ligase activity.. The amino acid number associated with the respective domains of the parkin protein are shown below the diagram. Abbreviations, UBL, ubiquitin like; R1, really interesting new gene (RING) 1; IBR, inbetween RING; R2, RING 2.

Experimental Paradigm and Goal of Dissertation

MPTP toxicity is dependent upon the dose and timing of MPTP administration. The majority of studies described herein will utilize a single injection of MPTP with experiments terminated within 24 h of toxicant administration. The use of this single-acute injection regimen allows for identification of early events that occur following toxicant administration, either deleterious or protective, which may play a role in subsequent terminal degeneration and cell death. Within the single -acute MPTP injection paradigm, the low exposure dose and short time course following MPTP causes dysfunction primarily within the DA axon terminal, such as loss of TH-ir and displacement of vesicular DA, independent of any overt cell death (Behrouz et al., 2007; JACKSONLEWIS et al., 1995; Petroske et al., 2001). These early changes in phenotypic markers of DA axon terminal homeostasis following MPTP can serve as a predictive index of later cellular degeneration. For example, one of the earliest indicators of MPTP toxicity is loss of TH protein and TH-ir cell bodies and axon terminals of NSDA neurons. It has been shown that loss of TH in NSDA neurons consistently precedes actual cell loss in MPTP treated monkeys and mice as well as in PD post mortem brain tissues (Jackson Lewis et al., 1995; Kastner et al., 1994; Kastner, Hirsch, Agid, & Javoy-Agid, 1993).

An additional dopaminergic phenotypic marker that predicts future toxicity is axon terminal DA concentrations. A consistent anomaly found when studying MPTP is the near complete resistance of rats to MPTP toxicity. Despite similar levels of MAO-B activity, DAT reuptake activity as well as MPP⁺ accumulation in NSDA neurons between the two species, mice are susceptible to MPTP toxicity while rats are resistant. The only species differences found between mice and rats following MPTP administration is an almost 3-fold increase in MPTP-induced extracellular DA concentrations in mice as compared to rats (Giovanni, Sieber,

Heikkila, & Sonsalla, 1994). This difference in the early response of axon terminal DA concentrations parallels the differential neurotoxicity observed between the two species. This data suggests that DA toxicity is paramount in MPTP toxicity, but also that initial changes in axon terminal DA stores can serve as a strong predictive index of eventual toxicity and degeneration.

At the low exposure level used in the current dissertation, only highly susceptible neurons will fail to cope with the cytotoxicity produced from a single injection of MPTP. By examining the early changes in DA phenotypic markers (such as axon terminal DA concentrations and TH-ir) or expression of neuroprotective proteins occurring in susceptible NSDA neurons and comparing them to early events within resistant TIDA neurons, it may be possible to identify cell-autonomous, phenotypic variations, which underlie the increased susceptibility of NSDA neurons in PD. Further, it may also be possible to identify mechanisms specific to TIDA neurons that render these neurons resistant to MPTP and PD, and could be the target of translational therapeutics aimed at saving damaged DA neurons that are damaged but not yet doomed. To this end, the effect of increased or decreased parkin expression in the differential susceptibility of TIDA and NSDA neurons to MPTP toxicity will be examined.

Summary

PD pathology is associated with the selective degeneration of midbrain NSDA neurons, while the TIDA neurons of the mediobasal hypothalamus remain intact. The same pattern of selective degeneration has been observed following exposure to MPTP, a neurotoxicant that recapitulates many of the molecular pathologies associated with PD. Factors mediating this differential susceptibility of central DA neurons to PD and MPTP are unknown, but could be

related to the ability to increase the expression of neuroprotective proteins under conditions of cellular stress. The protein parkin in particular, seems to be ideally suited to deal with DA neuron homeostasis, as it is a key player in several of the molecular pathways that have been implicated in both PD and MPTP toxicity. The experiments in this thesis were designed to characterize the differential susceptibility of TIDA and NSDA neurons to MPTP toxicity and investigate the role parkin plays in the protection of TIDA neurons following toxicant exposure.

Thesis Objective

The studies described in this dissertation were developed in order to test the central hypothesis that TIDA neuronal resistance to acute MPTP toxicity is mediated by a cell-autonomous ability to up-regulate parkin protein expression under conditions of cellular stress, whereas NSDA neuronal susceptibility to acute MPTP toxicity is due to an inability to increase parkin expression. The following Specific Aims and hypotheses were designed to test this central hypothesis.

1) Characterization of the differential susceptibility of TIDA and NSDA neurons to single-acute MPTP exposure.

Hypothesis: TIDA neurons are resistant, while NSDA neurons are susceptible to acute MPTP induced disruption of axon terminal DA homeostasis. The differential susceptibility of TIDA and NSDA neurons to acute MPTP toxicity is associated with the ability to increase the expression of neuroprotective proteins.

2) The role of toxicant exposure, prolactin activation and DA synthesis in the differential susceptibility of TIDA and NSDA neurons to single-acute MPTP toxicity.

Hypothesis: Toxicant bioavailability, DA synthesis or prolactin feedback activation do not account for the differential susceptibility of TIDA and NSDA neurons to acute MPTP toxicity.

3) Characterization of the differential susceptibility of TIDA and NSDA neurons to chronic MPTP exposure.

Hypothesis: TIDA neurons are resistant, while NSDA neurons are susceptible to chronic MPTP induced disruption of axon terminal DA homeostasis and cell loss. The differential susceptibility of TIDA and NSDA neurons to chronic MPTP toxicity is associated with the ability to increase the expression of neuroprotective proteins.

4) The role of parkin in the differential susceptibility of TIDA and NSDA neurons to single-acute toxicant exposure.

Hypothesis: the resistance of TIDA neurons to single-acute MPTP toxicity is mediated by the ability to up-regulate parkin protein expression following toxicant exposure, whereas NSDA neuronal susceptibility to acute MPTP toxicity is due to an inability to increase parkin expression.

The following chapters outline the research performed to address the above Specific Aims. The reader is referred to Chapter 2 for detailed methodology. Chapters 3-7 describe findings as they relate to the central hypothesis and the thesis objectives. Chapter 8 provides a general discussion on the relevance and the importance of this research as it relates to the previous findings and the information from the literature. Appendix A, describe the production or recombinant adeno-associated virus (rAAV) vectors containing parkin short hairpin RNA (shRNA) or human parkin transgenes.

Chapter 2. Materials and Methods

Animals

All experiments were conducted in 8-10 week old male C57Bl6/J mice purchased from Jackson Laboratories (Bar Harbor, MA). Animals were randomly assigned to treatment groups, and housed two to four per cage, maintained in a light-controlled (12 h light/dark cycle; lights on 0600 h), temperature-controlled ($22 \pm 1^\circ\text{C}$) room, with food and tap water provided *ad libitum*. The Michigan State University Institutional Animal Care & Use Committee approved all experiments using live animals (AUF 10/11-222-00).

Drugs and Administration

All drugs were purchased from Sigma-Aldrich (St. Louis, MO). Doses were calculated as the free base of the respective drug.

Single Acute MPTP: 1-methyl-4-phenyl-1,2,3,6-tetrahydropyridine (MPTP) was dissolved in 0.9% sterile saline. Mice received a single injection of either saline vehicle (10 ml/kg; s.c.) or MPTP (20 mg/kg; s.c) and the experiment was terminated at 4, 8, 16, 24 or 32 h after the MPTP injection. Saline control animals were sacrificed 4 h post-injection and used as zero time controls.

Chronic + Single Acute MPTP: Mice were treated with MPTP using an amended version of a previously described chronic administration regimen (Meredith et al., 2008; Petroske et al., 2001). Animals received ten MPTP (20 mg/kg; s.c.; every 3.5 days) or saline (10 ml/kg; s.c.;

every 3.5 days) injections with P-dipropylsulfamoyl-benzoic acid (probenecid), over the course of 35 days. Probenecid was dissolved in 0.1 N NaOH, which was stabilized with 1 M Tris-HCl to a pH of 7.4. All animals received injections of probenecid (250 mg/kg; i.p.) 30 min prior to MPTP or saline administration. Twenty-one days following the last chronic MPTP or saline injection, mice received a single injection of either MPTP (20 mg/kg; s.c.) or saline (10 ml/kg; s.c.) and were sacrificed 24 hr later. MPTP and probenecid were freshly prepared on each injection day. Probenecid is an organic cation transporter inhibitor used to decrease excretion of the active MPTP metabolite, MPP⁺, thereby maintaining brain levels of the neurotoxicant during the 3.5 day injection interval. It has previously been shown that probenecid does not interfere with neurochemical indices of DA axon terminal integrity (Meredith et al., 2008; Petroske et al., 2001).

NSD-1015: 3-hydroxybenzylhydrazine (NSD-1015) was dissolved in 0.9% sterile saline. At various times following MPTP administration mice were treated with the DOPA-decarboxylase inhibitor NSD-1015-dihydrochloride (100mg/Kg; i.p.), 30 min prior to sacrifice.

Bromocriptine: Mice were treated with the DA receptor agonist bromocriptine (3mg/kg; s.c.) dissolved in 0.9% sterile saline with 4% ethanol or vehicle (10ml/Kg; s.c.) 4 h prior to MPTP treatment.

Tissue Preparation

For neurochemical and Western blot analyses, mice were sacrificed by decapitation and brains were rapidly removed and placed on an ice-cooled glass stage. Under a dissecting

microscope the ME was collected using forceps and iridectomy scissors, and the remaining brain was quickly frozen on dry ice. Consecutive frozen coronal sections (500 μm) were prepared throughout the rostrocaudal extent of the regions containing DA subpopulations of interest using a cryostat set at $-10\text{ }^{\circ}\text{C}$ (CTD-Model Harris, International Equipment Co., Needham, MA), thaw mounted onto glass slides and immediately refrozen. The regions of interest were microdissected using a modification of the method described previously (Palkovits, 1973; Palkovits & Brownstein, 1983). Figure 2-1 and Figure 2-2 demonstrate the locations in the brain where tissue was collected. Using a dissecting microscope bilateral tissue punches were obtained from the ST (round 18-gauge: Figure 2-1 top) and the SN (oval 21-gauge: Figure 2-1 bottom) while single punches were obtained from two consecutive sections for the ARC (round 18-gauge: Figure 2-2). These tissue samples were used for neurochemical and Western blotting and were processed according to the appropriate protocols described below.

For immunohistochemical (IHC) analysis, mice were deeply anesthetized with a ketamine:xylazine cocktail (26.6 mg/kg: 4 mg/kg; s.c.). Once fully anesthetized (showing no withdrawal reflexes), mice were transcardially perfused with 0.9% saline followed by 4% paraformaldehyde. Brains were then removed and post fixed in 4% paraformaldehyde and cryoprotected in 20% sucrose.

Coronal sections (35 μm) through the entire rostrocaudal axis of the brain were prepared with a cryostat (-19°C) using and, in the case of brightfield IHC, Multiblock™ processing (Neuroscience Associates, Knoxville, TN).

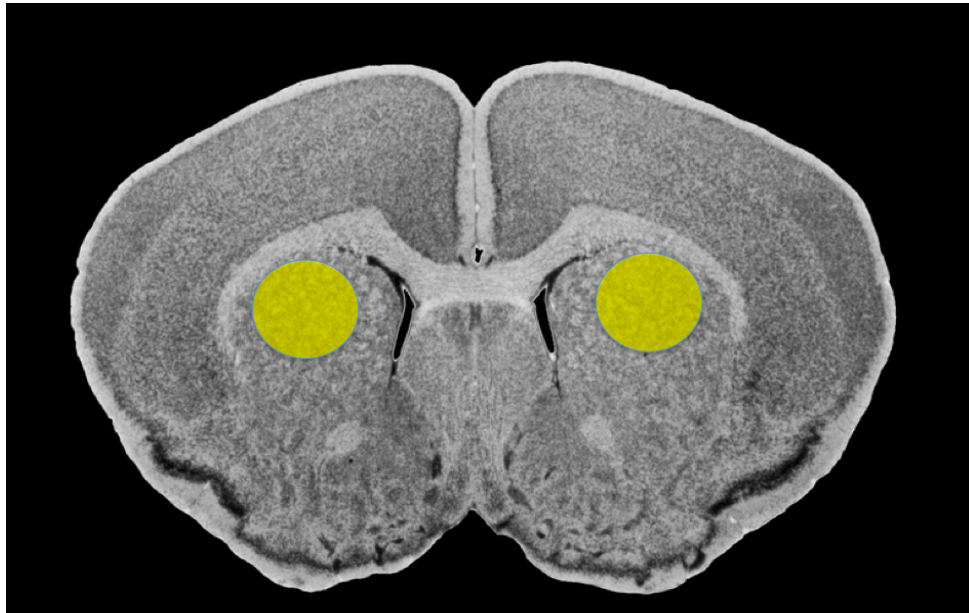


Figure 2-1. Diagram of coronal brain sections showing localization of micropunches used to dissect the ST (top) and SN (bottom). The yellow circles and ovals represent the location of the Palkovits micropunch. The ST (top) was dissected from a 500 μ M section 0.98mm rostral to Bregma. The SN (bottom) was dissected from a 500 μ M section 3.08 mm caudal to Bregma. Modified from mouse brain library (2010).

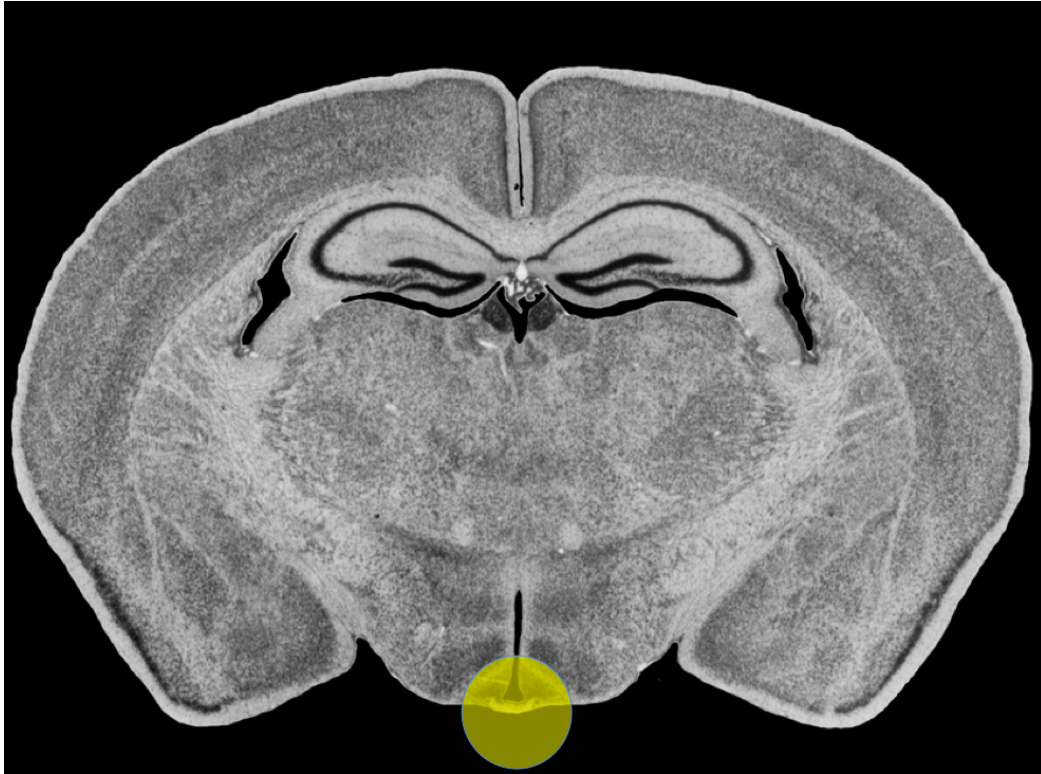


Figure 2-2. Diagram of coronal brain sections showing localization of micropunches used to dissect the ARC. The yellow circle represent the location of the Palkovits micropunch. The ARC was dissected from two consecutive 500 μ M section at 1.58 mm (shown) and 2.06 mm (not shown) caudal to Bregma. Modified from mouse brain library (2010).

Neurochemical Analyses

Microdissected brain tissue samples were placed into cold tissue buffer (0.1M phosphate-citrate buffer pH 2.5) and sonicated with three consecutive 1 sec bursts (Heat Systems Ultrasonics, Plainview NY). Protein was pelleted by centrifugation at 12,000 x g (Beckman Coulter Microfuge, Palo Alto, CA) for 1 min. The content of DA, DOPAC and DOPA in supernatants was determined with high pressure liquid chromatography coupled with electrochemical detection (HPLC-ED) using a Waters 515 HPLC pump (Waters Corporation, Milford, MA) and an ESA Coulochem 5100A electrochemical detector with an oxidation potential of +0.4V. MPP+ content in supernatants was determined using HPLC coupled with mass spectrometry (MS) as described previously (Lehner et al., 2011). Neurochemical standards and experimental samples were injected onto a C18 reverse phase analytical column (Bioanalytical Systems, West Lafayette, IN). The HPLC mobile phase (0.5M sodium phosphate, 0.03M citrate, 0.1mM EDTA, 0.2-0.3% sodium octylsulfate, 15-20% methanol, pH 2.5) was adjusted by altering concentrations of SOS and methanol in order to optimize neurotransmitter peak resolution. DA, DOPAC and DOPA content was quantified by comparing the peak heights of each sample to the peak heights of 1.0 ng standards.

Tissue pellets were re-suspended in 1 N NaOH and assayed for protein using the bicinchonic acid (BCA) protein assay (J. M. Walker, 2002). To correct for differences in sample size the neurochemical content was normalized to the amount of protein in each sample and expressed as a concentration of neurochemical in ng per mg protein.

Western Blot Analyses

Microdissected brain samples were sonicated in cold homogenization buffer (TBS containing 1% SDS, 0.1mM PMSF, 1mM DTT with Complete Mini Protease Inhibitor Cocktail Tablets; Roche Diagnostics, Mannheim, Germany) pH 7.4, and centrifuged (10,000 x g 10 min). The supernatants containing total cytoplasmic protein were removed and placed into fresh microcentrifuge tubes. The supernatants were assayed for protein content using the BCA protein method (J. M. Walker, 2002). Protein (10-15 μ g) from each sample was run on polyacrylamide gels (Bio-Rad, Hercules, CA) and transferred to 0.45 μ m PVDF or FL-PVDF membrane (Millipore, Pittsburgh, MA, USA) by electrophoresis. PVDF membranes were washed in 25mM Tris buffered saline (TBS), blocked with either 5% non-fat dry milk or blocking buffer (Li Cor, Inc., Lincoln, NE) for 1h and reacted with primary antibody in either 5% NFDM or blocking buffer overnight at 4°C. The source, dilution and company supplying each primary antibody used are shown in Table 2-1.

Following primary antibody incubation membranes were washed in TBS and incubated for 1h at room temperature with the appropriate secondary for 1 h at room temperature. The source, dilution and company supplying each secondary antibody used are shown in Table 2-2.

Membranes were washed and bound antibodies were visualized with the Odyssey-FC infrared imager (Li-Cor Biosciences). The density of each band was quantified by measuring the infrared absorbance using the Odyssey infrared imager and Odyssey software (Version 3.0, Li-Cor Biosciences). Relative density was obtained by normalizing the band density of target proteins to that of the control protein, used to account for variations in loading of samples onto the gel. Glyceraldehyde phosphate dehydrogenase (GAPDH) or β -actin were used as the control proteins, and their detection and visualization was linear. Expression levels of GAPDH

or β -actin were similar amongst the compared brain regions regardless of treatment. Each membrane contained representative samples from all experimental conditions.

Immunohistochemistry

Brightfield Immunohistochemistry:

Brightfield IHC was performed on free-floating sections using a primary rabbit anti-TH antibody (Millipore, Billerica, MA), followed by a biotin-conjugated, goat anti-rabbit secondary antibody (Jackson ImmunoResearch, West Grove, PA). Bound peroxidase was visualized with 0.05% 3,3'-diaminobenzidine tetrahydrochloride with 0.01% hydrogen peroxide using an ABC Elite kit (Vector Laboratories, Burlingame, VT). Sections were counter-stained with Cresyl Violet to determine if decreases in TH-ir cell counts correspond with loss of Nissl stained cells in the area.

Fluorescence Immunohistochemistry:

In order to visualize the location and spread of viral vector expression fluorescence IHC was performed on free-floating sections. Sections were washed in 0.05M phosphate buffer containing 0.1% Triton x-100 (PB-TX) and incubated overnight in primary antibody. The source, dilution and company supplying each primary antibody used are shown in Table 2-1. Following overnight incubation in primary antibody, sections were washed in PB-TX and incubated with secondary antibody for 1h at room temperature and protected from light. The source, dilution and company supplying each secondary antibody used are shown in Table 2-2. Sections were then washed and covered slipped using ProLong Gold antifade reagent (Molecular Probes, Eugene, OR). Sections were viewed on a Nikon TE-2000-U-Fluorescence Microscope (Melville, NY).

Primary Antibody	Dilution	Source	Company
TH	1:2000	Rabbit	Millipore (Ab152)
Parkin	1:1000	Mouse	Cell Signaling (4211)
UCH-L1	1:800	Rabbit	Cell Signaling (3524)
DAT	1:3500	Rat	Millipore (MAB369)
CHIP	1:1000	Rabbit	Cell Signaling (C3B6)
HSP70	1:1000	Rabbit	Cell Signaling (4872)
IBA 1	1:1000	Goat	Abcam (ab5076)
Nitrotyrosine	1:1000	Rabbit	Millipore (06-284)
β -Actin	1:1000	Mouse	Cell Signaling (3700)
GAPDH	1:5000	Mouse	Sigma (G8795)
GFP	1:1000	Chicken	Abcam (13970)
FLAG (DDDDK)	1:2000	Goat	Abcam (1257)

Table 2-1. Description of primary antibodies. Antibody characterization describes the standard dilution used for Western blotting or immunohistochemistry, the animal the antibody was derived from (source) as well as the company and catalog number describing where the antibody was purchased from (company). Abbreviations: TH, tyrosine hydroxylase; UCH-L1, ubiquitin carboxy terminal hydrolase-L1; DAT, dopamine transporter; CHIP, C-terminus of HSC-70 interacting protein; HSP70, heat shock 70kDa protein; IBA 1, ionized calcium-binding adaptor molecule 1; GAPDH, glyceraldehyde 3-phosphate dehydrogenase; GFP, green fluorescent protein.

Secondary Antibody	Dilution	Source	Company
Anti-Mouse IgG-HRP	1:8000	Horse	Cell Signaling (7076)
IRDye 680LT anti-Rabbit IgG	1:15,000	Goat	Li-Cor (926-68021)
IRDye800CW anti-Mouse IgG	1:10,000	Goat	Li-Cor (926-32210)
IRDye800CW anti-Rat IgG	1:10,000	Goat	Li-Cor (926-32219)
IRDye800CW anti-Goat IgG	1:10,000	Donkey	Li-Cor (926-32214)
Alexa Fluor 488 Anti-Chicken	1:1000	Goat	Invitrogen (A11039)
Alexa Fluor 488 Anti-Goat	1:1000	Donkey	Invitrogen (A11055)
Cy-3-conjugated Affinipure Anti-Rabbit	1:500	Goat	Jackson ImmunoResearch (111-165-003)

Table 2-2. Description of secondary antibodies. Antibody characterization describes the standard dilution used for Western blotting or immunohistochemistry, the animal the antibody was derived from (source) as well as the company and catalog number describing where the antibody was purchased from (company).

Unbiased Stereological Cell Counting

Using Stereo-Investigator software (Version 4.03 Microbrightfield, Inc. 2000), sections were viewed on a screen at low magnification (4x). The SN and ARC were delineated through the rostrocaudal extent of the respective nuclei. The first plane was a randomly chosen section within 180 μm of the most rostral plane of the area of interest as determined by a mouse atlas (Paxinos & Franklin, 2003). The delineated sections were evenly spaced apart (210 μm).

TH-ir neurons were counted using the Optical Fractionator method. This method results in a quantifiable estimate of the total population of cells within a given region independent of cell shape and size, or conformational changes in the tissue (Schmitz & Hof, 2005; West, Slomianka, & Gundersen, 1991). A counting frame (100 x 100 μm) was utilized and a fraction of the delineated cells were sampled. TH-ir cells were identified with a consistent distribution over the depth of the counting frame, thus confirming sufficient reagent penetration throughout the thickness of the tissue slice. Approximately 7-10 sections per animal were needed to count the entire SN, whereas 5-7 sections per animals were needed to count the ARC.

Counting TH-ir cells was performed using a 40x objective. Cells were counted only if they showed TH-ir in the cell body and the top of the nucleus came into focus within the virtual counting frame as well as within the delineated region of interest. For estimates of neuron number every sixth section was sampled. The coefficient of error for each estimate was calculated and was less than 0.1 (Gundersen, $m=1$) (Gundersen & Jensen, 1987).

Stereotaxic Surgery

Mice were anesthetized using 4-5% isoflurane while the surgical site was shaved and the animal was placed in the stereotaxic frame. Isoflurane was reduced to 2% for the remainder of the surgery. The surgical site was thoroughly scrubbed with a Betadine swab prior to incision. A single incision was made along the rostrocaudal axis of the skull and tissue overlying the skull was retracted to expose the skull surface. A Hamilton syringe (Hamilton, Reno, NV) with a 30 gauge blunt-tip needle was fitted with a siliconized pulled glass micropipette with an opening of 60-80 μ m. Bilateral ARC injections of 250nl/side were performed at a 10 degree angle in the following coordinates from Bregma: rostro-caudal -1.75, medio-lateral 1.25 and -1.25, and dorso-ventral -6.2 from the skull surface. Unilateral SN injections of 500nl were performed using the following coordinates from Bregma: rostro-caudal; -3.0, medio-lateral: -1.4, dorso-ventral: -4.4 from the skull. Figure 2-3 depicts the location of the bilateral ARC injections and unilateral SN injections. Recombinant adeno-associated viral (rAAV) vectors were injected at a titer of 1.4×10^{13} vg/ml for shRNAs and 3.4×10^{13} vg/ml for parkin cDNA. Lactacystin was injected at a concentration of 5 μ g/ μ l. Volumes were injected at a rate of approximately 125 nl/min using an automated micropump (World Precision Instruments). The needle was left in place for an additional 5 min to prevent reflux. The hole in the skull was filled with sterile bonewax, and the skin replaced and closed using surgical staples. Mice were kept on a heating pad until recovery from anesthesia and then returned to their home cages. Mice were checked daily for signs of infection/distress.



Figure 2-3. Localization of stereotaxic injections into the ARC (top) and the SN (bottom). Animals received 250 nl bilateral stereotaxic injections to the ARC (top) at the following coordinates from Bregma: R/C:-1.75, M/L: \pm 1.25, D/V: -6.2. Animals received 500nl unilateral stereotaxic injections to the SN (bottom) at the following coordinates from Bregma: R/C: -3.0, M/L: -1.4, D/V: -4.4. Modified from mouse brain library (2010).

Statistical Analysis

Power analyses were conducted to determine sample size required for each experiment based on an α of 0.05 for all planned comparisons and the expected standard error of measurement for each endpoint. For neurochemical endpoints, a sample size of 8 per group yields a power of 0.85 to detect a 15% difference between saline and MPTP treatment groups. For protein expression endpoints, a sample size of 10 per group yields a power of 0.80 to detect a 23% difference between saline and MPTP treatment groups. For cell count endpoints, a sample size of 4 per group yields a power of 0.94 to detect a 15% difference between saline and MPTP groups. The experimenter was blind to all experimental conditions during data collection and analysis.

One-way analysis of variance (ANOVA) tests were used to detect statistical significance between two or more groups with a single independent variable. Two-way ANOVA was used to detect statistical significance between two or more groups when there were two independent variables in the study. A *p value* of less than or equal to 0.05 was considered statistically significant. If the ANOVA revealed an interaction of statistical significance, post-hoc analysis was followed by between group comparisons using Tukey's test.

Chapter 3. Characterization of the differential susceptibility of TIDA and NSDA neurons to single-acute MPTP exposure.

Introduction

PD is a progressive neurodegenerative disorder characterized by motor abnormalities, which are primarily due to severe degeneration of NSDA neurons, and corresponding loss of DA neurotransmission in the ST (Schenkman, Wei Zhu, Cutson, & Whetten-Goldstein, 2001; Wermuth, Stenager, Stenager, & Boldsen, 2009). Synthesis and transmission of DA, one defining feature of NSDA neurons, has been intensively studied and proposed to contribute to the neurodegenerative process through the generation of reactive intermediates during the metabolism of cytoplasmic DA (Lotharius, Dugan, & O'Malley, 1999; Lotharius & O'Malley, 2000). However, separate DA neuronal populations with similar neurotransmitter synthetic and metabolic pathways, including hypothalamic TIDA neurons, do not degenerate in the PD brain, suggesting other deleterious or protective factors may be involved in determining the fate of DA neurons in PD (Braak et al., 2003; Langston & Forno, 1978). Beyond differences in DA reuptake mechanisms, the molecular machinery for synthesis, vesicular storage, release, and metabolism of DA are otherwise virtually identical between TIDA and NSDA neurons. As such, pathological stresses that theoretically disrupt DA homeostasis should produce similar deleterious effects in both TIDA and NSDA neuronal systems.

The MPTP neurotoxicant-based animal model produces a predictable injury and degeneration of NSDA nerve terminals and cell bodies, and efficiently recapitulates many of the molecular pathological features of PD, including oxidative stress, mitochondrial dysfunction, impairment of proteasome function, activation of programmed cell death, and neuroinflammation

(Burke et al., 2003; Chan et al., 1991; Dauer & Przedborski, 2003; Di Monte et al., 1986; Fornai et al., 2005; Jackson-Lewis & Przedborski, 2007; Johannessen, Adams, Schuller, Bacon, & Markey, 1986; Nicklas et al., 1987; Smith & Bennett, 1997; Zang & Misra, 1993; Zeng et al., 2006), Although there are noteworthy shortcomings for this and all current animal models of PD, the fact that NSDA neurons are severely damaged, while TIDA neurons are resistant to acute doses of MPTP, make this a reasonable model for studying differences between these DA neuronal populations (Behrouz et al., 2007; Melamed et al., 1985; Mogi et al., 1988; Sundström, Fredriksson, & Archer, 1990; Willis & Donnan, 1987).

The initial responses of TIDA and NSDA neurons to single systemic injection of MPTP are very similar, with both neuronal populations losing axon terminal DA stores by 4 h post treatment. The difference between these neuronal populations becomes evident by 8 h post-MPTP, when TIDA neurons begin recovering from DA loss eventually reaching full convalescence by 16 h. In contrast, NSDA neuronal DA stores remain depleted at 16 h and show evidence of apoptosis by 72 h post-MPTP (Behrouz et al., 2007; Lad, Fornstedt, Clark, & Carlsson, 2011; Perry et al., 1985). The narrow window of time during which resistant TIDA neurons recover and susceptible NSDA neurons remain damaged allows for examination of intrinsic, cell autonomous mechanisms, which may mediate their differential responses. To this end it is known that TIDA neuronal recovery from MPTP is protein synthesis dependent and associated with increases in levels of UCH-L1 and parkin mRNA (Benskey et al., 2012). However, it is unknown whether these increases in mRNA are actually translated into protein that could mediate the recovery of TIDA neurons. The studies presented here test the hypothesis that TIDA neurons are resistant, while NSDA neurons are susceptible, to acute MPTP-induced decreases in axon terminal DA phenotypic markers, and that this differential susceptibility is

associated with the ability to increase the expression of neuroprotective proteins. In order to test this hypothesis animals were administered a single dose of MPTP (20mg/Kg; s.c.) or saline vehicle (10ml/Kg; s.c.) and were sacrificed at 4, 8, 16 or 24 h post-MPTP. Changes in axon terminal DA and TH concentrations were measured in the ME and ST and changes in protein expression were measured in the ARC and SN.

Results

Time Course of the Neurochemical Responses of TIDA and NSDA Neurons to a Single injection of MPTP

Figure 3-1 depicts the time course of changes in axon terminal DA concentrations of TIDA and NSDA neurons to a single systemic injection of MPTP. ME and ST DA levels (reflecting DA stores in the terminal regions of TIDA and NSDA neurons, respectively) significantly decreased 4 h after MPTP treatment. ME DA levels recovered and were similar to controls by 24 h post-MPTP. In contrast, DA levels in the ST decreased further past the 4 h time point and remained low (~25% of controls) for up to 24 h post-MPTP.

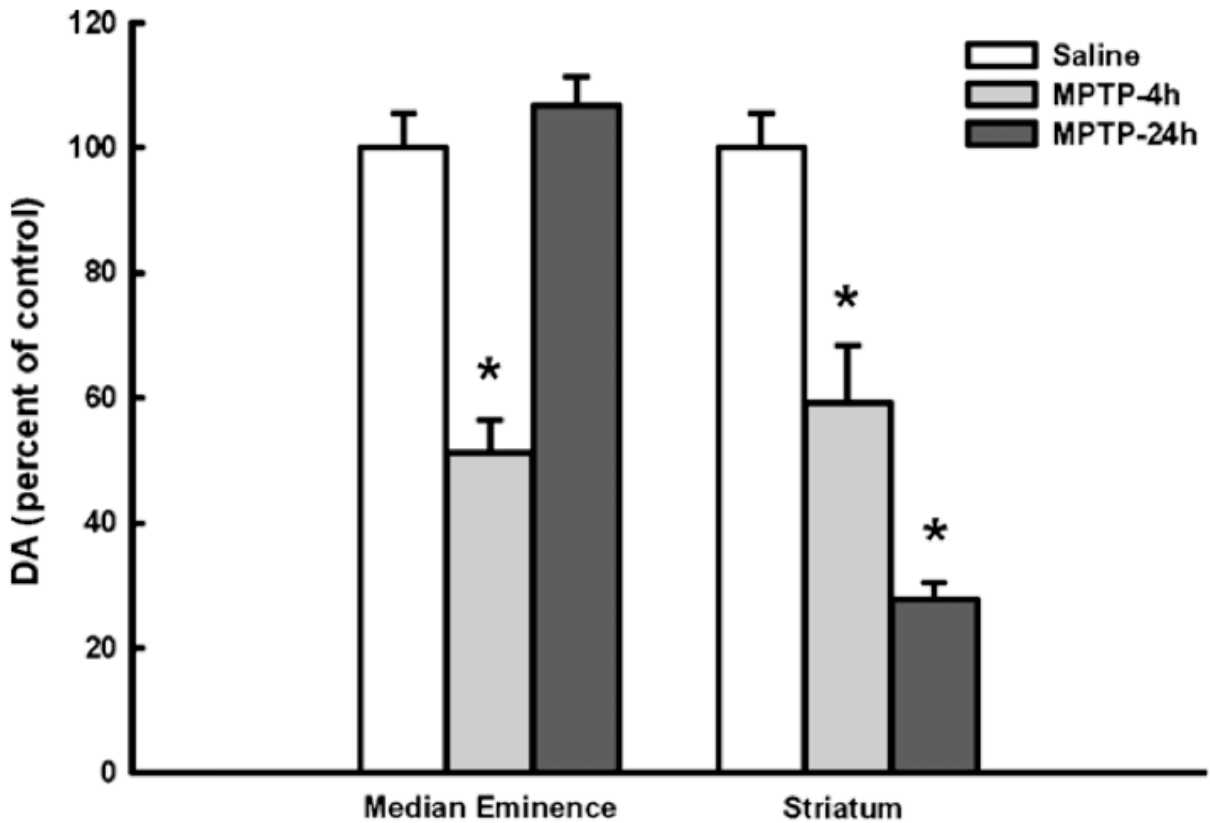


Figure 3-1. The time course of effects of a single injection of MPTP on DA concentrations in ME and ST. Male C57Bl/6J mice (n = 8/group) were treated with MPTP (20 mg/kg; s.c.) and killed by decapitation either 4 or 24 h later. Saline (10 ml/kg; s.c.) treated animals were killed 8 h post-injection and were used as zero time controls. DA levels are presented as percent of these saline-treated controls. Actual zero time control values (mean ng DA per mg protein) were 97 ± 7 and 102 ± 8 . Columns represent means of groups and vertical lines represent + 1 standard error of the mean. (*) Represent values for MPTP-treated mice that were significantly different ($p < 0.05$) from those of saline-treated zero time controls.

Time course of TH protein expression following a single injection of MPTP

Given that the ability of TIDA neurons to recover from MPTP is dependent on new protein synthesis, it is possible that there is a compensatory increase in TIDA expression of TH, which could mediate the recovery of ME DA via increased DA synthesis. Further, loss of TH in the soma and terminals of NSDA neurons is one of the earliest changes observed following MPTP toxicity and may serve as a predictive index of resistance to future toxicity (Ara et al., 1998; JACKSONLEWIS et al., 1995; Kastner et al., 1994; Kuhn, Aretha, & Geddes, 1999; Muroyama, Kobayashi, & Mitsumoto, 2011). In order to determine if changes in levels of TH are responsible for the recovery of TIDA neurons following MPTP, total TH protein was measured by Western blot over a 24 h period. Figure 3-2 shows that following single-acute MPTP treatment, total TH protein is unchanged in both the ME and the ST for 24 h post toxicant administration.

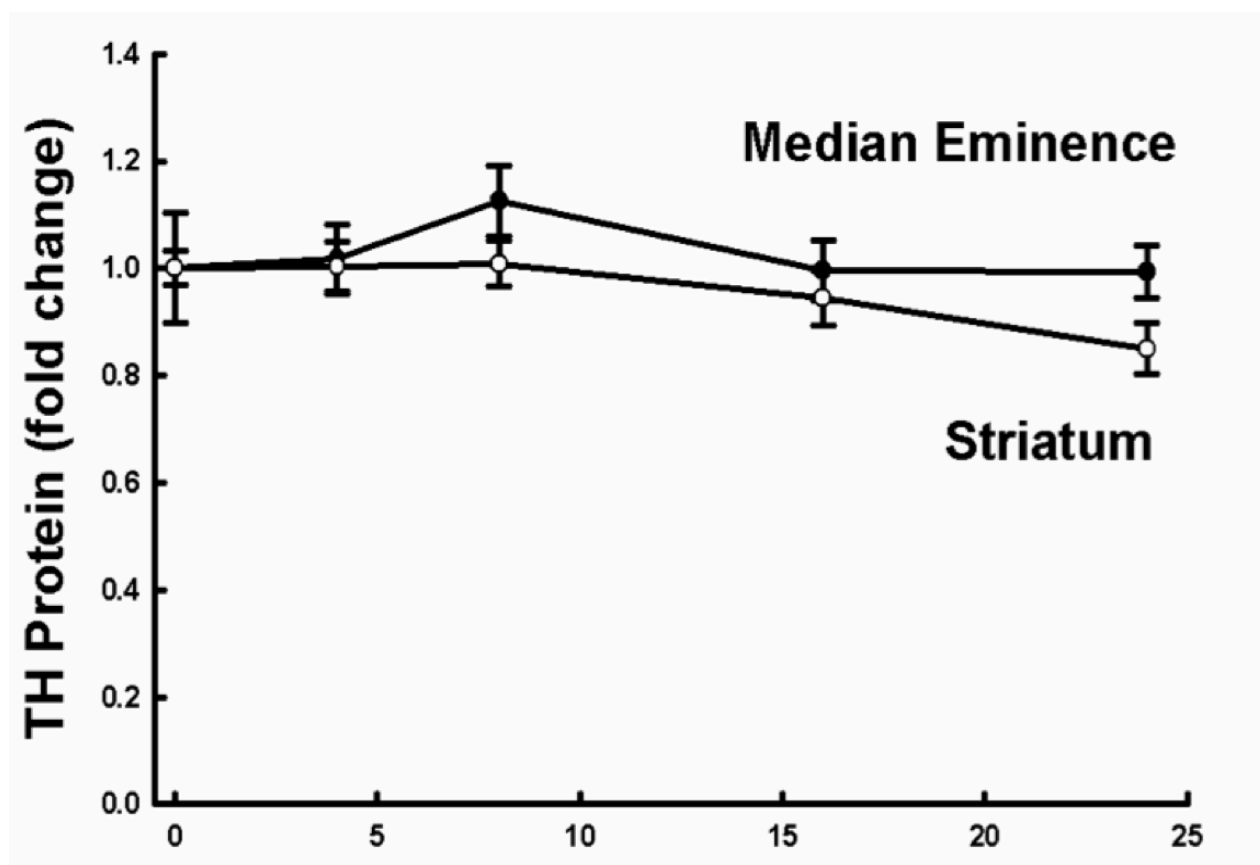
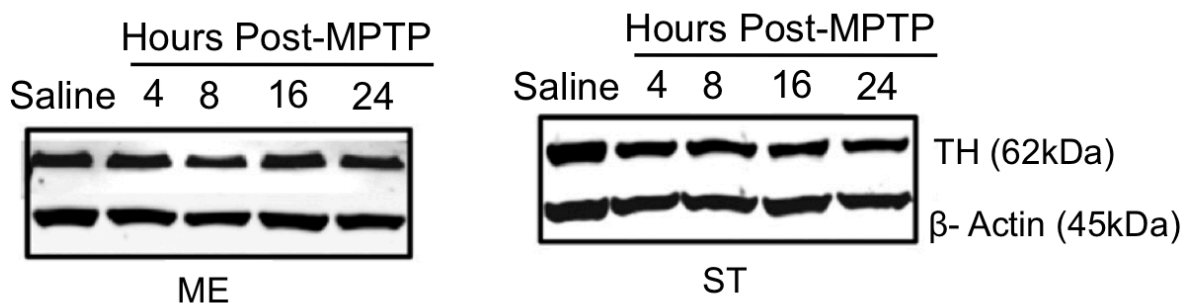


Figure 3-2. The time course of effects of a single injection of MPTP on total TH protein concentrations in the ME and ST. Male mice ($n = 8/\text{group}$) were treated with MPTP (20 mg/kg; s.c.) and killed by decapitation either 4, 8, 16 or 24 h later. Saline (10 ml/kg; s.c.) treated animals were killed 4 h post-injection and were used as zero time controls. The ME and ST were microdissected and protein was isolated from each region. Total TH concentrations were determined by Western blotting and normalized to β -actin. Total TH protein values are represented as mean fold change from saline \pm 1 standard error of the mean. Representative blots from all groups are shown above line graph.

Changes in UCH-L1 and Parkin Protein Expression in TIDA and NSDA Neurons Following a Single Injection of MPTP

It is currently known that the differential susceptibility of TIDA and NSDA neurons to MPTP toxicity is associated with increases in expression of the genes UCH-L1 and parkin (Benskey et al., 2012). However, it is not known if this message is translated into protein. In order to determine if UCH-L1 and parkin protein levels do increase in TIDA neurons following MPTP administration, UCH-L1 and parkin were measured by Western blot over a 24 h time course following toxicant administration. UCH-L1 protein levels increase in the ARC at the 16 h time point following MPTP administration (Figure 3-3). Conversely, UCH-L1 protein concentrations are decreased in the SN from 8-24 h post-MPTP administration (Figure 3-3). MPTP induced an increase in parkin protein in the ARC that was time-dependent, with progressively increasing protein levels at 6, 12, 24 and 36 h following MPTP (Figure 3-4). In contrast, parkin protein expression remains static in the SN for up to 12 h, followed by a decrease at 24 and 36 h following neurotoxicant injection (Figure 3-4).

Due to the known neuroprotective abilities of parkin, the role of parkin in the differential susceptibility of TIDA and NSDA neurons to MPTP toxicity is the main focus of this dissertation. As such changes in parkin expression were further characterized by measuring changes in parkin protein levels following incremental doses of MPTP. The MPTP-induced up-regulation of parkin protein expression in the ARC following MPTP was found to be dose-dependent (Figure 3-5), while there was a decrease in parkin protein expression in the SN at the higher doses (Figure 3-6).

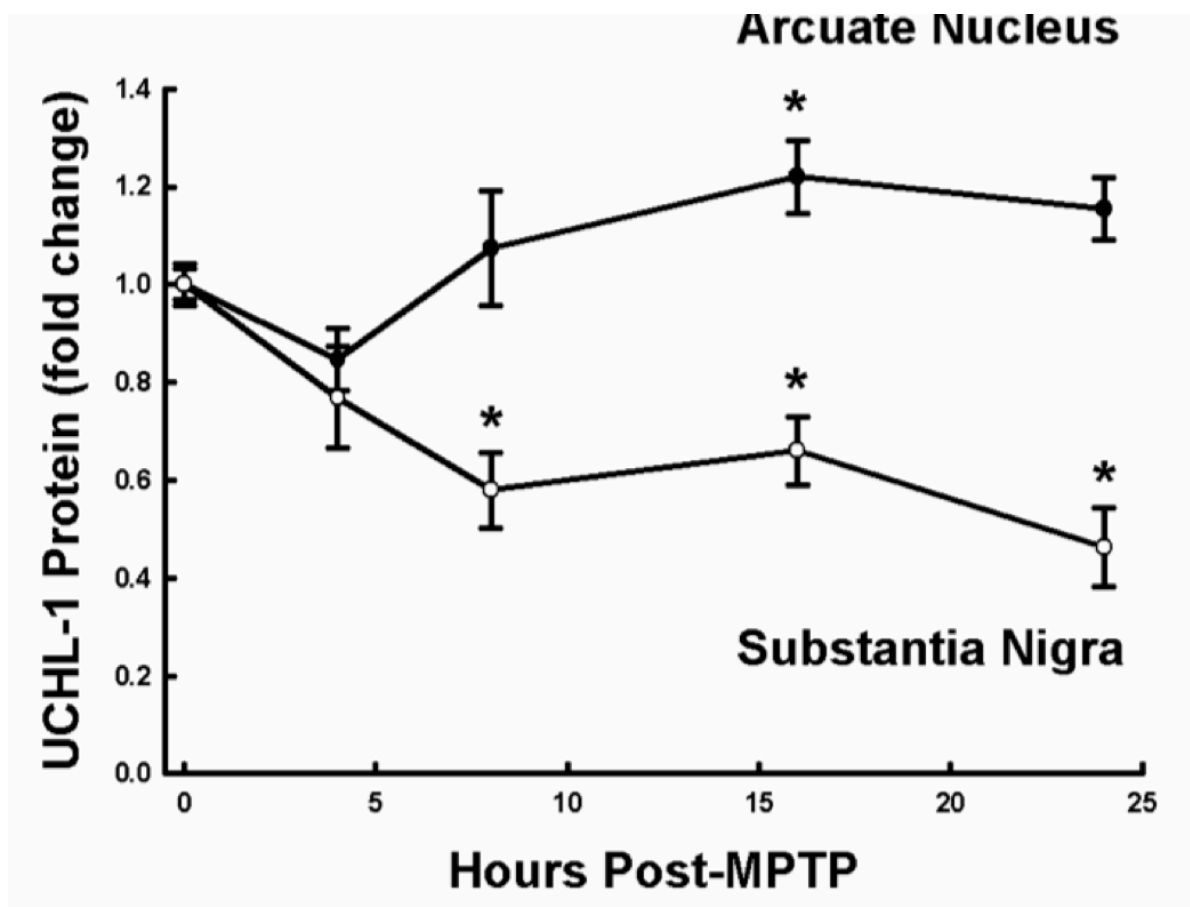
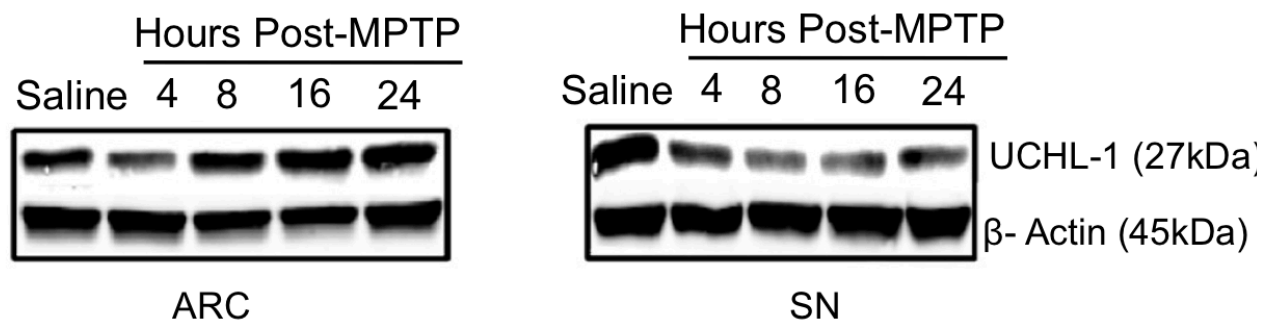


Figure 3-3. The time course of effects of a single injection of MPTP on UCH-L1 protein expression in the ARC and SN. Male mice ($n = 8/\text{group}$) were treated with MPTP (20 mg/kg; s.c.) and killed by decapitation either 4, 8, 16 or 24 h later. Saline (10 ml/kg; s.c.) treated animals were killed 4 h post-injection and were used as zero time controls. The area of the brain containing the ARC or SN, was microdissected and protein was isolated from each region. UCH-L1 levels were determined by Western blotting and normalized to β -actin. UCH-L1 protein values are represented as mean fold change from saline ± 1 standard error of the mean. Representative blots from all groups are shown above line graph. (*) Represent values for MPTP-treated mice that were significantly different ($p < 0.05$) from those of saline-treated zero time controls.

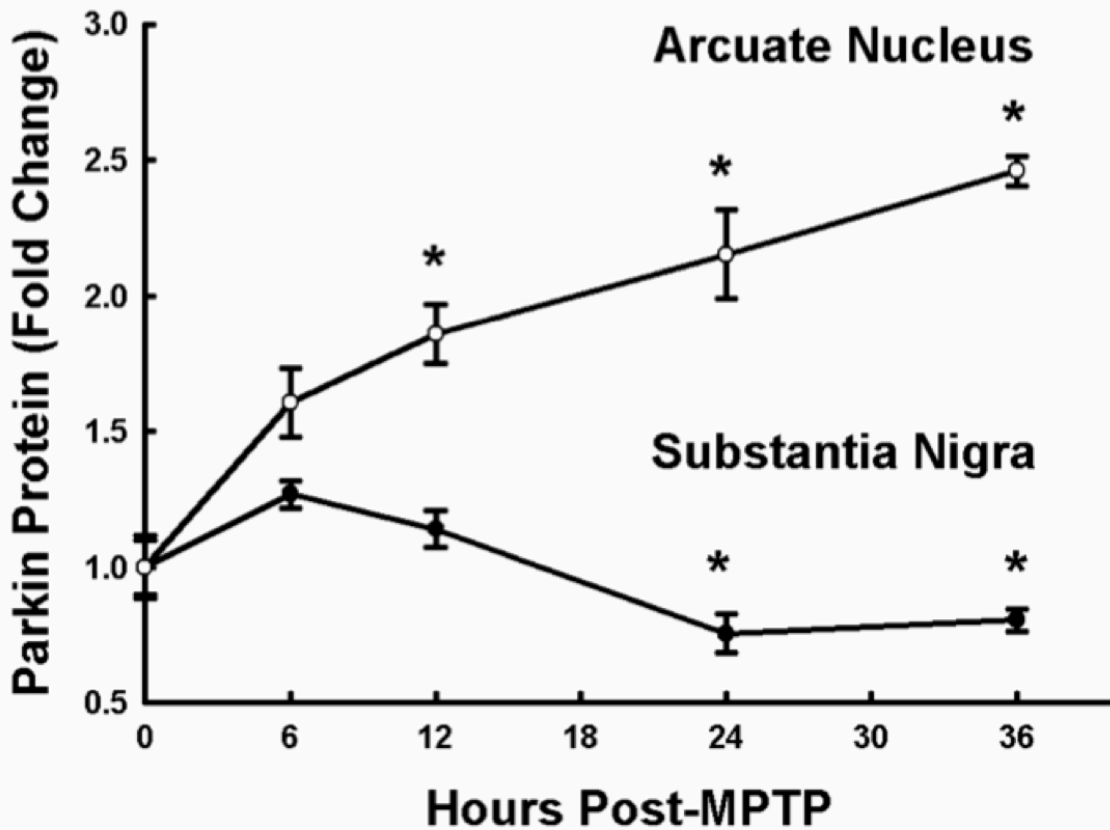
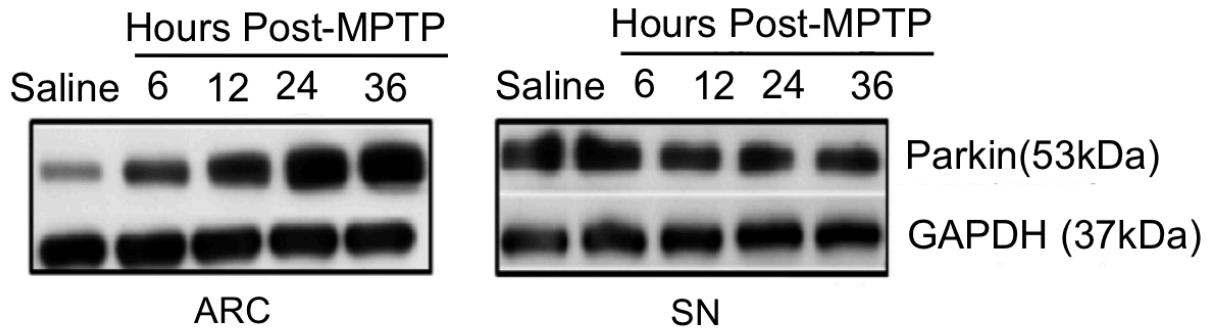


Figure 3-4. The time course of effects of a single injection of MPTP on parkin protein expression in the ARC and SN. Male mice ($n = 8/\text{group}$) were treated with MPTP (20 mg/kg; s.c.) and killed by decapitation either 6, 12, 24 or 36 h later. Saline (10 ml/kg; s.c.) treated animals were killed 12 h post-injection and were used as zero time controls. The area of the brain containing the ARC or SN, was microdissected and protein was isolated from each region. Parkin levels were determined by Western blotting and normalized to GAPDH. Parkin protein values are represented as mean fold change from saline \pm 1 standard error of the mean. Representative blots from all groups are shown above line graph. (*) Represent values for MPTP-treated mice that were significantly different ($p < 0.05$) from those of saline-treated zero time controls.

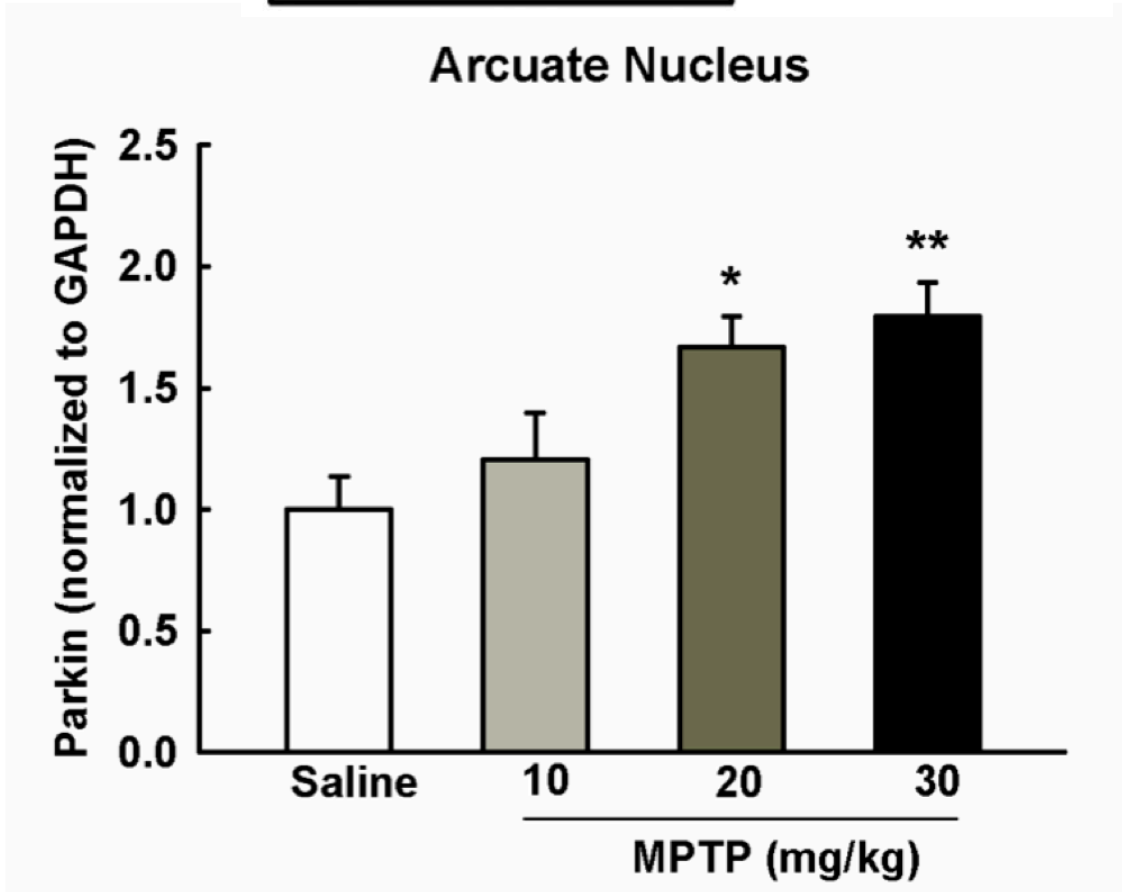
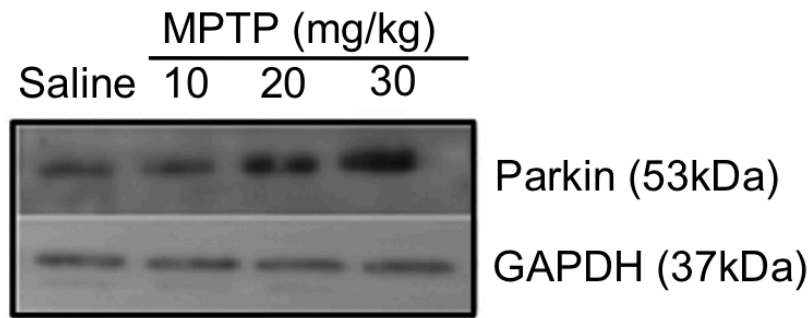


Figure 3-5. Dose–response changes in parkin expression in the ARC. Male C57Bl/6J mice were injected with either saline or MPTP (10, 20 or 30 mg/kg; s.c.) and killed 12 h later. The area of brain containing the ARC was microdissected and protein was isolated from each region. Parkin protein concentrations were determined by Western blotting and normalized to GAPDH. Columns represent means of groups and vertical bars represent + 1 standard error of the mean (n = 8/group). Representative blots from all groups are shown above histograms. (*) Indicates values significantly different from saline control, (**) indicates values significantly different from saline and 10 mg/kg MPTP-treated group. Corresponding ST DA concentrations were 205 ± 11 , 159 ± 14 , 137 ± 17 and 72 ± 11 ng/mg protein following saline or 10, 20 or 30 mg/kg MPTP, respectively.

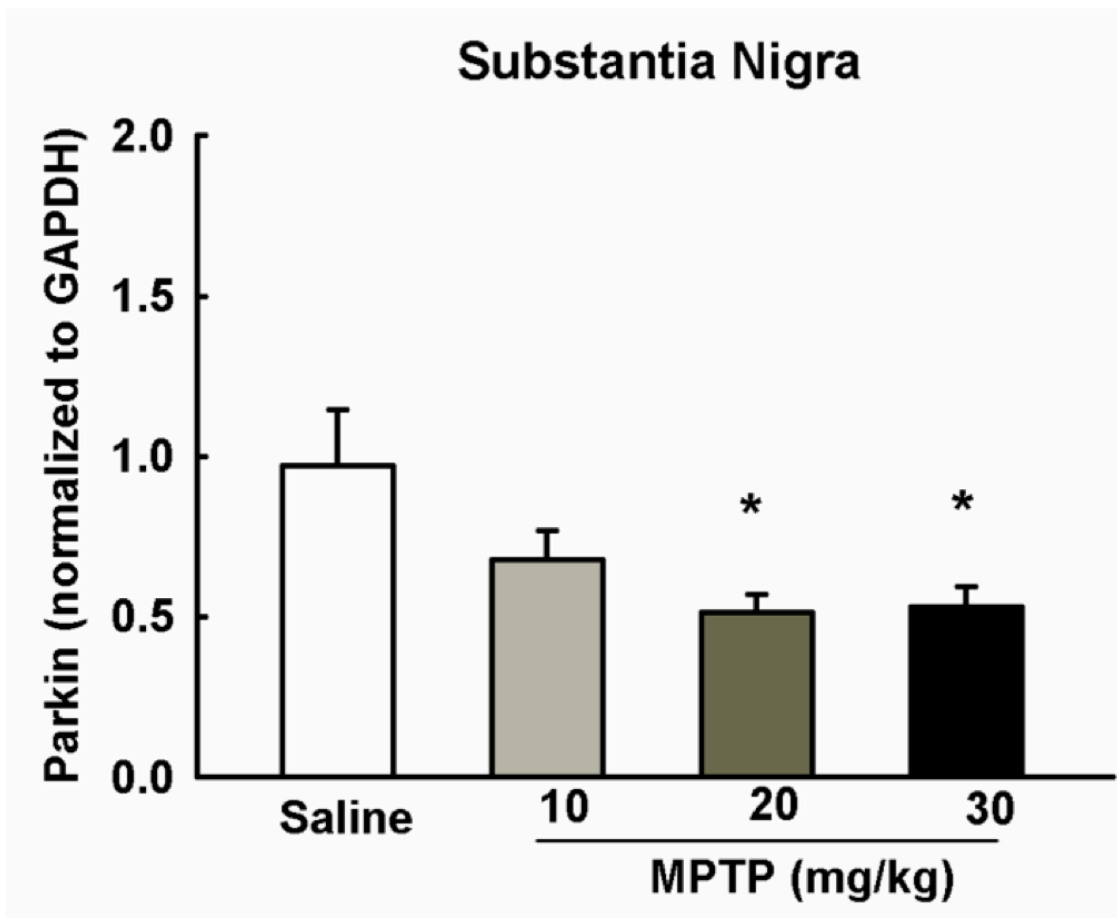
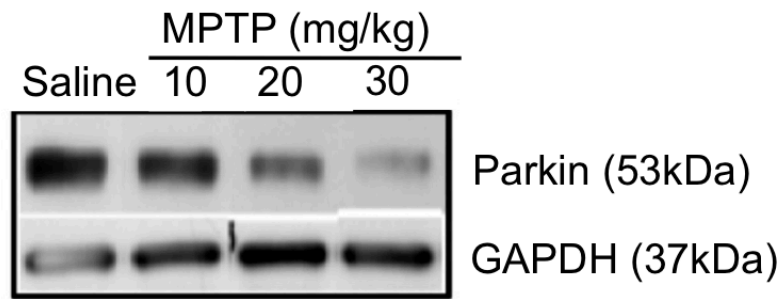


Figure 3-6. Dose–response changes in parkin expression in the SN. Male C57Bl/6J mice were injected with either saline or MPTP (10, 20 or 30 mg/kg; s.c.) and killed 12 h later. The area of brain containing the SN was microdissected and protein was isolated from each region. Parkin protein concentrations were determined by Western blotting and normalized to GAPDH. Columns represent means of groups and vertical bars represent + 1 standard error of the mean (n = 8/group). Representative blots from all groups are shown above histograms. (*) Indicates values significantly different from saline control. Corresponding ST DA concentrations were 205 ± 11 , 159 ± 14 , 137 ± 17 and 72 ± 11 ng/mg protein following saline or 10, 20 or 30 mg/kg MPTP, respectively.

Discussion

The ability of DA neurons to recover from toxic damage may be important in treatment of PD progression, especially in early stages, since there is likely a population of neurons that are injured but not yet doomed, similar to DA neurons following an acute dose of MPTP. The experiments presented herein examine how TIDA neurons, which survive in PD, differ from the highly susceptible NSDA neurons following single-acute injury with the neurotoxicant MPTP. TIDA neurons recover from single-acute MPTP-induced loss of terminal DA, while NSDA neurons exhibit a robust decrease in axon terminal DA concentrations that is sustained for up to 24 h. TIDA neuronal recovery is associated with an up-regulation of UCH-L1 and parkin protein following MPTP in TIDA (but not NSDA) neurons, implicating an involvement of these proteins in the recovery from acute neurotoxicant insult. Taken together, these data suggest that the ability of TIDA neurons to recover from an acute injury may be dependent, in part, on the ability of these neurons to increase expression of neuroprotective proteins.

Despite large sustained decreases in axon terminal DA concentrations of NSDA neurons following MPTP administration, axon terminal TH concentrations were less dramatic. Although there was a small decrease at the 24 h time point, this effect was not statistically significant. It was hypothesized that NSDA neurons would exhibit a decrease in axon terminal TH concentrations in addition to loss of terminal DA, yet the data presented here do not support this hypothesis. It must be noted that this result is in contrast to data reported in the literature (Hung & Lee, 1996; Hurley et al., 2003; Jackson Lewis et al., 1995; Kastner et al., 1994; Kuhn et al., 1999; Muroyama et al., 2011). The reason for this discrepancy is unknown, but could be due to experimental error or statistical artifact from multiple factorial levels. Accordingly, it will be necessary to repeat and confirm or disconfirm this result (as will be done in later chapters).

Furthermore, the use of early changes in DA phenotypic markers (such as axon terminal DA and TH concentrations) following a single-acute injury as an index of neuronal resistance to longer term or harsher toxicity must be vetted. That being said, the unique ability of TIDA neurons to endogenously recover from MPTP toxicity is a phenomenon that could be exploited in attempts to save damaged DA neurons in PD.

It seems the most critical events that determine acute MPTP toxicity occur between 4 and 16 h following injection, when TIDA neurons are able to up-regulate protein expression and completely recover from DA loss. In contrast, NSDA neurons are unable to up-regulate protein expression (at least for the proteins probed) and demonstrate continued and sustained DA loss. TIDA axons terminate in the ME, which is a circumventricular region where the blood brain barrier is relatively porous, potentially creating a micro-environment of increased toxicant exposure. In this context, it is possible that TIDA neurons have evolved the ability to rapidly up-regulate proteins that promote survival in the face of exposure to hazardous molecules that produce initial acute injury. Indeed, previous reports indicate that blockade of protein synthesis between 4 and 10 h following MPTP significantly impairs the ability of TIDA neurons to recover from DA loss by 16 h after toxicant treatment without affecting DA loss in NSDA neurons (Benskey et al., 2012).

Given the recovery of TIDA axon terminal DA stores is observed as early as 8 h after MPTP administration, it is likely that mechanisms which allow for this recovery must be readily available, either due to differential basal expression or inducible expression in response to cellular stress. Previously, basal mRNA expression levels of several candidate genes including parkin, UCH-L1, pink1, DJ-1, α -synuclein and Lrrk2 were shown to be similar in ARC and SN of control animals. However, mRNA levels of both parkin and UCH-L1 increase in ARC (but

not in the SN) 8 h following MPTP, suggesting their possible involvement in restoration of TIDA neuronal integrity following an initial injury (Benskey et al., 2012). Despite the correlation between MPTP-induced transcription of UCH-L1 and parkin and TIDA recovery, it was unknown whether this mRNA was translated into protein that could possibly mediate the resistance of TIDA neurons from MPTP.

The data herein demonstrates an increase in UCH-L1 and parkin protein expression in the ARC following MPTP. The time course of parkin protein expression following MPTP temporally parallels the recovery from DA loss in TIDA axon terminals. In contrast, both UCH-L1 and parkin protein expression is initially unaltered in NSDA neurons followed by a decrease, a pattern which correlates with further DA loss and notable absence of recovery of DA integrity in axon terminals of NSDA neurons. While these observations are drawn from a small subset of candidate proteins involved in PD, they are consistent with the hypothesis that induced expression (and not basal expression) is the key process underlying the differential response of TIDA and NSDA neurons to acute MPTP exposure. It is plausible, therefore, that the differential susceptibility of NSDA and TIDA neurons is a reflection of the intrinsic ability of TIDA neurons to selectively up-regulate protective protein expression, rather than NSDA neurons producing deleterious or maladaptive proteins.

Although increases in parkin and UCH-L1 proteins were observed in the ARC following MPTP exposure, these data do not necessarily mean these increases were occurring specifically within TIDA neurons. It is possible that other cell types within this region, both neuronal and non-neuronal, could be contributing to the observed up-regulation of protein synthesis. That said, previous experiments have shown that increases in parkin mRNA occur within TIDA neurons (Benskey et al., 2012). However, this does not exclude the possibility that other cell types may be

contributing to TIDA recovery or NSDA susceptibility, through the differential regulation of neuroprotective proteins (such as parkin), trophic support, inflammation or reactive gliosis (Hung & Lee, 1996; Hurley et al., 2003; Schwartz, Sheng, Mitsuo, Shirabe, & Nishiyama, 1993; Teismann & Ferger, 2001). The compensatory up-regulation of UCH-L1 and parkin protein within the ARC in response to acute neurotoxicant exposure is quite likely a component of a broad, yet region specific response to injury.

It is plausible that the differential susceptibility of NSDA and TIDA neurons is a reflection of the intrinsic, neuron specific ability of TIDA neurons to selectively up-regulate protective protein expression. The observations that the same proteins that are up-regulated in toxicant and PD resistant TIDA neurons are also decreased in susceptible NSDA neurons are consistent with this hypothesis. Of course, the data presented in this chapter are largely correlative regarding the individual proteins involved (e.g., parkin and UCHL-1) and require further investigation to validate a causal link between differential expression of specific proteins and recovery from toxicant-induced neuronal injury.

The data from these experiments suggest a novel, central DA neuronal system that physiologically increases expression of UCH-L1 and parkin as a mechanism to facilitate the prompt recovery from toxicant-induced damage. The molecular mechanisms regulating the differential expression of these proteins following acute injury in TIDA versus NSDA neurons are not known and is a compelling focus for future investigation. However, prior to this it will be necessary to determine if parkin and/or UCH-L1 are indeed mediating this recovery or if TIDA recover is simply due to extrinsic factors such as reduced toxicant exposure. The role of extrinsic factors in TIDA recovery will be the focus of Chapter 4.

Conclusions

The unique ability of TIDA neurons to recover from an acute toxicant-induced injury is dependent on induced synthesis of new proteins. Protein levels of both UCH-L1 and parkin increase following toxicant administrations in MPTP resistant TIDA neurons and decrease in MPTP susceptible NSDA neurons. Further, parkin protein increases in TIDA neurons with incremental doses of MPTP and decreases in NSDA neurons with higher doses of MPTP. The time- and dose-dependent correlation between parkin and the susceptibility of DA neurons to MPTP suggests that endogenous parkin may represent a plausible, cell autonomous candidate mediator of DA neuronal recovery from injury. However, before it can be concluded that TIDA recovery from MPTP is mediated by intrinsic factors, the contribution of extrinsic factors to the observed recovery must be examined.

Chapter 4. The role of toxicant exposure, prolactin activation and DA synthesis in the differential susceptibility of TIDA and NSDA neurons to single-acute MPTP toxicity.

Introduction

The ability of TIDA neurons to recover from acute MPTP toxicity is a novel phenomenon that could potentially be exploited in order to rescue NSDA neurons that have been damaged in PD but have not died. The finding that the ability of TIDA neurons to recover from MPTP toxicity is protein synthesis dependent and associated with compensatory increases in parkin and UCH-L1 expression suggests that these proteins may be involved in the recovery process. However, it is also possible that this recovery may simply be due to extrinsic factors, i.e. factors that are unrelated to the observed increase in protein expression. This chapter will explore the hypothesis that; toxicant bioavailability, DA synthesis or prolactin feedback activation cannot account for the differential susceptibility of TIDA and NSDA neurons to acute MPTP toxicity. The following introductory sections will give more background, rationale and methods for testing the individual components of this hypothesis.

Decreased Toxicant Exposure in the Recovery of TIDA Neurons from MPTP

It has long been suspected that the ability of TIDA neurons to recover from MPTP toxicity was mediated by decreased toxicant exposure within these neurons. As noted previously, the primary toxic metabolite of MPTP, MPP^+ , is a charged molecule that requires transporter facilitation for entry into the cell. Specifically, MPP^+ shows very high affinity for DAT, which explains the selective degeneration of DA neurons following MPTP administration (Javitch et al., 1985). However, the presence of DAT in the ME has remained highly

controversial. Accordingly, decreased DAT expression and a corresponding decreased uptake of MPP^+ into TIDA terminals could potentially explain the ability of these neurons to recover from MPTP toxicity.

Although the presence of DAT in TIDA neurons remains controversial there is evidence showing the presence of functional DAT in the ME. Indirect evidence supporting the presence of DAT in TIDA neurons was found when ME homogenates and synaptosomes were able to accumulate [^3H]DA (Cuello, Horn, Mackay, & Iversen, 1973; Demarest & Moore, 1979b; George & Van Loon, 1982). In addition, mazindol (a specific DAT blocker) as well as cocaine (a non-specific amine transporter blocker) are both able to decrease the amount of PRL mRNA in the anterior lobe (Demaria et al., 2000). Finally, IHC visualization of DAT within the ME has provided direct evidence for the expression of DAT by TIDA neurons (Revy et al., 1996). However, it should be noted that although the presence of DAT has been confirmed in TIDA neurons, DAT expressed by these neurons has a lower affinity for its substrate, showing a K_m value 2-3 fold higher than DAT in NSDA neurons (Cuello et al., 1973; Demarest & Moore, 1979a). Thus, it is possible that TIDA recovery from MPTP is mediated by decreased MPP^+ accumulation within these neurons. In order to test this hypothesis, animals will be treated with a single injection of either saline or MPTP, and MPP^+ concentrations will be measured over a 24 h time course within the terminals of TIDA and NSDA neurons

PRL Activation in the Recovery of TIDA Neurons from MPTP

An alternative mechanism that could explain the ability of TIDA neurons to recover from MPTP toxicity is through the activating effects of PRL on TIDA neurons. The main

physiological role of TIDA neurons is the regulation of PRL secretion from the anterior pituitary. DA released from the terminals of TIDA neurons will travel down the hypophysial portal circulation to the anterior pituitary where it will activate inhibitory D₂ DA receptors upon lactotrophs, thereby inhibiting PRL secretion (Durham, Eaton, Moore, & Lookingland, 1997). In turn, PRL released from the anterior pituitary will feed back to directly activate PRL receptors on TIDA neurons in order to increase DA synthesis, release and turnover from TIDA terminals (Di Carlo, Muccioli, Lando, & Bellussi, 1985; Hokfelt & Fuxe, 1972).

PRL induced activation of TIDA neurons occurs in two different phases. The first is the rapid “tonic” activation, in which TIDA neurons are activated in response to acute, minute to minute changes in circulating PRL. The second, termed the delayed or “inductive” component, is responsive to long-term elevations in circulating PRL. The latter of these components is protein synthesis dependent and can be blocked through the application of cyclohexamide (Demarest, Riegler, & Moore, 1986). It is through this elegant architecture of positive feedback to inhibitory afferents that lactotrophs control PRL concentrations.

PRL induced activation of TIDA neurons could explain the recovery of TIDA neurons from MPTP toxicity. Following administration of MPTP, TIDA axon terminal DA is found to decrease by 4 h post injection (Behrouz et al., 2007). This decrease in available axon terminal DA could potentially remove the tonic DA inhibition of PRL secretion from the anterior pituitary. Consequently, PRL secretion would increase, causing a subsequent activation of TIDA neurons and the recovery of TIDA axon terminal DA observed following MPTP.

Several lines of evidence support this hypothesis. First, due to the rapid recovery of TIDA neurons, the impetus for TIDA neuronal recovery would necessarily have to be working through a very fast acting mechanism. To this end, decreases in TIDA DA release have been shown to

cause an immediate increase in PRL levels (R. Y. R. Moore & Bloom, 1978). This fast acting increase in PRL could then mediate transient TIDA activation immediately through the rapid tonic mechanism, followed by continuing activation working through the induction component of PRL mediated TIDA activation. Supporting this view, TIDA recovery is blocked by protein synthesis inhibitors (Benskey et al., 2012), as is the induction component of PRL mediated TIDA activation (Demarest et al., 1986). Thus, it is feasible that an MPTP induced loss of DA stores causes an increase in circulating PRL levels, which in turn results in the activation of TIDA neurons, ultimately leading to recovery of these neurons.

To determine if TIDA recovery from MPTP is mediated by PRL, the ability of TIDA neurons to recover from MPTP toxicity will be probed in the presence of pharmacologically inhibited PRL secretion. The long acting DA D₂ receptor agonist, bromocriptine, will be administered 4 h prior to MPTP in order to suppress any increases in PRL secretion. Following, ME DA concentrations will be assayed at 4 h (when ME DA is known to be depleted) and 24 h (when ME DA is known to have recovered) following MPTP.

DA Synthesis in the Recovery of TIDA Neurons from MPTP

In addition to being a potent mitochondrial complex I inhibitor, MPP⁺ also shows high affinity for VMAT, being packaged into synaptic vesicle and purging DA into the cytosol in the process (Y. Liu et al., 1992). As such, it is likely that the initial depletion of terminal DA concentrations in both TIDA and NSDA neurons at 4 h post-MPTP administration represents an MPP⁺ -induced purging of vesicular DA. Large increases in cytosolic DA, beyond being highly toxic, can inhibit TH activity through end product inhibition, impairing DA synthesis and the ability to refill synaptic vesicles. If this is the case, then the differential ability of TIDA and

NSDA neurons to recover from acute MPTP toxicity may simply reflect the differential ability of these neurons to either maintain or increase TH activity (and thus DA synthesis) following toxicant exposure.

In order to determine if increased DA synthesis is responsible for the ability of TIDA neurons to recover from MPTP toxicity, TH activity will be monitored over a 24 h time course following MPTP administration. Following MPTP administration, animals will be pretreated with the AADC inhibitor 3-hydroxybenzylhydrazine (NSD-1015), 30 min prior to sacrifice and DOPA accumulation in the terminals of TIDA and NSDA neurons will be used as an index of TH activity following MPTP administration. In addition, the concentrations of total TH protein will be measured (in animals not treated with NSD-1015) in the terminals of TIDA and NSDA neurons 24 h following MPTP administration as an additional index of TH integrity.

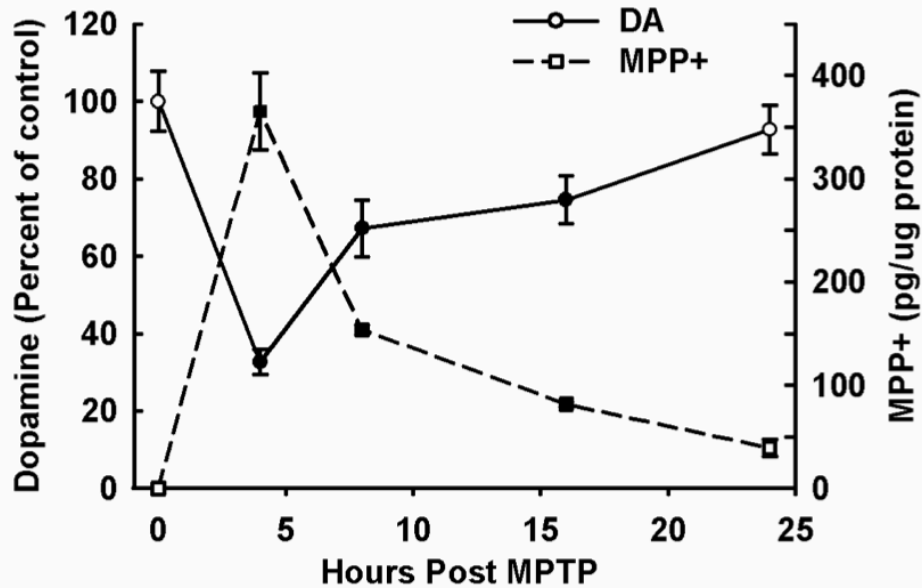
Results

Time Course of MPP⁺ Accumulation in the Median Eminence and Striatum Following Single-Acute MPTP Administration

TIDA neuronal recovery from a single injection of MPTP could be due to differential distribution and elimination of MPP⁺ in the ME and ST, thus MPP⁺ concentrations were measured in the axon terminal field regions of NSDA and TIDA neurons following MPTP treatment. Compared to saline-treated animals, there is a significant accumulation of MPP⁺ in the ME by 4 h post-MPTP administration (Figure 4-1, Panel A), which is slowly eliminated over the next 24 h post-injection with an approximate half-life of 5.9 h (Table 4-1). The accumulation and elimination of MPP⁺ in the axon terminal regions of TIDA neurons (ME) mirrored the

changes in DA concentrations within this region, i.e., ME DA concentrations reaches its lowest point at 4 h post-MPTP and recovers to pretreatment levels while MPP⁺ is concurrently eliminated. MPP⁺ concentrations in the ST reached maximal accumulation at 4 h post-MPTP (Figure 4-1, Panel B), followed by a relatively rapid elimination of the toxicant over the next 20 h with an approximate half-life of 1.8 h (Table 4-1). In contrast to ME DA, ST DA remains depleted for up to 24h post MPTP without any appreciable recovery. The absolute maximal concentrations of MPP⁺ were four times higher in the ME compared to the ST, with MPP⁺ concentrations of 365 ± 37 pg/mg in the ME and 78 ± 9 pg/mg in the ST. Elimination constants were calculated for MPP⁺ in the ME and ST (Table 4-1). MPP⁺ has a significantly higher elimination constant in the ST (0.38 ± 0.02) than in the ME (0.11 ± 0.01).

A)



B)

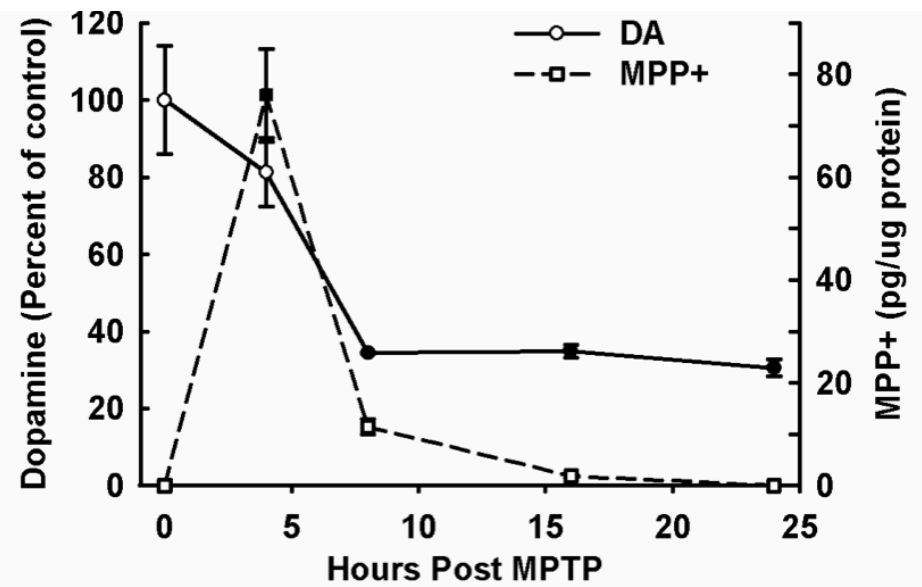


Figure 4-1. Time course of the effects of a single injection of MPTP on DA and MPP⁺ concentrations in the ME (Panel A) and ST (Panel B). Mice were injected with MPTP (20 mg/kg; s.c.) and sacrificed 4, 8, 16 or 24 h later. Zero time control mice were injected with saline (10 ml/kg; s.c.) and sacrificed 4 h later. DA (solid lines) concentrations were calculated as a percent of control animals and are represented on the left Y-axis. Actual zero time control values (mean ng DA per mg protein) were 104 ± 5 for the ST and 220 ± 16 for the ME.

MPP⁺ (dashed line). MPP⁺ concentrations were calculated as pg/mg protein and are represented on the right Y-axis. Symbols represent means of groups ($n = 8/\text{group}$) and vertical bars indicate 1.0 SEM. Filled symbols represent values from MPTP-treated groups that are significantly different from vehicle-treated controls ($p < 0.05$).

	Half life (h)	Elimination constant (\pm SE)
ME	5.9	0.11 ± 0.01
ST	1.8	$0.38 \pm 0.02^*$

Table 4-1. Half-lives and elimination constants of MPP⁺ in the terminal regions of TIDA and NSDA neurons following a single injection of MPTP. Mice were injected with MPTP (20 mg/kg; s.c.) and sacrificed 4, 8, 16 or 24 h later. Zero time control mice were injected with saline (10 ml/kg; s.c.) and sacrificed 4 h later. Elimination constants were calculated by plotting the linear regression of the natural log of MPP⁺ concentrations from all time points and obtaining the slope. Half-lives were then calculated by dividing this value into the natural log of 2. Represents MPP⁺ elimination constants within the ST that were significantly different ($p < 0.05$) than those of the ME.

The Effects of Bromocriptine-induced Suppression of PRL Secretion on the Ability of TIDA Neurons to Recover from Single-Acute MPTP Exposure

In order to suppress any possible increases in plasma PRL concentrations following MPTP, the DA D₂ receptor agonist bromocriptine, was administered 4 h prior to toxicant exposure. Figure 4-2 shows that administration of bromocriptine significantly decreased levels of plasma PRL as compared to saline treated controls. However, MPTP itself was also found to suppress plasma PRL levels in the absence of bromocriptine. In addition, bromocriptine and MPTP decrease PRL concentrations in a synergistic manner at the 4 h time point. These results show that instead of increasing PRL secretion, MPTP actually results in a large decrease in plasma PRL levels. Accordingly, there was no difference in the ability of saline or bromocriptine treated animals to recover axon terminal DA concentrations by the 24 h time point following MPTP administration (Figure 4-3).

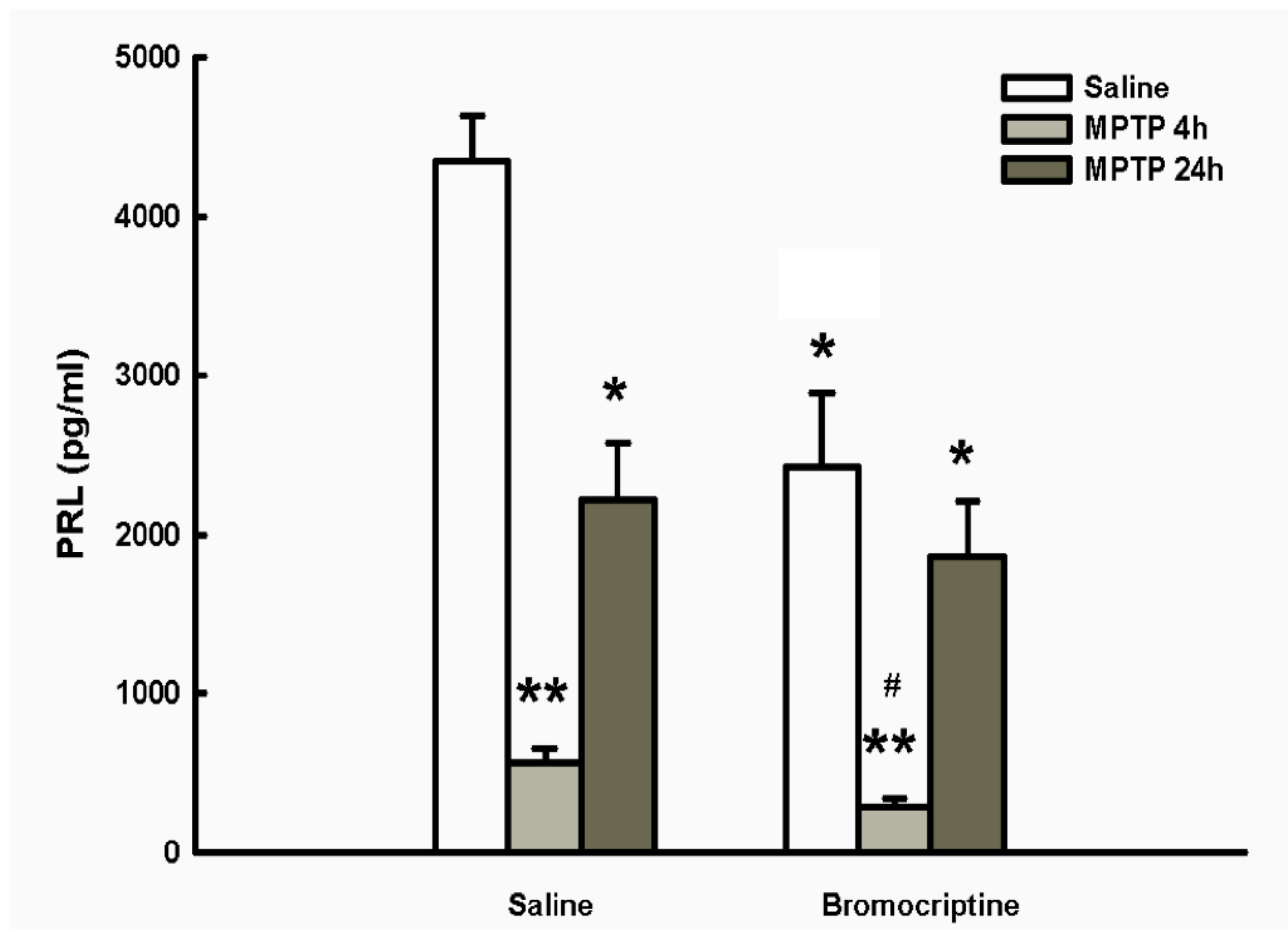


Figure 4-2. Effects of bromocriptine and MPTP on plasma PRL concentrations. Four h prior to toxicant administration mice were pre-treated with bromocriptine (3mg/kg; s.c.) or its vehicle (4% ethanol in saline; 10 ml/kg; s.c.). Following, mice were treated with saline vehicle (10ml/kg; s.c.) or MPTP (20 mg/kg; s.c.) and sacrificed 4 or 24 h later. Values represent mean PRL concentrations + 1.0 SEM. (*) Values that are significantly different from saline/saline treated control group. (**) Values that are significantly different than both saline and bromocriptine controls. (#) Values that are significantly different than 4 h saline/MPTP group ($p < 0.05$).

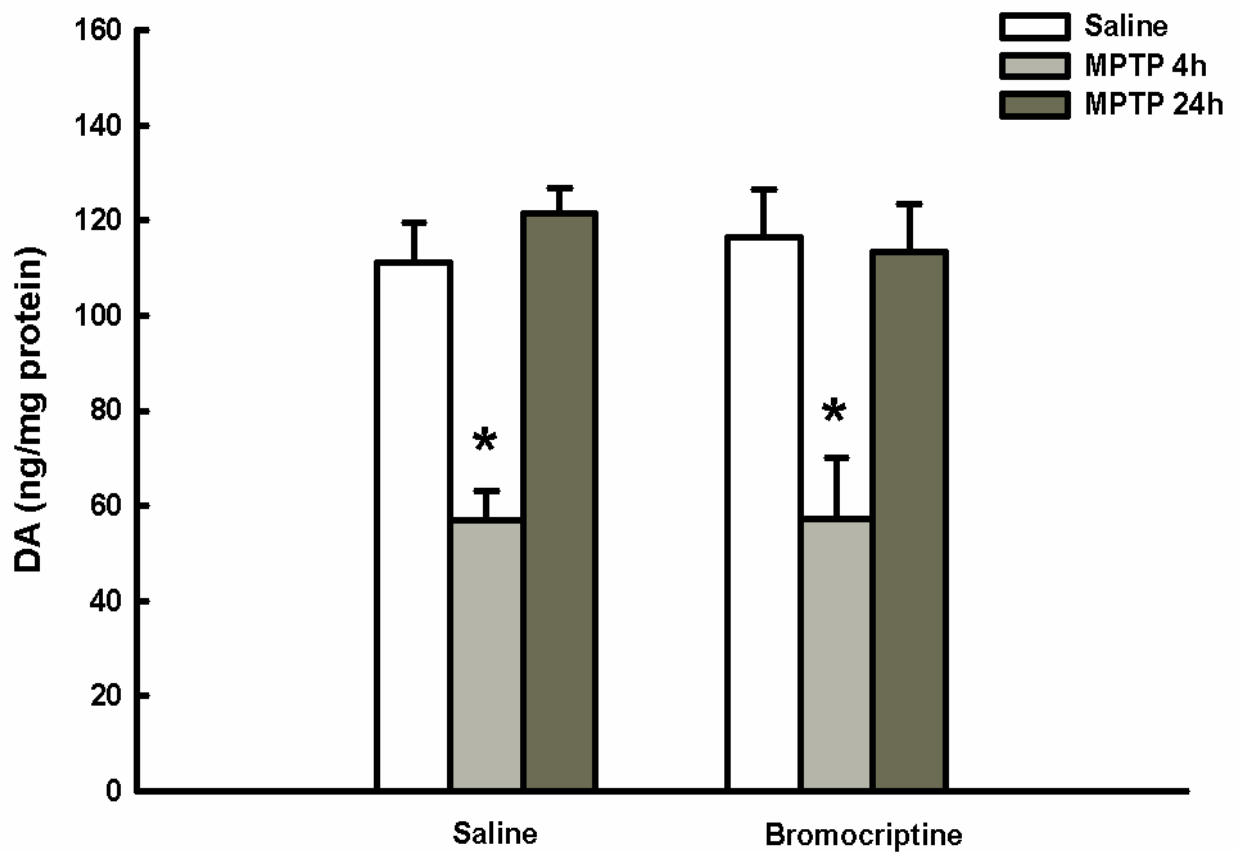


Figure 4-3. Effects of bromocriptine and MPTP on ME DA concentrations. Four h prior to toxicant administration mice were pre-treated with bromocriptine (3 mg/kg; s.c.) or its vehicle (4% ethanol in saline; 10 ml/kg; s.c.) or). Following, mice were treated with either MPTP (20 mg/kg; s.c.) and sacrificed 4 or 24 h later, or saline vehicle (10ml/kg; s.c.) and sacrificed 24 h later. Values represent mean DA concentrations + 1.0 SEM. (*) Values that are significantly different from saline/saline treated control group ($p < 0.05$).

The Role of DA Synthesis in the Differential Susceptibility of TIDA and NSDA Neurons to Single-Acute MPTP Toxicity

Differential activation of DA synthesis following MPTP administration may explain the differences in the ability of TIDA and NSDA neurons to recover axon terminal DA concentrations following MPTP. To determine if DA synthesis is involved in the differential susceptibility of TIDA and NSDA neurons, the AADC inhibitor NSD-1015 was administered 30 min prior to sacrifice and DOPA accumulation (an index of TH enzymatic activity) was measured in the ME and ST. Following treatment with MPTP, TH activity is significantly decreased at the 4 h time point compared to saline treated controls in both the ME and ST (Figure 4-4). TH activity remains decreased for up to 24 h post-MPTP in the ST. In contrast, TH activity partially recovers in the ME beginning at 8 h. Although TH activity remains low in the ME at later time points, this decrease is no longer statistically different than saline treated controls. Finally single-acute MPTP administration significantly decreased concentrations of TH protein in the ST, but not the ME, 24 h following toxicant exposure (Figure 4-5).

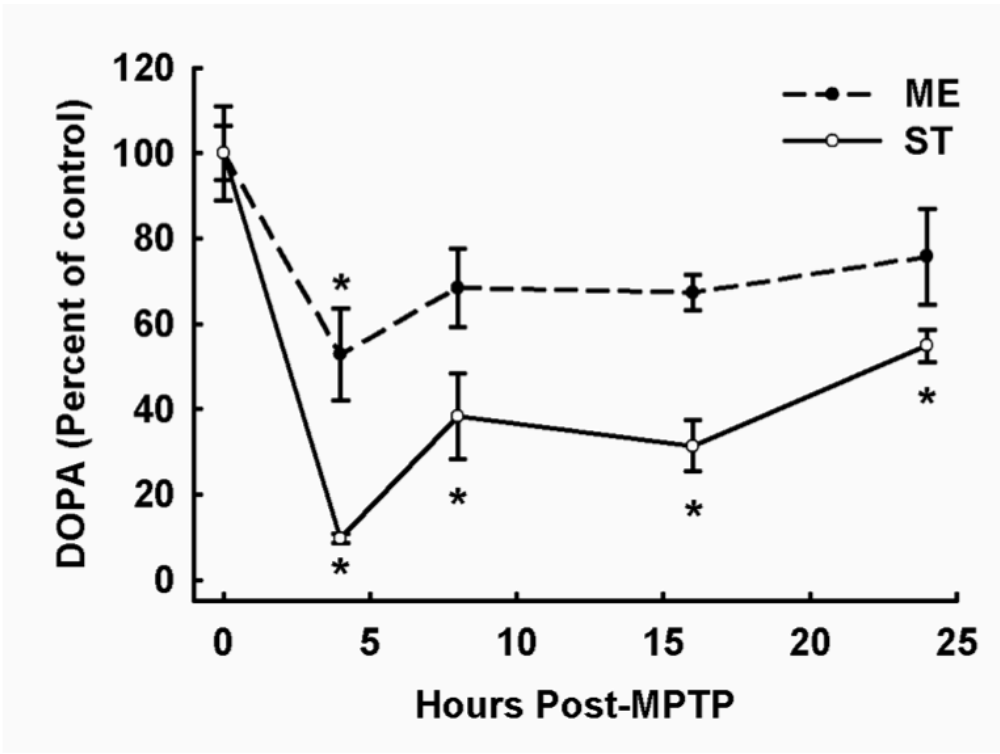


Figure 4-4. Effects of MPTP on DOPA accumulation in the ST and ME.

Male C57Bl/6J mice (n=8/group) were treated with MPTP (20 mg/kg; s.c.) and sacrificed either 4, 8, 16 or 24 h later. Zero time control mice were injected with saline (10 ml/kg; s.c.) and sacrificed 4 h later. All animals were treated with NSD-1015, 30 min prior to sacrifice. Data points represents means of groups expressed as percent control and vertical lines represent ± 1 SEM. Actual zero time control values (mean ng DOPA per mg protein) were 14.04 ± 2.66 in the ME and 21.87 ± 1.39 in the ST. (*) Represents values for MPTP-treated animals that were significantly different ($P < 0.05$) from those of saline-treated zero time controls.

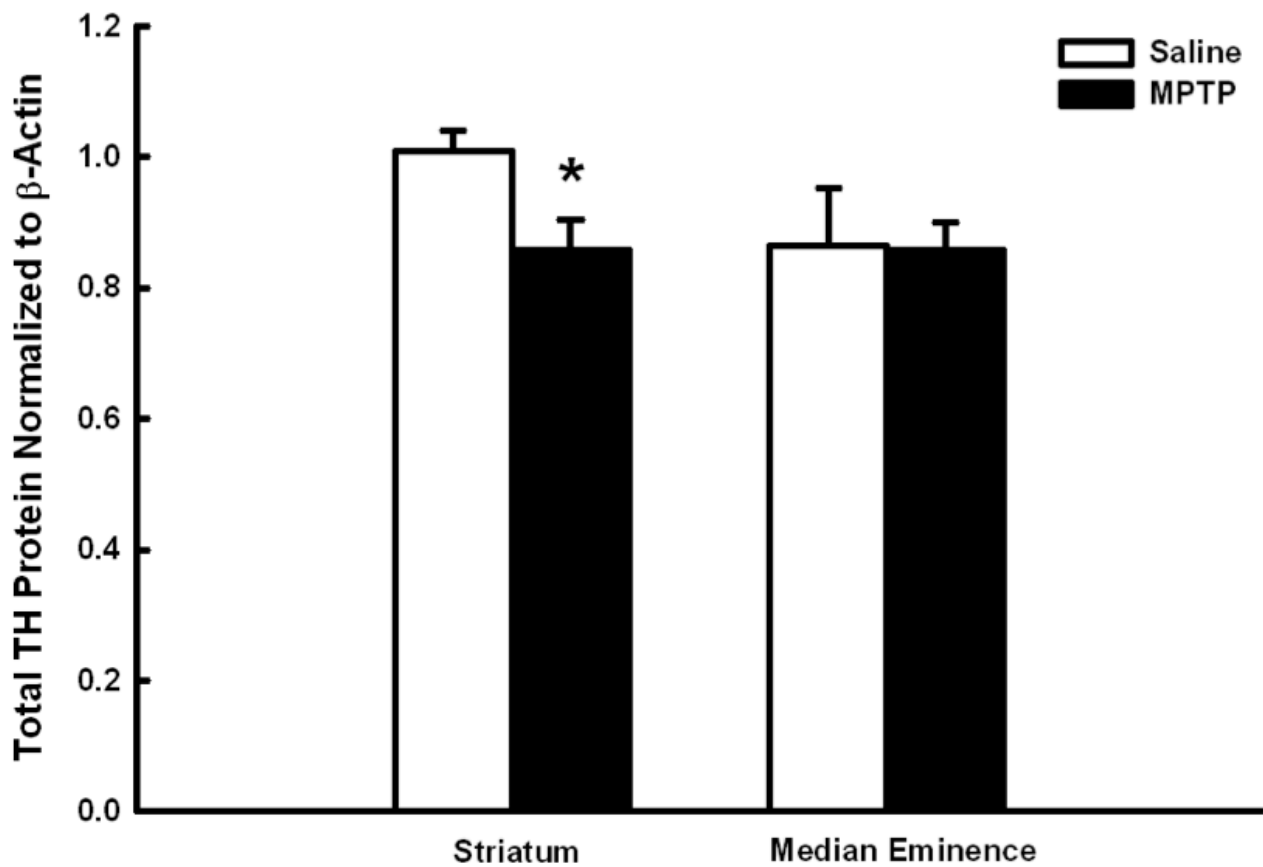


Figure 4-5. The effects of MPTP on total TH protein concentrations in the ST and ME. Male C57Bl/6J mice (n=8/group) were treated with either saline (10 ml/kg; s.c.) or MPTP (20 mg/kg; s.c.) and sacrificed 24 h later. Columns represent means of groups and vertical lines represent + 1 SEM. (*) Represents values for MPTP-treated animals that were significantly different ($P < 0.05$) from those of saline-treated controls

Discussion

The data presented in Chapter 3 of this dissertation are consistent with the hypothesis that TIDA neurons intrinsically up-regulate endogenous neuroprotective proteins in response to cellular stress. If this is the case, TIDA neurons represent a platform that could be used to exploit novel upstream and downstream mechanisms of parkin that could ultimately be used to rescue damaged DA neurons in PD. However, prior to exploring the role of parkin in the recovery of TIDA neurons, it is first necessary to investigate the most parsimonious explanations as to why TIDA neurons are able to recover from a single injection of MPTP whereas NSDA neurons cannot.

The data presented in this section shows that the recovery of TIDA neurons from MPTP toxicity is not due to extrinsic mechanisms, such as decreased toxicant exposure or the activating effects of PRL on TIDA neurons. However, the differential ability of TIDA and NSDA neurons to recover axon terminal DA concentrations following MPTP may be related to an intrinsic ability of TIDA neurons to recover TH activity and reconstitute DA synthesis in a more timely manner than NSDA neurons. The data presented herein are consistent with the idea that TIDA neuronal recovery from toxicant exposure is due to an intrinsic ability to restore cellular homeostasis following cytotoxicity.

Decreased Toxicant Exposure in the Recovery of TIDA Neurons from MPTP Toxicity

TIDA neurons have been thought to be resistant to the toxicant MPP⁺ due to lower expression of DAT (Annunziato et al., 1980; Demarest & Moore, 1979a; Revay et al., 1996). However, previous findings and the data presented herein indicate that this is not likely to be the

case. Previous studies from our laboratory have shown that pharmacological blockade of DAT prior to administration of MPTP does not prevent the initial loss of DA stores in TIDA neurons as it does in NSDA neurons, suggesting that the mode of MPP^+ entry into TIDA neurons is, at least partially, DAT-independent (Benskey et al., 2012). Reports characterizing a low affinity high volume transporter in TIDA neurons provide further evidence that these neurons utilize different mechanisms for uptake of DA-like substances (lookingland & Moore, 2005). Neurons in the ARC express high levels of non-specific cation transporters (Cui et al., 2009; P. J. Gasser, Orchinik, Raju, & Lowry, 2009), suggesting that these low affinity uptake transporters may be responsible for the entry and accumulation of MPP^+ in TIDA neurons.

Data from the current study shows that peak concentrations of MPP^+ are higher in regions containing axon terminals of TIDA neurons as compared to NSDA neurons, and the half-life of MPP^+ is shorter in the ST than in the ME. These data are consistent with previous reports demonstrating that MPP^+ does effectively enter as well as accumulate within hypothalamic DA neurons and is eliminated slower than in NSDA neurons (Del Zompo et al., 1993; Speciale, Liang, Sonsalla, Edwards, & German, 1998). Regardless of the mode of MPP^+ entry into the cell, both neuronal populations respond to toxicant treatment in a similar fashion, i.e., loss of DA stores in axon terminal regions is similar by 4 h post-MPTP, at a time when MPP^+ concentrations peak. Further, TIDA neurons are also resistant to an alternative mitochondrial complex I inhibitor rotenone (Behrouz et al., 2007). Rotenone is a highly lipophilic molecule and does not require bio-activation or transporter presence for entry to the cell. As such decreased transporter expression cannot account for TIDA neuronal resistance to rotenone. Taken together,

differences in the mode of toxicant entry into the cell or decreased toxicant accumulation as explanations for the unique ability of TIDA neurons to recover from an acute toxicant injury is not supported by the data.

PRL Activation in the Recovery of TIDA Neurons from MPTP Toxicity

The activating effect of PRL on TIDA neurons was also explored as a mechanism of TIDA recovery from acute MPTP toxicity. Despite the successful suppression of any increases in PRL concentrations, TIDA neurons were still able to recover in animals treated with bromocriptine. Thus, it seems that the recovery of TIDA terminal DA stores is not mediated by activation of these neurons by PRL. This conclusion is well supported by the data presented within this set of experiments.

Within the time points assayed there was never an increase in plasma PRL, even in animals treated with MPTP in the absence of bromocriptine. The working hypothesis of this experiment was that MPTP-induced loss of axon terminal DA stores would remove the tonic dopaminergic inhibition on anterior pituitary lactotrophs, resulting in an increase in PRL secretion. However, this scenario was not observed in this experiment, in contrast PRL was actually suppressed at all time points.

It is possible that in between the 4 and 24 h time points there may have been a transient increase in plasma PRL. However, the more likely explanation is that when MPTP displaces DA from the synaptic vesicles, the large increase in cytosolic DA leaks from the axon terminal into the extracellular space. In the case of TIDA neurons, the extracellular space is the hypophysial portal circulation. Thus, MPTP may actually act to indirectly suppress PRL by increasing the exocytosis-independent release of DA from TIDA neurons. Regardless of the mechanism of

PRL inhibition, it is clear that the ability of TIDA neurons to recover axon terminal DA concentrations following MPTP administration is not mediated by increases in tonic activation of these neurons by PRL.

DA Synthesis in the Recovery of TIDA Neurons from MPTP Toxicity

The final goal of the current set of experiments was to determine if differential levels of TH protein and/or TH enzymatic activity in the axon terminals of NSDA and TIDA neurons could account for the differential ability of these two neuronal subpopulations to recover DA concentrations following single-acute MPTP administration. Data presented herein shows that TH activity in the ST reaches a nadir at 4 h post-MPTP and remains significantly decreased for the entire 24 h time course. In contrast, TH activity is found to be decreased solely at the 4 h time point in the ME. This pattern of TH activity in the ST and ME roughly mirrors the pattern of DA concentrations in the same brain regions following MPTP. It is possible that the small and transient decrease in TH activity within the ME following MPTP could explain why these neurons are able to replenish axon terminal DA, whereas NSDA neurons, which show a large and sustained decrease in TH activity, show a corresponding sustained depletion of axon terminal DA.

In addition to showing differences in TH activity, concentrations of TH protein at the 24 h time point also support the role of DA synthesis in the differential ability of TIDA and NSDA neurons to recover axon terminal DA concentrations following MPTP. TH protein is decreased within the ST at 24 h post-MPTP but is unchanged in the ME. This experiment is a replication of a similar experiment measuring terminal TH protein concentrations that was performed in Chapter 3. In the previous experiment TH protein in the ST was decreased but not significantly

different from saline treated controls 24 h post-MPTP. The reason for this discrepancy is unknown, but likely represents either experimental error or the inability to detect a modest effect when using more stringent multiple levels of comparison. Regardless, the results from the current experiment are in line with the literature, however, this experiment will need to be repeated again in order to confirm that the results from Chapter 3 were spurious.

The differential ability of TIDA and NSDA neurons to recover axon terminal DA homeostasis may be due to their different cytoarchitecture and/or regulatory mechanisms. Unlike prototypical DA neurons, TIDA neurons do not form classic synapses but instead terminate near capillaries within the hypophysial portal system. TIDA neurons lack D₂ autoreceptors and have lower concentrations of DAT as compared to NSDA neurons (Timmerman, Deinum, Westerink, & Schuiling, 1995). Following entry into DA axon terminals, MPP⁺ has a high affinity for the vesicular monoamine transporter, being transported into synaptic vesicles and displacing stored DA into the cytosol (Lotharius & O'Malley, 2000; Moriyama, Amakatsu, & Futai, 1993). Within NSDA neurons, purged vesicular DA can diffuse from neurons into the synapse, activating D₂ autoreceptors, thereby inhibiting DA synthesis and release. Additionally, DA in the synaptic cleft can be transported back into the axon terminal by DAT, further inhibiting DA synthesis through end product inhibition. In contrast, due to lower levels of DAT, loss of released DA into the hypophysial portal blood, and the lack of D₂ autoreceptors, the reuptake and inhibition of DA synthesis would be severely reduced in TIDA neurons (Timmerman et al., 1995).

The contribution of this differential DA terminal regulation is supported by the temporal difference in the maximal effect of MPTP on ST and ME DA concentrations. Within TIDA neurons peak DA depletion is concurrent with peak MPP⁺ levels (consistent with DA

displacement from vesicles), after which time these neurons are able to refill vesicular DA, a timeframe that corresponds with the recovery of TH activity within the ME. In contrast, peak DA depletion occurs long after maximal MPP⁺ concentrations are observed within NSDA neurons. In the window of time following peak MPP⁺ concentrations, DA concentrations and TH activity remain low in the ST, even when MPP⁺ is no longer detectable. These latter results suggest sustained dopaminergic dysfunction and toxicity within NSDA neurons following exposure to MPTP. It is possible that the rapid ability of TIDA neurons to clear cytosolic DA (whether it be into vesicles or into portal circulation) may contribute to their observed resistance to the same forms of toxicity that severely injures NSDA neurons.

Differences in DA regulation may play some role in the differential susceptibility of TIDA and NSDA neurons; however, TIDA recovery from MPTP is protein synthesis dependent (Benskey et al., 2012). Accordingly differences in cytoarchitecture and DA regulation cannot account for the entirety of the observed phenomenon. It is possible that the unique neuroanatomical position of TIDA neurons may be responsible for their resilience. Having axons that terminate outside the protective blood brain barrier exposes TIDA neurons to bloodbourn toxicants. It is possible that this constant exposure to deleterious compounds, which other neuronal populations within the blood brain barrier never encounter, has forced these neurons to evolve a compensatory mechanisms to perform their physiological function in the face of a potentially neurotoxic environment. Data from Chapter 3 of this dissertation has revealed some of these potential compensatory mechanisms in the form of parkin and UCH-L1 up-regulation.

It is plausible that the ability of TIDA neurons to up-regulate parkin and UCH-L1 helps to maintain normal enzyme function in the face of cellular stress and thus reconstitute normal

DA synthesis and neurotransmission. UCH-L1 has been shown to increase following recovery from oxidative stress, while parkin has been shown to quell increases in oxidative and nitrosative stress (Hyun, Lee, Halliwell, & Jenner, 2005; H. H. Jiang et al., 2004; D. J. Moore et al., 2005; H. H. Shen, Sikorska, Leblanc, Walker, & Liu, 2006). Further, increases in nitrosative stress produced by MPTP have been shown to result in loss of TH protein and enzymatic activity (Ara et al., 1998; Blanchard-Fillion, 2001; Kuhn et al., 1999). This provides a possible link between the ability of TIDA neurons to up-regulate parkin expression and the ability to maintain DA synthesis following toxicant exposure. This link between parkin and the ability of TIDA and NSDA neurons to recover axon terminal DA homeostasis will be further explored in Chapter 7.

Alternatively, as the recovery of TIDA neurons from MPTP is protein synthesis dependent it may also be possible that these neurons are able to increase TH expression in order to compensate for loss of the enzyme within the early stages of cytotoxicity. Concentrations of TH protein in the ME do not increase following MPTP, however, this could reflect newly synthesized TH protein replacing damaged protein, resulting in no measurable change. As such, it would be interesting to measure changes in TH mRNA following MPTP in the ME and ST.

Conclusion

Data from this chapter has confirmed that neither decreased toxicant exposure nor PRL activation of TIDA neurons is responsible for the ability of these neurons to recover from acute MPTP toxicity. Further, it was shown that the ability to reconstitute normal DA synthesis likely plays a role in the ability of TIDA neurons to recover axon terminal DA concentrations following MPTP exposure. These data support the hypothesis that TIDA recovery is not

mediated by extrinsic mechanisms, but more likely by intrinsic mechanisms that are unique to these neurons.

Chapter 5. Characterization of the differential susceptibility of TIDA and NSDA neurons to chronic MPTP exposure.

Introduction

Previous studies in this dissertation have utilized an acute-single injection of MPTP in order to identify early events following MPTP administration that differ between TIDA and NSDA neurons (Behrouz et al., 2007, Benskey et al., 2012). In doing so it was discovered that TIDA neurons fully recover axon terminal DA stores within 24 h following a single administration of MPTP, while NSDA neurons show sustained depletion of DA stores for up to 72 h post-MPTP (Behrouz et al., 2007; Benskey et al., 2012). This differential susceptibility of TIDA and NSDA neurons to acute MPTP toxicity is associated with a differential expression of the proteins, parkin and UCH-L1 (Behrouz et al., 2007; Benskey et al., 2012). More specifically, up-regulation of both parkin and UCH-L1 is observed in the ARC within 24 h following MPTP, while there is a slight decrease in parkin and UCHL1 concentrations in the SN. Finally, TIDA resistance is not due to extrinsic factors such as reduced bioactivation or accumulation of MPP⁺ in the terminals of these neurons. Rather, TIDA recovery from MPTP appears to reflect an intrinsic capability to cope with cytotoxic stress, a neuronal phenotype that may rely on the compensatory up-regulation of neuroprotective proteins such as parkin and UCH-L1.

Despite this body of evidence detailing TIDA neuronal recovery, it is currently unclear whether the molecular events associated with recovery are limited to one-time low dose toxicant exposure or if TIDA neurons can also recover from repeated toxicant exposure. The appearance of NSDA cellular pathology in PD most likely does not result from a single event but, more plausibly, from the culmination of multiple deleterious events working in combination over time.

Similarly, prolonged toxicant exposure likely entails a multitude of primary and secondary cytotoxic events, which may differ from a simple one time exposure. Accordingly, investigations that aim to identify mechanisms unique to TIDA neuronal recovery must also consider the ability of these neurons to recover from prolonged exposure, in addition to how previous cytotoxicity affects the response profile to acute toxicity.

The purpose of the current study was to test the hypothesis that TIDA neurons are resistant, while NSDA neurons are susceptible to chronic MPTP induced disruption of axon terminal DA homeostasis and cell loss. Additionally, the differential susceptibility of TIDA and NSDA neurons to chronic MPTP toxicity is hypothesized to be associated with the ability to increase the expression of neuroprotective proteins. In order to test this hypothesis mice were chronically treated with MPTP (10 X 20 mg/kg; s.c.) or saline (10 X 10 ml/kg; s.c.) over the course of 35 days. Twenty-one days following the last chronic injection mice received an additional single injection of MPTP (20 mg/kg; s.c.) or saline (10 ml/kg; s.c.) and were killed by decapitation 24 h later.

This MPTP dosing paradigm will address whether chronic MPTP exposure results in TIDA neuronal degeneration or renders TIDA neurons susceptible to subsequent neurotoxicant exposure. Further, the ability of TIDA neurons to elicit, as well as maintain, the compensatory up-regulation of parkin and UCH-L1 following various MPTP dosing paradigms will be examined to determine if enhanced expression of these proteins is a transient or a sustained event. Finally, the response of TIDA neurons to a more protracted and harsher MPTP dosing regimen will determine if studying early molecular events following the single-acute MPTP regimen is an appropriate tool in determining mechanisms of recovery that could be adapted to damaged NSDA neurons in PD.

Results

The effects of MPTP on TH and DAT concentrations in the striatum: confirmation of successful neurotoxicant administration

In order to confirm successful neurotoxicant administration in all MPTP treatment paradigms, concentrations of TH and DAT in the ST were quantified using Western blot analyses. Striatal TH concentrations decreased to approximately 80% of saline treated controls following an acute injection of MPTP (Figure 5-1). Striatal TH concentrations are further reduced to approximately 20% of saline treated animals following chronic MPTP administration. Acute MPTP administration 21 days following the completion of the chronic MPTP regimen produced no further decrease in ST TH concentrations beyond that observed with the chronic regimen alone.

In addition to monitoring changes in TH concentrations in the ST, changes in DAT following MPTP were also measured in order to serve as an additional validating index of NSDA axon terminal density and positive control for successful MPTP administration. Similar to the pattern of TH loss, DAT concentrations are reduced to approximately 70% of saline treated animals following acute MPTP exposure (Figure 5-2). Chronic MPTP administration reduces ST DAT concentrations to approximately 10% of saline treated animals, and the acute injection of MPTP following completion of the chronic regimen had no further effect on DAT concentrations in the ST.

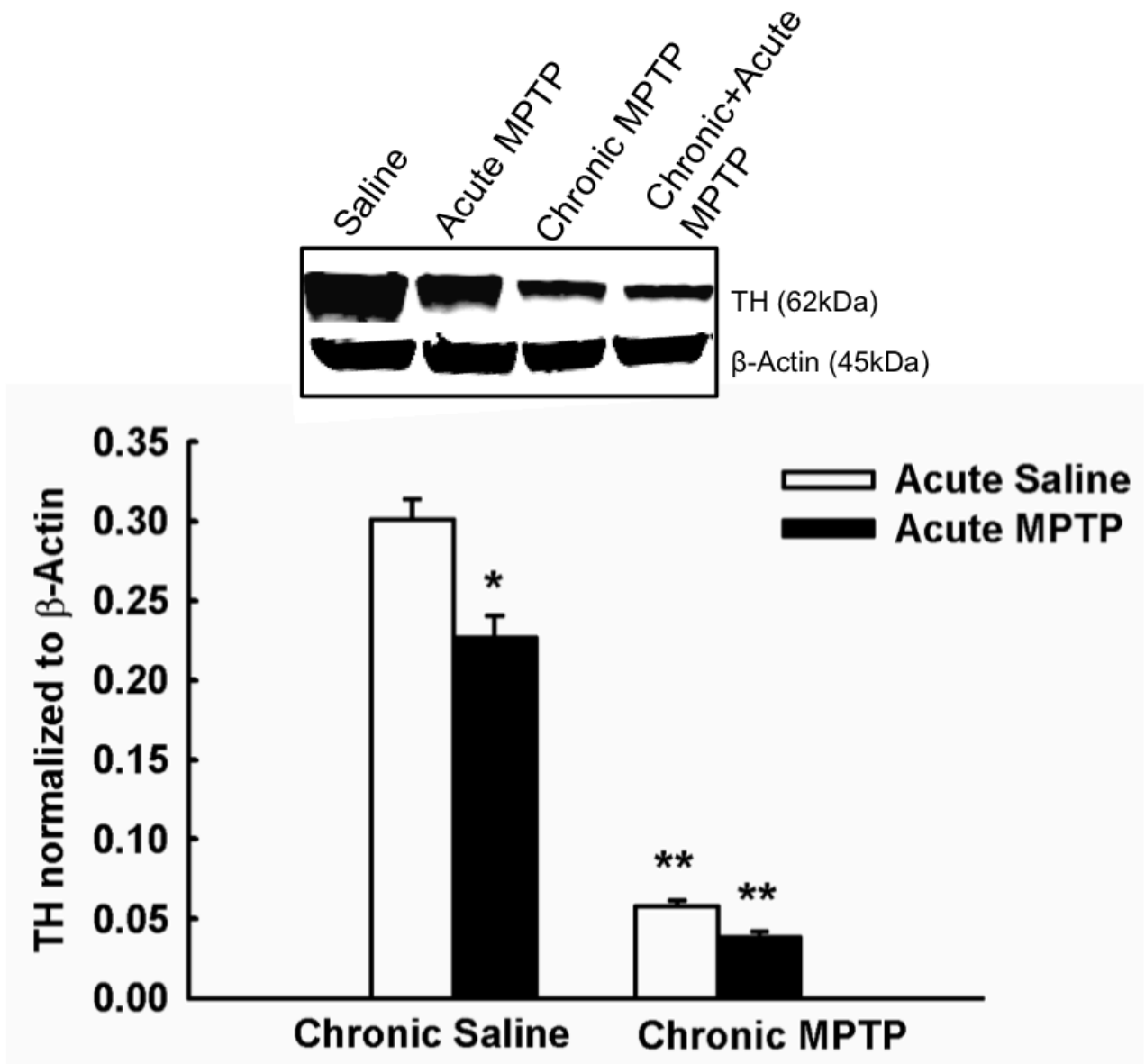


Figure 5-1. The effects of MPTP on TH concentrations in the ST: confirmation of successful neurotoxicant administration. Male C57BL/6J mice ($n = 10/\text{group}$) were chronically treated with MPTP ($10 \times 20 \text{ mg/kg}$; s.c.) or saline ($10 \times 10 \text{ ml/kg}$; s.c.) over the course of 35 days. Twenty-one days following the last chronic injection mice received a single additional injection of MPTP (20 mg/kg ; s.c., black columns) or saline (10 ml/kg ; s.c., white columns) and were killed by decapitation 24 h later. TH concentrations were determined by Western blotting and normalized to β -actin. Columns represent mean TH \pm 1 SEM. *TH concentrations significantly different ($p < 0.05$) from saline-treated controls. **TH concentrations significantly different ($p < 0.05$) from those of single-MPTP treated animals and saline treated controls. Representative blots from all groups are shown above graphs.

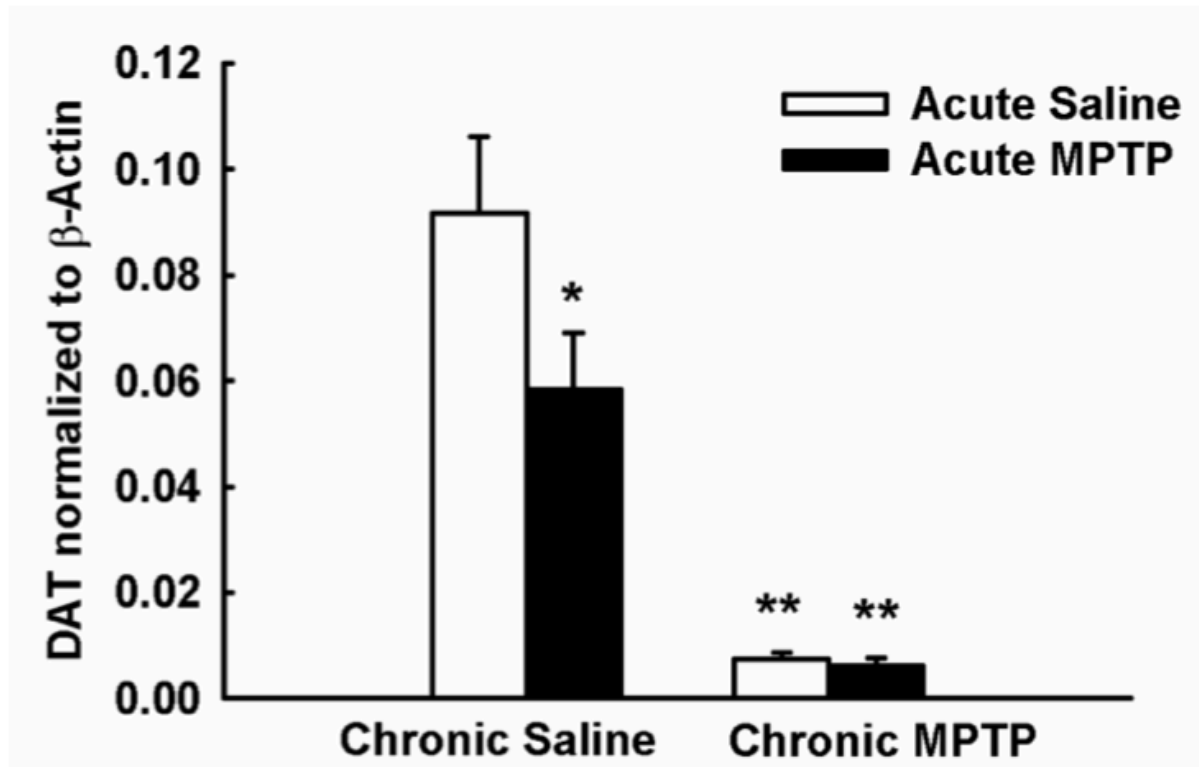
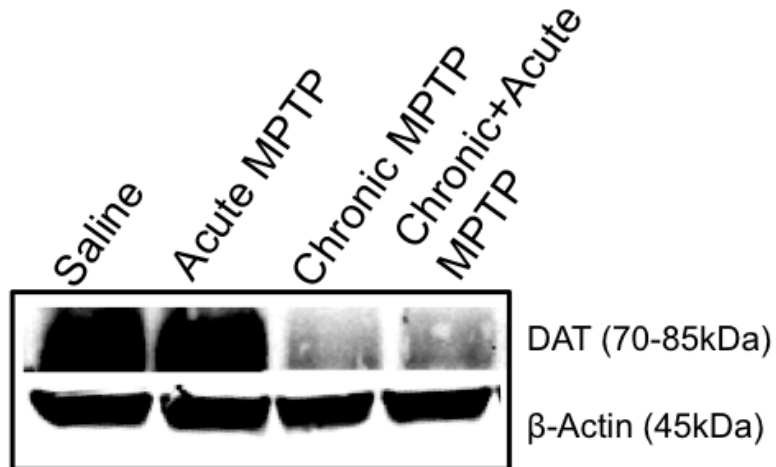


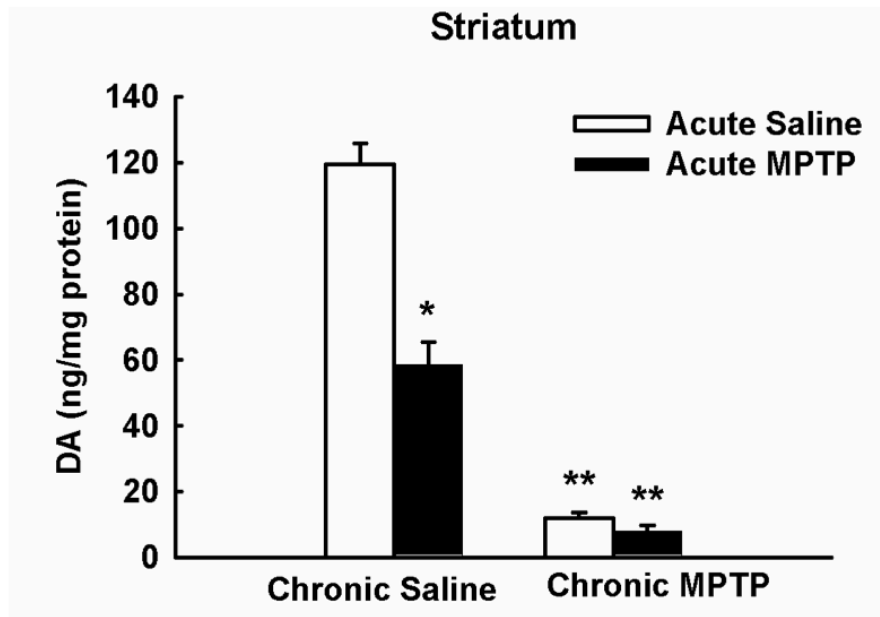
Figure 5-2. The effects of MPTP on DAT concentrations in the ST: confirmation of successful neurotoxicant administration. Male C57BL/6J mice ($n = 10/\text{group}$) were chronically treated with MPTP ($10 \times 20 \text{ mg/kg}$; s.c.) or saline ($10 \times 10 \text{ ml/kg}$; s.c.) over the course of 35 days. Twenty-one days following the last chronic injection mice received a single additional injection of MPTP (20 mg/kg ; s.c., black columns) or saline (10 ml/kg ; s.c., white columns) and were killed by decapitation 24 h later. DAT concentrations were determined by Western blotting and normalized to β -actin. Columns represent mean DAT + 1 SEM. (*) DAT concentrations significantly different ($p < 0.05$) from saline-treated controls. (**) DAT concentrations significantly different ($p < 0.05$) from those of single-MPTP treated animals and saline treated controls. Representative blots from all groups are shown above graphs.

The effects of MPTP on DA concentrations, DA metabolism and DA turnover in axon terminals of NSDA and TIDA neurons

Previous reports have shown that “PD-susceptible” NSDA neurons exhibit a profound and sustained loss of axon terminal DA stores following acute MPTP exposure, whereas “PD-resistant” TIDA neurons recover axon terminal DA within 24 h (Benskey et al., 2012). The ability of TIDA neurons to recover from single-acute MPTP toxicity following previous chronic toxicant exposure has not been examined. Figure 5-3 shows the neurochemical response profiles of NSDA and TIDA neurons following MPTP. Acute exposure to MPTP results in an approximately 50% reduction of DA concentrations in the ST compared to saline-treated control animals. Chronic MPTP treatment decreases ST DA to less than 10% of control animals, and single-acute MPTP administration following the chronic regimen had no significant effect beyond that of the chronic regimen alone (Figure 5-3, Panel A). In contrast, 24 h following an acute MPTP exposure, DA concentrations in the ME were not different than that of controls (Figure 5-3, Panel B). ME DA concentrations were not decreased following the chronic MPTP regimen, nor after acute MPTP administration following chronic exposure to MPTP (Figure 5-3, Panel B).

Chronic MPTP as well as chronic + acute MPTP administration resulted in a decrease in the DA metabolite DOPAC in the ST (Figure 5-4, Panel A). Further, all MPTP dosing regimens examined produced an increase in DA turnover within the ST, as indexed by the ratio of DOPAC to DA, indicative of increased activity of remaining NSDA neurons (Figure 5-4, Panel B). There was no change in the concentrations of DOPAC or the turnover of DA in the ME (Figure 5-5, Panels C & D).

A)



B)

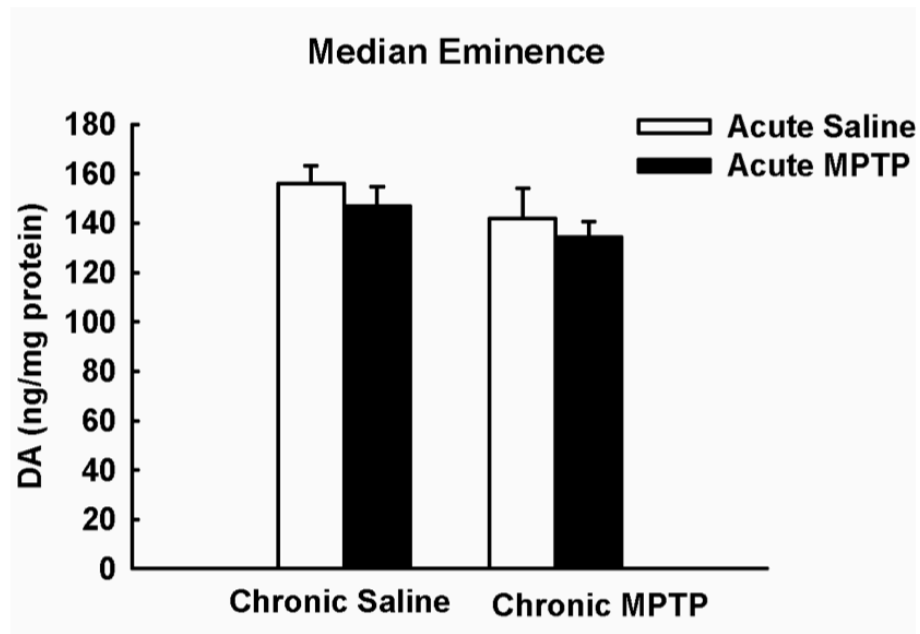
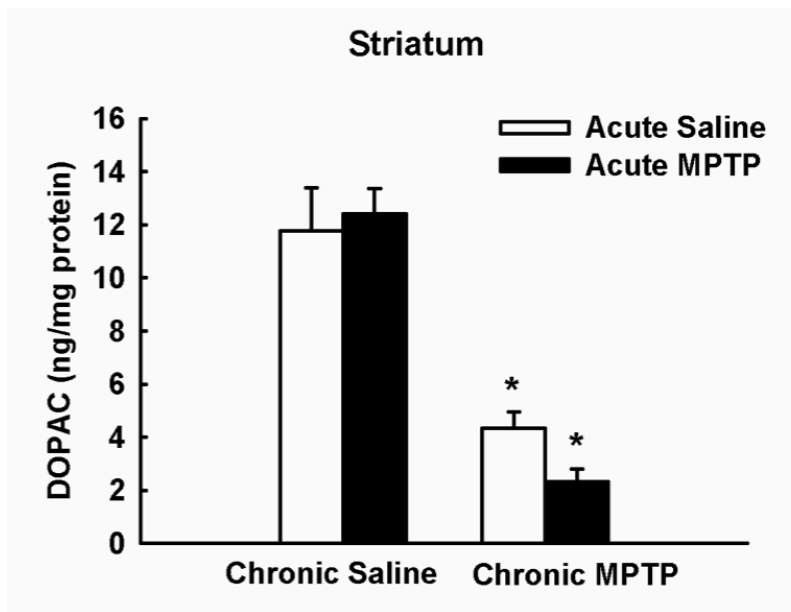


Figure 5-3. The effects of single-acute MPTP administration on DA concentrations in axon terminals of NSDA and TIDA neurons in mice chronically treated with MPTP. Male mice were chronically treated with MPTP or saline over the course of 35 days. Twenty-one days following the last chronic injection mice received a single additional injection of MPTP (black columns) or saline (white columns) and were sacrificed 24 h later. DA concentrations are expressed as ng/mg protein. Columns represent mean DA concentrations in the ST (Panel A) and ME (Panel B) + 1 SEM. (*) DA concentrations significantly different ($p < 0.05$) from those of saline treated controls. (**) DA concentrations significantly different ($p < 0.05$) from those of single-MPTP treated animals and saline treated controls.

A)



B)

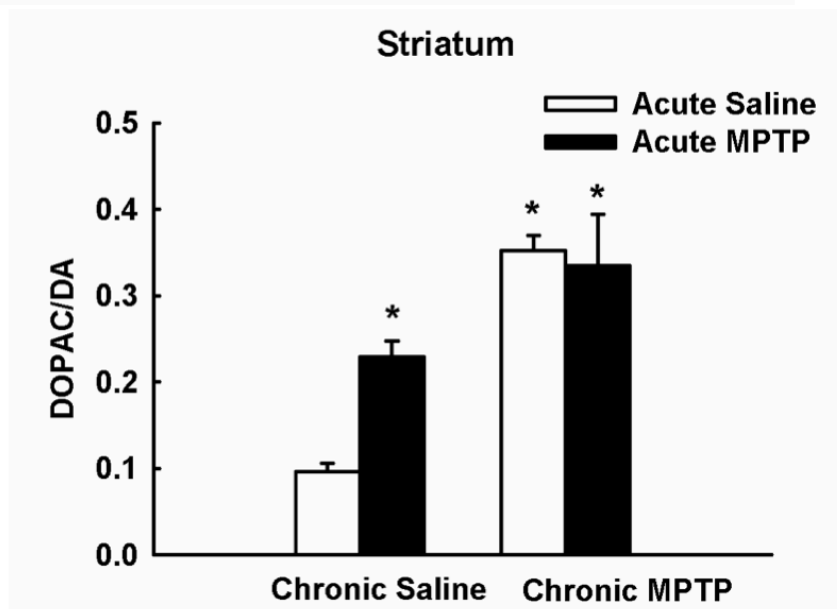
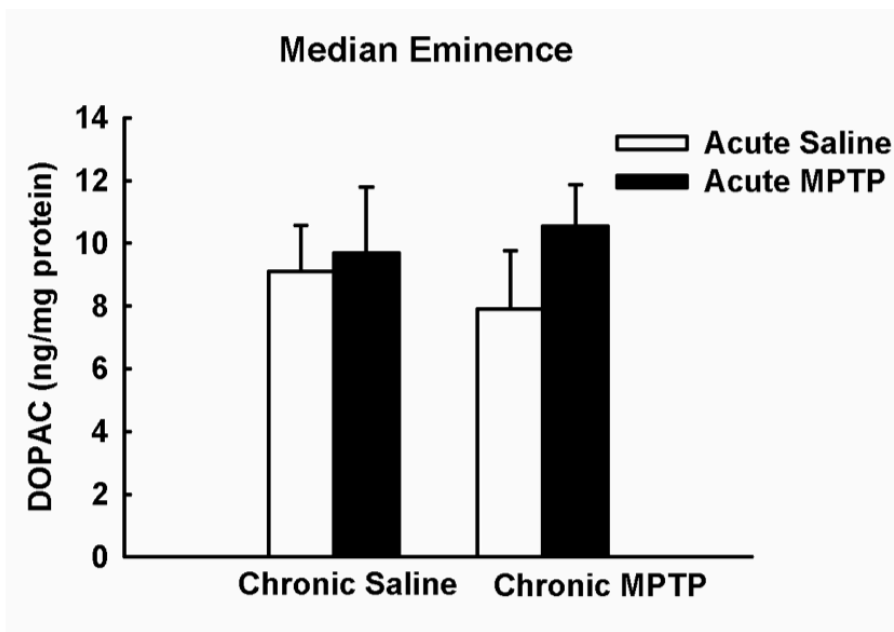


Figure 5-4. The effects of single-acute MPTP administration on DA metabolism and turnover in axon terminals of NSDA neurons in mice chronically treated with MPTP. Male C57BL/6J mice (n = 6/group) were chronically treated with MPTP (10 x 20 mg/kg; s.c.) or saline (10 x 10 ml/kg; s.c.) over the course of 35 days. Twenty-one days following the last chronic injection mice received a single additional injection of MPTP (20 mg/kg; s.c., black columns) or saline (10 ml/kg; s.c., white columns) and were sacrificed 24 h later. DOPAC concentrations (Panel A) are expressed as ng/mg protein. DA turnover is represented by the ratio of the DA metabolite DOPAC to DA (Panel B). Columns represent mean DOPAC concentrations or DOPAC/DA ratio + 1 SEM. (*) DOPAC concentrations or DOPAC/DA ratios significantly different (p < 0.05) from those of saline treated controls.

A)



B)

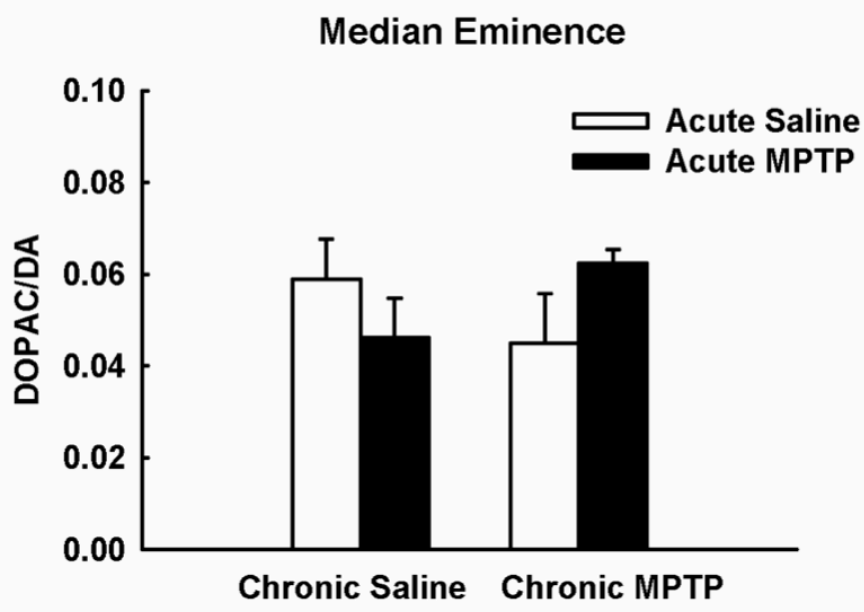


Figure 5-5. Lack of effects of single-acute MPTP administration on DA metabolism and turnover in axon terminals of TIDA neurons in mice chronically treated with MPTP. Male C57BL/6J mice ($n = 6/\text{group}$) were chronically treated with MPTP ($10 \times 20 \text{ mg/kg}$; s.c.) or saline ($10 \times 10 \text{ ml/kg}$; s.c.) over the course of 35 days. Twenty-one days following the last chronic injection mice received a single additional injection of MPTP (20 mg/kg ; s.c., black columns) or saline (10 ml/kg ; s.c., white columns) and were sacrificed 24 h later. DOPAC concentrations (Panel A) are expressed as ng/mg protein. DA turnover is represented by the ratio of the DA metabolite DOPAC to DA (Panel B). Columns represent mean DOPAC concentrations or DOPAC/DA ratio + 1 SEM. (*) DOPAC concentrations or DOPAC/DA ratios significantly different ($p < 0.05$) from those of saline treated controls.

The effects of MPTP on TH-ir cell numbers in the SN and ARC

TIDA neurons recover axon terminal DA concentrations following single-acute administration of MPTP (Benskey et al., 2012), but the effect of single-acute MPTP administration alone, or single-acute MPTP following previous chronic MPTP exposure on the number of TH-ir cells in the ARC is not known. Accordingly, TH-ir cells of the SN and ARC were quantified using unbiased stereology following MPTP. Figure 5-6 shows representative images of TH-ir cells in the ARC and SN following the MPTP paradigms investigated. The number of TH-ir cells in the SN was decreased to approximately 80% of vehicle treated controls following single-acute MPTP administration (Figure 5-7, Panel A). Despite decreased TH-ir cell numbers, there were no differences in the number of Nissl stained cells in the SN of vehicle ($19,575 \pm 1,163$) and single-acute MPTP-treated mice ($18,874 \pm 523$). Chronic MPTP exposure further decreases TH-ir cell numbers in the SN to approximately half that of saline treated controls, and this was associated with a concomitant decrease in the number of Nissl stained cells (9549 ± 527). The acute-single injection of MPTP in animals receiving prior chronic MPTP had no further loss of TH-ir or Nissl (9020 ± 364) cell numbers in the SN beyond that of the chronic paradigm alone. There was no significant change in TH-ir cell numbers within the ARC following any of the dosing regimens examined (Figure 5-7, Panel B).

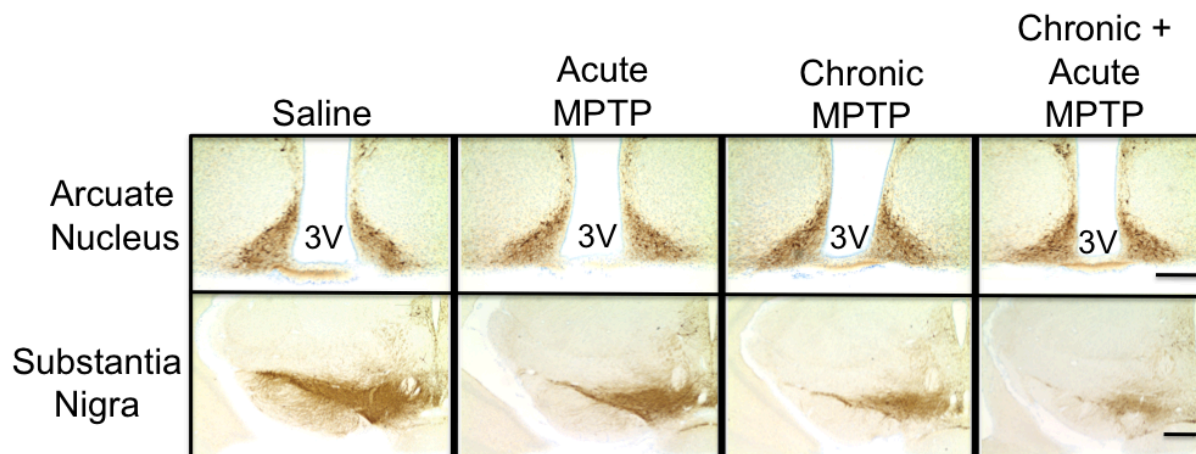
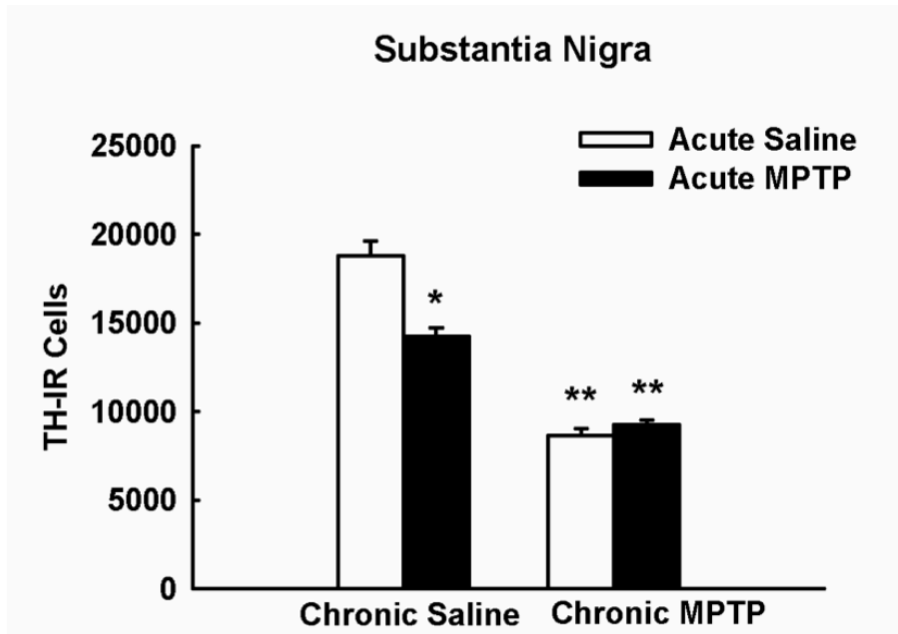


Figure 5-6. Representative photomicrographs of TH-ir cells in the SN and ARC following single acute and chronic MPTP administration. Male C57BL/6J mice (n = 6/group) were chronically treated with MPTP (10–20 mg/kg; s.c.) or saline (10–10 ml/kg; s.c.) over the course of 35 days. Twenty-one days following the last chronic injection mice received a single additional injection of MPTP (20 mg/kg; s.c., black columns) or saline (10 ml/kg; s.c., white columns) and were perfused 24 h later. Representative photomicrographs of TH-IR cells in the SN and ARC surrounding the third ventricle (3V) are shown. Scale bar is equal to 200 μ m in the upper right panel and 500 μ m in the lower left panel.

A)



B)

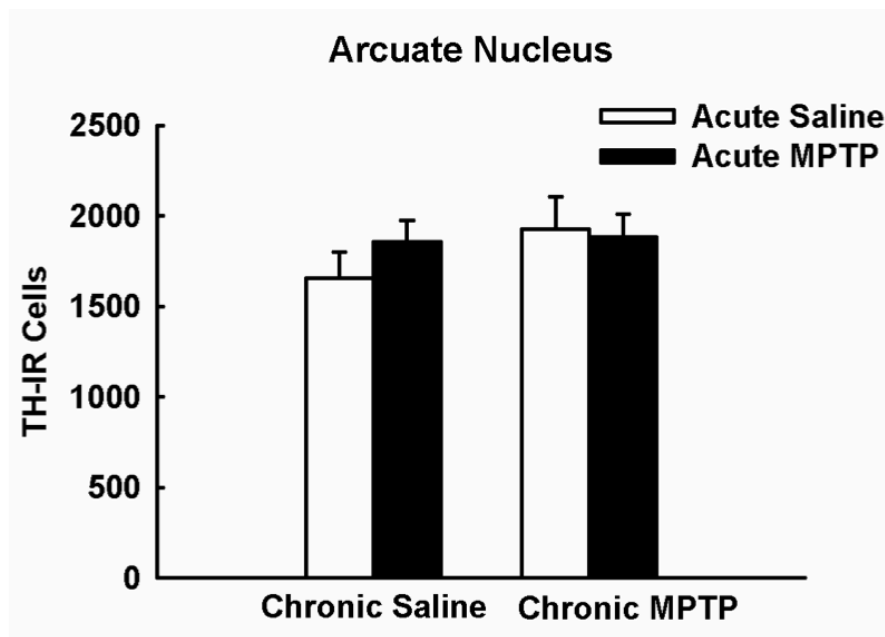


Figure 5-7. The effects of single-acute MPTP administration on TH-ir cell numbers in the SN and ARC in mice chronically treated with MPTP. Male C57BL/6J mice (n = 6/group) were chronically treated with MPTP (10 x 20 mg/kg; s.c.) or saline (10 x 10 ml/kg; s.c.) over the course of 35 days. Twenty-one days following the last chronic injection mice received a single additional injection of MPTP (20 mg/kg; s.c., black columns) or saline (10 ml/kg; s.c., white columns) and were perfused 24 h later. Numbers of TH-ir cells were estimated using unbiased stereology in the SN (Panel A) and ARC (Panel B). Columns represent mean TH-IR cell numbers + 1 SEM. (*) TH-IR cell numbers significantly different (p < 0.05) from saline-treated controls. (**) TH-IR cell numbers significantly different (p < 0.05) from single MPTP-treated animals and saline-treated controls.

Changes in protein concentrations in the SN and ARC following MPTP administration

Recent studies have shown that recovery of THDA neurons from a single dose of MPTP is correlated with an acute increase in the expression of the PD-associated genes, UCH-L1 and parkin in the ARC (Benskey et al., 2012). Conversely, following a single dose of MPTP, these same proteins show a decrease in the cell body regions of the highly susceptible NSDA neurons. If an increase in these proteins was serving a neuroprotective role, then the same differential expression pattern should be observed following the chronic MPTP paradigms used in the current study.

Figure 5-8 shows changes in UCH-L1 protein concentrations in the SN following the various MPTP treatment regimens. UCH-L1 protein concentrations in the SN are decreased 24 h following an acute injection of MPTP. Twenty-one days following the completion of the chronic MPTP regimen UCH-L1 protein concentrations are no longer different than those of control animals. Single-acute MPTP administration reduced UCH-L1 concentrations in animals with prior chronic MPTP exposure .

Changes in UCH-L1 protein concentrations in the ARC following MPTP treatment are shown in Figure 5-9. As has been previously reported, UCH-L1 protein concentrations are increased 24 h following a single-acute injection of MPTP (Benskey et al., 2012). Twenty-one days following completion of the chronic MPTP regimen, UCH-L1 concentrations in the ARC are not different from saline treated animals, and acute MPTP administration increased UCH-L1 protein concentrations in animals receiving prior chronic MPTP exposure as compared to vehicle-treated controls.

Figure 5-10 depicts changes in parkin protein expression in the SN following the single-acute, chronic and chronic + single acute MPTP dosing paradigms. Parkin protein

concentrations in the SN are reduced from control levels 24 h following acute MPTP administration. Parkin protein concentrations return to control levels 21 days following the completion of the chronic MPTP paradigm. Acute MPTP administration reduced parkin protein concentrations in animals receiving prior chronic MPTP exposure as compared to vehicle-treated controls.

Figure 5-11 replicates previous findings, showing parkin protein concentrations in the ARC to be increased 24 h following single-acute MPTP administration, demonstrating the reproducibility of this unique response to toxicant-induced injury. The increase in parkin protein in the ARC is sustained for 21 days following completion of the chronic MPTP regimen. Acute MPTP administration in animals receiving prior chronic MPTP exposure did not increase parkin concentrations beyond the elevated levels observed in animals receiving the chronic MPTP regimen.

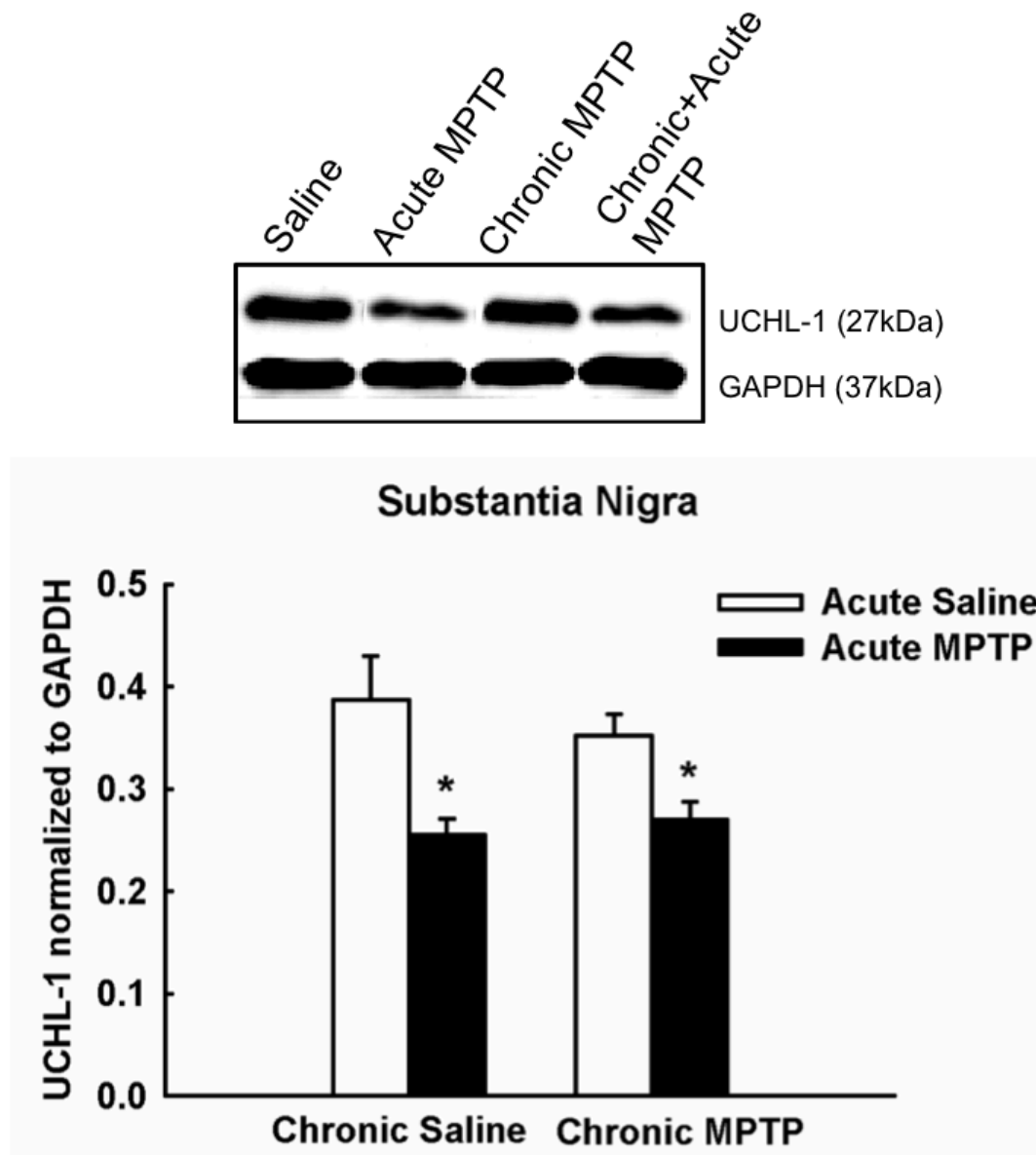


Figure 5-8. Changes in UCH-L1 protein concentrations in the SN following single-acute MPTP administration in mice chronically treated with MPTP. Male C57BL/6J mice (n = 10/group) were chronically treated with MPTP (10 x 20 mg/kg; s.c.) or saline (10 x 10 ml/kg; s.c.) over the course of 35 days. Twenty-one days following the last chronic injection mice received a single additional injection of MPTP (20 mg/kg; s.c., black columns) or saline (10 ml/kg; s.c., white columns) and were killed by decapitation 24 h later. UCH-L1 concentrations were determined by Western blotting and normalized to GAPDH. Columns represent mean UCH-L1 concentrations + 1 SEM. (*) UCH-L1 concentrations significantly different ($p < 0.05$) from saline-treated controls. Representative blots from all groups are shown above graphs.

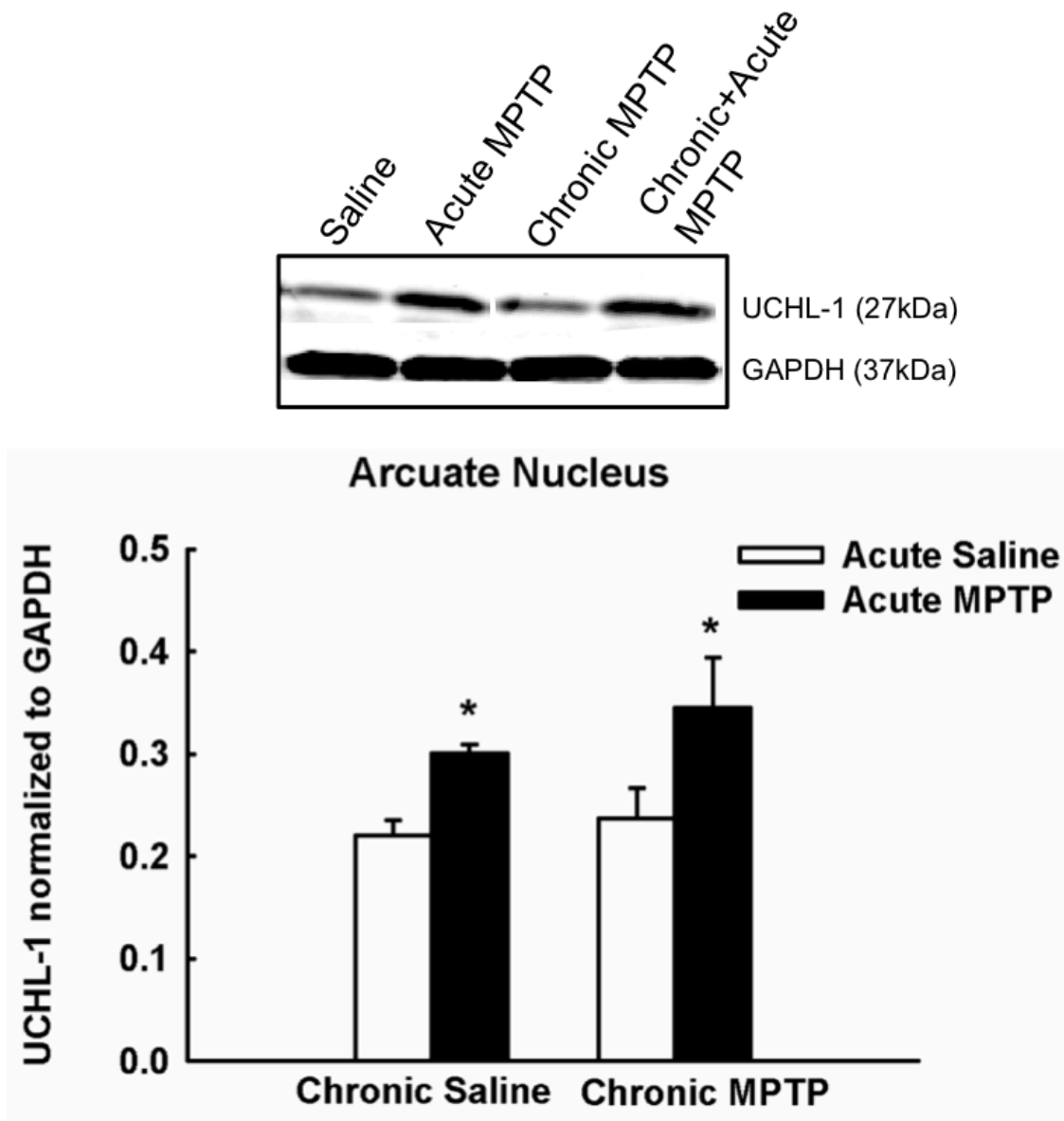


Figure 5-9. Changes in UCH-L1 protein concentrations in the ARC following single acute MPTP administration in mice chronically treated with MPTP. Male C57BL/6J mice ($n = 10/\text{group}$) were chronically treated with MPTP ($10 \times 20 \text{ mg/kg}$; s.c.) or saline ($10 \times 10 \text{ ml/kg}$; s.c.) over the course of 35 days. Twenty-one days following the last chronic injection mice received a single additional injection of MPTP (20 mg/kg ; s.c., black columns) or saline (10 ml/kg ; s.c., white columns) and were killed by decapitation 24 h later. UCH-L1 concentrations were determined by Western blotting and normalized to GAPDH. Columns represent mean UCH-L1 concentrations + 1 SEM. (*) UCH-L1 concentrations significantly different ($p < 0.05$) from saline-treated controls. Representative blots from all groups are shown above graphs.

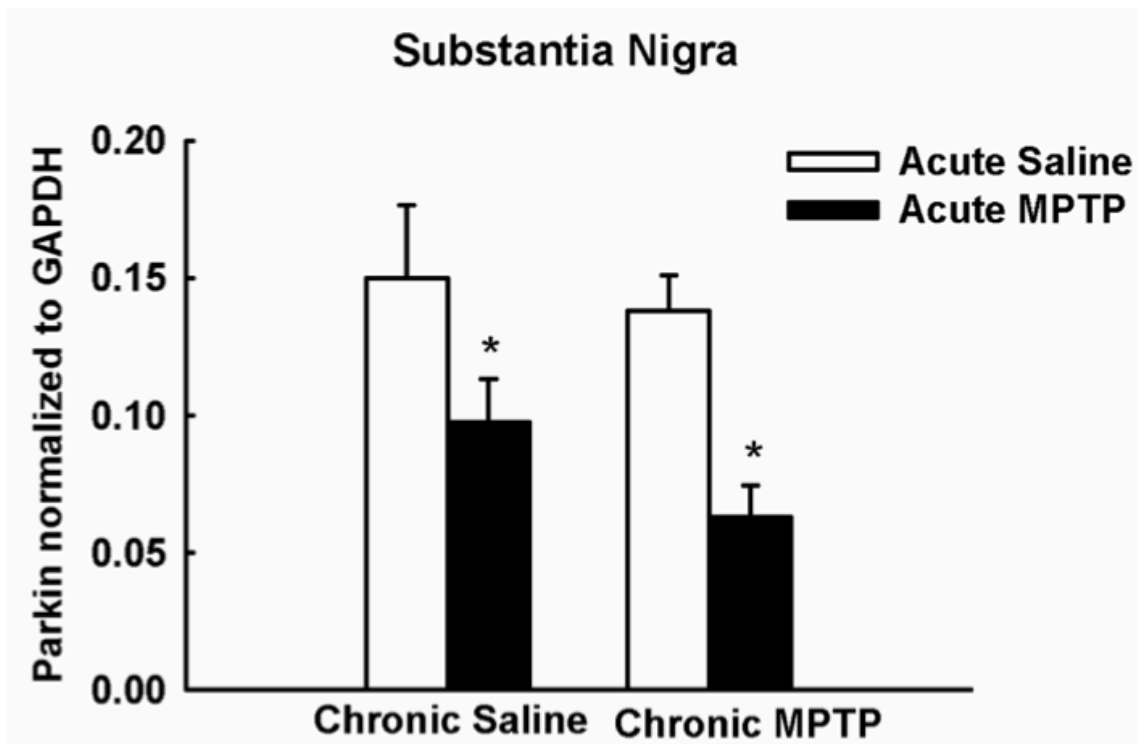
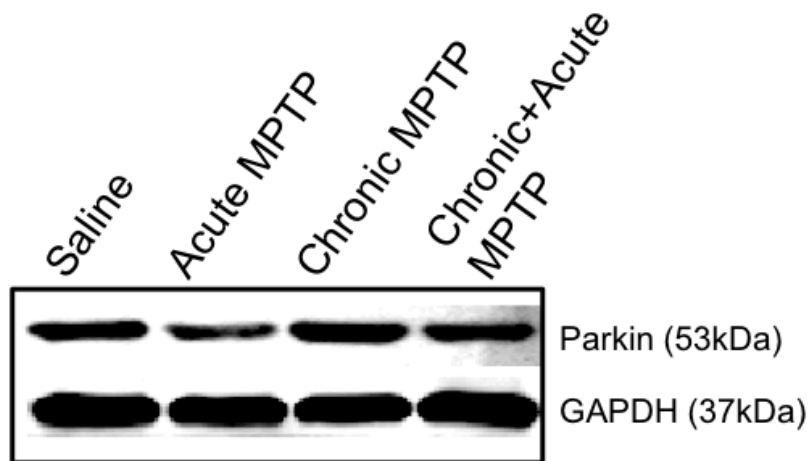


Figure 5-10. Changes in parkin protein concentrations in the SN following single-acute MPTP administration in mice chronically treated with MPTP. Male C57BL/6J mice (n = 10/group) were chronically treated with MPTP (10 x 20 mg/kg; s.c.) or saline (10 x 10 ml/kg; s.c.) over the course of 35 days. Twenty-one days following the last chronic injection mice received a single additional injection of MPTP (20 mg/kg; s.c., black columns) or saline (10 ml/kg; s.c., white columns) and were killed by decapitation 24 h later. Parkin concentrations were determined by Western blotting and normalized to GAPDH. Columns represent mean parkin concentrations + 1 SEM. (*) Parkin concentrations significantly different ($p < 0.05$) from saline-treated controls. Representative blots from all groups are shown above graphs.

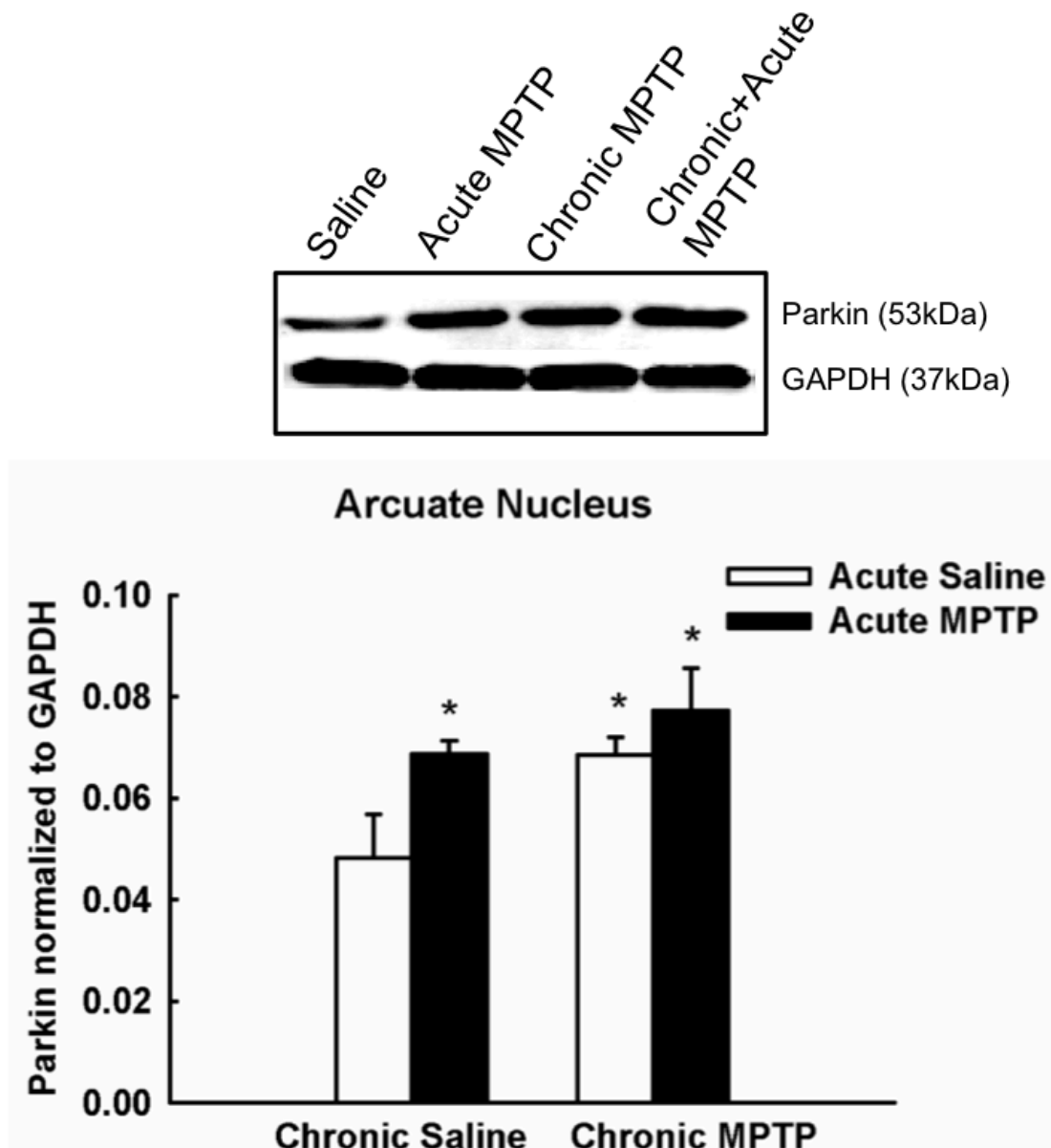


Figure 5-11. Changes in parkin protein concentrations in the ARC following single-acute MPTP administration in mice chronically treated with MPTP. Male C57BL/6J mice (n = 10/group) were chronically treated with MPTP (10 x 20 mg/kg; s.c.) or saline (10 x 10 ml/kg; s.c.) over the course of 35 days. Twenty-one days following the last chronic injection mice received a single additional injection of MPTP (20 mg/kg; s.c., black columns) or saline (10 ml/kg; s.c., white columns) and were killed by decapitation 24 h later. Parkin concentrations were determined by Western blotting and normalized to GAPDH. Columns represent mean parkin concentrations + 1 SEM. (*) Parkin concentrations significantly different ($p < 0.05$) from saline-treated controls. Representative blots from all groups are shown above graphs.

Discussion

In the present study the ability of TIDA neurons to recover from cytotoxicity produced by different MPTP dosing paradigms was examined. In addition to investigating the effects of acute and chronic MPTP administration alone, mice received an acute MPTP administration 21 days following chronic MPTP exposure. The use of a second insult superimposed on a chronic injury was employed as a strategy to determine if a repeated MPTP-induced injury sensitizes TIDA neurons to subsequent toxicant-induced injury and whether the compensatory increase in protein expression (i.e. parkin and UCH-L1 expression) found following an acute injury persists after prolonged MPTP-induced toxicity.

The results from these studies show that TIDA neurons are highly resistant to DA-associated toxicity caused by chronic MPTP exposure and do not suffer the loss of protective proteins that are thought to play a role in the demise of NSDA neurons. These data validate the utility of studying the early molecular events and phenotypic changes occurring in TIDA neurons following single-acute MPTP, and confirms that these changes are an appropriate predictive index of resistance to longer term, harsher toxicity.

The demise of NSDA neurons observed in PD is generally believed to result from a combination of several cellular dysfunctions, culminating in irreversible cytotoxicity. Environmental toxicant exposure, NSDA cellular structure, mitochondrial dysfunction, UPP impairment, cytosolic DA oxidation, and the loss of protective proteins are factors which are posited to work in concert to cause NSDA cell loss (Betarbet et al., 2000; Greenamyre, MacKenzie, & Peng, 1999; McNaught & Jenner, 2001; Priyadarshi, 2001; Sulzer, 2007). Due to the complexity of the interactions that contribute to NSDA cellular pathology, investigations

aimed at translating mechanisms unique to TIDA neuronal recovery into therapeutics must also consider the ability of TIDA neurons to recover from several modalities of cytotoxicity.

The majority of the key cellular dysfunctions known to contribute to NSDA cell death in PD are recapitulated by MPTP, however the underlying mechanisms and severity of toxicity are dependent upon the dose and timing of MPTP administration. A single exposure to MPTP will predominantly result in transient dysfunction within the dopaminergic axon terminal; including reduction in vesicular DA, ATP loss and free radical formation (Chan et al., 1991; Di Monte et al., 1986; Hasegawa, Takeshige, Oishi, Murai, & Minakami, 1990; JACKSONLEWIS et al., 1995; Lotharius & O'Malley, 2000; Scotcher, Irwin, DeLanney, Langston, & Di Monte, 1990). In contrast, chronic MPTP exposure has been shown to result in sustained DA axon terminal degeneration, motor abnormalities, as well as necrotic and apoptotic like cell death (Jackson-Lewis & Przedborski, 2007; Lotharius & O'Malley, 2000; Petroske et al., 2001; Tatton & Kish, 1997). Accordingly, the use of chronic MPTP exposure more accurately recapitulates the insidious nature of DA neurotoxicity observed in PD.

The active metabolite of MPTP, MPP^+ , is taken up into DA axon terminals by DAT and causes retrograde axonopathy in NSDA neurons. As such, indices of DA axon terminals in the ST (TH and DAT protein) were measured as a positive control of successful neurotoxicant administration. NSDA neurons exhibit drastic reductions in concentrations of DAT and TH in the ST, confirming successful MPTP administration. Concomitant with these changes is a severe depletion of DA stores in axon terminals in the ST. In contrast, TIDA neurons showed no change in axon terminal DA concentrations following acute or chronic toxicant administration, nor did repeated MPTP exposure sensitize TIDA neurons to subsequent insult.

NSDA neurons, which exhibit axon terminal DA dysfunction, also exhibited loss of TH-ir cell bodies in the SN in a manner that was consistent with the severity of the dosing regimen. In contrast, there was no cell loss observed in the ARC following any of the MPTP dosing regimens examined. Loss of TH-ir cells in the SN following a single injection of MPTP most likely does not reflect actual cell death, but rather a reduction in viable TH protein within the SN. Animals in this group were sacrificed 24h following the single injection, and are thus in the active phase of MPTP-induced neurodegeneration. During this phase, which extends up to 4 days following MPTP administration, counts of TH-ir cells are consistently lower than counts of Nissl stained neurons (JACKSONLEWIS et al., 1995).

MPTP causes transient disappearance of TH in the absence of actual cell loss in several different cell types including NSDA neurons, cultured embryonic neurons, as well as retinal cells (JACKSONLEWIS et al., 1995; Sanchez-Ramos, Michel, Weiner, & Hefti, 1988; Sanchez-Ramos, Barrett, & Goldstein, 1986; Tatton & Kish, 1997). As such, the decrease in the number of observable TH-ir cells in the SN following a single injection of MPTP reflects loss of TH within these cells as opposed to dopaminergic cell death. In accordance with this idea, acute MPTP exposure had no effect on Nissl counts which reflect the total number of cells within the SN.

A deficit in protective proteins is one mechanism thought to play a role in the cellular pathology of NSDA neurons in the PD brain. Two such proteins that have been implicated in PD-pathogenesis, UCH-L1 and parkin, were differentially altered in the ARC and SN following MPTP administration in the current study. UCH-L1 concentrations were transiently decreased in the SN and transiently increased in the ARC following MPTP exposure. Previous *in vitro* studies using mouse neuroblastoma cells have shown that UCH-L1 decreases during times of maximal

oxidative stress, followed by a compensatory increase during recovery (H. H. Shen et al., 2006). In agreement, *in vivo* studies from Chapter 3 have shown that UCH-L1 concentrations in the ARC decrease 4h post-MPTP, a time when MPP⁺ concentrations are highest in TIDA neurons and the MPP⁺-induced oxidative stress is likely to be maximal (Benskey et al., 2012). This initial decrease in UCH-L1 is followed by a compensatory increase in UCH-L1 protein, which is consistent with initial injury followed by rapid recovery.

Similarly, in the present study UCH-L1 protein concentrations are increased in the cell body region of TIDA neurons 24h following acute MPTP administration, a time when these neurons have fully recovered DA homeostasis. Conversely, UCH-L1 concentrations remain low for up to 24 h in NSDA neurons. Data from Chapter 4 showed that MPP⁺ is no longer detectable in the ST at 16 h post-MPTP. Yet NSDA neurons display sustained UCH-L1 and DA depletion for up to 24 h post-MPTP, consistent with ongoing oxidative stress and dopaminergic dysfunction in the NSDA terminals. Taken together, these data are consistent with the hypothesis that TIDA neurons have a high intrinsic capacity to quell increases in oxidative stress and thus maintain a homeostatic cellular environment. The high correlation between the ability of DA neurons to increase UCH-L1 and the maintenance of axon terminal DA suggest UCH-L1 (like parkin) may play a role in this process.

In support of the idea that TIDA and NSDA neurons have a differential ability to cope with oxidative stress is the differential expression profile of parkin in the SN and ARC following MPTP. Transient decreases in parkin protein concentrations were observed in the SN for up to 24 h following the last injection of MPTP but returned to basal levels following the 21-day recovery period. Similar to the decrease in UCH-L1, the transient decrease in parkin concentrations in the

SN within 24 h of MPTP exposure is potentially mediated by increases in oxidative and nitrosative stress within NSDA neurons. Parkin is known to be nitrosylated, causing a shift in sub-cellular location from the soluble to the insoluble fraction (C. Wang, 2005). Further nitrosylation has been shown to reduce the enzymatic and protective capabilities of parkin (C. Wang, 2005; C. C. Wang et al., 2005). However, whether the observed decrease in parkin within NSDA neurons following MPTP represents oxidative or nitrosative modification is unknown and more in depth studies are needed to answer this question.

In stark contrast to the transient changes in parkin concentrations within the SN, the increase in parkin expression in the ARC following MPTP exposure is robust, reproducible and sustained. Parkin concentrations are increased within 24 h following the final injection of MPTP, but also following a 21-day recovery period. However, there appears to be a ceiling effect in the ability of MPTP to elicit an increase in parkin expression, as the additional acute MPTP administration in mice treated chronically with MPTP yielded no further increases of parkin in the ARC. Parkin mRNA increases following a single injection of MPTP (Behrouz et al., 2007), yet it is not known whether this compensatory increase in gene expression continues throughout the course of repeated toxicant exposure, or if parkin mRNA and/or protein degradation is inhibited. More detailed studies are needed to address these issues. However, it is known that there is a long-lasting change in the expression profile of the neuroprotective protein parkin in TIDA neurons following repeated exposure to MPTP and that this phenotype is distinct from that of susceptible NSDA neurons. The ability of TIDA neurons to elicit such a long lasting adaptation is likely a major determinant in their resistance to chronic toxicant exposure.

The data presented herein reveal a pattern of susceptibility in both loss of axon terminal DA stores and TH-ir cell numbers to MPTP toxicity that is highly correlated with the presence or

absence of the PD-associated proteins parkin and UCHL-1. Although previous studies have shown that parkin expression does increase specifically within DA neurons of the ARC (Benskey et al., 2012), the possibility that parkin also increases in non-DA neurons or glial cells in the same brain region cannot be excluded and may be contributory. Although likely, it is not known if the observed increase in UCHL-1 concentrations occurs within TIDA neurons themselves, or in other surrounding neurons or glia.

UCH-L1 is known to be an important component of the UPP that responds to oxidative stress, while parkin specifically seems to play a pivotal role in dopaminergic homeostasis, displaying an impressively wide range of neuroprotective benefits including; protection against oxidative stress, proteosomal dysfunction, and regulation of mitochondrial quality control (H. H. Jiang et al., 2004; Narendra et al., 2010; Petrucelli et al., 2002; Poole et al., 2008). Parkin up-regulation, whether endogenously or exogenously, protects from rotenone, paraquat, alpha synuclein, 6-hydroxydopamine and most apropos to the current study, MPTP toxicity (Manfredsson et al., 2007; Vercammen et al., 2006; C. C. Wang et al., 2005; Yamada, Mizuno, & Mochizuki, 2005; Yasuda et al., 2011). Further, the compensatory increase in the PD-associated proteins parkin and UCHL-1 following MPTP seems to be specific, as expression of other PD related genes (alpha synuclein, DJ-1, Pink1 and LRRK2) do not change (Benskey et al., 2012).

Parkin and UCHL-1 are both components of the UPP, suggesting that the ability to maintain a homeostatic environment for proper protein function plays a role in the ability of DA neurons to recover from toxicity. More detailed studies are needed in order to confirm that either parkin and/or UCHL-1 are necessary and sufficient to protect DA neurons from MPTP. To determine the role of parkin in the differential susceptibility of TIDA and NSDA neurons to

MPTP rAAV expressing parkin shRNA or a human parkin transgene were developed (Appendix A). These vectors will then be used to decrease parkin expression in TIDA neurons and over express parkin in NSDA neurons. Following the ability of TIDA and NSDA neurons to recover from a single injection of MPTP will be determined (Chapter 6).

Conclusion

Data from this chapter has shown that TIDA neurons, but not NSDA neurons, are resistant to chronic MPTP-induced loss of axon terminal DA and TH-ir cells. Further, this resistance of TIDA neurons is associated with a transient increase in UCH-L1 expression and a sustained increase in parkin expression. The findings that parkin and UCH-L1 are decreased in the soma regions of the highly susceptible NSDA neurons and increased in the soma regions of the highly resilient TIDA neurons, supports the idea that the loss of protective proteins is a contributing factor to the demise of DA neurons. Further, it appears that TIDA neurons specifically, are highly resilient due to their ability to alter expression of the neuroprotective protein parkin, an ability that is not only rapid but can also be sustained. Although the data presented herein is not causal, there remains a very high correlation between the presence of the proteins parkin and UCHL-1, and the ability of central DA neurons to recover from MPTP toxicity.

Chapter 6. The role of parkin in the differential susceptibility of TIDA and NSDA neurons to single-acute toxicant exposure

Introduction

The loss of neuroprotective proteins is thought to contribute to the demise of DA neurons in PD. Indeed, one of the major findings of this dissertation is the correlation between synthesis of key PD related proteins and the ability of TIDA neurons to recover from acute MPTP toxicity. Specifically, TIDA neurons recover axon terminal DA stores within 24 h following a single injection of MPTP and this recovery is correlated with rapid and sustained up-regulation of parkin. In contrast, NSDA neurons show sustained DA depletion along with decreased parkin protein concentrations (Behrouz et al., 2007; Benskey et al., 2012). TIDA neurons are also resistant to chronic MPTP toxicity, demonstrating that TIDA recovery is not limited to low-dose, one-time exposure (Benskey, Lee, Parikh, Lookingland, & Goudreau, 2013). The ability of TIDA neurons to recover from the same toxicity that severely damages NSDA neurons is not due to extrinsic factors. Rather TIDA neuronal recovery is thought to be mediated by an intrinsic ability to up-regulate neuroprotective proteins following cellular stress. The fact that TIDA neuronal recovery from MPTP is protein synthesis dependent supports the role of parkin expression in the recovery process (Benskey et al., 2012).

The ability of TIDA neurons to up-regulate parkin expression could account for the recovery from the neurotoxicant MPTP. Parkin has been shown to be neuroprotective against many of the cellular pathologies produced by MPTP, including proteasomal stress, mitochondrial dysfunction and DA associated toxicity (H. H. Jiang et al., 2004; Narendra, Tanaka, Suen, & Youle, 2008; Petrucelli et al., 2002). Further, exogenous overexpression of parkin can protect

against some forms of MPTP toxicity (Paterna, Leng, Weber, Feldon, & Bueler, 2007; Yasuda et al., 2011), while decreased parkin concentrations are associated with NSDA neuron vulnerability to MPTP toxicity (Benskey et al., 2012; 2013). Accordingly, parkin is an attractive candidate for an endogenous mechanism that could be responsible for the homeostatic maintenance of DA neurons as well as the recovery of DA neurons from MPTP. However, the data presented thus far is largely correlative. As such, experiments in this chapter will aim to manipulate the levels of parkin and probe the ability of TIDA and NSDA neurons to recover from MPTP toxicity in the context of decreased or increased parkin expression. In order to determine the role of parkin in the differential recovery of DA neurons from MPTP, rAAV vectors containing either parkin shRNA or a human parkin transgene were created (for details on shRNA, parkin transgene constructs or vector production see Appendix A).

AAV is a single stranded DNA dependovirus belonging to the parvovirus family. AAV has the ability to infect both mitotic and post-mitotic cells of multiple lineages, including myocytes, hepatocytes, haemopoietic progenitor cells, photoreceptors and neurons (Tenenbaum et al., 2004; Xiao, Li, McCown, & Samulski, 1997). In the current study the AAV serotype 2 will be used. This serotype is the most extensively characterized and presents natural tropism to skeletal muscles, smooth muscle and neurons. AAV 2 has been used to deliver nucleic acids to many anatomical subdivisions of the central nervous system (CNS) and primarily transduces neurons. AAV 2 has been extensively used in clinical trials and has never been associated with any human disease giving it the highest biosafety level rating of any viral vector system currently in use (Grimm & Kleinschmidt, 1999).

More specifically the experiments in this dissertation will utilize rAAV2/5. The designation of 2/5 results from the mixing of a viral genome of one serotype (in this case 2) with

the capsid from another serotype (in this case 5) creating pseudotypes of rAAV. As with different serotypes, different pseudotypes will display different tropisms as well as time courses of expression. AAV2/5 was chosen because it has previously been used to transduce DA neurons in the hypothalamus (Manfredsson et al., 2009). AAV 2/5 also shows a superior distribution of expression and multiplicity of infection as compared to a purely AAV 2 serotype (Reimsnider, Manfredsson, Muzyczka, & Mandel, 2007), allowing for increased transduction using fewer viral particles, decreasing the risk of eliciting an immune response.

Experiments detailed in this chapter will test the hypothesis that the recovery of TIDA neurons from single-acute MPTP toxicity is mediated by the ability to up-regulate parkin protein expression following toxicant exposure, whereas NSDA neuronal susceptibility to acute MPTP toxicity is due to an inability to increase parkin expression. In order to test this hypothesis, parkin expression will be knocked down in the ARC using rAAV containing parkin shRNA. Alternatively, parkin will be exogenously overexpressed in the SN using a rAAV FLAG-tagged human parkin (F-hParkin). Four-weeks following rAAV administration, mice will receive a single injection of MPTP and the ability of TIDA and NSDA neurons to recover axon terminal DA and TH concentrations will be examined 24 h post-injection.

Results

Characterization of rAAV Parkin-shRNA Vector Expression and Knockdown of Endogenous Parkin in the Medial Basal Hypothalamus

Mice received bilateral stereotaxic injection of rAAV-parkin shRNA and 4 weeks later the ability of this vector to transduce DA neurons of the MBH was determined. The rAAV vector contains a GFP reporter construct for visualization of cellular expression. Figure 6-1 shows

immunohistochemical characterization of GFP (green) and TH (red) neurons. DA neurons that have been successfully transduced will express both TH and GFP, and will appear yellow. Bilateral injection of rAAV was able to transduce the entire rostrocaudal axis of the MBH. This transduction includes vector expression within both DA and non-DA cells of the hypothalamus. Importantly rAAV expression was observed in both the cell bodies as well as the axon terminals of TIDA neurons.

Knowing that rAAV could be used to successfully transduce TIDA neurons of the hypothalamus, the ability of the parkin-shRNA to knockdown endogenous parkin expression in the ARC was determined. Four-weeks following vector injection, the ARC was removed and parkin protein was measured with Western blot. Figure 6-2 shows that 4 weeks following rAAV-parkin shRNA administration, endogenous parkin protein levels were decreased to approximately half that of non-injected controls. Administration of parkin shRNA was able to knockdown both the 44kDa and 53kDa isoforms of parkin. However, as the 53kDa MW isoform is thought to be the primary native form of the protein (Horowitz, Myers, Stachowiak, & Torres, 1999), this isoform will be used as an index of parkin concentrations in all future experiments.

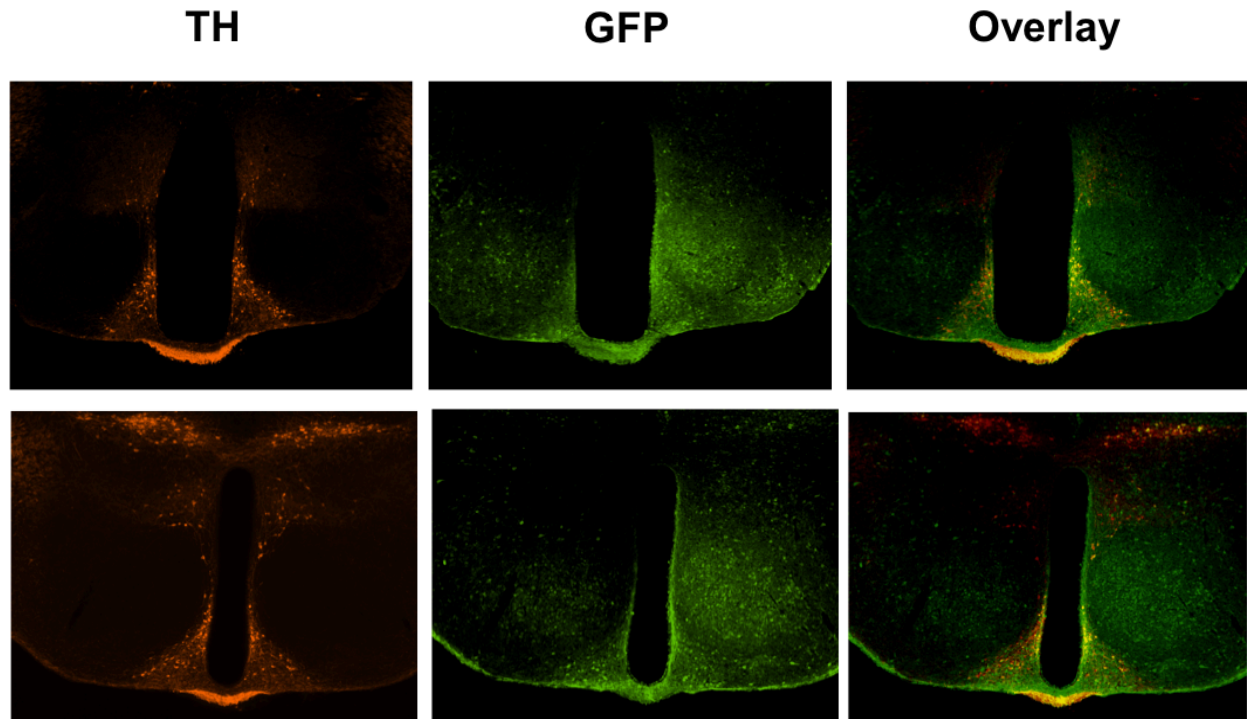


Figure 6-1. Immunohistochemical characterization of rAAV expression in the ARC.

Mice received bilateral 250nl stereotaxic injections of rAAV-parkin shRNA (3.5×10^{13}) into the ARC. Four-weeks following injection mice were sacrificed and brains were processed for IHC to visualize TH (red) and GFP (green). TIDA neurons are shown as TH-ir (red) cells surrounding the third ventricle. TIDA neurons expressing rAAV are shown as yellow cells and axon terminals in the overlay column. Approximate rostrocaudal coordinates of the representative images shown are: -1.58 (top row), -2.06 (lower row) from Bregma.

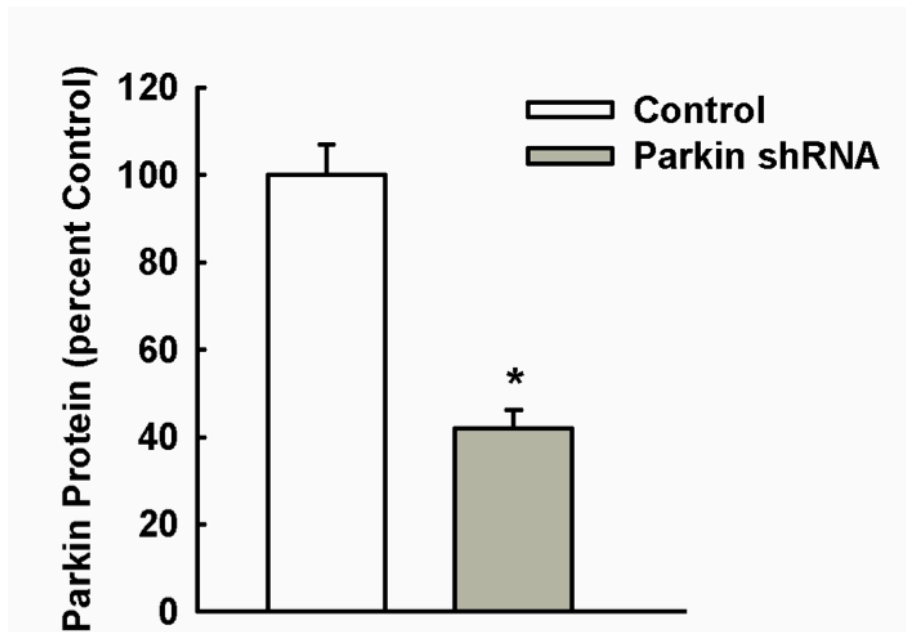
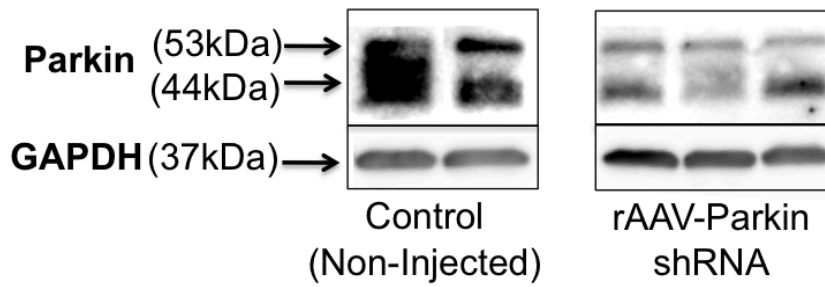


Figure 6-2. The effects of rAAV-parkin shRNA on endogenous parkin expression in the ARC. Mice (n=4/group) received bilateral 250nl stereotaxic injections of rAAV-parkin shRNA (3.5×10^{13}) into the ARC. Non-injected (NI) control animals remained naïve to surgery. Four-weeks following injection, mice were sacrificed and parkin protein was measured in the ARC by Western blot. Data is represented as parkin normalized to GAPDH expressed as percent of control treated animals. Columns represent means of groups + 1 SEM in non-injected (white column) and rAAV-parkin shRNA (grey column) treated mice. Representative blots showing the 53kDa and 44kDa isoforms of parkin are shown.

The Ability of TIDA Neurons to Recover from Single-Acute MPTP Toxicity following Knockdown of Parkin in the ARC

To determine the role of parkin in the ability of TIDA neurons to recover from MPTP, parkin was knocked down in the ARC. Mice received either scrambled parkin control shRNA, parkin shRNA, or remained naïve to surgery. Four-weeks following surgery, mice received a single injection of MPTP. Figure 6-3 shows changes in parkin protein expression in the ARC 24 h following MPTP administration. Parkin protein concentrations were increased in the ARC of non-injected, MPTP treated animals, as compared to saline treated controls in the non-injected surgery group. Injection of the scrambled shRNA had no effect on this increase of parkin protein in the ARC 24 h post-MPTP. In contrast, the parkin-shRNA knocked down parkin expression by approximately 40% compared to saline treated animals that remained naïve to surgery. This data shows that the parkin shRNA, but not the scrambled control shRNA, is able to effectively decrease parkin protein expression in the ARC, blunting the ability of TIDA neurons to up-regulate parkin expression following MPTP.

Following knockdown of parkin, TIDA axon terminal DA concentrations were measured 24 h post-MPTP. Figure 6-4 shows that in the non-injected surgery group, ME DA concentration in MPTP treated animals are no different than saline treated controls, reproducing the recovery of TIDA neurons to recover DA concentrations following a single injection of MPTP. The scrambled shRNA had no effect on the ability of TIDA neurons to recover ME DA concentrations following MPTP. However, after knockdown of parkin in the ARC, the ability of TIDA neurons to recover axon terminal DA was significantly attenuated, recovering to a mere 50% of saline treated control animals.

Knocking down parkin protein concentrations in the ARC rendered TIDA neurons susceptible to MPTP-induced DA loss, similar to that observed in NSDA neurons. Within

NSDA neurons, the loss of axon terminal DA concentrations occurs with a concomitant loss of TH protein in the ST. To determine if TIDA neurons show the same MPTP-induced decreases in TH as NSDA neurons, ME TH protein concentrations were measured in saline and MPTP treated animals following knock down of parkin in the ARC. Figure 6-5 demonstrates that despite decreased parkin protein concentrations, MPTP had no effect on TH protein concentrations in the ME.

Finally, the inability of TIDA neurons to recover from MPTP-induced DA loss following knockdown of parkin could represent off target toxicity produced by an immune response elicited by rAAV. To test the possibility of an immune response, concentrations of a marker of activated microglia, ionized calcium-binding adapter molecule 1 (IBA1), were monitored in the ARC. Figure 6-6 shows that there was no increase in IBA1 expression following rAAV administration in saline or MPTP treated animals. It should be noted that due to limitations in animals numbers the scrambled shRNA group was not included in the analysis of TH or IBA-1. However, as the scrambled shRNA had no effect on the DA profile in the ME following MPTP, nor did the parkin shRNA have an effect on TH or IBA-1, this should not confound the interpretation of the results.

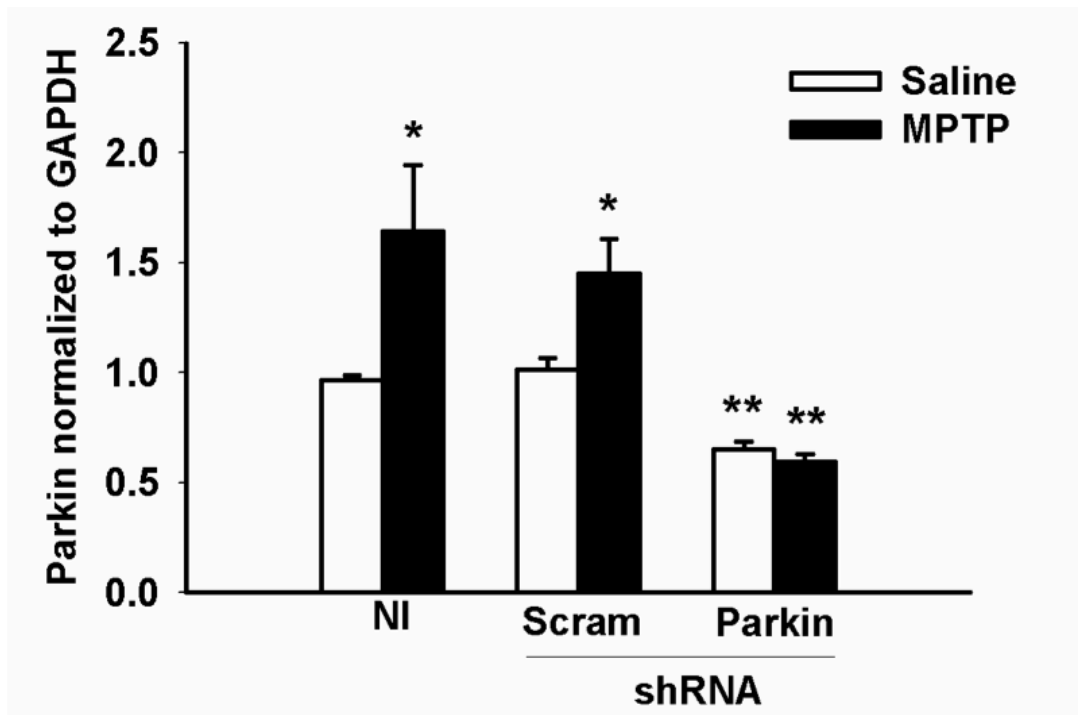
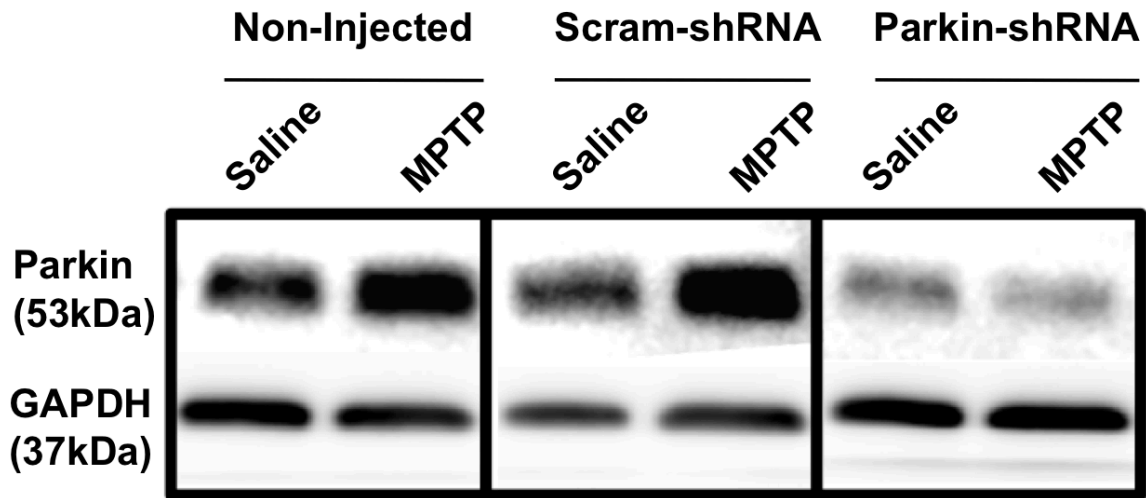


Figure 6-3. Parkin protein concentrations in the ARC following administration of scrambled or parkin shRNA in saline and MPTP treated mice. Mice (n=8/group) received bilateral 250nl stereotaxic ARC injections of rAAV (3.5×10^{13}) containing scrambled shRNA or parkin shRNA. Non-injected (NI) control animals remained naïve to surgery. Four-weeks following injection, mice were treated with a single injection of saline (10ml/kg; s.c.) or MPTP (20mg/kg; s.c.) and were sacrificed 24 h later. Parkin protein concentrations were determined by Western blotting and normalized to GAPDH. Columns represent mean parkin concentrations + 1 SEM. (*) Parkin concentrations significantly different ($p < 0.05$) from saline-treated controls. (**) Parkin concentrations significantly different than saline and MPTP treated mice in the non-injected or scrambled shRNA surgery groups. Representative blots from all groups are shown above graphs.

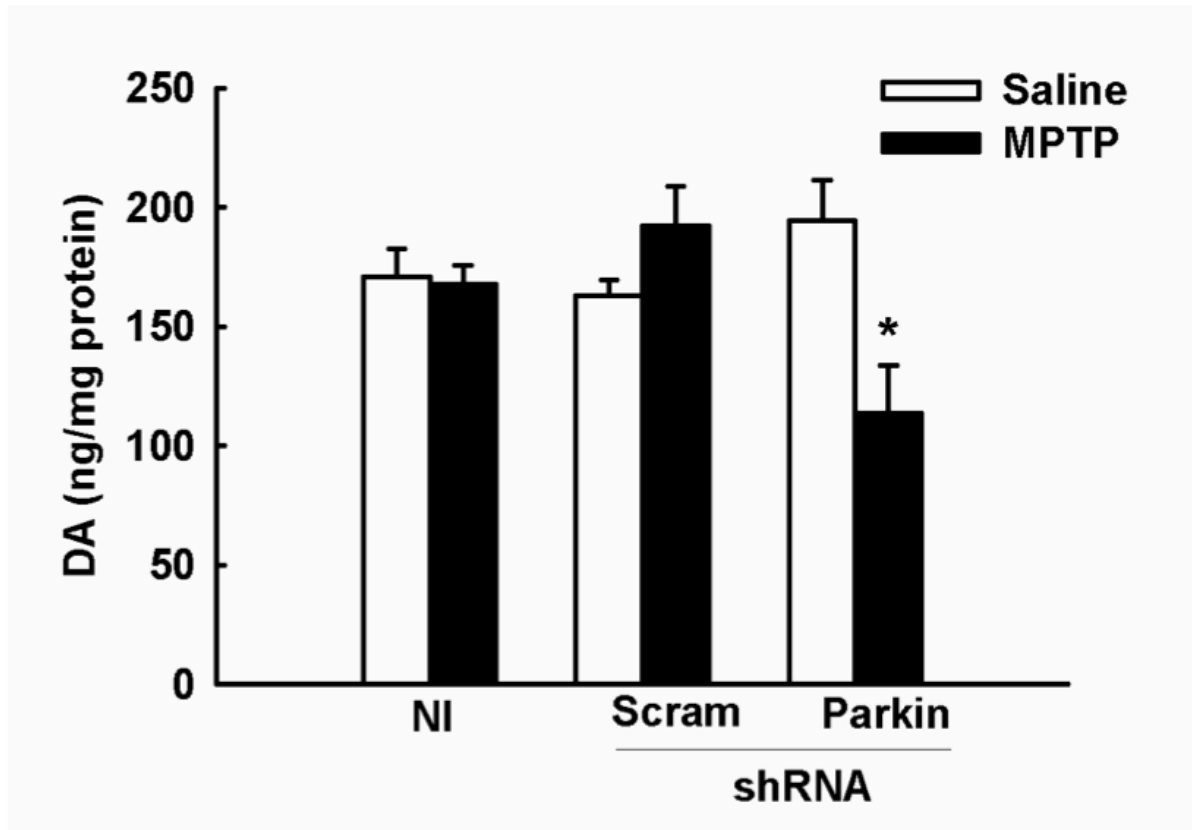


Figure 6-4. The effects of parkin knockdown on TIDA axon terminal DA concentrations following single-acute MPTP exposure. Mice (n=8/group) received bilateral 250nl stereotaxic ARC injections of rAAV (3.5×10^{13}) containing scrambled shRNA or parkin shRNA. Non-injected (NI) control animals remained naïve to surgery. Four-weeks following injection, mice were treated with a single injection of saline (10ml/kg; s.c.) or MPTP (20mg/kg; s.c.) and were sacrificed 24 h later. ME DA concentrations were determined by HPLC-ED. Columns represent mean DA concentrations + 1 SEM. (*) ME DA concentrations significantly different ($p < 0.05$) from saline-treated controls.

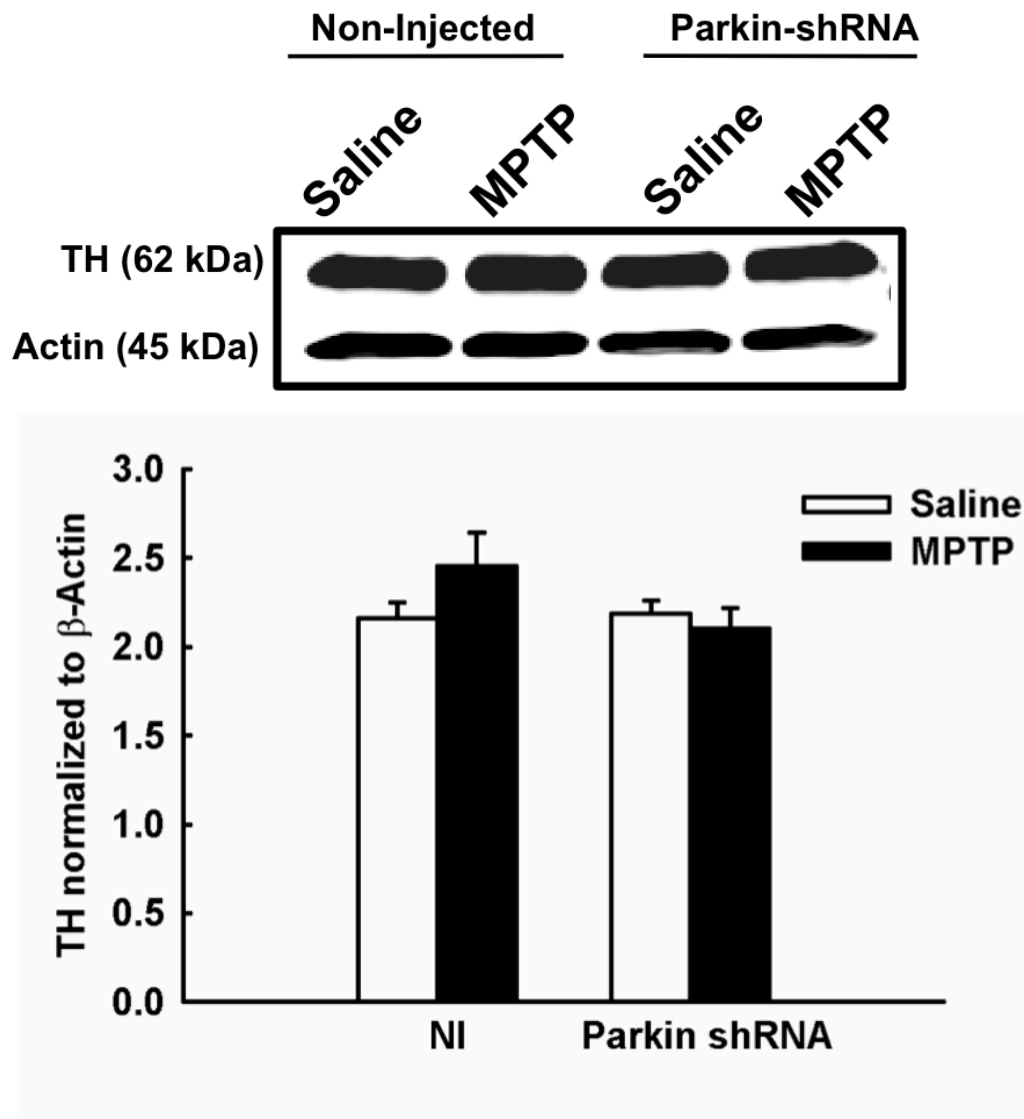


Figure 6-5. The effects of parkin knockdown on TIDA axon terminal TH concentrations following single-acute MPTP exposure. Mice (n=8/group) received bilateral 250nl stereotaxic ARC injections of rAAV (3.5×10^{13}) containing parkin shRNA. Non-injected (NI) control animals remained naïve to surgery. Four-weeks following injection, mice were treated with a single injection of saline (10ml/kg; s.c.) or MPTP (20mg/kg; s.c.) and were sacrificed 24 h later. TH protein concentrations were determined by Western blotting and normalized to β -Actin. Columns represent mean TH concentrations + 1 SEM. Representative blots from all groups are shown above graphs.

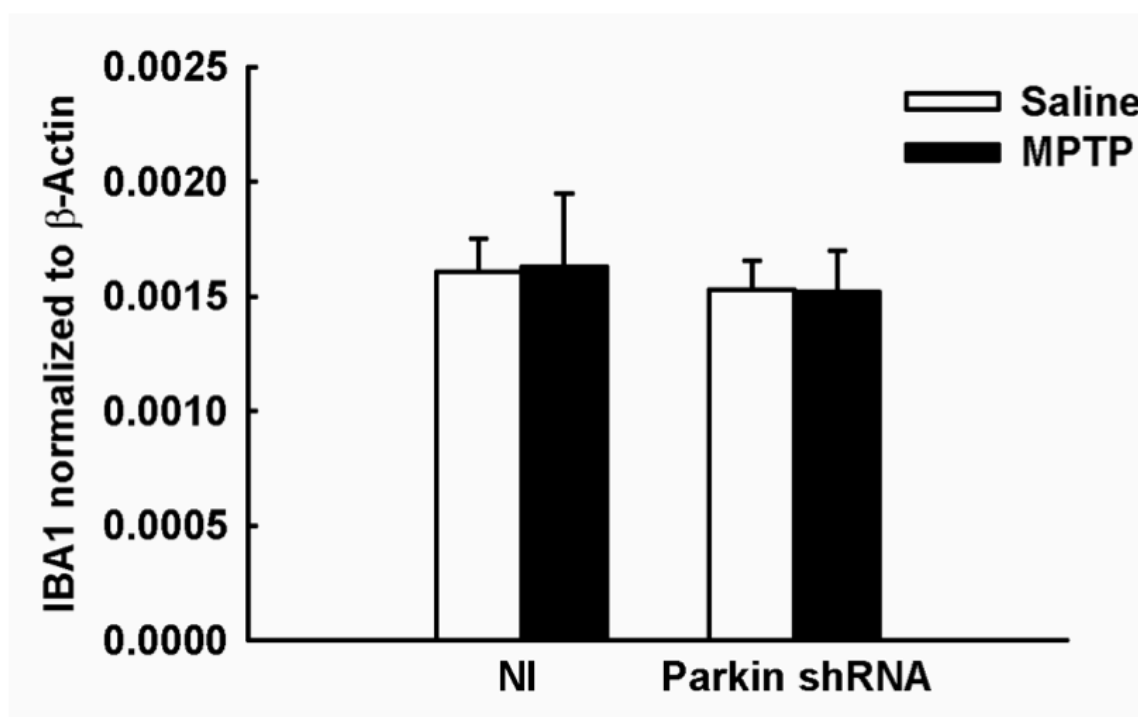
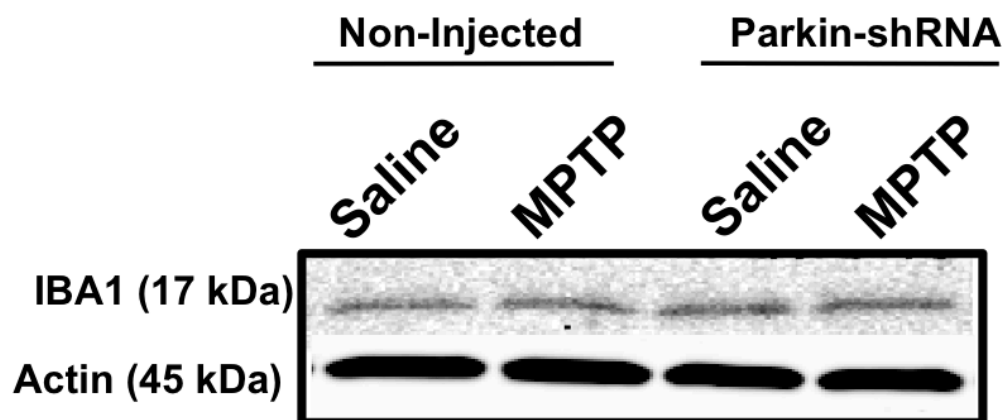


Figure 6-6. The effects of rAAV administration on neuroinflammation in the ARC. Mice (n=8/group) received bilateral 250nl stereotaxic ARC injections of rAAV (3.5×10^{13}) containing parkin shRNA. Non-injected (NI) control animals remained naïve to surgery. Four-weeks following injection, mice were treated with a single injection of saline (10ml/kg; s.c.) or MPTP (20mg/kg; s.c.) and were sacrificed 24 h later. IBA1 protein concentrations, an index of activated microglia, were determined by Western blotting and normalized to β -Actin. Columns represent mean IBA1 concentrations + 1 SEM. Representative blots from all groups are shown above graphs.

Characterization of rAAV Vector Expression and F-hParkin Protein Expression in the SN

Mice received unilateral injections of rAAV expressing F-hParkin into the left SN, allowing the use of the right SN as an internal control. Figure 6-7 shows immunohistochemical characterization of FLAG tag (green) and TH (red) expressing neurons. DA neurons that have been successfully transduced will show immunoreactivity for both FLAG and TH and will appear yellow. Figure 6-7 (Upper Panels) shows the successful transduction of the left, ipsilateral SN, leaving the contralateral SN relatively unaffected. The rAAV vector was expressed in both DA and non-DA cells in the midbrain. A large portion of the DA neurons in the SN show co-localization of FLAG and TH, confirming the successful expression of the F-hParkin protein in NSDA neurons (Figure 6-7, Lower Panels).

To further confirm the expression of F-hParkin, specifically within NSDA neurons, Western blotting was performed on tissue from the SN and ST. Following transduction of NSDA neurons, the F-hParkin protein should show anterograde transport down the NSDA axon and be detectable in the ST. Indeed, Figure 6-8, shows the presence of the exogenous F-hParkin in both the SN and ST. Further, the expression of the F-hParkin protein was limited to the SN and ST of the ipsilateral hemisphere only, confirming that the contralateral SN was not infected by the virus. This data further confirms the successful expression of F-hParkin within NSDA neurons and also validates the use of the NSDA neurons of the contralateral hemisphere as an internal control.

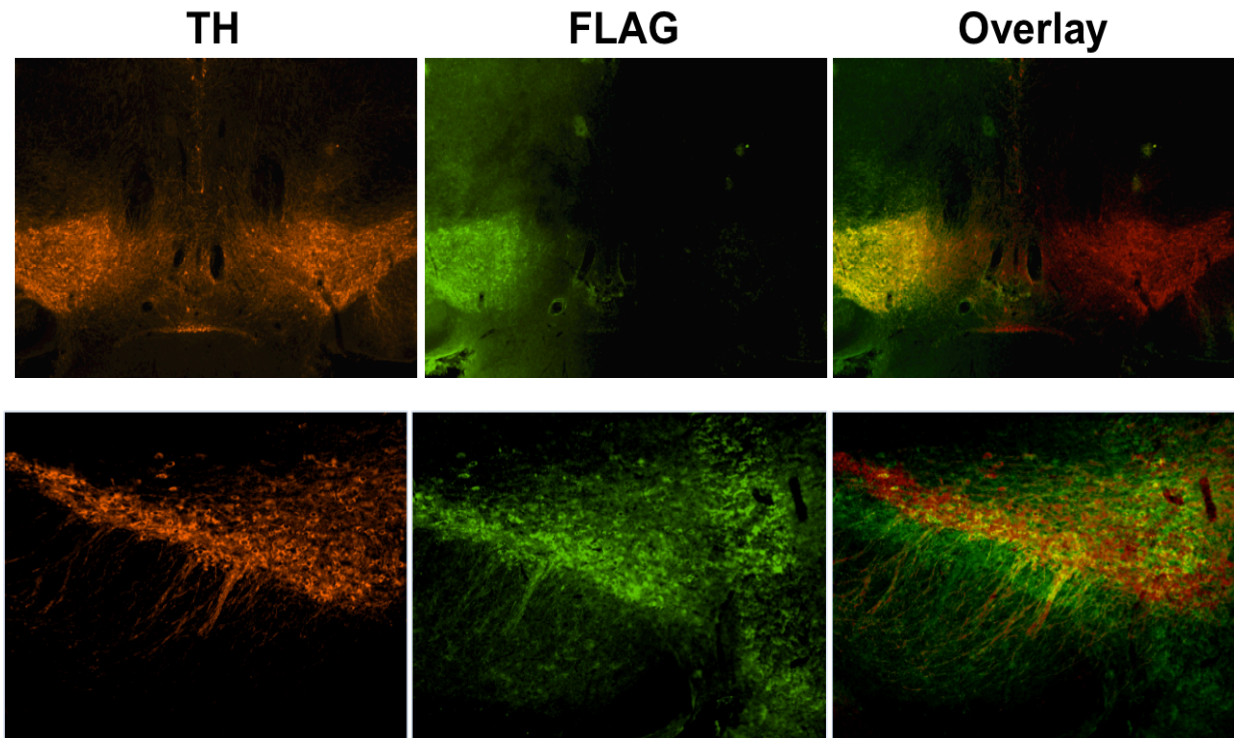


Figure 6-7. Immunohistochemical characterization of rAAV expression in the SN. Mice received unilateral 500nl stereotaxic injections of rAAV-F-hParkin (3.4×10^{13}) into the left, ipsilateral SN. The right, contralateral SN was un-injected and used as an internal control. Four-weeks following injection mice were sacrificed and brains were processed for IHC to visualize TH (red) and FLAG (green). NSDA neurons are shown as TH-ir (red). NSDA neurons expressing rAAV are shown as yellow cells in the overlay column. Upper panels demonstrate FLAG expression in the left SN, leaving the right SN devoid of exogenous parkin overexpression. Lower Panels, show co-localization of FLAG within TH expressing neurons of the left SN.

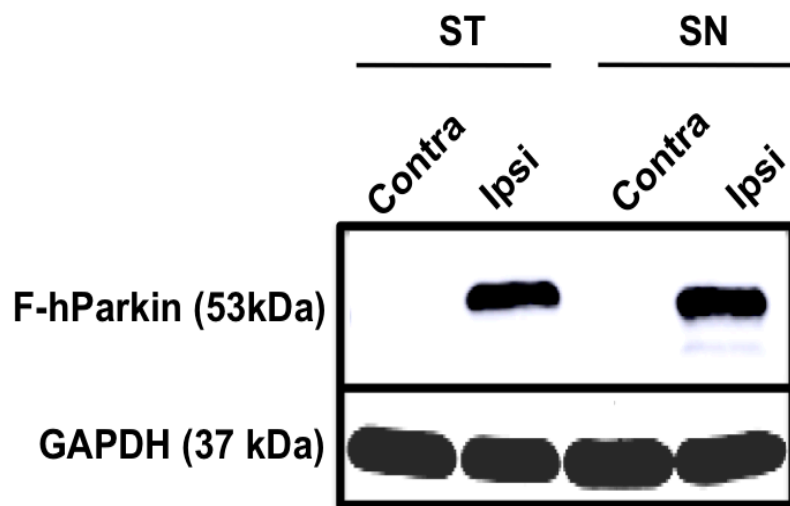


Figure 6-8. Confirmation of F-hParkin expression within the SN and ST. Mice (n=4/group) received unilateral 500nl stereotaxic injections of rAAV-F-hParkin (3.4×10^{13}) into the left, ipsilateral SN. The right, contralateral SN was un-injected and was used as an internal control. Four-weeks following injection, mice were sacrificed and F-hParkin protein was measured in the SN and ST of the ipsilateral and contralateral hemispheres by Western blot.

The ability of NSDA neurons to Recover from Single-Acute MPTP Toxicity Following Overexpression of Parkin in the SN

To determine if decreases in protective proteins following MPTP administration contributes to the pathology observed in NSDA neurons, the ability of parkin to rescue NSDA neurons from MPTP-induced decreases in striatal DA and TH was examined. Four-weeks post surgery mice were injected with a single dose of MPTP and sacrificed 24 h later. Figure 6-9 shows ST DA concentrations in the ipsilateral (injected) and contralateral (non-injected) hemispheres. Despite the successful expression of exogenous F-hParkin in the SN (Figure 6-9; Panel A) ST DA concentrations remain significantly depleted in both the ipsilateral and contralateral hemispheres 24 h post-MPTP (Figure 6-9; Panel B). However, despite the inability to rescue axon terminal DA concentrations, overexpression of parkin in NSDA neurons completely rescued the decrease in TH protein concentrations within the ST (Figure 6-10) and SN (Figure 6-11) observed 24 h post-MPTP.

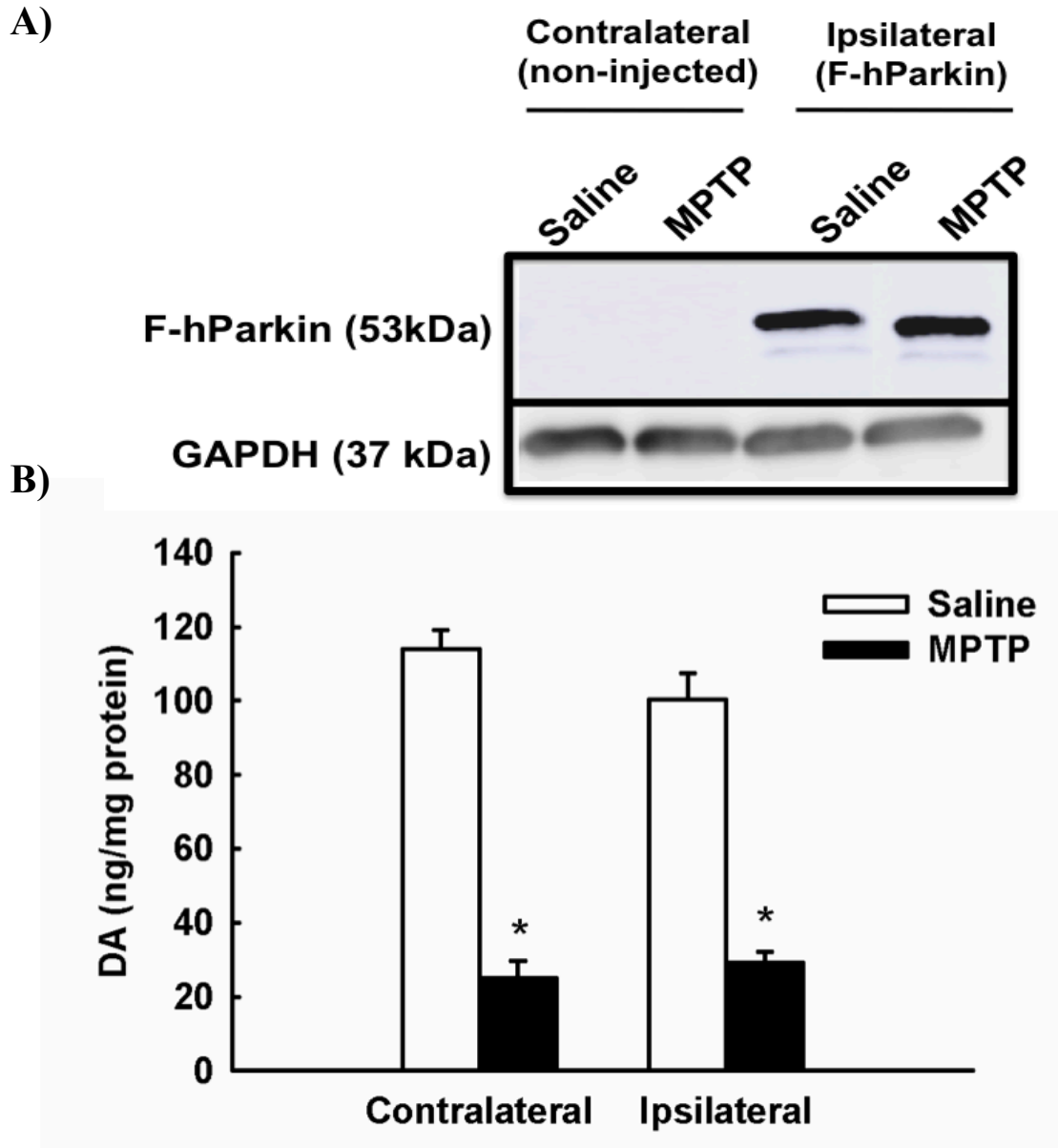


Figure 6-9. The effects of parkin overexpression on NSDA axon terminal DA concentrations following single-acute MPTP exposure. Mice ($n=8/\text{group}$) received unilateral 500nl stereotaxic injections of rAAV-F-hParkin (3.4×10^{13}) into the left SN. The right SN was un-injected and was used as an internal control. Four-weeks following injection, mice were treated with a single injection of saline (10ml/kg; s.c.) or MPTP (20mg/kg; s.c.) and were sacrificed 24 h later. Panel A, F-hParkin concentrations in the SN were determined by Western blot to confirm successful transduction of NSDA neurons in the ipsilateral hemisphere. Panel B, ST DA concentrations were determined by HPLC-ED. Columns represent mean DA concentrations + 1 SEM in the ipsilateral (injected) and contralateral (non-injected) hemispheres. (*) ST DA concentrations significantly different ($p < 0.05$) from saline-treated controls.

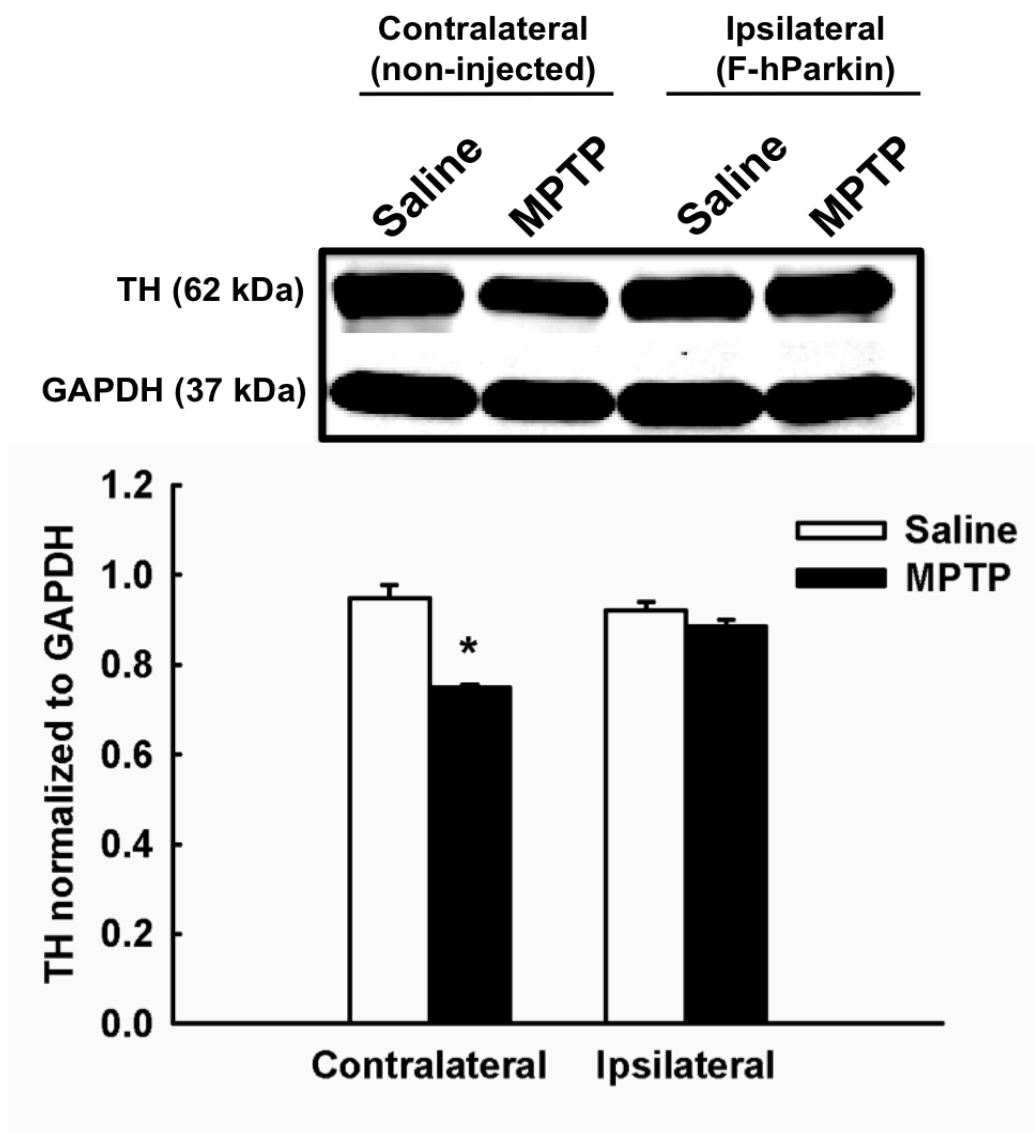


Figure 6-10. The effects of parkin overexpression on NSDA axon terminal TH concentrations following single-acute MPTP exposure. Mice (n=8/group) received unilateral 500nl stereotaxic injections of rAAV-F-hParkin (3.4×10^{13}) into the left SN. The Right SN was un-injected and was used as an internal control Four-weeks following injection, mice were treated with a single injection of saline (10ml/Kg; s.c.) or MPTP (20mg/Kg; s.c.) and were sacrificed 24 h later. TH concentrations in the ST were determined by Western blot and were normalized to GAPDH. Columns represent mean TH concentrations + 1 SEM in the ipsilateral (injected) and contralateral (non-injected) hemispheres. (*) ST TH concentrations significantly different ($p < 0.05$) from saline-treated controls.

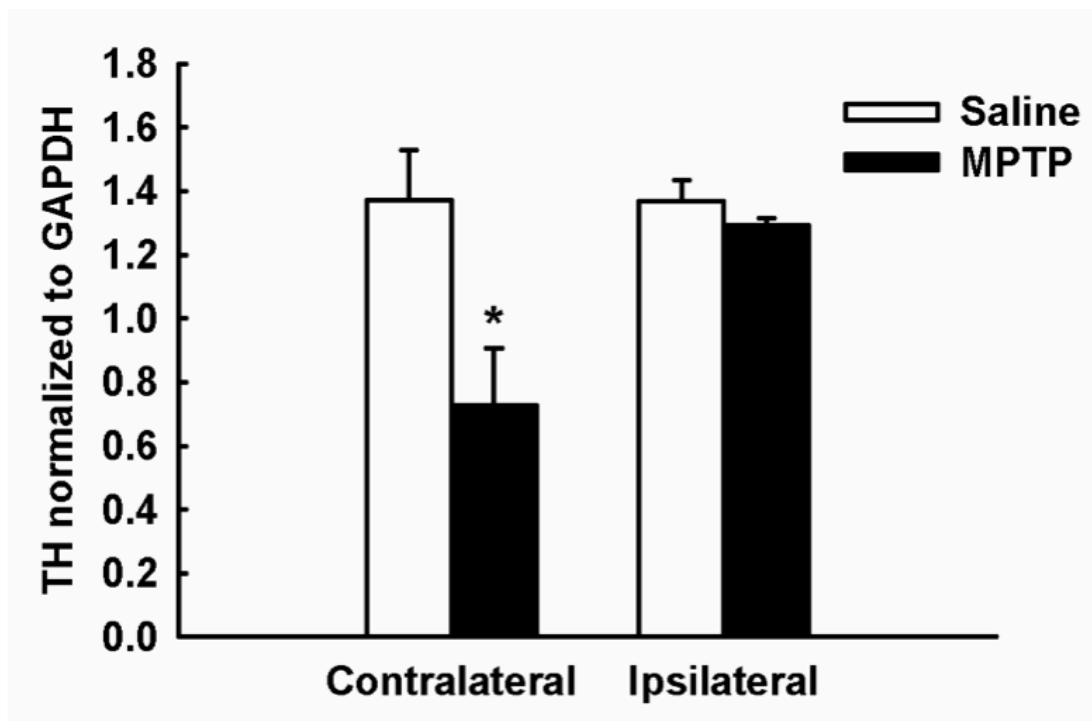
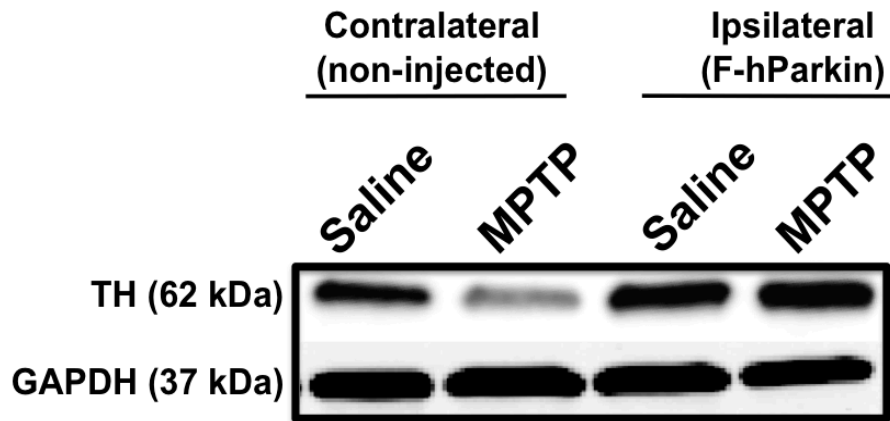


Figure 6-11. The effects of parkin overexpression on NSDA cell body TH concentrations following single-acute MPTP exposure. Mice (n=8/group) received unilateral 500nl stereotaxic injections of rAAV-F-hParkin (3.4×10^{13}) into the left SN. The Right SN was uninjected and was used as an internal control. Four-weeks following injection, mice were treated with a single injection of saline (10ml/kg; s.c.) or MPTP (20mg/kg; s.c.) and were sacrificed 24 h later. TH concentrations in the SN were determined by Western blot and were normalized to GAPDH. Columns represent mean TH concentrations + 1 SEM in the ipsilateral (injected) and contralateral (non-injected) hemispheres. (*) SN TH concentrations significantly different ($p < 0.05$) from saline-treated controls.

Discussion

There is currently increasing evidence that parkin is crucial in the homeostatic maintenance of central DA neurons. Mutations in the parkin gene cause NSDA neuronal degeneration in autosomal recessive juvenile parkinsonism (ARJP). Conversely, the ability of TIDA neurons to up-regulate parkin following cellular stress was hypothesized to mediate the recovery and/or resistance of TIDA neurons to several neurotoxicants. Data presented in this chapter confirms the role of parkin in the ability of DA neurons to maintain terminal DA homeostasis following acute MPTP toxicity. Specifically, the knockdown of endogenous parkin expression in the ARC (and the ability of TIDA neurons to increase parkin following cytotoxicity) significantly attenuated the ability of TIDA neurons to recover axon terminal DA concentrations within 24 h of MPTP administration. Further, overexpression of parkin in the SN completely rescued the MPTP-induced loss of TH in both the SN and ST. This data confirms the role of parkin in the maintenance of DA homeostasis following cellular stress. Further, the results presented herein validate the utility of exploring parkin-mediated translational therapeutics aimed at saving damaged DA neurons.

The experiments in this chapter utilized the rAAV vector in order to deliver shRNA as well as human transgenes to both the MBH and the ventral midbrain. The use of viral vector mediated manipulation of gene expression was chosen over other methods of genetic manipulation (such as transgenic or conditional mutant animals) due to the effects of developmental variables that complicate the interpretation of results. Further, the stereotaxic delivery of rAAV allows for highly precise temporal and spatial control of genetic manipulation within specific subdivisions of the CNS. Within the current studies the use of rAAV allowed for the specific knockdown of parkin expression within TIDA neurons of the ARC as well as

overexpression of parkin within NSDA neurons of the SN and ST. The ability to very precisely manipulate the levels of the parkin protein within these discrete brain regions provided an elegant platform upon which to investigate the role of parkin in the recovery of TIDA and NSDA neurons from acute MPTP toxicity.

The successful transduction of TIDA neurons in the ARC with rAAV expressing parkin shRNA, significantly decreased endogenous parkin protein concentrations. Additionally, and possibly more importantly, the MPTP-induced up-regulation of parkin in the ARC was abolished. In this context of decreased parkin expression TIDA neurons were unable to reconstitute axon terminal DA concentrations within 24 h of single-acute MPTP exposure. It is currently unclear if TIDA neurons were rendered susceptible to MPTP toxicity due to an actual decrease in parkin expression or merely an inability to up-regulate parkin following toxicant exposure. The fact that TIDA neurons show a similar inability to recover ME DA following exposure to a protein synthesis inhibitor (without directly knocking down parkin expression) supports the latter of these two possibilities. Regardless, this data confirms that parkin is, at least partially, responsible for mediating the recovery of ME DA following acute MPTP toxicity.

Although unlikely, it is possible that the inability of TIDA neurons to recover from MPTP-induced axon terminal DA loss following shRNA mediated knockdown of parkin represents an off target effect of the shRNA. This possibility is not likely due to the fact that the neither the scrambled shRNA control nor the parkin shRNA had any effects on the axon terminal DA profile of TIDA neurons under basal conditions. Further, the scrambled shRNA control did not affect the ability of TIDA neurons to recover; illustrating that merely activating the RNA-induced silencing complex (RISC) is not sufficient to render TIDA neurons susceptible to MPTP toxicity. In contrast, it took the specific knockdown of parkin prior to MPTP administration to

render TIDA neurons susceptible. Nonetheless, in order to confirm that this phenomenon is truly parkin mediated, it is necessary to repeat the same results using an alternative parkin shRNA directed toward a different target region of the parkin transcript. Additionally, the ability to rescue TIDA neurons from MPTP induced DA loss by re-introducing parkin in the ARC following knockdown of endogenous parkin expression would provide incontrovertible evidence that TIDA recovery of axon terminal DA is truly a parkin mediated phenomenon.

In contrast to the effects on ME DA, knock down of endogenous parkin in the ARC had no effect on the concentrations of TH protein in the ME within 24 h of toxicant administration. Following MPTP administration, NSDA neurons exhibit loss of axon terminal DA and TH concentrations that corresponds to a loss of parkin in the SN. As such, it was hypothesized that by decreasing parkin expression in TIDA neurons, a similar pattern of susceptibility would be seen following MPTP. However, this decrease in TH was not observed. It is possible that TH concentrations were decreased following MPTP and parkin knockdown but were not detected because they were decreased earlier within the time course. Alternatively, it is possible that the mere 40% reduction in parkin expression was not sufficient to render TIDA neurons susceptible to terminal TH loss, and a more robust knock down is needed to achieve this pathology. An additional possibility is that TIDA neurons are able to increase TH expression following MPTP exposure. Finally, the data presented herein could reflect that parkin is acting differently in separate DA neuronal populations. More detailed studies are needed to answer these questions and should be the focus of future investigations.

The AAV 2/5 vector was chosen in the current set of experiments, partially due to the low immune response associated with this vector system. However, despite the low levels of inflammation associated with AAV, there is always the risk of eliciting an immune response

when introducing a foreign substance into a host, especially when the substance is a virus. Further, MPTP has been shown to result in relatively large increases in neuroinflammation that are believed to contribute to the pathological cascade (Lofrumento et al., 2011). Indeed, administration of anti-inflammatory drugs have been found to rescue NSDA neurons from MPTP-induced loss of axon terminal DA and TH-ir cell bodies (Teismann & Ferger, 2001). As such, it is possible that the combination of rAAV and MPTP toxicity resulted in a synergistic increase in neuroinflammation in the ARC, which resulted in toxicity to TIDA neurons. To explore this possibility, concentrations of IBA1 were monitored in the ARC as an index of the presence of activated microglia. IBA1 is a protein found specifically within microglia and is up-regulated (in activated microglia) under conditions of neuroinflammation (Imai et al., 2001; Ito et al., 1998; Ito, Tanaka, Suzuki, Dembo, & Fukuuchi, 2001). The administration of rAAV, MPTP or the combination of rAAV and MPTP did not result in a measurable increase in IBA1 protein within the time frame examined. This data supports the idea that the inability of TIDA neurons to recover axon terminal DA concentrations following MPTP was mediated by decreased parkin expression and not an increase in neuroinflammation.

Finally, a note must be made on the exclusion of the scrambled shRNA surgery group in certain experimental conditions. The scrambled shRNA group was a control for the administration of an shRNA and activation of RISC within transduced neurons. Knock down of parkin was shown to decrease the ability of TIDA neurons to recover ME DA following MPTP, and as such it was necessary to confirm that the observed effect was not simply due to the activation of the RISC complex. Due to limitations in animal numbers the scrambled shRNA group was excluded from the experiments investigating the effects of parkin knockdown on TH and IBA1 concentrations. Nonetheless, if the rAAV parkin-shRNA was shown to either decrease

concentrations of TH or increase levels of IBA1, it would be necessary to include the scrambled shRNA to control for RISC activation. However, this situation was not observed and as such, the exclusion of this control should not confound the interpretation of data.

Unlike TIDA neurons, which show up-regulation of parkin following MPTP exposure and corresponding recovery, NSDA neurons show a deficit in parkin and corresponding susceptibility to MPTP toxicity. To further explore the role of parkin in maintaining DA neuronal homeostasis, the ability of exogenous parkin overexpression to rescue NSDA neurons from MPTP-induced losses of DA and TH were also investigated. rAAV containing F-hParkin was administered to the left SN, leaving NSDA neurons of the right, contralateral, hemisphere devoid of parkin overexpression for use as an internal control. F-hParkin expression was only detected in the ipsilateral SN and ST, again demonstrating the precision of stereotaxic delivery of rAAV as a tool to manipulate gene expression. Despite successful overexpression of within the ipsilateral SN 24 h post-MPTP, there was no difference in the concentrations of ST DA between the ipsilateral and contralateral hemispheres. In contrast, exogenous overexpression of parkin completely rescued the MPTP-induced loss of TH in both the ipsilateral ST and SN.

This data is in line with results from the literature. Paterna et al., 2007, found that overexpression of parkin in the SN significantly rescued MPTP-induced TH-ir cell loss but had no effect on DA depletion within the ST. While previous studies have found parkin to rescue actual TH-ir cell death following MPTP, the dosing paradigm used in the current study does not produce cell death within the time frame examined (Benskey et al., 2013). However, MPTP has been found to produce transient loss of TH in many different cell types in the absence of actual cell death (JACKSONLEWIS et al., 1995; Sanchez-Ramos et al., 1986; 1988; Tatton & Kish, 1997). Further, loss of TH is within this active phase of degeneration is one of the earliest

pathologies observed following MPTP exposure and consistently precedes further cytotoxicity and degeneration (Jackson-Lewis & Przedborski, 2007; Kastner et al., 1993; 1994). As such, the ability of parkin to prevent this initial loss of TH is likely important and may translate into a more pronounced protective benefit given time.

The mechanism by which MPTP induces loss of TH is unknown but has been attributed to nitrosative damage of TH within the active phase of MPTP induced degeneration (Ara et al., 1998; Blanchard-Fillion, 2001; Jackson-Lewis & Przedborski, 2007; Kuhn et al., 1999). Parkin overexpression has been shown to decrease levels of nitrated proteins (Hyun et al., 2005). Accordingly, it is possible that parkin is rescuing concentrations of TH in NSDA neurons through the ability to quell increases in oxidative and nitrosative protein damage. Further, parkin has also been shown to form a protein complex with C-terminus of HSC-70 interacting protein (CHIP) and heat shock protein -70kDa (HSP-70) and act as a chaperone to help refold damaged proteins (Imai et al., 2001). Although parkin has never been shown to mediate degradation of TH within the UPP, parkin may be working in concert with other protein in order to repair damaged TH through chaperone functions. Alternatively, parkin may be working upstream of TH, to indirectly maintain enzyme integrity by degrading or refolding a regulator of TH. Additionally, it is also unclear if parkin overexpression is able to rescue TH by increasing in parkin over basal levels or through the prevention of the MPTP-induced loss of parkin. Additional studies are needed to determine the mechanism by which parkin protects TH protein concentrations.

Although parkin overexpression showed pronounced protective effects on TH concentrations, parkin had no effect on loss of ST DA following MPTP. This inability of parkin to rescue DA loss in NSDA neurons could reflect the sustained inhibition of DA synthesis produced by MPP⁺.

This situation is supported by data from Chapter 4, in which MPTP causes a mere 15% reduction in TH protein in the ST, yet there is an approximate 80% decrease in TH activity. Thus despite the ability of parkin overexpression to maintain normal levels of viable TH protein in NSDA neurons, it is possible that DA synthesis is continually inhibited by the MPP⁺-induced increase in cytosolic DA, rendering NSDA neurons unable to recover ST DA concentrations.

Within TIDA neurons, MPP⁺-induced increases in cytosolic DA will leak into the hypophysial portal and be washed away from the cell. This is supported by the inhibition of PRL secretion following MPTP administration (Chapter 4). As such TIDA neurons are able to reconstitute normal DA synthesis much faster than NSDA neurons. Following, the ability of these neurons to efficiently refill synaptic vesicles is reflected in recovery of ME DA concentrations within 24 h of toxicant administration. Parkin likely plays a role in the refilling of synaptic vesicle through its ability to interact with and stabilize the microtubule (MT) framework. Parkin binds to MT and this interaction has been shown to drastically increase stability and prevent depolymerization of MTs (Ren, Jiang, Yang, Nakaso, & Feng, 2008; Yang et al., 2005). While parkin supports MT stability, MPP⁺ causes large increases in MT depolymerization and also inhibits tubulin polymerization (Cappelletti, Maggioni, & Maci, 1999; Cappelletti, Pedrotti, Maggioni, & Maci, 2001; Cappelletti, Surrey, & Maci, 2005; Ren, Liu, Jiang, Jiang, & Feng, 2005). This breakdown of a stable MT framework impairs the ability of the cell to efficiently traffic vesicles to and from the membrane, and consequently the ability to refill synaptic vesicles.

Thus, following MPTP administration, the MPP⁺-induced depolymerization of MTs is prevented by parkin, maintaining a stable MT framework. Under normal conditions, TIDA neurons are able to quickly reconstitute DA synthesis following MPTP administration. At the

same time, the ability of parkin to maintain a stable MT framework allows for quick and efficient vesicular trafficking and repackaging, and the observed recovery of ME DA. Following knock down of parkin in TIDA neurons, it is likely that the ability to refill vesicles is compromised thereby accounting for the deficit in ME DA observed 24 h post-MPTP. This same scenario would not benefit NSDA neurons due to the sustained decrease in DA synthesis observed in the ST following MPTP. Thus, it is possible that parkin overexpression rescues MT depolymerization within NSDA neurons, however, due to sustained decreases in DA synthesis, vesicular DA remains depleted.

An alternative explanation is that the benefits of endogenous parkin up-regulation differ from that of exogenous parkin overexpression. The human parkin construct used in the current experiments contained an N-terminal FLAG tag. The FLAG moiety is essentially a string of highly charged aspartic acid residues. Although, this same FLAG tagged parkin construct has been functionally validated and used in many mechanistic studies (Geisler et al., 2010; Imai et al., 2001; Imai, Soda, & Takahashi, 2000; D. J. D. Moore, 2006), the possibility remains that for the specific end points examined, the FLAG tag interfered with the normal function of parkin (e.g. MT stabilization). The work by Paterna et al., 2007, in which parkin overexpression was unable to rescue ST DA depletion following MPTP, supports this. Although the parkin construct used in these studies did not have an N-terminal FLAG tag, it did have an N-terminal HA tag, suggesting that the N-terminal domain may be important in the ability of endogenous parkin to rescue axon terminal DA concentrations within TIDA neurons. Although there are many possibilities that could explain the discrepancy in the effects of parkin on axon terminal DA and TH within TIDA and NSDA neurons, these possibilities are merely speculation. Accordingly

additional studies are needed to elucidate the mechanism by which parkin is mediating neuroprotection in these separate DA subpopulations.

Conclusion

The data presented in this chapter confirm that the ability of TIDA neurons to recover axon terminal DA concentrations following MPTP administration is mediated by an ability to increase parkin expression. Although parkin is up-regulated specifically within TIDA neurons following MPTP, the possibility that parkin also increases in non-DA neurons or glial cells in the same brain region cannot be excluded and may be contributory. Additionally, while this work confirms that parkin does play some role in TIDA neuronal recovery following acute toxic insult, the contribution of other proteins (e.g. UCH-L1) cannot be excluded and may also aid the recovery of these neurons.

Parkin was shown to rescue MPTP-induced decreases in TH within the ST and SN. These results confirm that the loss of protective proteins plays at least some part in the MPTP-induced degeneration of NSDA neurons. Using a combination of knock down of endogenous parkin to render TIDA neurons MPTP-susceptible, and the over expression of exogenous parkin to partially rescue NSDA neurons from MPTP provides strong support for the role of parkin in DA homeostasis. The data presented herein supports the role of parkin in the protection of DA neurons and suggests that parkin represents a promising target for translational therapeutics aimed at halting NSDA neuron degeneration in PD.

Chapter 7. General Discussion and Concluding Remarks

One of the major defining features of PD pathology is that it is primarily relegated to central DA neurons. However, not all central DA neurons are affected to the same extent in PD. Specifically, NSDA neurons show profound degeneration while TIDA neurons are spared (Ahlskog, 2005; Braak et al., 2003; Langston & Forno, 1978; Matzuk & Saper, 1985). A similar pattern of differential susceptibility is observed following administration of the DA-neuron specific neurotoxicant MPTP (Behrouz et al., 2007; Benskey et al., 2012; 2013). This dissertation describes in detail, the early events that occur following MPTP administration in TIDA and NSDA neurons. By investigating the narrow window of time following MPTP administration in which TIDA neurons recover and NSDA neurons display sustained pathology, it was the goal of this dissertation to identify early molecular events which are responsible for the differential susceptibility of central DA neurons to toxicity. To this end, it was found that the protein parkin plays an integral role in the ability of DA neurons to recover from toxicant administration. The findings presented in this dissertation provide further support for the development of parkin-based translation therapeutics that could be targeted to halt the degeneration of DA neurons in PD.

The Single-Acute MPTP Paradigm

The majority of experiments presented in this dissertation describe the initial events that occur in DA neurons following an acute dose of MPTP. The purpose of using a small, one-time dose with a short time course thereafter was to identify earlier mediators of cytotoxicity and/or recovery that differ between NSDA and TIDA neurons. Following identification of differential cellular responses between TIDA and NSDA neurons to acute toxicant administration, these

early changes were used as a predictive index of neuronal resistance (or susceptibility) to a more insidious MPTP dosing paradigm, which closer resembles the toxicity observed in PD. Finally, the early molecular events identified during the recovery of TIDA neurons were adapted to NSDA neurons in an attempt to protect these cells from toxicity. Within the limited scope of the endpoints examined in this dissertation, the purpose of this experimental paradigm was achieved.

Following a single injection of MPTP, TIDA neurons are able to recover ME DA concentrations and show no change in ME TH concentrations. As a predictive index, this would suggest that TIDA neurons are resistant to chronic MPTP toxicity as well. Indeed, TIDA neurons were completely resistant to chronic MPTP-induced cell death as well as decreases in ME DA. In contrast, NSDA neurons are extremely vulnerable to a single injection of MPTP, displaying decreased concentrations of DA and TH in the ST. Again, these initial pathologies were predictive of future toxicity, as NSDA neurons exhibited robust decreases in axon terminal DA, DOPAC, TH and DAT as well as significant cell death following chronic toxicant exposure. Further, the ability of TIDA neurons to recover from MPTP was associated with an increase in parkin expression (following both single-acute and chronic MPTP), while NSDA susceptibility was associated with decreases in parkin protein concentrations. These early differences in parkin suggested that this protein was involved in the ability of DA neurons to recover from MPTP. This was also confirmed, as decreasing parkin rendered TIDA neurons susceptible to MPTP toxicity. Accordingly, the neuroprotective effects of parkin up-regulation were adapted and translated to NSDA neurons and parkin overexpression partially rescued NSDA neurons from MPTP. This data validates the exploration of early events following single acute MPTP exposure as a method to identify mechanism that mediate recovery or susceptibility of DA neurons to cytotoxicity.

Additionally, examination of the early events in DA neuronal toxicity is important to the understanding of the complex interactions of toxicity that result in DA neuronal degeneration in PD. The degeneration of DA neurons in PD most likely does not result from a single event, but more plausibly from multiple deleterious events, which together, culminate in irreversible toxicity. Similarly, chronic MPTP exposure is not truly chronic, but more accurately a series of single-acute toxic events administered sequentially. As such, in order to truly understand the complex nature of DA neuronal degeneration it is necessary to understand how the constitutive components of neurotoxicity contribute to the final manifestation of pathology. Only then is it possible to understand the additive or synergistic effects of individual deleterious events to the gestalt of PD pathology. Described in this dissertation is a comprehensive characterization of the effects of a single injection of MPTP (including axon terminal DA, DA metabolite, MPP⁺, TH protein, TH activity, as well as TH-ir and Nissl cell numbers) within two sets of DA neurons that are differentially affected by MPTP and PD. It is the hope that this information can be used a building block in order to dissect the complex interaction which ultimately contribute to the susceptibility or resistance of DA neurons to PD pathology.

The Role of DA Clearance in the Endogenous Neuroprotective Capability of TIDA Neurons

TIDA neurons are a unique subpopulation of central DA neurons that are resistant to PD and are able to recover from initial toxicity produced by the parkinsonian toxicant MPTP. Specifically, TIDA neurons are able to recover axon terminal DA concentration after an initial, but pronounced, MPTP-induced loss of terminal DA. The major motor symptoms observed in PD are the result of degeneration of NSDA neurons and a corresponding loss of DA neurotransmission in the ST. However, in the progression of PD pathology, especially early in

the disease, there is likely a set of NSDA neurons that have sustained damage but have not yet died. Thus, discerning the mechanisms underlying the ability of TIDA neurons to recover normal DA neurotransmission following initial toxicity is a phenomenon that could potentially be translated to treatment of early stage PD patients in order to restore and maintain DA neurotransmission in the ST.

Although the ability of TIDA neurons to recover DA concentrations following acute MPTP toxicity was shown to be independent of extrinsic factors (such as reduced toxicant exposure or hormonal activation), there is indirect evidence presented in this dissertation that the ability to mitigate large and sustained increases in cytosolic DA plays a role in the recovery of these neurons. At 4 h post-MPTP administration, axon terminal DA is severely decreased in TIDA neurons, corresponding to a time when MPP^+ concentrations are maximal in the ME. It is likely that this initial decrease in vesicular DA represents an MPP^+ -induced purging of DA from synaptic vesicles into the cytosol. This is supported by a decrease in DA synthesis at the 4 h time point, most likely representing end product inhibition of TH activity. However, following this initial insult, TIDA neurons are able to quickly reconstitute normal DA synthesis and recover vesicular DA stores. It is possible that the recovery of DA homeostasis within TIDA neurons is the result of a quick and efficient clearance of cytosolic DA into the extracellular fluid.

It is possible that the hypophysial portal circulation contributes to the clearance of cytosolic DA. MPP^+ -induced increases in cytosolic DA will leak from the cell and enter the hypophysial portal circulation, at which point the DA will be transported away from TIDA neurons. This theory is supported by the large decrease in PRL secretion at the 4 h time point,

when ME DA concentrations are low and MPP⁺ concentrations are high. During the early time points following MPTP administration a similar situation is observed in the ST, however unlike TIDA neurons, NSDA neurons show sustained depletion of vesicular DA and DA synthesis. Increases in NSDA cytosolic DA are also purged to the extracellular space (Giovanni et al., 1994), however in the case of NSDA neurons this extracellular DA can then activate D₂ autoreceptors or reenter the NSDA cytosol through the actions of DAT. The inability to clear or repackage this DA results in sustained DA synthesis inhibition and generates a cycle of toxicity. Again this is supported by the enduring decreases in striatal DA and DA synthesis observed long after MPTP administration, even when MPP⁺ is no longer detectable in the ST.

Beyond the inhibition of DA synthesis, prolonged increases in cytosolic DA will render DA vulnerable to autooxidation, resulting in severe cytotoxicity (Lotharius et al., 1999; Lotharius & O'Malley, 2000). These findings support the role of aberrant DA metabolism and DA toxicity in the early stages of DA neuronal toxicity. Accordingly, potential therapeutics could be aimed at quelling sustained increases in cytosolic DA. Although TIDA neurons are able to accomplish this based on their unique neuroanatomical location, this could potentially be accomplished in NSDA neurons by increasing DA vesicular sequestration or developing a more efficient DA chelating mechanism. These therapeutics targets may seem counterintuitive, as the majority of PD treatments aim at increasing DA within NSDA neurons. However, it is likely that early in the progression of PD, increased cytosolic DA plays a role in the pathological cascade. As such, the ability to clear or repackage cytosolic DA could hold therapeutic efficacy. As our diagnostic capabilities increase and PD patients are identified prior to massive NSDA degeneration, the utility of DA clearance based therapeutics may increase.

The Role of Protein Synthesis in the Endogenous Neuroprotective Capability of TIDA Neurons

The recovery of TIDA neurons from MPTP has also been shown to be protein synthesis dependent, thus, although the ability of these neurons to clear cytosolic DA likely plays a role, it cannot fully account for recovery from MPTP. Within this dissertation it was confirmed that the ability of TIDA neurons to up-regulate parkin expression following MPTP is at least partially responsible for the restoration of ME DA concentrations. These data confirm that TIDA neurons represent a novel, central DA neuronal system that physiologically increases expression of parkin as a mechanism to facilitate the prompt recovery from toxicant-induced damage. Demonstration of an endogenous, cell autonomous, parkin-mediated mechanism that promotes DA neuronal recovery from injury lends support to the strategy of exogenously increasing parkin expression as a therapy to restore DA homeostasis within damaged DA neurons. However, when parkin was overexpressed within NSDA neurons it was unable to restore normal ST DA concentrations following MPTP.

The inability of parkin overexpression to maintain ST DA concentrations following MPTP could be due to technical factors. For example the use of exogenous human parkin, as opposed to the endogenous murine parkin that is upregulated in TIDA neurons, could have affected the ability of parkin to mediate DA recovery. It is also possible that the level of parkin overexpression achieved was not high enough for recovery or the presence of the FLAG-tag interfered with the ability of parkin to restore normal DA concentrations.

Alternatively, it is possible that the compensatory up-regulation of parkin within TIDA neurons in response to an acute neuronal disruption is a component of a broad, yet region specific response to injury. Accordingly, it is possible that overexpression of other neuroprotective proteins in addition to parkin is necessary to maintain ST DA following MPTP.

The work in this dissertation has shown that beyond parkin, UCH-L1 concentrations are also up-regulated in the ARC following MPTP. As such, this protein represents another interesting target that could potentially be used to rescue NSDA neurons.

TIDA axons terminate in the ME, a circumventricular region where the blood brain barrier is relatively porous, potentially creating a microenvironment of increased toxicant exposure. In this context, it is possible that TIDA neurons are specially suited to rapidly up-regulate proteins, like parkin and UCHL-1, which allow for survival in the face of exposure to potentially hazardous molecules that produce acute injury. Thus, although parkin was identified and confirmed to represent a neuroprotective protein that is used by TIDA neurons to ameliorate the damage caused by acute toxicity, the translation of this mechanism to NSDA neurons produced only modest protection. Accordingly a more powerful tool would be to identify the suite of genes that are up-regulated by TIDA neurons and express these in NSDA neurons.

This could potentially be done using gene therapy to administer multiple genes expressing proteins with overlapping and coordinated effects. However, a more elegant solution would be to determine the combination of transcription factors that work in concert in order to produce the rapid and coordinated up-regulation of neuroprotective proteins in TIDA neurons following MPTP. It could be possible to tease apart the signaling pathways and transcription factors responsible for the toxicant-induced coordinated up-regulation of neuroprotective proteins, and apply these to NSDA neurons. This could potentially enable NSDA neurons to respond to neurotoxicity with a cell autonomous, toxicant-induced up-regulation of neuroprotective proteins, similar to that observed in TIDA neurons. However, it is first necessary to determine all aspects of TIDA neuroprotection as well as the mechanism by which this neuroprotection is initiated and implemented.

The ability of TIDA neurons to increase expression of neuroprotective proteins may still represent only a portion the ability of these neurons (or this brain region) to respond to toxicity. It is possible that the ability to increase trophic support or quell neuroinflammation may also play a role in the recovery of these neurons. Thus, TIDA neurons seem to represent a subset of neurons with an innate capability for self-protection in the face of toxicity. Taken together, TIDA neurons represent a novel platform to study endogenous neuroprotection with the potential to translate a self sustaining therapy that would allow DA neurons to initiate self-protective mechanism in the face of the toxicity that is associated with PD.

The Role of Decreased Parkin in the Degeneration of DA Neurons

Since the discovery of familial linked PD, the loss of neuroprotective proteins has been suspected to contribute to degeneration of NSDA neurons in PD. Data from this dissertation provides evidence that beyond genetic mutation, NSDA neuron are susceptible to toxicant-induced loss of proteins. In contrast to TIDA neurons, NSDA neurons displayed decreased concentrations in both parkin and UCH-L1 following a single injection of MPTP. These decreases in protein concentrations correlate with sustained dysfunction within the NSDA axon terminal. The loss of parkin following MPTP was confirmed to contribute to the pathology of NSDA neurons, as parkin overexpression was able to completely rescue MPTP-induced loss of TH in the ST and SN. These data confirm that parkin mediates neuroprotection within NSDA neurons and loss of parkin results in dysfunction. However, it also calls into question the contribution that the loss of protein function plays in idiopathic PD.

Mutations in parkin, and corresponding loss of protein function, produce rare forms of familial PD (Kitada et al., 1998). This finding clearly demonstrates that parkin is important in

NSDA neuronal survival; however, familial forms of PD are very rare and only represent approximately 5-10% of all cases of PD (de Lau & Breteler, 2006). It has recently been suggested that a mere reduction in functional parkin, as opposed to the complete ablation of parkin, is sufficient to cause NSDA neuronal degeneration. Parkin associated ARJP is caused by either homozygous or compound heterozygous parkin mutations, in either case, both alleles are affected (Kitada et al., 1998; Rainer von Coelln, Dawson, & Dawson, 2004). However recent reports have found cases of PD in which only one allele is affected, indicating that haploinsufficiency of parkin is sufficient to induce parkinsonism (Farrer et al., 2001; Rainer von Coelln et al., 2004).

As decreased parkin due to haploinsufficiency seems to be sufficient to render NSDA neurons susceptible to degeneration, it has been theorized that loss of parkin function could also play a role in idiopathic PD. The discovery that two forms of oxidative stress negatively affect the function of parkin has confirmed this theory. Parkin is S-nitrosylated within the cysteine rich catalytic RING domains of the parkin protein. S-nitrosylation severely impairs the enzymatic activity of parkin and thus also impairs the neuroprotective capabilities of the protein. Increased concentrations of S-nitrosylated parkin have been documented in animal models of PD as well as post mortem tissue from the SN of PD patients (Chung et al., 2001; Yao et al., 2004).

Further, DA has also been shown to negatively modify parkin. Following DA autooxidation, the DA-quinone covalently binds to parkin resulting in an aggregate-prone, loss-of-function form of parkin. The covalent DA modification of parkin has also been identified in neural tissue from post mortem PD patients (Lavoie, Ostaszewski, Weihofen, Schlossmacher, & Selkoe, 2005). This further supports the role of cytosolic DA toxicity in NSDA degeneration but more importantly, these data provide the first direct link between loss of parkin and idiopathic

PD, indicating that toxicant induced modification of parkin could recapitulate the loss of function that is associated with parkin mutations.

The data in this dissertation are in line with these reports from the literature. Following exposure to a single injection of MPTP, parkin protein concentrations are decreased in the SN. Within DA neurons MPP⁺ causes large increases in reactive nitrogen species and cytosolic DA (Chung, 2004; Lotharius & O'Malley, 2000). Thus, through two distinct mechanisms, MPTP administration likely results in loss of function modification of parkin through s-nitrosylation as well as DA-quinone modification. Supporting this theory, MPTP has been shown to increase S-nitrosylation of parkin (Chung, 2004). As such, it is likely that the loss of parkin in the SN following MPTP observed in the current study represents oxidative modification of parkin. Further supporting this scenario, parkin mRNA is unchanged in the SN following MPTP administration (Benskey et al., 2012), thus decreases in parkin protein do not represent decreased parkin expression but most likely protein modification. Both S-nitrosylation and DA quinone modification of parkin result in an aggregate prone form of the protein (Chung, 2004; Lavoie et al., 2005; Tsang & Chung, 2009; Yao et al., 2004). Accordingly, it would be interesting to determine if the loss of parkin observed in the SN following a single injection of MPTP is associated with a corresponding increase of parkin protein concentrations within the insoluble fraction. Additional studies should be undertaken to determine if parkin is oxidatively modified within the SN following a single injection of MPTP.

Ironically, parkin seems to be severely sensitive to the same toxicity that it can protect against. Thus, it is likely that the ability of TIDA neurons to up-regulate parkin allows these cells to overcome deficits produced by oxidative and nitrosative modification of parkin. As demonstrated in this dissertation, up-regulation of parkin obviates the loss of parkin-mediated

neuroprotective benefits and allows TIDA neurons to recover from MPTP toxicity. It is clear that the ability to up-regulate, or at least maintain, normal parkin function is crucial for the survival of DA neurons. It has been shown that decreased parkin results in NSDA neuronal degeneration; however, it is not clear if all NSDA neurons are equally prone to loss of parkin. Following MPTP administration or within the PD brain, there are likely surviving NSDA neurons that are presumably more resistant to toxicity than other NSDA neurons that have degenerated. As such, it would be very interesting to sample these “resistant” NSDA neurons to determine if they display increases in parkin or other neuroprotective proteins. This would provide further support for the role of parkin in the survival of DA neurons in the face of toxicity.

Taken together it is clear that loss of parkin due to mutations, oxidative modification or knockdown render DA neurons susceptible to toxicity. In contrast, increased parkin expression through endogenous up-regulation or exogenous overexpression is protective. Thus, parkin is clearly a crucial component in the homeostasis and survival of DA neurons. Yet despite the strong body of evidence showing parkin-mediated protection the precise pathways involved in its pro-survival properties remain elusive.

Mechanisms of Parkin Neuroprotection

As was detailed in the General Introduction (Chapter 1), parkin acts as an E3 ligase in the UPP and has been shown to mediate K48 linked polyubiquitination, leading to proteasomal degradation. In addition, parkin can mediate alternative K63 linked polyubiquitination and monoubiquitination, leading to autophagic degradation or post-translation modification of target proteins (Lim, 2005; Lim et al., 2006). Parkin is also involved in mitochondrial homeostasis. Under conditions of oxidative stress, parkin is recruited to the outer membrane of dysfunctional

mitochondria where it appears to play a role in mitophagy in order to maintain mitochondrial homeostasis. As the majority of parkin mutations or oxidative modifications inhibit the E3 ligase activity of parkin (Chung, 2004; Henn, Gostner, Lackner, Tatzelt, & Winklhofer, 2005; Imai & Takahashi, 2004; Lavoie et al., 2005; Matsuda et al., 2006), it is speculated that loss of functional parkin causes aberrant or decreased ubiquitination, leading to corresponding deficits in the UPP or mitochondria. Thus, it is possible that in the current experiments toxicant administration causes oxidative loss-of-function parkin modifications, resulting in the accumulation of toxic substrates or the inability to maintain mitochondrial function within NSDA neurons. In contrast, the up-regulation of parkin observed within TIDA neurons following MPTP would allow for maintenance of mitochondrial function and efficient degradation of potentially toxic substrates.

Since the discovery that parkin is an E3 ubiquitin ligase, there have been many putative parkin substrates identified. However, recent research has cast doubt on the authenticity of some parkin substrates, as they do not accumulate in the brains of parkin KO mice or ARJP patients. Currently, the list of “authentic” parkin substrates includes aminoacyl-tRNA synthetase interacting multifunctional protein type 2 (AIMP2), far upstream element-binding protein 1 (FBP-1) and PARIS (Ko, 2005; 2006; Shin et al., 2011). The contribution of AIMP2 and FBP-1 to the degeneration of NSDA neurons is currently not clear. However, the recently identified PARIS has been linked to parkin and the UPP as well as mitochondrial maintenance.

PARIS acts as a transcriptional repressor of peroxisome proliferator-activated receptor gamma (PPAR γ) coactivator-1 α (PGC-2 α). PGC-1 α is in turn a transcriptional regulator of many genes that are involved in cellular metabolism, including genes necessary for mitochondrial biogenesis, mitochondrial respiration and ROS metabolism. Decreased levels of functional parkin lead to accumulation of PARIS, which are toxic to DA neurons, and this toxic

accumulation of PARIS has been documented in the brains of PD patients and in animal models of PD (Shin et al., 2011).

Accordingly, it is possible that following MPTP administration, parkin is oxidatively modified resulting in loss of function. Within NSDA neurons loss of parkin following MPTP could result in increase levels of PARIS, increased suppression of PGC-1 α and subsequent toxicity. Following MPTP administration, the up-regulation and activation of parkin within TIDA neurons would mediate the degradation of damaged mitochondria through mitophagy, while at the same time, parkin-mediated degradation of PARIS would allow increased PGC-1 α activity to compensate for the lost mitochondria. In contrast, within NSDA neurons, MPTP would inhibit this process by directly damaging mitochondria as well as inhibiting the parkin-mediated repair of mitochondria. The continual presence of damaged mitochondria could then result in severe cytotoxicity through the production of ROS, decreases in ATP, or in terminal stages, the release of pro-apoptotic proteins.

Although this scenario could account for the differential susceptibility of TIDA and NSDA neurons to MPTP, the experiments detailed within this dissertation examined early events following MPTP administration. Thus, it is unclear if this series of events could result in toxicity within the short window of time examined. It is also possible that parkin is acting through a more acute mechanism. Recent work has shown that following exposure to ROS, oxidatively damaged proteins of the electron transport chain are quickly removed from the mitochondria by mitochondrial-derived vesicles, and parkin is implicated in this process (Soubannier et al., 2012). Alternatively, as discussed in Chapter 6, the effects of parkin observed within this dissertation may simply reflect the stabilization of MTs (Ren et al., 2008). Due to the fact that parkin seems to be a multifaceted neuroprotective protein, it is difficult to determine the specific pathway by

which parkin is protecting DA neurons. Accordingly, future experiments should aim to determine the exact pathways important for parkin-mediated recovery of DA neurons following MPTP.

Although the precise mechanism by which parkin protects DA neurons is unclear. The data presented within this dissertation and the literature confirm that parkin is crucial in the maintenance and survival of DA neurons. As such, parkin mediated therapies show great promise in the treatment of PD. Within the current set of experiments the effects of parkin overexpression were modest. Thus, using gene therapy to overexpress parkin may not be a feasible option in the treatment of PD. In contrast, the ability of TIDA neurons to endogenously up-regulate parkin seems to render these neurons extremely resistant to long term toxicity. Accordingly, research should be undertaken in order to determine the mechanism used by TIDA neurons, which allows for a rapid and sustained up-regulation of parkin expression. Alternatively, downstream mechanisms of increased parkin activity represent another avenue that could be used to save damaged DA neurons. Future studies investigating the upstream mechanisms of parkin up-regulation as well as the down stream effects of parkin expression within TIDA neurons would greatly contribute to our understanding DA neuronal homeostasis and recovery, which would in turn further our understanding of NSDA pathology in PD.

Concluding Remarks

TIDA neurons represent a novel platform upon which to investigate endogenous neuroprotective mechanisms unique to DA neurons. Experiments presented in this dissertation have identified the ability to increase parkin expression following toxicant exposure as one neuroprotective mechanism used by TIDA neurons. Using this TIDA neuronal system as a

model, parkin overexpression was adapted to NSDA neurons and was successful in preventing some aspects of MPTP-induced toxicity. These results identify toxicant-induced loss of parkin as a potential risk factor for NSDA neuronal degeneration. The work presented in this dissertation suggest that future research into mechanism of TIDA neuronal recovery from toxicant exposure has the potential to elucidate mechanisms of endogenous neuroprotection that could be used to prevent DA neuronal degeneration. Additionally, the work presented here suggests that parkin specifically, as well as the up- and downstream events associated with parkin up-regulation in TIDA neurons, represent an ideal focus for a translational therapeutic aimed at halting the degeneration of DA neurons in PD.

APPENDIX

The Production of rAAV Vectors Containing Parkin shRNA or Human Parkin Transgenes

Introduction

rAAV vectors containing shRNA directed toward the murine parkin gene were created. This allows for temporal as well as spatial control over parkin knockdown in order to determine the role of parkin in the recovery of TIDA neurons from MPTP. In addition, several parkin transgene constructs were also created which will be used in an attempt to rescue the highly susceptible NSDA neurons from MPTP toxicity, experiments in Chapter 6 aim to change the MPTP-resistant TIDA phenotype to MPTP-susceptible by knocking down parkin (using parkin shRNA), in addition to changing the MPTP-susceptible NSDA phenotype to MPTP-resistant using over expression of parkin transgenes.

AAV is a single stranded DNA dependovirus belonging to the parvovirus family. AAV has the ability to infect both dividing and non-dividing cells of multiple lineages, including myocytes, hepatocytes, haemopoetic progenitor cells, photoreceptors and most importantly neurons. AAV has never been associated with any human disease giving it the highest biosafety level rating of any viral vector system currently in use (Grimm & Kleinschmidt, 1999).

Under normal circumstances AAV requires the presence of a helper virus, such as adeno- or herpes-virus, in order to replicate its genome, earning it the title of a naturally defective, replication deficient virus. The AAV genome entails a single DNA strand approximately 5 kilobases (kb) in length, which consists of two open reading frames encoding the *rep* and *cap* genes flanked between two inverted terminal repeats (ITR). The *rep* sequences is composed of four overlapping genes encoding Rep proteins required for replication of the AAV genome, while the *cap* sequence encodes a series of structural capsid proteins which are responsible for

the formation of the icosahedral capsid (Walther & Stein, 2000). The ITR sequences, so named due to their palindromic symmetry, are required for the successful multiplication and packaging of the AAV genome. These sequences are able to fold back on themselves; thereby creating a hairpin, initiating a self-priming that allows a primase-independent synthesis of a second, complimentary AAV-DNA strand. These ITR sequences have been shown to be the only components of the AAV genome necessary for viral replication and integration into a host genome (Bohenzky, LeFebvre, & Berns, 1988). Thus, in clinical or research use, the *rep* and *cap* genes can be removed from the AAV genome and replaced by a transgene of interest (e.g. parkin), leaving only the ITR flanking the transgene with the desired promoter (Figure A-1). One limitation in the use of AAV is the relatively small size of the genome. Removal of the *rep* and *cap* genes allows for the insertion of transgene ranging in size from 4.1 to 4.9 kb (Walther & Stein, 2000). Luckily this will not be a problem in the current study due to the size of the parkin gene (about 1.4 kb).

This Appendix will describe the production of 2 parkin shRNA (one target and one scrambled control) constructs. In addition, 3 human parkin transgene constructs were created; a wild type (WT) human parkin (hParkin) construct, a C-terminal (C-Term) truncated version of hParkin and a Q311 stop mutant (Q311).

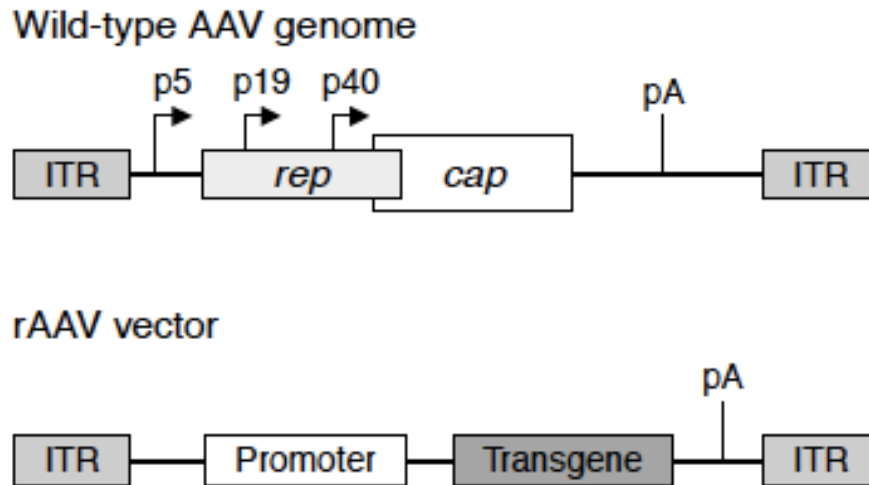


Figure A-1. Structure of wild-type and recombinant AAV genome. The wild-type AAV consists of the viral genes *rep* and *cap*, the AAV promoters (p5, p19, p40), the pA and the ITR sequences. In rAAV vectors, the viral *rep* and *cap* genes are replaced by a transgene cassette; consisting of the desired promoter, the transgene and the pA-site. Abbreviations: pA, polyadenylation site; ITR, inverted terminal repeats. Image modified from Walther and Stein, 2000.

Triage of Parkin shRNA Sequences: The Dual Luciferase Assay

Prior to packaging the desired parkin shRNA molecule into the final AAV genome, several parkin shRNA constructs with different sequences were triaged in order to determine the shRNA with the highest knockdown capability. Triage of parkin shRNA was performed using the commercially available Dual-Luciferase Reporter Assay system (Promega).

The dual reporter system utilizes two individual reporter enzymes, expressed and measured simultaneously within a single *in vitro* system. In this system, one reporter is designated as an “experimental reporter” and is used to measure the effect of an experimental manipulation, while the other enzyme is designated as a “control reporter” and is used as an internal control. In the current experiment the reporter enzymes used were the *firefly luciferase gene* (hluc+), used as the control reporter and the *renilla luciferases gene* (hRluc) used as the experimental reporter.

In brief, the assay was set-up and conducted as follows: First, the gene of interest is subcloned into the restriction site immediately following hRluc within the psiCHECK vector. The gene of interest will now be expressed when the experimental reporter, *hRluc*, is expressed. Following, the psiCHECK vector was transfected into a cell, allowing for transcription and translation of the genes within the vector, i.e. the gene of interest attached to the experimental reporter and the control reporter alone. Following, the activities of both reporters were measured sequentially by adding specific substrates and measuring the luciferase activity of each individual enzyme. The ability to normalize the experimental reporter to the control reporter minimizes variability due to transfection efficiency or cell viability, and allows for an efficient and reliable system for measurement of gene expression.

In order to utilize this system to triage shRNAs, a separate plasmid containing an shRNA of interest was co-transfected along with the psiCHECK vector. The presence of the shRNA will activate the RNA induced silencing complex (RISC) to initiate degradation of any RNA with a homologous sequence. Thus, transfection of a parkin shRNA will cause the cell to degrade any parkin mRNA as well as the experimental reporter transcript that is attached to it. The efficacy of a particular shRNA was quantified by measuring a reduction in the luciferase activity of the experimental reporter.

Parkin shRNA Sequences

The target sequences and hairpin sequences of the parkin shRNAs were chosen from The RNAi Consortium (TRC), a publically available service. Triage of three target shRNAs and one scrambled control was performed. The target sequences and shRNA sequences are shown in Figure A-2.

Due to the relatively short length of the shRNA sequences, the entire oligomeric sequence was ordered through Integrated DNA technologies (IDT). For each shRNA construct, a sense and antisense oligomer was ordered. All shRNA sense strands were designed with a 5' sequence recognized by the restriction enzyme BAMH1 (5'..GATCC..3'), while all antisense strands were designed with 5' sequences recognized by the restriction enzyme HINDIII (5'..AGCTT..3'). Different restriction sites on the complementary strands ensures proper directionality when subcloning the double stranded shRNA into the holder plasmid. Both sense and antisense strands were ordered with a 5' phosphate group necessary for ligation.

shRNA trcn000041143

Target Sequence:

CGTTTCATTATCTGCAACTTT

Hairpin Sequence:

5'-CCGG-CGTTTCATTATCTGCAACTTT-CTCGAG-
AAAGTTGCAGATAATGAAACG-TTTTTG-3'

shRNA trcn000041145

Target Sequence:

CGGAGGATGTATGCACATGAA

Hairpin Sequence:

5'-CCGG-CGGAGGATGTATGCACATGAA-CTCGAG-
TTCATGTGCATACATCCTCCG-TTTTTG-3'

shRNA trcn000041147

Target Sequence:

GACCTGGAACAACAGAGTATT

Hairpin Sequence:

5'-CCGG-GACCTGGAACAACAGAGTATT-CTCGAG-
AATACTCTGTTGTTCCAGGTC-TTTTTG-3'

Figure A-2. The sequence of parkin shRNA constructs. Three separate target parkin shRNA constructs were obtained from The RNAi Consortium. The sequence of the mouse parkin gene that each individual shRNA targets as well as the sequence of the hairpin loop of each shRNA is shown.

Cloning Parkin shRNA into the pSilencer Plasmid

The pSilencer plasmid was used to hold the shRNA being triaged. The sense and antisense oligomers were diluted to a final concentration of 300pM. The sense and antisense strands were then annealed at 95°C for 3 min, yielding a double stranded DNA molecule. The pSilencer plasmid was incubated with the restriction enzymes BAMH1 and HINDIII at 37°C for 2 h in order to linearize DNA backbone.

During the ligation reaction, the DNA ligase enzyme will catalyze the formation of a phosphodiester bond between any adjacent nucleotides containing a 5'-phosphate group and a 3'-hydroxyl group. Thus, the previously linearized backbone will readily close in on itself if the 5' end of the DNA still has a phosphate exposed. To solve this problem the linearized DNA is dephosphorylated in order to prevent closing of the plasmid. The pre-digested DNA was incubated with thermosensitive alkaline phosphatase (TSAP) for 30 min at 37°C in order to dephosphorylate the DNA. The prepared Psilencer backbone and double stranded DNA were then ligated together using the T4 DNA ligase at 16°C overnight. The resultant pSilencer plasmid containing the shRNAs of interest were transformed into One Shot Top 10 electrocompetent cells (Invitrogen) by electroporation and incubated in LB media for 1 h at 37°C. Cells were then plated on to LB agar plates that had previously been coated with ampicillin (100mg/ml in 50%EtOH). The pSilencer plasmid contains an ampicillin resistance gene, thus only bacterial colonies that had successfully integrated the pSilence plasmid would grow on the ampicillin coated agar plate. Colonies were picked from the plate and expanded by incubating in LB broth (containing ampicillin) overnight at 37°C. Following, plasmid DNA was isolated from the bacteria using a plasmid miniprep kit (Sigma). Isolated plasmid DNA was then cut with the restriction enzymes BAMH1 and HINDIII and the presence of the shRNA and

pSilencer backbone was confirmed by running on a 1.2 % agarose gel. DNA from colonies that visually showed the presence of the pSilencer backbone as well as the shRNA insert was then sequenced for final confirmation. Unfortunately, when performing this early aspect of the process I did not use the correct percentage of agarose in the gels and thus I had no visual records to show successful cloning of the shRNAs into the pSilencer plasmid, however all DNA was sequenced confirmed. Cells from colonies with the sequenced-confirmed presence of the parkin shRNA in the pSilencer plasmid were transferred to an 80% glycerol solution for long-term storage at -80C.

Cloning Mouse Parkin gene

In order to determine the efficacy of parkin knockdown by the shRNAs of interest using the Dual Luciferase Assay, the mouse parkin gene must be cloned and then subcloned into the psiCHECK plasmid. PCR primers for the mouse parkin gene were designed by our collaborator Dr. Fredric Manfredsson. The sense and antisense primers were as follows:

Sense

5- GCG GCC GCA TGA TAGTGTTTGTC A GGTT -3

Antisense

5- GCG GCC GCC TAC ACG TCA AAC CAG TGA TCT -3

Primers were diluted to a concentration of 300pM and a PCR reaction was performed using the expand high fidelity PCR system (Roche Applied Sciences) and mouse cDNA as a template (BioChain). PCR reactions were carried out for 25 cycles with an annealing temperature of 55°C and an elongation time of 1 min. PCR products were then run out on a 0.7% agarose gel and visualized (Figure A-3). The PCR product resolving at the correct molecular weight (MW) was then cut and purified from the gel using the commercially available Wizard SV gel and PCR clean up system (Promega).

Parkin Clone (PC-D6)

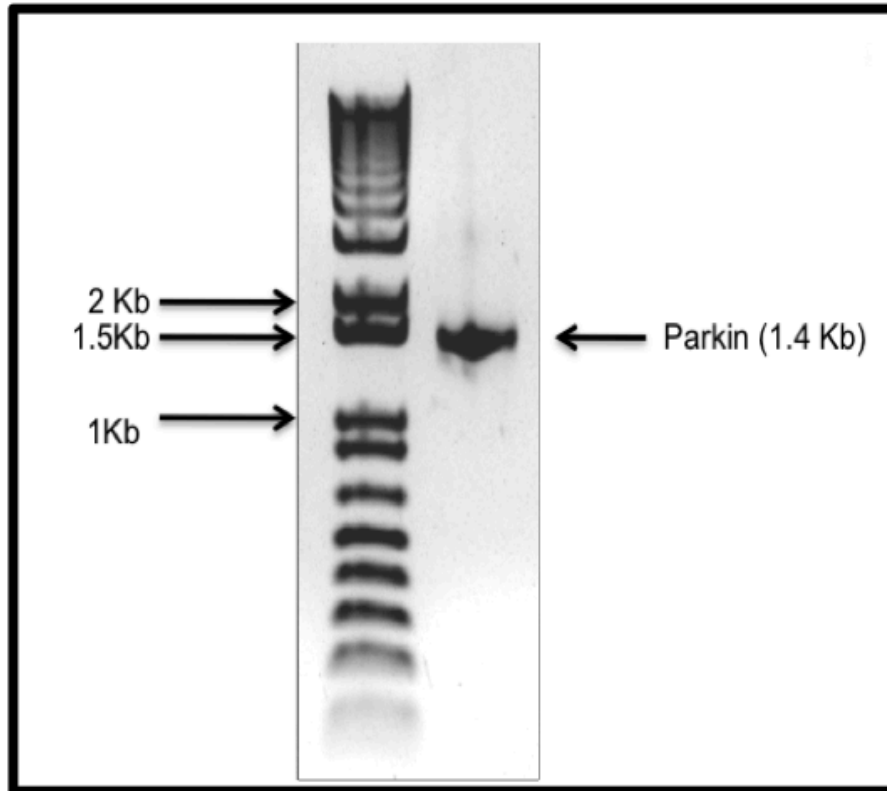


Figure A-3. Confirmation of parkin PCR product. Primers for the murine parkin gene were diluted to a concentration of 300pM and a PCR reaction was performed for 25 cycles with an annealing temperature of 55°C and an elongation time of 1 min. PCR products were then run out on a 0.7% agarose gel and visualized. The mouse parkin gene is shown resolving at 1.4Kb.

Subcloning the Parkin Gene into the psiCHECK Plasmid: Part I, TOPO TA Cloning

Directly cloning large pieces of DNA into a plasmid backbone can prove to be very difficult. As such, in order to facilitate the subcloning of the parkin gene into the psiCHECK vector, an intermediate subcloning step was performed with the TOPO TA cloning kit (Invitrogen).

The TOPO TA cloning system is a highly efficient strategy for direct insert of *taq* DNA polymerase amplified PCR products into a plasmid. The TOPO system takes advantage of the fact that *taq* polymerase has a non-template dependent, terminal transferase activity that will add an adenine (A) residue to the 3' end of any PCR product. The pre-linearized TOPO plasmid vector comes with an overhanging thymine (T) residue on each 3' end. This allows for efficient insertion of a *taq* polymerase PCR product to the TOPO backbone by complementation of the A-overhang on the PCR product and the T-overhang on the backbone.

As shown in Figure A-4, the final ligation of the PCR product to the backbone is mediated with the help of a DNA topoisomerase I enzyme that is covalently attached to the 3' ends of the linear vector. Normally, the topoisomerase enzyme works to cleave and rejoin supercoiled DNA during replication. The topoisomerase used in the TOPO TA cloning system is isolated from the Vaccinia virus and will bind specifically to DNA sequence 5'-(C/T)CCTT-3'. The TOPO vector is designed to contain this sequence at the two linear ends where the topoisomerase I enzyme is attached. Once the PCR product is inserted into the TOPO vector (by the aforementioned A-T complementarity), the bound topoisomerase I will recognize and cleave the phosphodiester bond after DNA sequence 5'-CCCTT. The formation of a new, temporary bond between a tyrosine residue within the enzyme itself and the 3' phosphate of the cleaved strand, conserves the energy from the broken bond. This newly formed intermediate phospho-

tyrosyl bond will be attacked by the 5' hydroxyl group of the PCR insert, forming a phosphodiester bond between the A and T overhangs after which point the topoisomerase I will be cleaved off and escape.

The purified parkin PCR product (PC-D6) was prepared for subcloning into the TOPO vector by first adding A-overhangs by incubating with *taq* DNA polymerase (Invitrogen). The entire PCR product was incubated with *taq* and deoxynucleotide triphosphates (dNTPs) for 10 min at 72C. Some of the product of this reaction was then run out on an agarose gel (0.7%) to confirm the presence of the correct MW band. Following, the A-overhang PCR product and the linearized TOPO vector were incubated according to manufacturers instructions for 5 min at room temperature. The newly ligated vector was then transformed into One Shot Top 10 electrocompetent cells by electroporation and incubated in LB media for 1h at 37C.

Cells were plated onto LB agar plates that had previously been coated with ampicillin (100mg/ml in 50% ethanol) as well as X-Gal (40mg/ml of DMSO) in order to perform blue-white screening. The TOPO vector contains a *lacZ* gene, which codes for the protein β -galactosidase. β -galactosidase is an enzyme that catalyzes the hydrolysis of galactosides such as lactose into simple monosaccharides. X-Gal, a lactose analog, is cleaved by β -galactosidase to form 5-bromo-4-chloro-indoxyl, which undergoes spontaneous dimerization and oxidation to form a bright blue insoluble pigment, 5,5'-dibromo-4,4'-dichloro-indigo. The multiple cloning site (MCS: containing T-overhangs) in the TOPO vector is in the middle of the *lacZ* gene. Thus, when the DNA insert is successfully cloned into the TOPO vector it will disrupt the *lacZ* gene and no functional β -galactosidase will be expressed. With no functional β -galactosidase, cells will fail to metabolize the X-Gal and white colonies will be observed instead of blue. Screening

for white colonies can than be performed for a convenient method of detection of the recombinant plasmid.

White colonies were picked and expanded in LB broth containing ampicillin overnight at 37C after which DNA was isolated and purified with a plasmid miniprep kit. DNA was than cut with the restriction enzyme NOT1 (recognizing the restriction site 5'-GCGGCCGC-3' which flanks the insert in the MCS) and the resultant DNA was run out and viewed on an agarose gel (0.7%). DNA from colonies that had the TOPO backbone and parkin gene resolving at the correct MW was sequenced for final confirmation. Cells from colonies with the sequenced-confirmed presence of the parkin clone in the TOPO plasmid were transferred to an 80% glycerol solution for long-term storage at -80C.

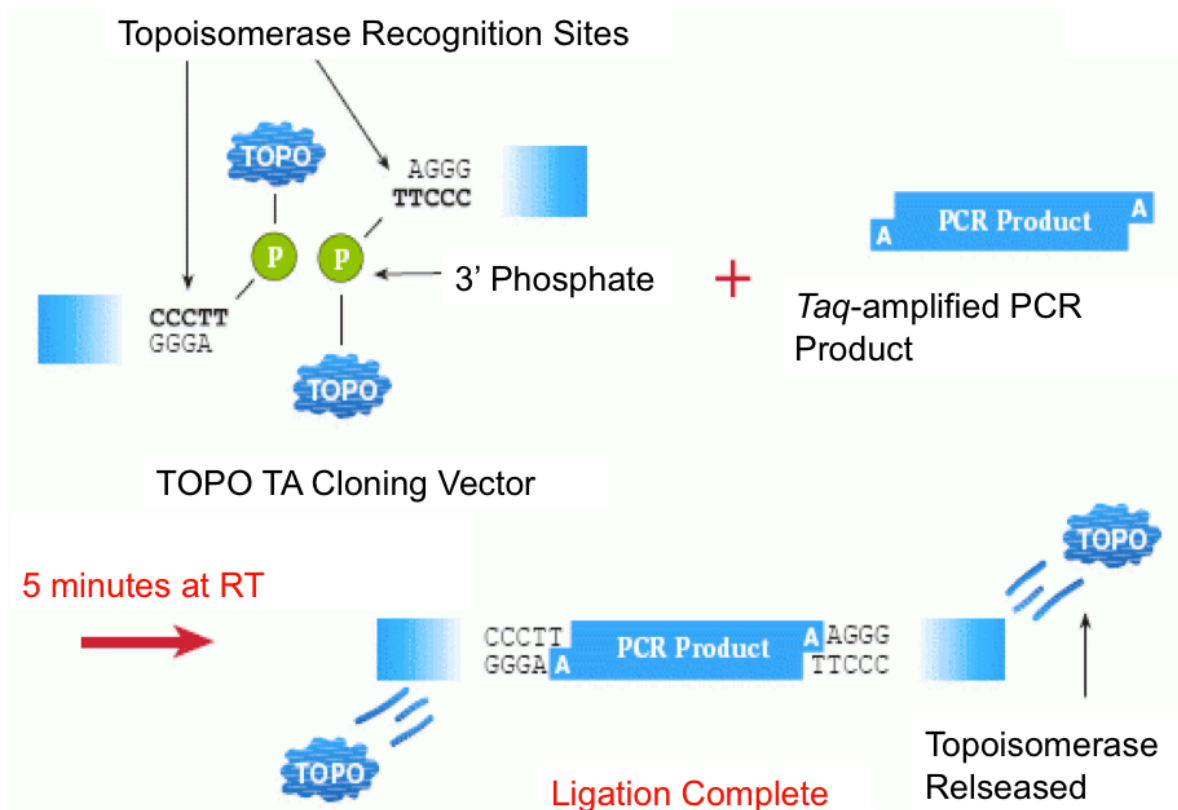


Figure A-4. Diagrammatic representation of PCR product subcloning using the TOPO TA cloning system. . The pre-linearized TOPO plasmid vector comes with an overhanging thymine (T) residue and a topoisomerase I recognition site on each 3' end. Incubation of the TOPO plasmid with a *Taq* amplified PCR product will cause A-T complimentarity and initial interaction of the PCR insert and the TOPO backbone. Following the Topoisomerase enzyme will cleave the TOPO backbone at the recognition site, creating a temporary phospho-tyrosyl bond. Finally, the free 5' hydroxyl group romm the PCR insert can attack this phospho-tyrosyl bond, freeing the topoisomerase enzyme and ligating the insert into the TOPO backbone. Abbreviations: TOPO, topoisomerase I. Figure modified from Life Technologies, 25-0276, (2012).

The purified parkin PCR product (PC-D6) was prepared for subcloning into the TOPO vector by first adding A-overhangs by incubating with *taq* DNA polymerase (Invitrogen). The entire PCR product was incubated with *taq* and deoxynucleotide triphosphates (dNTPs) for 10 min at 72C. Some of the product of this reaction was then run out on an agarose gel (0.7%) to confirm the presence of the correct MW band. Following, the A-overhang PCR product and the linearized TOPO vector were incubated according to manufacturers instructions for 5 min at room temperature. The newly ligated vector was then transformed into One Shot Top 10 electrocompetent cells by electroporation and incubated in LB media for 1h at 37C.

Cells were then plated onto LB agar plates that had previously been coated with ampicillin (100mg/ml in 50% ethanol) as well as X-Gal (40mg/ml of DMSO) in order to perform blue-white screening. The TOPO vector contains a *lacZ* gene, which codes for the protein β -galactosidase. β -galactosidase is an enzyme that catalyzes the hydrolysis of galactosides such as lactose into simple monosaccharides. X-Gal, a lactose analog, is cleaved by β -galactosidase to form 5-bromo-4-chloro-indoxyl, which undergoes spontaneous dimerization and oxidation to form a bright blue insoluble pigment, 5,5'-dibromo-4,4'-dichloro-indigo. The multiple cloning site (MCS: containing T-overhangs) in the TOPO vector is in the middle of the *lacZ* gene. Thus, when the DNA insert is successfully cloned into the TOPO vector it will disrupt the *lacZ* gene and no functional β -galactosidase will be expressed. With no functional β -galactosidase, cells will fail to metabolize the X-Gal and white colonies will be observed instead of blue. Screening for white colonies can then be performed for a convenient method of detection of the recombinant plasmid.

White colonies were picked and expanded in LB broth containing ampicillin overnight at 37C after which DNA was isolated and purified with a plasmid miniprep kit. DNA was then cut with the restriction enzyme NOT1 (recognizing the restriction site 5'-GCGGCCGC-3' which flanks the insert in the MCS) and the resultant DNA was run out and viewed on an agarose gel (0.7%) (Figure A-5). DNA from colonies that had the TOPO backbone and parkin gene resolving at the correct MW was sequenced for final confirmation. Cells from colonies with the sequenced-confirmed presence of the parkin clone in the TOPO plasmid were transferred to an 80% glycerol solution for long-term storage at -80C.

Parkin Clone (PC-D6) in TOPO
(Digested with NOT1)

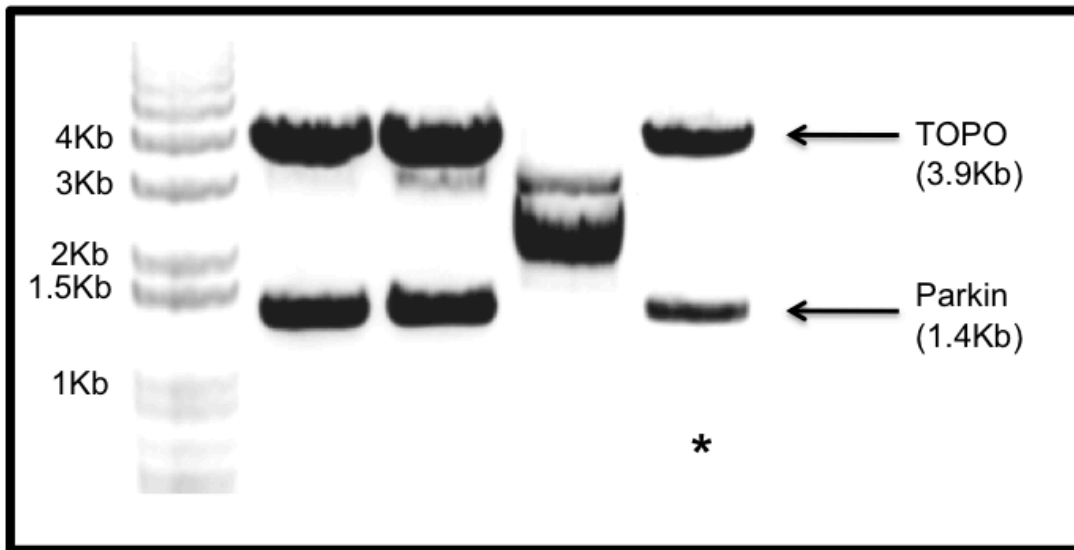


Figure A-5. Confirmation of successful insertion of parkin clone into TOPO vector. The murine parkin gene was cloned and then subcloned into the TOPO vector. Following ligation of parkin PCR product and the TOPO vector, purified plasmid DNA was cut with the restriction enzyme NOT1 and run on a 0.7% agarose gel. * Indicates lane with sequenced confirmed construct.

Subcloning the Parkin Gene into the psiCHECK Plasmid: Part II Subcloning from TOPO to the psiCHECK Plasmid

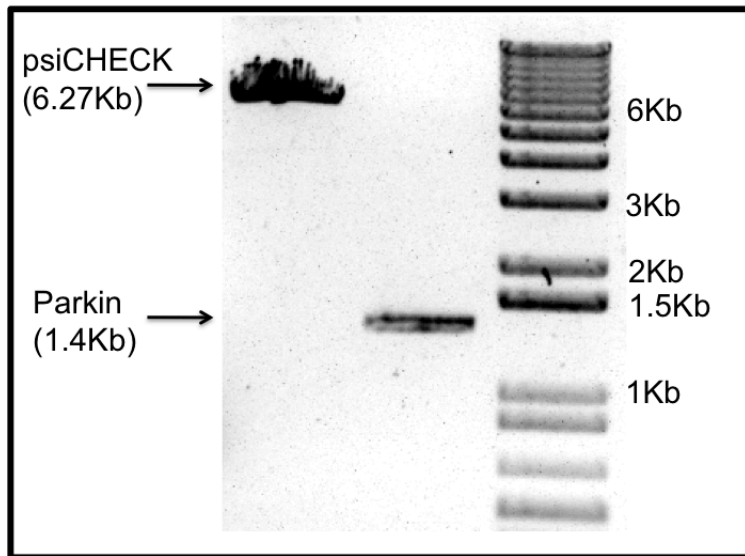
Using the TOPO TA cloning system, the parkin clone was inserted into the TOPO vector in a position that is flanked by multiple restriction sites. Thus, in addition to allowing for easy insertion of DNA into the TOPO vector, cutting the recombinant plasmid with an appropriate restriction enzyme the PCR product can pick up one of the flanking restriction sites, which can be used for future subcloning. As seen in Figure A-2, the psiCHECK vector contains NOT1 restriction sites flanking the MCS.

After clonal expansion, the parkin clone (PC-D6) was cut out of the TOPO vector with NOT1 (yielding approximately 10 μ g of insert). Additionally, the psiCHECK plasmid (approximately 9 μ g) was prepared by cutting with NOT1 to yield complementary 3' and 5' ends on the backbone and insert. The backbone was also dephosphorylated by incubating with TSAP. Both the cut parkin insert and the linearized, dephosphorylated psiCHECK backbone were run on an agarose gel (0.7%), and DNA resolving at the correct MW for parkin (1.4kB) and psiCHECK (6.3kB) was cut from the gel and purified with the wized SV cleanup system (Promega) (Figure A-6, Panel A).

The parkin clone was ligated into the prepared psiCHECK backbone by incubating the insert and the backbone at an 8:1 molar ratio in the presence of the T4 DNA ligase (Invitrogen). The reaction was carried out for 1h at room temperature. The ligated DNA was then transformed into XL10-Gold Ultracompetent Cells (Stratagene) through chemical poration. In brief, 5 μ l of the ligated DNA was added to 40 μ l of XL10-Gold cells and chilled on ice for 10 min. The cells were then heat-shocked at 42C for 30 sec, followed by incubation in ice for 2 min. The transformed cells were then incubated in LB broth for 30 min at 37C. Cells were finally plated

onto LB agar plates containing ampicillin and allowed to grow overnight. Colonies were picked and expanded in LB broth containing ampicillin for 12-16h. Plasmid DNA was then isolated and cut with the restriction enzyme NOT1. DNA was then visualized on an agarose gel (0.7%) in order to confirm the presence of the NOT1 digested insert and backbone (Figure A-6, Panel B). DNA containing the backbone and insert was sequenced for final confirmation of successful subcloning. Cells from colonies with the sequenced-confirmed parkin-psiCHECK plasmid were transferred to an 80% glycerol solution for long-term storage at -80C.

**Parkin Clone (PC-DC) and psiCHECK
backbone
(Digested with NOT1)**



**Parkin Clone (PC-D6) in psiCHECK
(Digested with NOT1)**

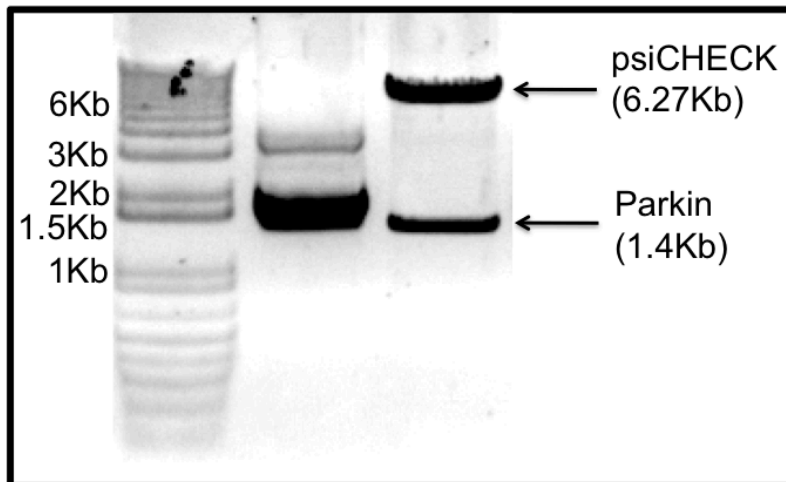


Figure A-6. Confirmation of successful insertion of parkin clone into psiCHECK plasmid. The parkin clone and psiCHECK backbone were individually cut with NOT1 and run on a 0.7% gel (Panel A). The DNA was extracted, purified and used to ligate the parkin clone into the psiCHECK vector. Following ligation of the parkin clone into the psiCHECK vector, purified plasmid DNA was cut with the restriction enzyme NOT1 and run on a 0.7% agarose gel (Panel B). DNA containing the correct MW psiCHECK and parkin bands was sequenced, confirming successful insertion of the parkin clone into the psiCHECK vector.

Dual Luciferase Assay

To perform the Dual Luciferase assay, the parkin-psiCHECK plasmid was co-transfected with either 1 of the 3 target shRNAs, the scrambled shRNA, an off target shRNA or an AAV-GFP construct (used as a transfection control) into HEK-293 cells. In brief, lipofectamine was diluted in OMEM at a ratio of 1:25. The OMEM-lipofectamine mixture was then added to HEK-293 cells (50 μ l/well) and incubated at RT for 20 min. Following, DNA (respective reporter and shRNA for each condition; Table A-1) was mixed with OMEM and added directly to wells. Cells were then incubated overnight with gentle rocking.

After overnight incubation, confirmation of successful transfection was determined by observing GFP (from the UF11 transfection control) fluorescence using a fluorescent microscope. Cells were then rinsed once with PBS and lysed by incubation with PLB for 15 min at RT. Lysates (20 μ l) were added to a 96 well plate and the dual luciferase assay was performed according to manufacturers instructions. Figure A-7 shows the results of the dual luciferase assay. The parkin shRNA construct 1 (trcn 41143) showed no knock down, while the parkin shRNA constructs 2 and 3 (trcn 41145-1 and 41145-2, respectively) showed an approximate 80% knockdown of parkin expression. Parkin sRNA construct 2 was chosen to be packaged into the final AAV backbone.

Experimental Condition	Reporter	shRNA	Transfection Control
Negative control	x	x	UF11 (0.8μg)
Control	psiCHECK-Parkin (0.1μg)	x	UF11 (0.7μg)
shRNA 41143	psiCHECK-Parkin (0.1μg)	shRNA41143 (0.4μg)	UF11 (0.3μg)
shRNA 41145-1	psiCHECK-Parkin (0.1μg)	shRNA41145-1 (0.4μg)	UF11 (0.3μg)
shRNA 41145-2	psiCHECK-Parkin (0.1μg)	shRNA41145-2 (0.4μg)	UF11 (0.3μg)
shRNA-Scrambled	psiCHECK-Parkin (0.1μg)	shRNA Scrambled (0.4μg)	UF11 (0.3μg)
shRNA-Off target	psiCHECK-Parkin (0.1μg)	shRNA-Beta101 (0.4μg)	UF11 (0.3μg)

Table A-1. Experimental design used for the dual luciferase assay. Each row represents the reporter and shRNA construct transfected to HEK293 cells. Following successful transfection cells were lysed and the resultant lysate was used for the dual luciferase assay.

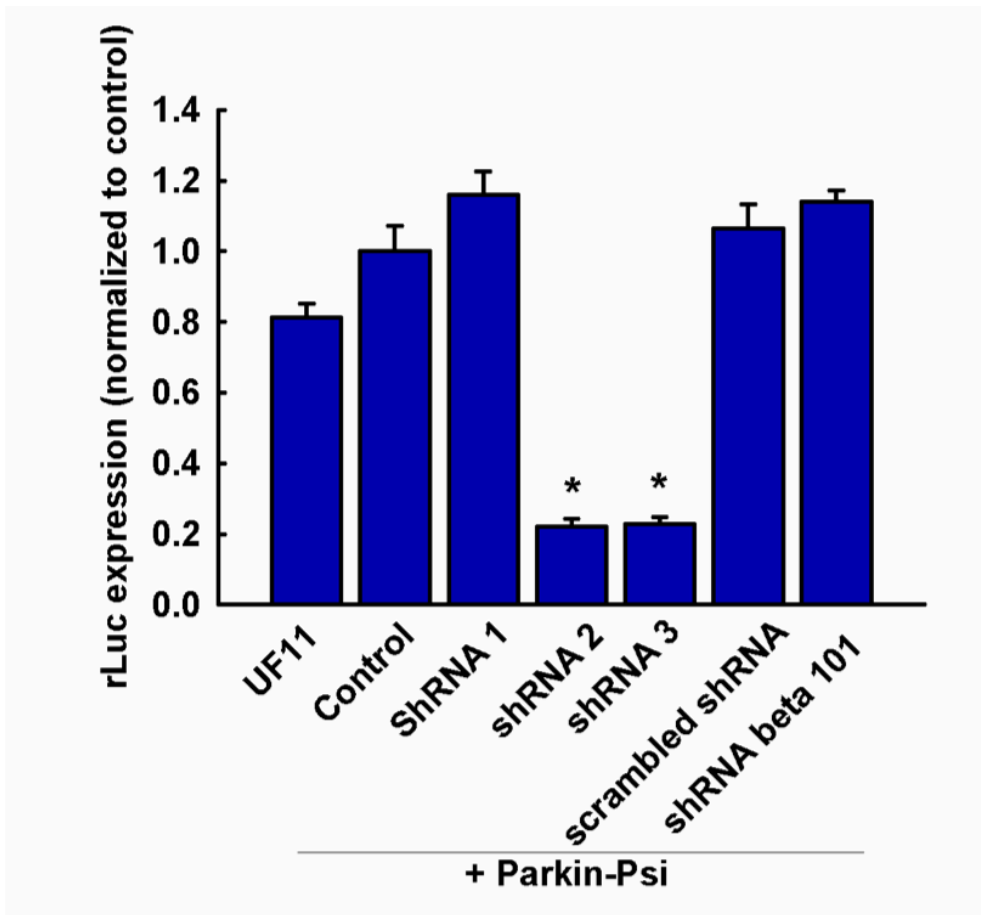


Figure A-7. shRNA mediated knockdown of parkin expression in HEK 293 cells. The Parkin-psiCHECK reporter plasmid and different shRNA constructs were transfected into HEK293 cells. Cells were lysed, substrate was added and luminescence was measured using a luminometer. Columns represent experimental reporter luciferase (rLuc) activity normalized to the control luciferase activity (luc+) + 1 SEM. * Represents significantly different than control group (P<0.05).

Cloning Parkin shRNA into the AAV Backbone

Following triage of the different parkin shRNA constructs, shRNA 2 (trcn 411451) was chosen to package into the final AAV backbone. The scrambled parkin shRNA was also packaged into the AAV backbone. Parkin shRNA and the scrambled shRNA were cloned out of the psiCHECK plasmid using new primers designed to flank the shRNA sequence with SalI restriction sites (5'-GTCGAC-3') to be used for subcloning in later steps.

Parkin shRNA

Sense

5'-GTC GAC AAT TCA TAT TTG CAT GTC GC-3'

Antisense

5'-GTC GAC TTT CCA AAA AAC GGA GGA TGT-3'

Scrambled shRNA

Sense

5'-GTC GAC AAT TCA TAT TTG CAT GTC GC-3'

Antisense

5'-GTC GAC AAG CTT TTC CAA AAA ACA AC-3'

Primers were diluted to a concentration of 300pM and a PCR reaction was performed using the respective pSilencer-shRNA plasmids as a template. PCR products were run out on an agarose gel (1.2%) and visualized. DNA resolving at the correct MW range was cut from gel

and purified. As detailed above purified PCR product was prepped and subcloned into the TOPO vector using the TOPO TA cloning system. Following selection and expansion of white colonies, DNA was cut with the restriction enzyme SalI and run on an agarose gel. DNA from colonies that had the TOPO backbone and parkin shRNA or scrambled shRNA resolving at the correct MW were sequenced for final confirmation. Cells from colonies with the sequenced-confirmed presence of the parkin shRNA and the scrambled shRNA constructs in the TOPO plasmid were transferred to an 80% glycerol solution for long-term storage at -80C.

The parkin and scrambled shRNAs were cut from the TOPO vector with the restriction enzyme SalI. In addition, the final AAV2 backbone pTR-UF11 (Figure A-8) was cut with SalI. Both the shRNA constructs and the linearized AAV backbone were run out on an agarose gel. Insert and backbone DNA were purified, and the AAV backbone was dephosphorylated by incubating with TSAP for 1 h. Finally, the shRNA constructs were ligated into the AAV backbone. Briefly, the purified shRNA and backbone were incubated in the presence of the T4 DNA ligase at a 1:5 molar ratio at 16C overnight. Ligated DNA was then transformed into XL10-Gold cells, incubated, expanded and plated as described above. DNA from selected colonies was isolated and cut with SalI. DNA from colonies containing the insert of interest were then checked for the integrity of ITRs.

Due to the repetitive nature and the secondary structures formed by the ITR sequences, these spans of DNA are highly prone to recombination and deletion events, which can result in a loss of the intact and correct ITR sequence. As the ITRs are crucial for AAV replication and packaging, it is necessary to select only the plasmids that have the desired insert present, in addition to intact ITR sequences. In order to determine the integrity of the ITRs, DNA from colonies that showed the presence of the desired insert, was digested with the restriction enzyme

SmaI (recognizing 5'-CCCGGG-3'). The ITR sequences contain SmaI sites, thus cutting the plasmid with SmaI should result in 2 high MW bands if the ITRs are intact. If ITRs are not intact one higher molecular weight band will appear. Under normal circumstances, the newly ligated DNA will be a mixed population of plasmids with ITRs intact and those without ITRs (Figure A-9). In this case DNA from these colonies will then be repeatedly transformed into SURE (Stop Unwanted Rearrangement Events) electroporation competent cells until a population with highly enriched ITRs (having 80-90% SmaI cut DNA) is achieved.

As the name implies, SURE cells lack components of the recombination pathways that catalyze the rearrangement and deletion of nonstandard secondary and tertiary structures, including cruciforms formed by ITRs. This allows high integrity cloning of the entire recombinant AAV genome within these cells. DNA was screened until colonies containing the scrambled or parkin shRNA and intact ITRs were present. Colonies were then expanded using the plasmid giga prep kit (Qiagen) according to vendor's recommendations. The resultant DNA was cut and visualized on an agarose gel as well as sequenced for final insert and ITR confirmation (Figure A-10).

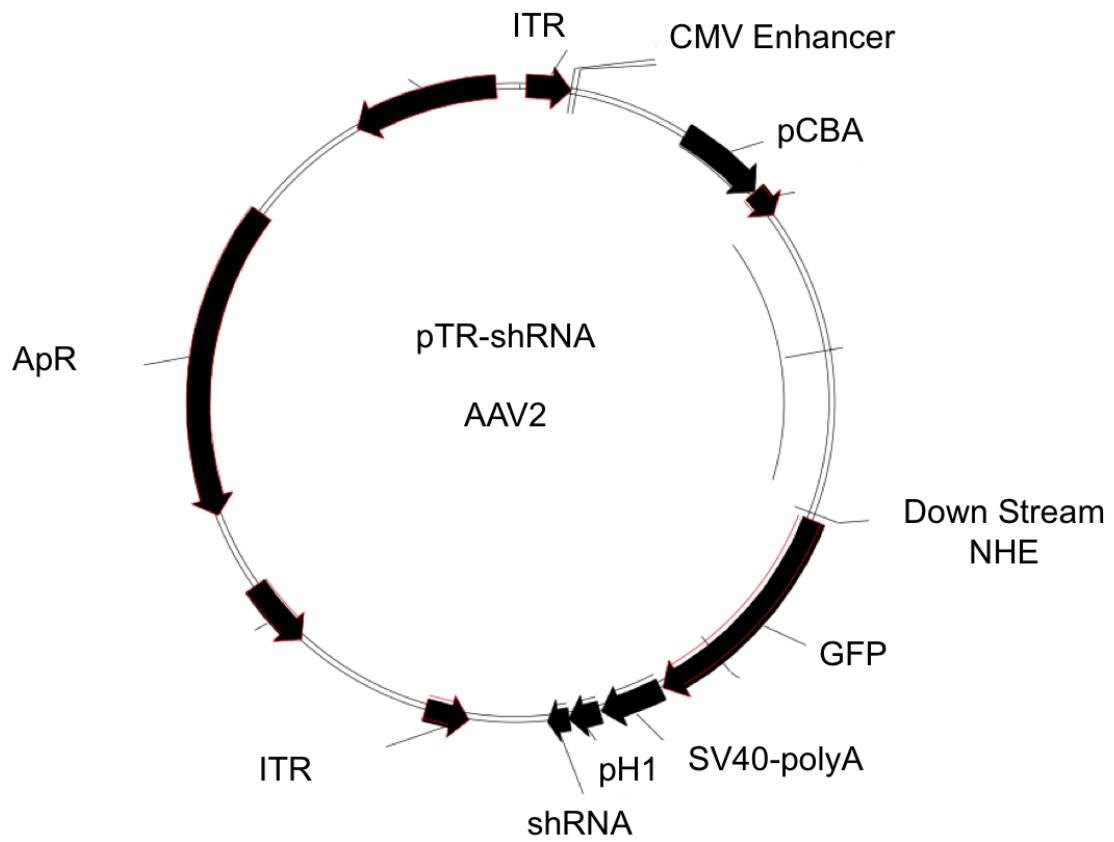


Figure A-8. Site Map of the recombinant AAV genome pTR UF11 expressing shRNA. Plasmid consisting of AAV2 ITR, a GFP reporter construct and shRNA inserts by flanked by SalI restriction sites down stream of the H1 promoter.

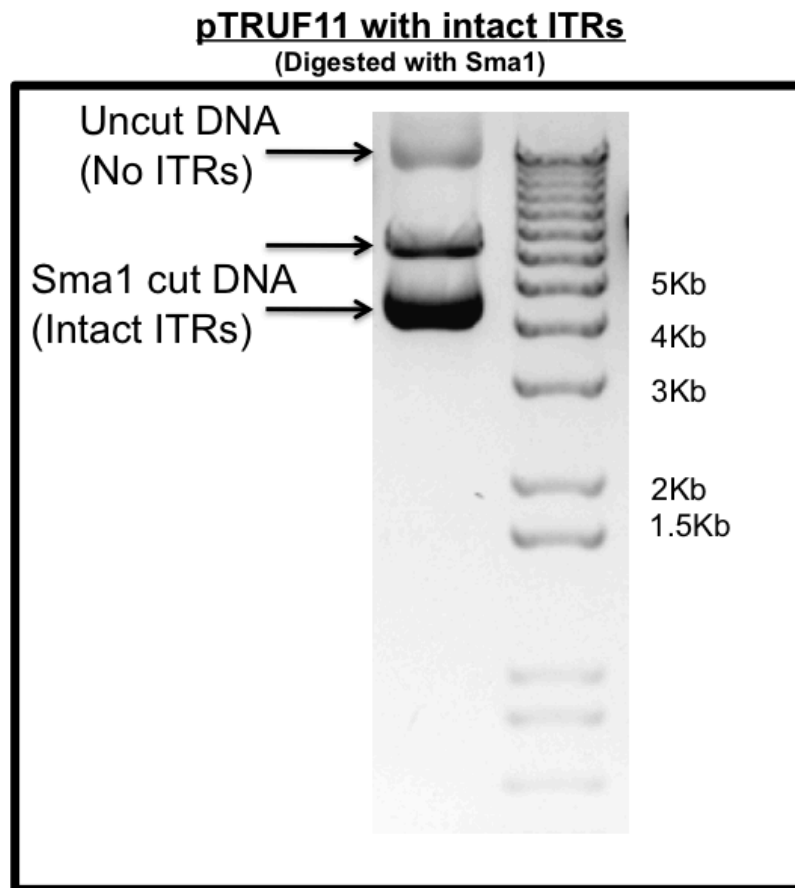


Figure A-9. pTRUF11 plasmid digested with Sma1 demonstrating the presence of both intact and damaged ITR. The ITR sequences contain Sma1 sites, thus cutting the plasmid with Sma1 should result in 2 high MW bands if the ITRs are intact. If ITRs are not intact one higher molecular weight band will appear. Uncut DNA indicates the absence of the Sma1 containing ITRs. Plasmid DNA containing ITRs which is cut with Sma1 yields 2 bands between 4-7Kb depending on insert size

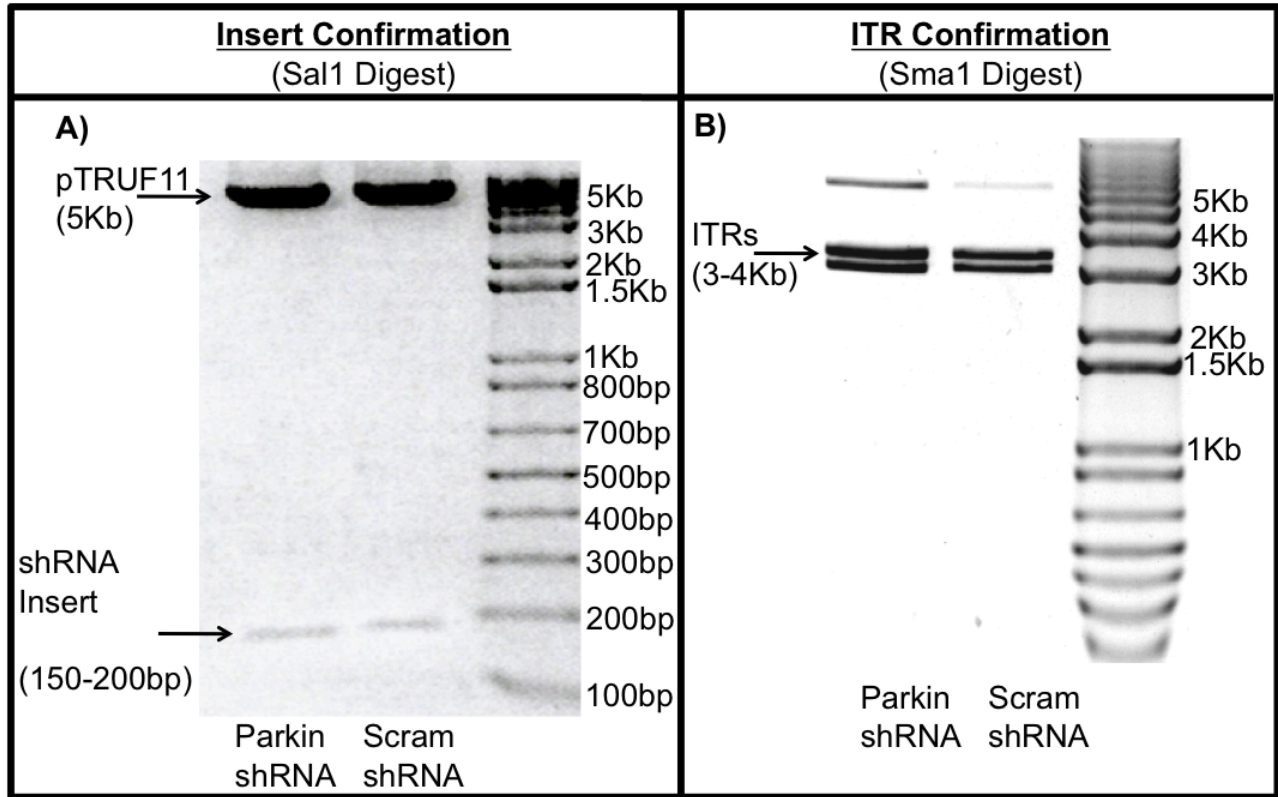


Figure A-10. Final insert and terminal repeat confirmation of shRNA-AAV constructs. Parkin shRNA and a scrambled shRNA were subcloned into the AAV backbone (pTRUF11). Successful insertion of shRNA sequences and maintained integrity of AAV inverted terminal repeats (ITR) was confirmed by digesting the plasmid DNA with the restriction enzymes Sal1 (Panel A) or Sma1 (Panel B), respectively. DNA was visualized on 1.2% (panel A) or 0.7% (panel B) agarose gels.

Cloning Parkin Transgene Constructs into the AAV Backbone

Three different parkin transgene products were packaged into the final AAV backbone. A WT version of the hParkin gene, a C-Terminal truncated hParkin and a Q311 premature stop mutant. The C-Term mutant form of parkin was generated by mutating amino acid 137 to methionine, creating a truncated mutant lacking all RING moieties. The Q311 hParkin mutant was generated by replacing amino acid 348 with a stop codon, yielding a dominant negative form of the protein. The use of these different mutants will enable mechanistic studies as to which functional moiety of parkin is mediating any potential effects observed. Further, all hparkin constructs were designed to include a FLAG tag at the N-terminal of the parkin protein for interaction studies as well as visualization in the brain (Figure A-11).

All hParkin constructs were obtained courtesy of Dr. Fredric Manfredsson. The 3 FLAG-hParkin (F-hParkin) constructs were generated by first cloning the different constructs out of a previously used pTRUF11 plasmid using primers encoding a 5' in-frame FLAG epitope.

Primers were diluted to a concentration of 300pM and a PCR reaction was performed using the 3 separate hParkin constructs (WT, C-Term and Q311) in pTRUF11 as a template. PCR products were run out on an agarose gel (0.7%) and visualized (Figure A-12). DNA resolving at the correct MW range was cut from gel and purified. Sequenced confirmed purified PCR product was prepped and subcloned into the TOPO vector using the TOPO TA cloning system. Following selection and expansion of white colonies, DNA was cut with the restriction enzyme NOT1 and run on an agarose gel. DNA from colonies that had the TOPO backbone and the WT-FLAG-hParkin, C-Term-FLAG-hParkin and Q311-FLAG-hParkin resolving at the correct MW were sequenced for final confirmation. Cells from colonies with the sequenced-

confirmed presence of the 3 distinct parkin constructs in the TOPO plasmid were transferred to an 80% glycerol solution for long-term storage at -80C.

Finally, WT, C-Term and Q311 FLAG-hParkin cDNA was cut from the TOPO vector with the restriction enzyme NOT1, and 1.5 µg of the final AAV backbone pTRUF11 was cut with NOT1. Both the FLAG-hParkin cDNA and the linearized AAV backbone were run out on an agarose gel. Insert and backbone DNA were purified. The AAV backbone was dephosphorylated. Finally, as described above the constructs were ligated into the AAV backbone (1:5 molar ratio of backbone to insert) and transformed to XL10-Gold cells, DNA from selected colonies was isolated and cut with NOT1. DNA from colonies containing the insert of interest was then checked for the integrity of ITRs. Plasmids containing the insert of interest and high integrity ITRs were repeatedly transformed into SURE cells until a population with highly enriched ITRs (having 80-90% Sma1 cut DNA) was achieved.

For the studies within this dissertation only the WT F-hParkin was needed and as such it was the only parkin transgene construct packaged into the viral capsid. Colonies containing the AAV2-f-hParkin construct were expanded using the plasmid giga prep kit (Qiagen) according to vendors recommendations. The resultant DNA was cut and visualized on an agarose gel (Figure A-13) as well as sequenced for final insert and ITR confirmation. Purified DNA (3-7mg) was sent to the Powell Gene Therapy Vector Core Lab at the University of Florida for packing into the viral capsid.

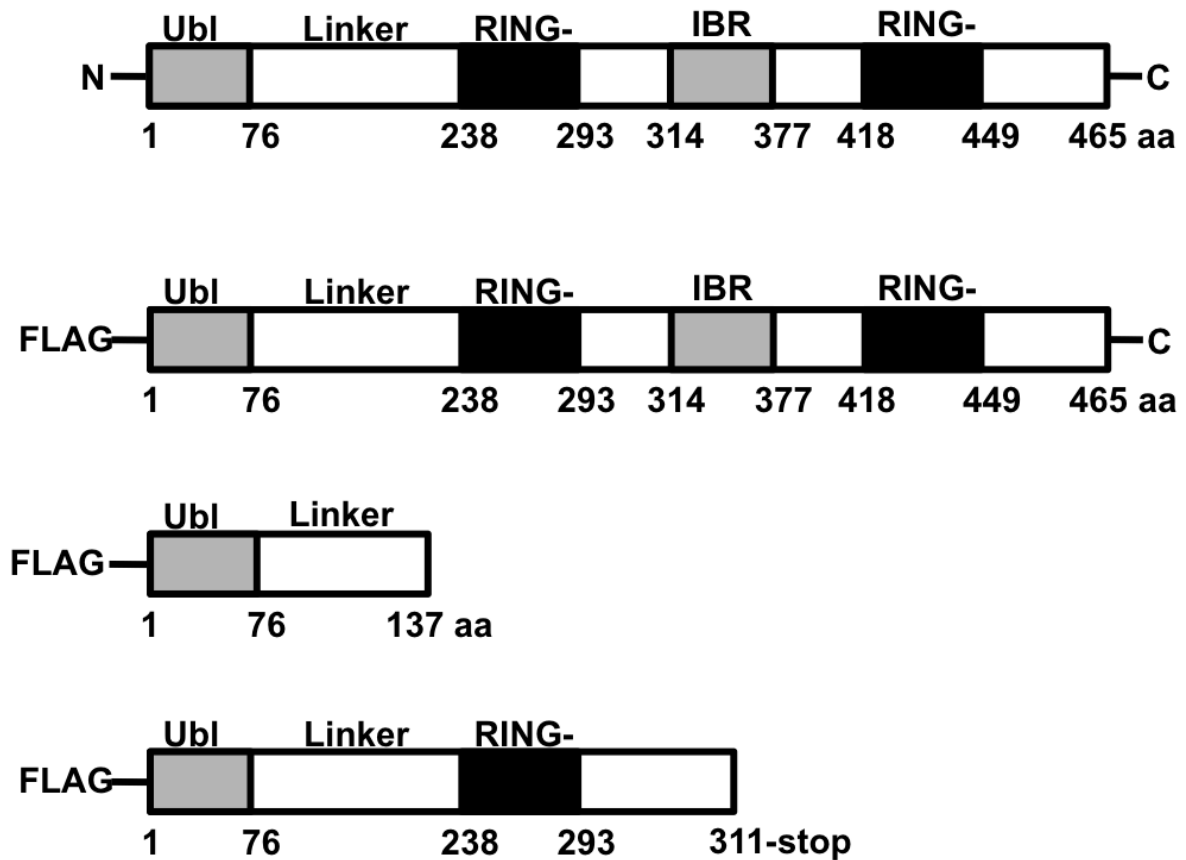


Figure A-11. Site map of parkin protein isoforms. (Panel A) WT hParkin protein containing the N Ubl, the linker region, RING-1, IBR and RING-2 domains. (Panel B) FLAG-hParkin-WT with an N-terminal FLAG tag on hParkin WT. (Panel C) FLAG-hParkin-C-Term mutant, lacking all RING domains. (Panel D) FLAG-hParkin-Q311 mutant with a premature stop codon substitution at amino acid 348.

FLAG-hParkin Constructs

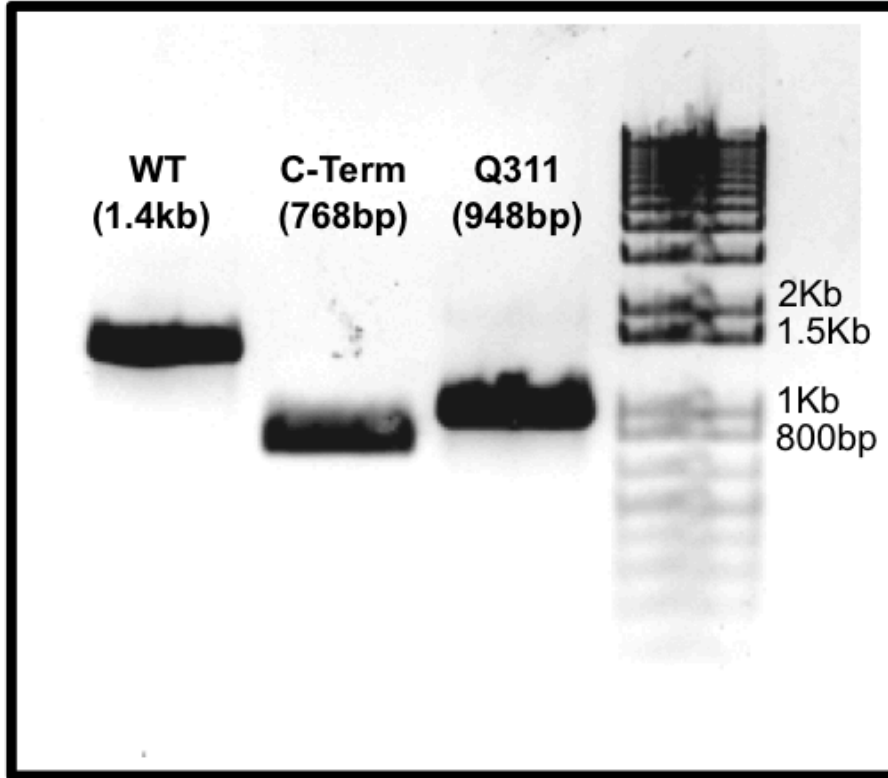


Figure A-12. FLAG-hParkin PCR products. Wild Type (WT), C-Terminal Truncated (C-Term) and Q311 stop (Q311) human parkin constructs were cloned out of the pTRUF11 backbone with PCR primers containing a 5' FLAG epitope. DNA was purified and run on a 0.7% agarose gel.

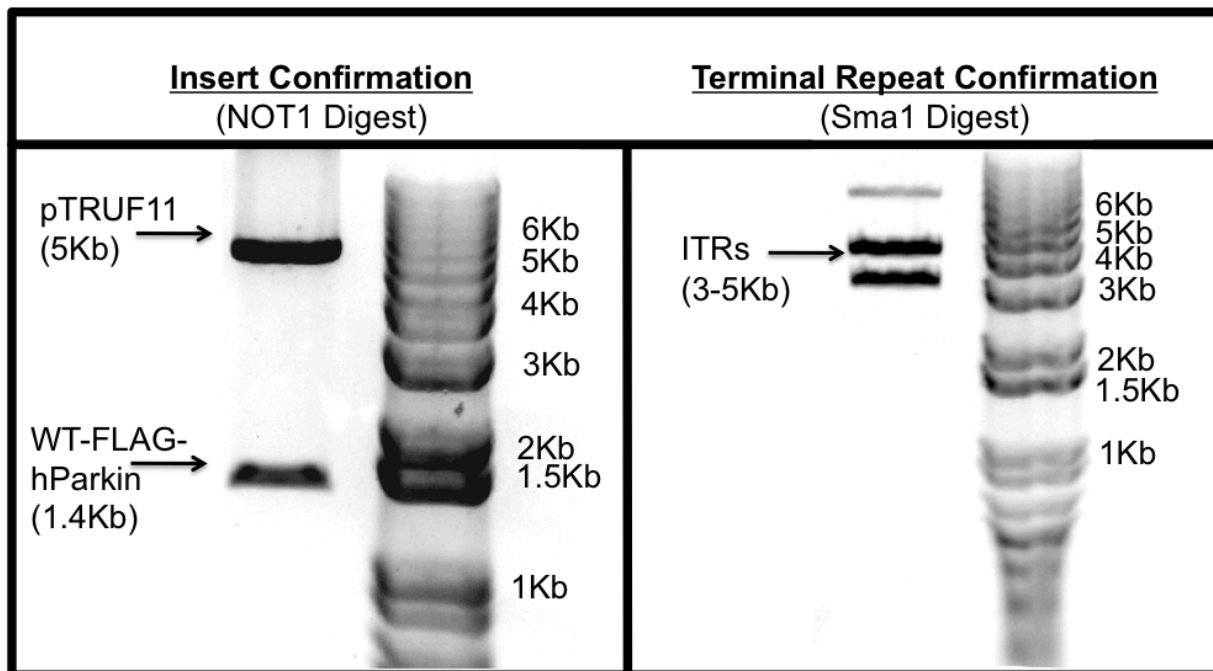


Figure A-13. Final insert and terminal repeat confirmation of WT FLAG-hParkin-AAV constructs. FLAG-hParkin-WT was subcloned into the AAV backbone (pTRUF11). Successful insertion of transgenes and maintained integrity of AAV inverted terminal repeats (ITR) was confirmed by digesting the plasmid DNA with the restriction enzymes NOT1 (**Left panels**) or Sma1 (**Right panels**), respectively. DNA was visualized on or 0.7% agarose gels.

REFERENCES

REFERENCES

- Ahlskog, J. E. J. (2005). Challenging conventional wisdom: the etiologic role of dopamine oxidative stress in Parkinson's disease. *Movement disorders : official journal of the Movement Disorder Society*, *20*(3), 271–282. doi:10.1002/mds.20362
- Amino acid assignment to one of three blood-brain barrier amino acid carriers. (2003). Amino acid assignment to one of three blood-brain barrier amino acid carriers, 1–5.
- Annunziato, L. L., Leblanc, P. P., Kordon, C. C., & Weiner, R. I. R. (1980). Differences in the kinetics of dopamine uptake in synaptosome preparations of the median eminence relative to other dopaminergically innervated brain regions. *Neuroendocrinology*, *31*(5), 316–320.
- Ara, J., Przedborski, S., Naini, A. B., Jackson-Lewis, V., Trifiletti, R. R., Horwitz, J., & Ischiropoulos, H. (1998). Inactivation of tyrosine hydroxylase by nitration following exposure to peroxynitrite and 1-methyl-4-phenyl-1,2,3,6-tetrahydropyridine (MPTP). *PNAS*, *95*(13), 7659–7663.
- Ballard, P. A., Tetrad, J. W., & Langston, J. W. (1985). Permanent human parkinsonism due to 1-methyl-4-phenyl-1,2,3,6-tetrahydropyridine (MPTP): Seven cases. *Neurology*, *35*(7), 949–949. doi:10.1212/WNL.35.7.949
- Barzilai, A. A., Melamed, E. E., & Shirvan, A. A. (2001). Is there a rationale for neuroprotection against dopamine toxicity in Parkinson's disease? *Cellular and Molecular Neurobiology*, *21*(3), 215–235.
- Behrouz, B., Drolet, R. E., Sayed, Z. A., Lookingland, K. J., & Goudreau, J. L. (2007). Unique responses to mitochondrial complex I inhibition in tuberoinfundibular dopamine neurons may impart resistance to toxic insult. *Neuroscience*, *147*(3), 592–598. doi:10.1016/j.neuroscience.2007.05.007
- Bence, N. F., Sampat, R. M., & Kopito, R. R. (2001). Impairment of the ubiquitin-proteasome system by protein aggregation. *Science*, *292*(5521), 1552–1555.

- Benskey, M., Behrouz, B., Sunryd, J., Pappas, S. S., Baek, S.-H., Huebner, M., et al. (2012). Recovery of hypothalamic tuberoinfundibular dopamine neurons from acute toxicant exposure is dependent upon protein synthesis and associated with an increase in parkin and ubiquitin carboxy-terminal hydrolase-L1 expression. *Neurotoxicology*, 33(3), 321–331. doi:10.1016/j.neuro.2012.02.001
- Benskey, M., Lee, K. Y., Parikh, K., lookingland, K. J., & Goudreau, J. L. (2013). Sustained resistance to acute MPTP toxicity by hypothalamic dopamine neurons following chronic neurotoxicant exposure is associated with sustained up-regulation of parkin protein. *Neurotoxicology*, 1–12. doi:10.1016/j.neuro.2013.04.002
- Berman, S. B., & Hastings, T. G. (1999). Dopamine oxidation alters mitochondrial respiration and induces permeability transition in brain mitochondria: Implications for Parkinson's disease. *Journal of Neurochemistry*, 73(3), 1127–1137. doi:10.1046/j.1471-4159.1999.0731127.x
- Betarbet, R., Sherer, T. B., MacKenzie, G., Garcia-Osuna, M., Panov, A. V., & Greenamyre, J. T. (2000). Chronic systemic pesticide exposure reproduces features of Parkinson's disease. *Nature neuroscience*, 3(12), 1301–1306. doi:10.1038/81834
- Blanchard-Fillion, B. (2001). Nitration and Inactivation of Tyrosine Hydroxylase by Peroxynitrite. *Journal of Biological Chemistry*, 276(49), 46017–46023. doi:10.1074/jbc.M105564200
- Blin, O., Desnuelle, C., Rascol, O., Borg, M., Peyro Saint Paul, H., Azulay, J. P., et al. (1994). Mitochondrial respiratory failure in skeletal muscle from patients with Parkinson's disease and multiple system atrophy. *Journal of the neurological sciences*, 125(1), 95–101. doi:10.1016/0022-510X(94)90248-8
- Bohenzky, R. A. R., LeFebvre, R. B. R., & Berns, K. I. K. (1988). Sequence and symmetry requirements within the internal palindromic sequences of the adeno-associated virus terminal repeat. *Virology*, 166(2), 316–327. doi:10.1016/0042-6822(88)90502-8
- Braak, H., Del Tredici, K., Rüb, U., de Vos, R. A. I., Jansen Steur, E. N. H., & Braak, E. (2003). Staging of brain pathology related to sporadic Parkinson's disease. *Neurobiology of aging*, 24(2), 197–211.
- Burke, W. J. W., Li, S. W. S., Williams, E. A. E., Nonneman, R. R., & Zahm, D. S. D. (2003).

3,4-Dihydroxyphenylacetaldehyde is the toxic dopamine metabolite in vivo: implications for Parkinson's disease pathogenesis. *Brain research*, 989(2), 9–9. doi:10.1016/S0006-8993(03)03354-7

Caneda-Ferrón, B., De Girolamo, L. A., Costa, T., Beck, K. E., Layfield, R., & Billett, E. E. (2008). Assessment of the direct and indirect effects of MPP+ and dopamine on the human proteasome: implications for Parkinson's disease aetiology. *Journal of Neurochemistry*, 105(1), 225–238. doi:10.1111/j.1471-4159.2007.05130.x

Cappelletti, G. G., Maggioni, M. G. M., & Maci, R. R. (1999). Influence of MPP+ on the state of tubulin polymerisation in NGF-differentiated PC12 cells. *Journal of neuroscience research*, 56(1), 28–35. doi:10.1002/(SICI)1097-4547(19990401)56:1<28::AID-JNR4>3.0.CO;2-2

Cappelletti, G. G., Pedrotti, B. B., Maggioni, M. G. M., & Maci, R. R. (2001). MICROTUBULE ASSEMBLY IS DIRECTLY AFFECTED BY MPP+ IN VITRO. *Cell Biology International*, 25(10), 4–4. doi:10.1006/cbir.2001.0772

Cappelletti, G. G., Surrey, T. T., & Maci, R. R. (2005). The parkinsonism producing neurotoxin MPP+ affects microtubule dynamics by acting as a destabilising factor. *FEBS Letters*, 579(21), 4781–4786. doi:10.1016/j.febslet.2005.07.058

Cassarino, D. S., Fall, C. P., Swerdlow, R. H., Smith, T. S., Halvorsen, E. M., Miller, S. W., et al. (1997). Elevated reactive oxygen species and antioxidant enzyme activities in animal and cellular models of Parkinson's disease. *Biochimica et biophysica acta*, 1362(1), 77–86.

Chan, P., DeLanney, L. E., Irwin, I., Langston, J. W., & Di Monte, D. (1991). Rapid ATP loss caused by 1-methyl-4-phenyl-1,2,3,6-tetrahydropyridine in mouse brain. *Journal of Neurochemistry*, 57(1), 348–351.

Chen, R., Wei, J., Fowler, S. C., & Wu, J.-Y. (2003). Demonstration of Functional Coupling between Dopamine Synthesis and Its Packaging into Synaptic Vesicles. *Journal of Biomedical Science*, 10(6), 774–781. doi:10.1159/000073965

Chiba, K. K., Trevor, A. A., & Castagnoli, N. N. (1984). Metabolism of the neurotoxic tertiary amine, MPTP, by brain monoamine oxidase. *Biochemical and biophysical research communications*, 120(2), 574–578. doi:10.1016/0006-291X(84)91293-2

- Christiansen, J., & Squires, R. F. (1974). Antagonistic effects of apomorphine and haloperidol on rat striatal synaptosomal tyrosine hydroxylase. *Journal of pharmacy and pharmacology*, *26*, 367–369.
- Chung, K. K. K. (2004). S-Nitrosylation of Parkin Regulates Ubiquitination and Compromises Parkin's Protective Function. *Science*, *304*(5675), 1328–1331. doi:10.1126/science.1093891
- Chung, K. K. K., Zhang, Y., Lim, K.-L., Tanaka, Y., Huang, H., Gao, J., et al. (2001). Parkin ubiquitinates the α -synuclein-interacting protein, synphilin-1: implications for Lewy-body formation in Parkinson disease. *Nature medicine*, *7*(10), 1144–1150. doi:10.1038/nm1001-1144
- Coelln, von, R., Thomas, B., Savitt, J. M., Lim, K. L., Sasaki, M., Hess, E. J., et al. (2004). Loss of locus coeruleus neurons and reduced startle in parkin null mice. *PNAS*, *101*, 10744–10749.
- Cohen, G., & Kesler, N. (1999). Monoamine oxidase and mitochondrial respiration. *Journal of Neurochemistry*, *73*(6), 2310–2315. doi:10.1046/j.1471-4159.1999.0732310.x
- Cuello, A. C., Horn, A. S., Mackay, A. V., & Iversen, L. L. (1973). Letter: Catecholamines in the median eminence: new evidence for a major noradrenergic input. *Nature*, *243*(5408), 465–467. doi:10.1038/243465a0
- Cui, M., Aras, R., Christian, W. V., Rappold, P. M., Hatwar, M., Panza, J., et al. (2009). The organic cation transporter-3 is a pivotal modulator of neurodegeneration in the nigrostriatal dopaminergic pathway. *PNAS*, *106*(19), 8043–8048. doi:10.1073/pnas.0900358106
- Dauer, W., & Przedborski, S. (2003). Parkinson's Disease: Mechanisms and Models. *Neuron*.
- de Lau, L., & Breteler, M. (2006). Epidemiology of Parkinson's disease. *The Lancet Neurology*, *5*(6), 525–535.
- Del Zompo, M. M., Piccardi, M. P. M., Ruiu, S. S., Quartu, M. M., Gessa, G. L. G., & Vaccari, A. A. (1993). Selective MPP⁺ uptake into synaptic dopamine vesicles: possible involvement in MPTP neurotoxicity. *British Journal of Pharmacology*, *109*(2), 411–414.
- Demarest, K. T. K., Riegler, G. D. G., & Moore, K. E. K. (1986). The rapid 'tonic' and the delayed "induction" components of the prolactin-induced activation of tuberoinfundibular

dopaminergic neurons following the systemic administration of prolactin. *Neuroendocrinology*, 43(3), 291–299.

- Demarest, K. T., & Moore, K. E. (1979a). Comparison of dopamine synthesis regulation in the terminals of nigrostriatal, mesolimbic, tuberoinfundibular and tuberohypophyseal neurons. *Journal of neural transmission*, 46(4), 263–277. doi:10.1007/BF01259333
- Demarest, K. T., & Moore, K. E. (1979b). Lack of a high affinity transport system for dopamine in the median eminence and posterior pituitary. *Brain research*, 171(3), 545–551.
- Demaria, J. E. J., Nagy, G. M. G., Lerant, A. A. A., Fekete, M. I. M., Levenson, C. W. C., & Freeman, M. E. M. (2000). Dopamine transporters participate in the physiological regulation of prolactin. *Endocrinology*, 141(1), 366–374. doi:10.1210/en.141.1.366
- Deng, H., Dodson, M. W., Huang, H., & Guo, M. (2008). The Parkinson's disease genes pink1 and parkin promote mitochondrial fission and/or inhibit fusion in *Drosophila*. *PNAS*, 105(38), 14503–14508.
- Di Carlo, R. R., Muccioli, G. G., Lando, D. D., & Bellussi, G. G. (1985). Further evidence for the presence of specific binding sites for prolactin in the rabbit brain. Preferential distribution in the hypothalamus and substantia nigra. *Life Sciences*, 36(4), 375–382.
- Di Monte, D., Jewell, S. A., Ekström, G., & Sandy, M. S. (1986). 1-methyl-4-phenyl-1,2,3,6-tetrahydropyridine (MPTP) and 1-methyl-4-phenylpyridine (MPP+) cause rapid ATP depletion in isolated hepatocytes. *Biochemical*
- Dodson, M. W., & Guo, M. (2007). Pink1, Parkin, DJ-1 and mitochondrial dysfunction in Parkinson's disease. *Current opinion in neurobiology*, 17(3), 331–337. doi:10.1016/j.conb.2007.04.010
- Durham, R. A. R., Eaton, M. J. M., Moore, K. E. K., & Lookingland, K. J. K. (1997). Effects of selective activation of dopamine D2 and D3 receptors on prolactin secretion and the activity of tuberoinfundibular dopamine neurons. *European Journal of Pharmacology*, 335(1), 37–42. doi:10.1016/S0014-2999(97)01179-5
- Exner, N., Treske, B., Paquet, D., Holmstrom, K., Schiesling, C., Gispert, S., et al. (2007). Loss-of-Function of Human PINK1 Results in Mitochondrial Pathology and Can Be Rescued by

Parkin. *Journal of Neuroscience*, 27(45), 12413–12418. doi:10.1523/JNEUROSCI.0719-07.2007

Fahn, S. (2003). Description of Parkinson's disease as a clinical syndrome. *Annals of the New York Academy of Sciences*, 991, 1–14.

Farrer, M., Chan, P., Chen, R., Tan, L., Lincoln, S., Hernandez, D., et al. (2001). Lewy bodies and parkinsonism in families with parkin mutations. *Annals of neurology*, 50(3), 293–300

Fernstrom, J. D., & Fernstrom, M. H. (2007). Tyrosine, phenylalanine, and catecholamine synthesis and function in the brain. *The Journal of nutrition*, 137(6), 1539S–1547S.

Fornai, F. F., Schlüter, O. M. O., Lenzi, P. P., Gesi, M. M., Ruffoli, R. R., Ferrucci, M. M., et al. (2005). Parkinson-like syndrome induced by continuous MPTP infusion: convergent roles of the ubiquitin-proteasome system and alpha-synuclein. *PNAS*, 102(9), 3413–3418. doi:10.2307/3374940

Gasser, P. J., Orchinik, M., Raju, I., & Lowry, C. A. (2009). Distribution of organic cation transporter 3, a corticosterone-sensitive monoamine transporter, in the rat brain. *Journal of Comparative Neurology*, 512(4), 529–555. doi:10.1002/cne.21921

Gasser, T. (2007). Update on the genetics of Parkinson's disease. *Movement disorders : official journal of the Movement Disorder Society*, 22(S17), S343–S350. doi:10.1002/mds.21676

Geisler, S. S., Holmström, K. M. K., Treis, A. A., Skujat, D. D., Weber, S. S. S., Fiesel, F. C. F., et al. (2010). The PINK1/Parkin-mediated mitophagy is compromised by PD-associated mutations. *Autophagy*, 6(7), 871–878. doi:10.4161/auto.6.7.13286

George, S. R., & Van Loon, G. R. (1982). Characterization of high affinity dopamine uptake into the dopamine neurons of the hypothalamus. *Brain research*, 234(2), 339–355.

Giovanni, A. A., Sieber, B. A. B., Heikkila, R. E. R., & Sonsalla, P. K. P. (1994). Studies on species sensitivity to the dopaminergic neurotoxin 1-methyl-4-phenyl-1,2,3,6-tetrahydropyridine. Part 1: Systemic administration. *The Journal of pharmacology and experimental therapeutics*, 270(3), 1000–1007.

- Gowers, W. R. (1896). *A Manual of Diseases of the Nervous System: Diseases of the nerves and spinal cord*.
- Graham, D. G. D., Tiffany, S. M. S., Bell, W. R. W., & Gutknecht, W. F. W. (1978). Autoxidation versus covalent binding of quinones as the mechanism of toxicity of dopamine, 6-hydroxydopamine, and related compounds toward C1300 neuroblastoma cells in vitro. *Molecular Pharmacology*, *14*(4), 644–653.
- Greenamyre, J. T., MacKenzie, G., & Peng, T. I. (1999). Mitochondrial dysfunction in Parkinson's disease. *Biochem Soc*.
- Grimm, D., & Kleinschmidt, J. A. (1999). Progress in adeno-associated virus type 2 vector production: promises and prospects for clinical use. *Human Gene Therapy*, *10*(15), 2445–2450. doi:10.1089/10430349950016799
- Gundersen, H. J., & Jensen, E. B. (1987). The efficiency of systematic sampling in stereology and its prediction. *Journal of Microscopy*, 229–263.
- Haas, R. H., Nasirian, F., Nakano, K., Ward, D., Pay, M., Hill, R., & Shults, C. W. (1995). Low platelet mitochondrial complex I and complex II/III activity in early untreated Parkinson's disease. *Annals of neurology*, *37*(6), 714–722. doi:10.1002/ana.410370604
- Hafer, G. G., Agarwal, D. P. D., & Goedde, H. W. H. (1987). Human brain aldehyde dehydrogenase: activity with DOPAL and isozyme distribution. *Alcohol*, *4*(5), 413–418.
- Hasegawa, E. E., Takeshige, K. K., Oishi, T. T., Murai, Y. Y., & Minakami, S. S. (1990). 1-Methyl-4-phenylpyridinium (MPP+) induces NADH-dependent superoxide formation and enhances NADH-dependent lipid peroxidation in bovine heart submitochondrial particles. *Biochemical and biophysical research communications*, *170*(3), 1049–1055. doi:10.1016/0006-291X(90)90498-C
- Henn, I. H. I., Gostner, J. M. J., Lackner, P. P., Tatzelt, J. J., & Winklhofer, K. F. K. (2005). Pathogenic mutations inactivate parkin by distinct mechanisms. *Journal of Neurochemistry*, *92*(1), 114–122. doi:10.1111/j.1471-4159.2004.02854.x
- Hokfelt, T., & Fuxe, K. (1972). Effects of prolactin and ergot alkaloids on the tubero-infundibular dopamine (DA) neurons. *Audio and Electroacoustics Newsletter, IEEE*, *9*(2),

100–122.

Holloway, R. (2000). Pramipexole vs levodopa as initial treatment for Parkinson disease-A randomized controlled trial. *Journal of the American Medical Association*, *284*, 1931–1938.

Horowitz, J. M. J., Myers, J. J., Stachowiak, M. K. M., & Torres, G. G. (1999). Identification and distribution of Parkin in rat brain. *Neuroreport*, *10*(16), 3393–3397.

Höglinger, G. U., Carrard, G., Michel, P. P., Medja, F., Lombès, A., Ruberg, M., et al. (2003). Dysfunction of mitochondrial complex I and the proteasome: interactions between two biochemical deficits in a cellular model of Parkinson's disease. *Journal of Neurochemistry*, *86*(5), 1297–1307. doi:10.1046/j.1471-4159.2003.01952.x

Höllerhage, M., Matusch, A., Champy, P., Lombès, A., Ruberg, M., Oertel, W. H., & Höglinger, G. U. (2009). Experimental Neurology. *Experimental neurology*, *220*(1), 133–142. doi:10.1016/j.expneurol.2009.08.004

Hung, H. C. H., & Lee, E. H. E. (1996). The mesolimbic dopaminergic pathway is more resistant than the nigrostriatal dopaminergic pathway to MPTP and MPP+ toxicity: role of BDNF gene expression. *Molecular Brain Research*, *41*(1-2), 14–26.

Hurley, S. D. S., O'Banion, M. K. M., Song, D. D. D., Arana, F. S. F., Olschowka, J. A. J., & Haber, S. N. S. (2003). Microglial response is poorly correlated with neurodegeneration following chronic, low-dose MPTP administration in monkeys. *Experimental neurology*, *184*(2), 10–10. doi:10.1016/S0014-4886(03)00273-5

Hyun, D.-H. D., Lee, M. M., Halliwell, B. B., & Jenner, P. P. (2005). Effect of overexpression of wild-type or mutant parkin on the cellular response induced by toxic insults. *Journal of neuroscience research*, *82*(2), 232–244. doi:10.1002/jnr.20638

Imai, Y., & Takahashi, R. (2004). How do Parkin mutations result in neurodegeneration? *Current opinion in neurobiology*, *14*(3), 384–389. doi:10.1016/j.conb.2004.04.002

Imai, Y., Soda, M., & Takahashi, R. (2000). Parkin suppresses unfolded protein stress-induced cell death through its E3 ubiquitin-protein ligase activity. *The Journal of biological chemistry*, *275*(46), 35661–35664. doi:10.1074/jbc.C000447200

Imai, Y., Soda, M., Inoue, H., Hattori, N., Mizuno, Y., & Takahashi, R. (2001). An unfolded

putative transmembrane polypeptide, which can lead to endoplasmic reticulum stress, is a substrate of Parkin. *Cell*, 105(7), 891–902.

Innis, R. B. R., Seibyl, J. P. J., Scanley, B. E. B., Laruelle, M. M., Abi-Dargham, A. A., Wallace, E. E., et al. (1993). Single photon emission computed tomographic imaging demonstrates loss of striatal dopamine transporters in Parkinson disease. *PNAS*, 90(24), 11965–11969.

Isobe, C., Abe, T., & Terayama, Y. (2010). Levels of reduced and oxidized coenzymeQ-10 and 8-hydroxy-2'-deoxyguanosine in the cerebrospinal fluid of patients with living Parkinson's disease demonstrate that mitochondrial oxidative damage and/or oxidative DNA damage contributes to the neurodegenerative process. *Neuroscience Letters*, 469(1), 159–163. doi:10.1016/j.neulet.2009.11.065

Ito, D., Imai, Y., Ohsawa, K., Nakajima, K., Fukuuchi, Y., & Kohsaka, S. (1998). Microglia-specific localisation of a novel calcium binding protein, Iba1. *Molecular Brain Research*, 57(1), 1–9.

Ito, D., Tanaka, K., Suzuki, S., Dembo, T., & Fukuuchi, Y. (2001). Enhanced expression of Iba1, ionized calcium-binding adapter molecule 1, after transient focal cerebral ischemia in rat brain. *Stroke; a journal of cerebral circulation*, 32(5), 1208–1215.

Jackson-Lewis, V., & Przedborski, S. (2007). Protocol for the MPTP mouse model of Parkinson's disease. *Nature Protocols*, 2(1), 141–151. doi:10.1038/nprot.2006.342

JACKSONLEWIS, V., JAKOWEC, M., BURKE, R. E., & Przedborski, S. (1995). Time-Course and Morphology of Dopaminergic Neuronal Death Caused by the Neurotoxin 1-Methyl-4-Phenyl-1,2,3,6-Tetrahydropyridine. *Neurodegeneration*, 4(3), 257–269. doi:10.1016/1055-8330(95)90015-2

Javitch, J. A., D'Amato, R. J., Strittmatter, S. M., & Snyder, S. H. (1985). Parkinsonism-inducing neurotoxin, N-methyl-4-phenyl-1,2,3,6 -tetrahydropyridine: uptake of the metabolite N-methyl-4-phenylpyridine by dopamine neurons explains selective toxicity. *Audio and Electroacoustics Newsletter, IEEE*, 82(7), 2173–2177. doi:10.2307/25058

Jiang, H. H., Ren, Y. Y., Zhao, J. J., & Feng, J. J. (2004). Parkin protects human dopaminergic neuroblastoma cells against dopamine-induced apoptosis. *Human Molecular Genetics*, 13(16), 1745–1754. doi:10.1093/hmg/ddh180

- Johannessen, J. N. J., Adams, J. D. J., Schuller, H. M. H., Bacon, J. P. J., & Markey, S. P. S. (1986). *1e Sciences*, 38(8), 743–749. doi:10.1016/0024-3205(86)90589-8
- Kastner, A., Herrero, M. T., Hirsch, E. C., Guillen, J., Luquin, M. R., Javoy-Agid, F., et al. (1994). Decreased tyrosine hydroxylase content in the dopaminergic neurons of MPTP-intoxicated monkeys: effect of levodopa and GM1 ganglioside therapy. *Annals of neurology*, 36(2), 206–214. doi:10.1002/ana.410360213
- Kastner, A., Hirsch, E. C., Agid, Y., & Javoy-Agid, F. (1993). Tyrosine hydroxylase protein and messenger RNA in the dopaminergic nigral neurons of patients with Parkinson's disease. *Brain research*, 606(2), 341–345.
- Kebabian, J. W., & Calne, D. B. (1979). Multiple Receptros for dopamine. *Nature*, 277, 93–96.
- Keeney, P. M., Xie, J., Capaldi, R. A., & Bennett, J. P. (2006). Parkinson's disease brain mitochondrial complex I has oxidatively damaged subunits and is functionally impaired and misassembled. *Journal of Neuroscience*, 26(19), 5256–5264. doi:10.1523/JNEUROSCI.0984-06.2006
- Kitada, T., Asakawa, S., Hattori, N., Matsumine, H., Yamamura, Y., Minoshima, S., et al. (1998). Mutations in the parkin gene cause autosomal recessive juvenile parkinsonism. *Nature*, 392(6676), 605–608. doi:10.1038/33416
- Kitada, T., Tong, Y., Gautier, C. A., & Shen, J. (2009). Absence of nigral degeneration in aged parkin/DJ-1/PINK1 triple knockout mice. *Journal of Neurochemistry*, 111(3), 696–702. doi:10.1111/j.1471-4159.2009.06350.x
- Ko, H. S. (2005). Accumulation of the Authentic Parkin Substrate Aminoacyl-tRNA Synthetase Cofactor, p38/JTV-1, Leads to Catecholaminergic Cell Death. *Journal of Neuroscience*, 25(35), 7968–7978. doi:10.1523/JNEUROSCI.2172-05.2005
- Ko, H. S. (2006). Identification of Far Upstream Element-binding Protein-1 as an Authentic Parkin Substrate. *Journal of Biological Chemistry*, 281(24), 16193–16196. doi:10.1074/jbc.C600041200
- Kuhn, D. M., Aretha, C. W., & Geddes, T. J. (1999). Peroxynitrite inactivation of tyrosine

hydroxylase: mediation by sulfhydryl oxidation, not tyrosine nitration. *The Journal of neuroscience : the official journal of the Society for Neuroscience*, 19(23), 10289–10294.

- Lad, E. P. L., Fornstedt, B., Clark, D., & Carlsson, A. (2011). Acute effects of 1-methyl-4-phenyl-1,2,3,6-tetrahydropyridine on dopamine metabolism in mouse and rat striatum. *Journal of pharmacy and pharmacology*, 37(10), 707–711. doi:10.1111/j.2042-7158.1985.tb04947.x
- Lamensdorf, I., Eisenhofer, G., Harvey-White, J., Nechustan, A., Kirk, K., & Kopin, I. J. (2000). 3,4-Dihydroxyphenylacetaldehyde potentiates the toxic effects of metabolic stress in PC12 cells. *Brain research*, 868(2), 191–201. doi:10.1016/S0006-8993(00)02309-X
- Langston, J. W. J., Ballard, P. P., Tetrud, J. W. J., & Irwin, I. I. (1983). Chronic Parkinsonism in humans due to a product of meperidine-analog synthesis. *Science*, 219(4587), 979–980.
- Langston, J. W. J., Forno, L. S. L., Tetrud, J. J., Reeves, A. G. A., Kaplan, J. A. J., & Karluk, D. D. (1999). Evidence of active nerve cell degeneration in the substantia nigra of humans years after 1-methyl-4-phenyl-1,2,3,6-tetrahydropyridine exposure. *Annals of neurology*, 46(4), 598–605. doi:10.1002/1531-8249(199910)46:4<598::AID-ANA7>3.0.CO;2-F
- Langston, J. W., & Forno, L. S. (1978). The hypothalamus in Parkinson disease. *Annals of neurology*, 3(2), 129–133. doi:10.1002/ana.410030207
- LaVoie, M. J. M., & Hastings, T. G. T. (1999). Dopamine quinone formation and protein modification associated with the striatal neurotoxicity of methamphetamine: evidence against a role for extracellular dopamine. *The Journal of neuroscience : the official journal of the Society for Neuroscience*, 19(4), 1484–1491.
- Lavoie, M. J., Ostaszewski, B. L., Weihofen, A., Schlossmacher, M. G., & Selkoe, D. J. (2005). Dopamine covalently modifies and functionally inactivates parkin. *Nature medicine*, 11(11), 1214–1221. doi:10.1038/nm1314
- Leroy, E., Boyer, R., Auburger, G., Leube, B., Ulm, G., Mezey, E., et al. (1998). The ubiquitin pathway in Parkinson's disease. *Nature*, 395(6701), 451–452.
- Levitt, M., Spector, S., Sjoerdsma, A., & Udenfriend, S. (1965). Elucidation of the rate-limiting step in norepinephrine biosynthesis in the perfused guinea-pig heart. *Journal of*

Pharmacology and Experimental Therapeutics, 148(1), 1–8.

- Lim, K. L. (2005). Parkin Mediates Nonclassical, Proteasomal-Independent Ubiquitination of Synphilin-1: Implications for Lewy Body Formation. *Journal of Neuroscience*, 25(8), 2002–2009. doi:10.1523/JNEUROSCI.4474-04.2005
- Lim, K.-L., Dawson, V. L., & Dawson, T. M. (2006). Parkin-mediated lysine 63-linked polyubiquitination: A link to protein inclusions formation in Parkinson's and other conformational diseases? *Neurobiology of aging*, 27(4), 524–529. doi:10.1016/j.neurobiolaging.2005.07.023
- Liu, Y. Y., Fallon, L. L., Lashuel, H. A. H., Liu, Z. Z., & Lansbury, P. T. P. (2002). The UCH-L1 Gene Encodes Two Opposing Enzymatic Activities that Affect α -Synuclein Degradation and Parkinson's Disease Susceptibility. *Cell*, 111(2), 10–10. doi:10.1016/S0092-8674(02)01012-7
- Liu, Y., Roghani, A., & Edwards, R. H. (1992). Gene transfer of a reserpine-sensitive mechanism of resistance to N-methyl-4-phenylpyridinium. *PNAS*, 89(19), 9074–9078.
- Lofrumento, D. D., Saponaro, C., Cianciulli, A., De Nuccio, F., Mitolo, V., Nicolardi, G., & Panaro, M. A. (2011). MPTP-induced neuroinflammation increases the expression of pro-inflammatory cytokines and their receptors in mouse brain. *Neuroimmunomodulation*, 18(2), 79–88. doi:10.1159/000320027
- lookingland, K. J., & Moore, K. E. (2005). Functional neuroanatomy of hypothalamic dopaminergic neuroendocrine systems. (S. B. Dunnett, M. Bentivoglio, A. Bjorklund, & T. Hokfelt, Eds.) *Handbook of Chemical Neuroanatomy*, 21, 433–521.
- Lotharius, J. J., Dugan, L. L. L., & O'Malley, K. L. K. (1999). Distinct mechanisms underlie neurotoxin-mediated cell death in cultured dopaminergic neurons. *The Journal of neuroscience : the official journal of the Society for Neuroscience*, 19(4), 1284–1293.
- Lotharius, J., & O'Malley, K. L. (2000). The parkinsonism-inducing drug 1-methyl-4-phenylpyridinium triggers intracellular dopamine oxidation. A novel mechanism of toxicity. *The Journal of biological chemistry*, 275(49), 38581–38588. doi:10.1074/jbc.M005385200
- Lovenberg, W., Weissbach, H., & Udenfriend, S. (1962). Aromatic L-amino acid decarboxylase. *The Journal of biological chemistry*, 237(1), 89–93.

- Manfredsson, F. P., Burger, C., Sullivan, L. F., Muzyczka, N., Lewin, A. S., & Mandel, R. J. (2007). rAAV-mediated nigral human parkin over-expression partially ameliorates motor deficits via enhanced dopamine neurotransmission in a rat model of Parkinson's disease. *Experimental neurology*, *207*(2), 13–13. doi:10.1016/j.expneurol.2007.06.019
- Manfredsson, F. P., Tumer, N., Erdos, B., Landa, T., Broxson, C. S., Sullivan, L. F., et al. (2009). Nigrostriatal rAAV-mediated GDNF overexpression induces robust weight loss in a rat model of age-related obesity. *Molecular Therapy*, *17*(6), 980–991. doi:10.1038/mt.2009.45
- Marchitti, S. A. S., Deitrich, R. A. R., & Vasiliou, V. V. (2007). Neurotoxicity and metabolism of the catecholamine-derived 3,4-dihydroxyphenylacetaldehyde and 3,4-dihydroxyphenylglycolaldehyde: the role of aldehyde dehydrogenase. *Pharmacological Reviews*, *59*(2), 125–150. doi:10.1124/pr.59.2.1
- Matsuda, N., Kitami, T., Suzuki, T., Mizuno, Y., Hattori, N., & Tanaka, K. (2006). Diverse effects of pathogenic mutations of Parkin that catalyze multiple monoubiquitylation in vitro. *The Journal of biological chemistry*, *281*(6), 3204–3209.
- Matzuk, M. M., & Saper, C. B. (1985). Preservation of hypothalamic dopaminergic neurons in Parkinson's disease. *Annals of neurology*, *18*(5), 552–555. doi:10.1002/ana.410180507
- McCormack, A. L. A., Thiruchelvam, M. M., Manning-Bog, A. B. A., Thiffault, C. C., Langston, J. W. J., Cory-Slechta, D. A. D., & Di Monte, D. A. D. (2002). Environmental risk factors and Parkinson's disease: selective degeneration of nigral dopaminergic neurons caused by the herbicide paraquat. *Neurobiology of disease*, *10*(2), 119–127. doi:10.1006/nbdi.2002.0507
- McNaught, K. S. P. K., Belizaire, R. R., Jenner, P. P., Olanow, C. W. C., & Isacson, O. O. (2002). Selective loss of 20S proteasome alpha-subunits in the substantia nigra pars compacta in Parkinson's disease. *Neuroscience Letters*, *326*(3), 155–158. doi:10.1016/S0304-3940(02)00296-3
- McNaught, K. S. P., Belizaire, R., Isacson, O., Jenner, P., & Olanow, C. W. (2003). Altered proteasomal function in sporadic Parkinson's disease. *Experimental neurology*, *179*(1), 38–46.

- McNaught, K. S. P., Perl, D. P., Brownell, A.-L., & Olanow, C. W. (2004). Systemic exposure to proteasome inhibitors causes a progressive model of Parkinson's disease. *Annals of neurology*, *56*(1), 149–162. doi:10.1002/ana.20186
- McNaught, K. S., & Jenner, P. (2001). Proteasomal function is impaired in substantia nigra in Parkinson's disease. *Neuroscience Letters*, *297*(3), 191–194.
- Melamed, E. E., Rosenthal, J. J., Globus, M. M., Cohen, O. O., Frucht, Y. Y., & Uzzan, A. A. (1985). Mesolimbic dopaminergic neurons are not spared by MPTP neurotoxicity in mice. *European Journal of Pharmacology*, *114*(1), 97–100.
- Meredith, G. E., Totterdell, S., Potashkin, J. A., & Surmeier, D. J. (2008). Modeling PD pathogenesis in mice: Advantages of a chronic MPTP protocol. *Parkinsonism & related disorders*, *14*, S112–S115. doi:10.1016/j.parkreldis.2008.04.012
- Mizuno, Y., Ohta, S., Tanaka, M., Takamiya, S., Suzuki, K., Sato, T., et al. (1989). Deficiencies in complex I subunits of the respiratory chain in Parkinson's disease. *Biochemical and biophysical research communications*, *163*(3), 1450–1455.
- Mogi, M. M., Harada, M. M., Kojima, K. K., Kiuchi, K. K., & Nagatsu, T. T. (1988). Effects of systemic administration of 1-methyl-4-phenyl-1,2,3,6-tetrahydropyridine to mice on tyrosine hydroxylase, L-3,4-dihydroxyphenylalanine decarboxylase, dopamine beta-hydroxylase, and monoamine oxidase activities in the striatum and hypothalamus. *Journal of Neurochemistry*, *50*(4), 1053–1056. doi:10.1111/j.1471-4159.1988.tb10572.x
- Moore, D. J. D. (2006). Parkin: a multifaceted ubiquitin ligase. *Biochemical Society Transactions*, *34*(Pt 5), 749–753. doi:10.1042/BST0340749
- Moore, D. J., Zhang, L., Troncoso, J., Lee, M. K., Hattori, N., Mizuno, Y., et al. (2005). Association of DJ-1 and parkin mediated by pathogenic DJ-1 mutations and oxidative stress. *Human Molecular Genetics*, *14*(1), 71–84. doi:10.1093/hmg/ddi007
- Moore, R. Y. R., & Bloom, F. E. F. (1978). Central catecholamine neuron systems: anatomy and physiology of the dopamine systems. *Neuroscience*, *1*, 129–169. doi:10.1146/annurev.ne.01.030178.001021

- Moriyama, Y., Amakatsu, K., & Futai, M. (1993). Uptake of the neurotoxin, 4-methylphenylpyridinium, into chromaffin granules and synaptic vesicles: a proton gradient drives its uptake through monoamine transporter. *Archives of Biochemistry and Biophysics*, 305(2), 271–277. doi:10.1006/abbi.1993.1422
- Muroyama, A., Kobayashi, S., & Mitsumoto, Y. (2011). Loss of striatal dopaminergic terminals during the early stage in response to MPTP injection in C57BL/6 mice. *Neuroscience Research*, 69(4), 352–355. doi:10.1016/j.neures.2010.12.009
- Mytilineou, C. C., Werner, P. P., Molinari, S. S., Di Rocco, A. A., Cohen, G. G., & Yahr, M. D. M. (1994). Impaired oxidative decarboxylation of pyruvate in fibroblasts from patients with Parkinson's disease. *Journal of Neural Transmission - Parkinsons Disease and Dementia Section*, 8(3), 223–228.
- Narendra, D., Kane, L. A., Hauser, D. N., Fearnley, I. M., & Youle, R. J. (2010). p62/SQSTM1 is required for Parkin-induced mitochondrial clustering but not mitophagy; VDAC1 is dispensable for both. *Autophagy*, 6(8), 1090–1106. doi:10.4161/auto.6.8.13426
- Narendra, D., Tanaka, A., Suen, D. F., & Youle, R. J. (2008). Parkin is recruited selectively to impaired mitochondria and promotes their autophagy. *The Journal of cell biology*, 183(5), 795–803. doi:10.1073/pnas.0711845105
- Nicklas, W. J., Youngster, S. K., Kindt, M., & Heikkila, R. E. (1987). IV. MPTP, MPP+ and mitochondrial function. *Life Sciences*.
- Niznik, H. B. (1987). Dopamine receptors: molecular structure and function. *Molecular and cellular endocrinology*, 54(1), 1–22.
- O'Carroll, A. M., Fowler, C. J., Phillips, J. P., Tobbia, I., & Tipton, K. F. (1983). The deamination of dopamine by human brain monoamine oxidase. Specificity for the two enzyme forms in seven brain regions. *Naunyn-Schmiedeberg's archives of pharmacology*, 322(3), 198–202.
- Okuno, S., & Fujisawa, H. (1985). A new mechanism for regulation of tyrosine 3-monooxygenase by end product and cyclic AMP-dependent protein kinase. *The Journal of biological chemistry*, 260(5), 2633–2635.

- Ouchi, Y. Y., Yoshikawa, E. E., Sekine, Y. Y., Futatsubashi, M. M., Kanno, T. T., Ogusu, T. T., & Torizuka, T. T. (2005). Microglial activation and dopamine terminal loss in early Parkinson's disease. *Annals of neurology*, *57*(2), 168–175. doi:10.1002/ana.20338
- Palkovits, M. (1973). Isolated Removal of Hypothalamic or other Brain Nuclei of the Rat. *Brain Res*, 449–450.
- Palkovits, M., & Brownstein, M. (1983). Microdissection of Brain Areas by the Punch Technique. *Brain Microdissection Techniques 2*, 1–36.
- Parker, W. D., Parks, J. K., & Swerdlow, R. H. (2008). Complex I deficiency in Parkinson's disease frontal cortex. *Brain research*, *1189*, 215–218. doi:10.1016/j.brainres.2007.10.061
- Paterna, J.-C., Leng, A., Weber, E., Feldon, J., & Bueler, H. (2007). DJ-1 and Parkin modulate dopamine-dependent behavior and inhibit MPTP-induced nigral dopamine neuron loss in mice. *Molecular Therapy*, *15*(4), 698–704. doi:10.1038/sj.mt.6300067
- Paxinos, G., & Franklin, K. (2003, July 8). *The Mouse Brain in Stereotaxic Coordinates*. San Diego Academic.
- Perry, T. L., Yong, V. W., Jones, K., Wall, R. A., Clavier, R. M., Foulks, J. G., & Wright, J. M. (1985). Effects of N-methyl-4-phenyl-1,2,3,6-tetrahydropyridine and its metabolite, N-methyl-4-phenylpyridinium ion, on dopaminergic nigrostriatal neurons in the mouse. *Neuroscience Letters*, *58*(3), 321–326.
- Petroske, E., Meredith, G. E., Callen, S., Totterdell, S., & Lau, Y. S. (2001). Mouse model of Parkinsonism: a comparison between subacute MPTP and chronic MPTP/probenecid treatment. *Neuroscience*, *106*(3), 589–601.
- Petrucelli, L., O'Farrell, C., Lockhart, P. J., Baptista, M., Kehoe, K., Vink, L., et al. (2002). Parkin protects against the toxicity associated with mutant alpha-synuclein: proteasome dysfunction selectively affects catecholaminergic neurons. *Neuron*, *36*(6), 1007–1019.
- Poole, A. C., Thomas, R. E., Andrews, L. A., McBride, H. M., Whitworth, A. J., & Pallanck, L. J. (2008). The PINK1/Parkin pathway regulates mitochondrial morphology. *PNAS*, *105*(5), 1638–1643. doi:10.1073/pnas.0709336105

- Priyadarshi, A. (2001). Environmental Risk Factors and Parkinson's Disease: A Metaanalysis. *Environmental Research*, 86(2), 122–127. doi:10.1006/enrs.2001.4264
- Qiu, J. H., Asai, A., Chi, S., Saito, N., Hamada, H., & Kirino, T. (2000). Proteasome inhibitors induce cytochrome c-caspase-3-like protease-mediated apoptosis in cultured cortical neurons. *The Journal of neuroscience : the official journal of the Society for Neuroscience*, 20(1), 259–265.
- Rainer von Coelln, Dawson, V. L., & Dawson, T. M. (2004). Parkin-associated Parkinson's disease. *Cell and Tissue Research*, 318(1), 175–184. doi:10.1007/s00441-004-0924-4
- Ramsay, R. R., & Singer, T. P. (1986). Energy-dependent uptake of N-methyl-4-phenylpyridinium, the neurotoxic metabolite of 1-methyl-4-phenyl-1,2,3,6-tetrahydropyridine, by mitochondria. *The Journal of biological chemistry*, 261(17), 7585–7587.
- Rapisardi, S. C., Warrington, V. O., & Wilson, J. S. (1990). Effects of MPTP on the fine structure of neurons in substantia nigra of dogs. *Brain research*, 512(1), 147–154.
- Reimsnider, S., Manfredsson, F. P., Muzyczka, N., & Mandel, R. J. (2007). Time Course of Transgene Expression After Intrastratial Pseudotyped rAAV2/1, rAAV2/2, rAAV2/5, and rAAV2/8 Transduction in the Rat. *Molecular Therapy*, 15(8), 1504–1511. doi:10.1038/sj.mt.6300227
- Ren, Y. Y., Liu, W. W., Jiang, H. H., Jiang, Q. Q., & Feng, J. J. (2005). Selective vulnerability of dopaminergic neurons to microtubule depolymerization. *The Journal of biological chemistry*, 280(40), 34105–34112. doi:10.1074/jbc.M503483200
- Ren, Y., Jiang, H., Yang, F., Nakaso, K., & Feng, J. (2008). Parkin Protects Dopaminergic Neurons against Microtubule-depolymerizing Toxins by Attenuating Microtubule-associated Protein Kinase Activation. *The Journal of biological chemistry*, 284(6), 4009–4017. doi:10.1074/jbc.M806245200
- Revay, R., Vaughan, R., Grant, S., & Kuhar, M. J. (1996). Dopamine transporter immunohistochemistry in median eminence, amygdala, and other areas of the rat brain. *Synapse*, 22(2), 93–99. doi:10.1002/(SICI)1098-2396(199602)22:2<93::AID-SYN1>3.0.CO;2-C

- RS, S., AG, E., Pschkanzer, D. C., & Young, R. R. (1969). Amantadine in the Treatment of Parkinson Disease. *Journal of the American Medical Association*, *208*, 11168–11170.
- Salach, J. I., Singer, T. P., Castagnoli, N., & Trevor, A. (1984). Oxidation of the neurotoxic amine 1-methyl-4-phenyl-1,2,3,6-tetrahydropyridine (MPTP) by monoamine oxidases A and B and suicide inactivation of the enzymes by MPTP. *Biochemical and Biophysical Research Communications*, *125*(2), 831–835. doi:10.1016/0006-291X(84)90614-4
- Sanchez-Ramos, J. R. J., Michel, P. P., Weiner, W. J. W., & Hefti, F. F. (1988). Selective destruction of cultured dopaminergic neurons from fetal rat mesencephalon by 1-methyl-4-phenylpyridinium: cytochemical and morphological evidence. *Journal of Neurochemistry*, *50*(6), 1934–1944. doi:10.1111/j.1471-4159.1988.tb02500.x
- Sanchez-Ramos, J., Barrett, J. N., & Goldstein, M. (1986). 1-Methyl-4-phenylpyridinium (MPP+) but not 1-methyl-4-phenyl-1,2,3,6-tetrahydropyridine (MPTP) selectively destroys dopaminergic neurons in cultures of dissociated rat mesencephalic neurons. *Neuroscience*.
- Schapira, A. H., Cooper, D., Dexter, D., Clark, J. D., & Jenner, P. (1990). Mitochondrial Complex I Deficiency in Parkinson's Disease. *Journal of Neurochemistry*, *54*, 823–827.
- Schenkman, M., Wei Zhu, C., Cutson, T. M., & Whetten-Goldstein, K. (2001). Longitudinal evaluation of economic and physical impact of Parkinson's disease. *Parkinsonism & Related Disorders*, *8*(1), 41–50.
- Schmitz, C., & Hof, P. R. (2005). Design-based stereology in neuroscience. *Neuroscience*, *130*(4), 813–831. doi:10.1016/j.neuroscience.2004.08.050
- Schneider, J. S. J., Yuwiler, A. A., & Markham, C. H. C. (1986). Production of a Parkinson-like syndrome in the cat with N-methyl-4-phenyl-1,2,3,6-tetrahydropyridine (MPTP): behavior, histology, and biochemistry. *Experimental Neurology*, *91*(2), 293–307.
- Schulz, J. B. J., Henshaw, D. R. D., Matthews, R. T. R., & Beal, M. F. M. (1995). Coenzyme Q₁₀ and nicotinamide and a free radical spin trap protect against MPTP neurotoxicity. *Experimental Neurology*, *132*(2), 5–5. doi:10.1016/0014-4886(95)90033-0
- Schwartz, J. P. J., Sheng, J. G. J., Mitsuo, K. K., Shirabe, S. S., & Nishiyama, N. N. (1993).

Trophic factor production by reactive astrocytes in injured brain. *Annals of the New York Academy of Sciences*, 679, 226–234. doi:10.1111/j.1749-6632.1993.tb18302.x

Scotcher, K. P. K., Irwin, I. I., DeLanney, L. E. L., Langston, J. W. J., & Di Monte, D. D. (1990). Effects of 1-methyl-4-phenyl-1,2,3,6-tetrahydropyridine and 1-methyl-4-phenylpyridinium ion on ATP levels of mouse brain synaptosomes. *Journal of Neurochemistry*, 54(4), 1295–1301. doi:10.1111/j.1471-4159.1990.tb01962.x

Semchuck, K. M., Love, E. J., & Lee, R. G. (1991). Parkinson's disease and exposure to rural environmental factors: a population based case-control study. *The Canadian Journal of Neurological Sciences*, 18, 279–286.

Shamoto-Nagai, M., Maruyama, W., Kato, Y., Isobe, K., Tanaka, M., Naoi, M., & Osawa, T. (2003). An inhibitor of mitochondrial complex I, rotenone, inactivates proteasome by oxidative modification and induces aggregation of oxidized proteins in SH-SY5Y cells. *Journal of neuroscience research*, 74(4), 589–597. doi:10.1002/jnr.10777

Sharma, N., McLean, P. J., Kawamata, H., Irizarry, M. C., & Hyman, B. T. (2001). Alpha-synuclein has an altered conformation and shows a tight intermolecular interaction with ubiquitin in Lewy bodies. *Acta neuropathologica*, 102(4), 329–334.

Sheehan, J. P., Swerdlow, R. H., Parker, W. D., Miller, S. W., Davis, R. E., & Tuttle, J. B. (1997). Altered calcium homeostasis in cells transformed by mitochondria from individuals with Parkinson's disease. *Journal of Neurochemistry*, 68(3), 1221–1233. doi:10.1046/j.1471-4159.1997.68031221.x

Shen, H. H., Sikorska, M. M., Leblanc, J. J., Walker, P. R. P., & Liu, Q. Y. Q. (2006). Oxidative stress regulated expression of ubiquitin Carboxyl-terminal Hydrolase-L1: role in cell survival. *Apoptosis : an international journal on programmed cell death*, 11(6), 1049–1059. doi:10.1007/s10495-006-6303-8

Shimada, S., Kitayama, S., Lin, C. L., Patel, A., Nanthakumar, E., Gregor, P., et al. (1991). Cloning and expression of a cocaine-sensitive dopamine transporter complementary DNA. *Science*, 254(5031), 576–578.

Shimura, H. H., Schlossmacher, M. G. M., Hattori, N. N., Frosch, M. P. M., Trockenbacher, A. A., Schneider, R. R., et al. (2001). Ubiquitination of a new form of alpha-synuclein by parkin from human brain: implications for Parkinson's disease. *Science*, 293(5528), 263–

269. doi:10.1126/science.1060627
- Shin, J.-H., Ko, H. S., Kang, H., Lee, Y., Lee, Y.-I., Pletinkova, O., et al. (2011). PARIS (ZNF746) Repression of PGC-1 α Contributes to Neurodegeneration in Parkinson's Disease. *Cell*, 144(5), 689–702. doi:10.1016/j.cell.2011.02.010
- Smith, T. S., & Bennett, J. P., Jr. (1997). Mitochondrial toxins in models of neurodegenerative diseases. I: in vivo brain hydroxyl radical production during systemic MPTP treatment or following microdialysis infusion of methylpyridinium or azide ions. *Brain research*.
- Snyder, H., Mensah, K., Theisler, C., Lee, J., Matouschek, A., & Wolozin, B. (2003). Aggregated and monomeric alpha-synuclein bind to the S6 ' proteasomal protein and inhibit proteasomal function. *The Journal of biological chemistry*, 278(14), 11753–11759. doi:10.1074/jbc.M208641200
- Soubannier, V. V., McLelland, G.-L. G., Zunino, R. R., Braschi, E. E., Rippstein, P. P., Fon, E. A. E., & McBride, H. M. H. (2012). A vesicular transport pathway shuttles cargo from mitochondria to lysosomes. *Current biology : CB*, 22(2), 135–141. doi:10.1016/j.cub.2011.11.057
- Speciale, S. G. S., Liang, C. L. C., Sonsalla, P. K. P., Edwards, R. H. R., & German, D. C. D. (1998). The neurotoxin 1-methyl-4-phenylpyridinium is sequestered within neurons that contain the vesicular monoamine transporter. *Neuroscience*, 84(4), 9–9. doi:10.1016/S0306-4522(97)00570-8
- Subramaniam, S. R., & Chesselet, M.-F. (2013). Mitochondrial dysfunction and oxidative stress in Parkinson's disease. *Progress in Neurobiology*, –. doi:10.1016/j.pneurobio.2013.04.004
- Sulzer, D. (2007). Multiple hit hypotheses for dopamine neuron loss in Parkinson's disease. *Trends in Neurosciences*, 30(5), 244–250. doi:10.1016/j.tins.2007.03.009
- Sundström, E., Fredriksson, A., & Archer, T. (1990). Chronic neurochemical and behavioral changes in MPTP-lesioned C57BL/6 mice: a model for Parkinson's disease. *Brain research*, 528(2), 181–188. doi:10.1016/0006-8993(90)91656-2
- Surmeier, D. J., Ding, J., Day, M., Wang, Z., & Shen, W. (2007). D1 and D2 dopamine-receptor modulation of striatal glutamatergic signaling in striatal medium spiny neurons. *Trends in Neurosciences*, 30, 228–235.

- Tanaka, Y., Engelender, S., Igarashi, S., Rao, R. K., Wanner, T., Tanzi, R. E., et al. (2001). Inducible expression of mutant alpha-synuclein decreases proteasome activity and increases sensitivity to mitochondria-dependent apoptosis. *Human Molecular Genetics*, *10*(9), 919–926.
- Tang, L., Todd, R. D., & O'Malley, K. L. (1994). Dopamine D2 and D3 receptors inhibit dopamine release. *The Journal of pharmacology and experimental therapeutics*, *270*(2), 475–479.
- Tatton, N. A. N., & Kish, S. J. S. (1997). In situ detection of apoptotic nuclei in the substantia nigra compacta of 1-methyl-4-phenyl-1,2,3,6-tetrahydropyridine-treated mice using terminal deoxynucleotidyl transferase labelling and acridine orange staining. *Neuroscience*, *77*(4), 1037–1048. doi:10.1016/S0306-4522(96)00545-3
- Teismann, P. P., & Ferger, B. B. (2001). Inhibition of the cyclooxygenase isoenzymes COX-1 and COX-2 provide neuroprotection in the MPTP-mouse model of Parkinson's disease. *Synapse*, *39*(2), 167–174. doi:10.1002/1098-2396(200102)39:2<167::AID-SYN8>3.0.CO;2-U
- Tenenbaum, L., Chtarto, A., Lehtonen, E., Velu, T., Brotchi, J., & Levivier, M. (2004). Recombinant AAV-mediated gene delivery to the central nervous system. *The Journal of Gene Medicine*, *6*(S1), S212–S222. doi:10.1002/jgm.506
- Timmerman, W. W., Deinum, M. E. M., Westerink, B. H. B., & Schuiling, G. A. G. (1995). Lack of evidence for dopamine autoreceptors in the mediobasal hypothalamus: a microdialysis study in awake rats. *Neuroscience Letters*, *195*(2), 113–116.
- Tsang, A. H. K., & Chung, K. K. K. (2009). Oxidative and nitrosative stress in Parkinson's disease. *Biochimica et Biophysica Acta (BBA) - Molecular Basis of Disease*, *1792*(7), 643–650. doi:10.1016/j.bbadis.2008.12.006
- Usiello, A., Baik, J. H., Rougé-Pont, F., Picetti, R., Dierich, A., LeMeur, M., et al. (2000). Distinct functions of the two isoforms of dopamine D2 receptors. *Nature*, *408*(6809), 199–203. doi:10.1038/35041572
- Vercammen, L., Van der Perren, A., Vaudano, E., Gijssbers, R., Debyser, Z., Van den Haute, C., & Baekelandt, V. (2006). Parkin Protects against Neurotoxicity in the 6-Hydroxydopamine

Rat Model for Parkinson's Disease. *Molecular Therapy*, 14(5), 8–8.
doi:10.1016/j.ymthe.2006.06.009

Wakabayashi, K., Engelender, S., Yoshimoto, M., Tsuji, S., Ross, C. A., & Takahashi, H. (2000). Synphilin-1 is present in Lewy bodies in Parkinson's disease. *Annals of neurology*, 47(4), 521–523. doi:10.1002/1531-8249(200004)47:4<521::AID-ANA18>3.0.CO;2-B

Walker, J. M. (2002). The Bicinchoninic Acid (BCA) Assay for Protein Quantitation . *The protein Protocols Handbook*, 3–14.

Walther, W., & Stein, U. (2000). Viral Vectors for Gene Transfer. *Drugs*, 60(2), 249–271.
doi:10.2165/00003495-200060020-00002

Wang, C. (2005). Stress-induced alterations in parkin solubility promote parkin aggregation and compromise parkin's protective function. *Human Molecular Genetics*, 14(24), 3885–3897.
doi:10.1093/hmg/ddi413

Wang, C. C., Tan, J. M. M. J., Ho, M. W. L. M., Zaiden, N. N., Wong, S. H. S., Chew, C. L. C. C., et al. (2005). Alterations in the solubility and intracellular localization of parkin by several familial Parkinson's disease-linked point mutations. *Journal of Neurochemistry*, 93(2), 422–431. doi:10.1111/j.1471-4159.2005.03023.x

Watabe, M., & Nakaki, T. (2008). Mitochondrial complex I inhibitor rotenone inhibits and redistributes vesicular monoamine transporter 2 via nitration in human dopaminergic SH-SY5Y cells. *Molecular Pharmacology*, 74(4), 933–940. doi:10.1124/mol.108.048546

Weihe, E., Schäfer, M. K.-H., Erickson, J. D., & Eiden, L. E. (1994). Localization of vesicular monoamine transporter isoforms (VMAT1 and VMAT2) to endocrine cells and neurons in rat. *Journal of molecular neuroscience : MN*, 5(3), 149–164.

Wermuth, L., Stenager, E. N., Stenager, E., & Boldsen, J. (2009). Mortality in patients with Parkinson's disease. *Acta Neurologica Scandinavica*, 92(1), 55–58. doi:10.1111/j.1600-0404.1995.tb00466.x

West, M. J., Slomianka, L., & Gundersen, H. J. (1991). Unbiased stereological estimation of the total number of neurons in the subdivisions of the rat hippocampus using the optical fractionator. *The Anatomical record*, 231(4), 482–497. doi:10.1002/ar.1092310411

- Wilkinson, K. D., Lee, K. M., Deshpande, S., Duerksen-Hughes, P., Boss, J. M., & Pohl, J. (1989). The neuron-specific protein PGP 9.5 is a ubiquitin carboxyl-terminal hydrolase. *Science*, *246*(4930), 670–673.
- Willis, G. L., & Donnan, G. A. (1987). Histochemical, biochemical and behavioural consequences of MPTP treatment in C-57 black mice. *Brain research*, *402*(2), 269–274.
- Winklhofer, K. F., & Haass, C. (2010). Mitochondrial dysfunction in Parkinson's disease. *Biochimica et Biophysica Acta (BBA) - Molecular Basis of Disease*, *1802*(1), 29–44. doi:10.1016/j.bbadis.2009.08.013
- Wirdefeldt, K., Bogdanovic, N., Westerberg, L., Payami, H., Schalling, M., & Murdoch, G. (2001). Expression of alpha-synuclein in the human brain: relation to Lewy body disease. *Molecular Brain Research*, *92*(1-2), 58–65.
- Xiao, X., Li, J., McCown, T. J., & Samulski, R. J. (1997). Gene transfer by adeno-associated virus vectors into the central nervous system. *Experimental neurology*, *144*(1), 113–124. doi:10.1006/exnr.1996.6396
- Yamada, M. M., Mizuno, Y. Y., & Mochizuki, H. H. (2005). Parkin gene therapy for alpha-synucleinopathy: a rat model of Parkinson's disease. *Human Gene Therapy*, *16*(2), 262–270. doi:10.1089/hum.2005.16.262
- Yang, F. F., Jiang, Q. Q., Zhao, J. J., Ren, Y. Y., Sutton, M. D. M., & Feng, J. J. (2005). Parkin stabilizes microtubules through strong binding mediated by three independent domains. *The Journal of biological chemistry*, *280*(17), 17154–17162.
- Yao, D., Gu, Z., Nakamura, T., Shi, Z.-Q., Ma, Y., Gaston, B., et al. (2004). Nitrosative stress linked to sporadic Parkinson's disease: S-nitrosylation of parkin regulates its E3 ubiquitin ligase activity. *PNAS*, *101*(29), 10810–10814.
- Yasuda, T. T., Hayakawa, H. H., Nihira, T. T., Ren, Y.-R. Y., Nakata, Y. Y., Nagai, M. M., et al. (2011). Parkin-mediated protection of dopaminergic neurons in a chronic MPTP-minipump mouse model of Parkinson disease. *Journal of neuropathology and experimental neurology*, *70*(8), 686–697. doi:10.1097/NEN.0b013e3182269ecd
- Youdim, M. B. H., & Bakhle, Y. S. (2009). Monoamine oxidase: isoforms and inhibitors in

Parkinson's disease and depressive illness. *British Journal of Pharmacology*, 147(S1), S287–S296. doi:10.1038/sj.bjp.0706464

Zang, L. Y. L., & Misra, H. P. H. (1993). Generation of reactive oxygen species during the monoamine oxidase-catalyzed oxidation of the neurotoxicant, 1-methyl-4-phenyl-1,2,3,6-tetrahydropyridine. *The Journal of biological chemistry*, 268(22), 16504–16512.

Zeng, B.-Y., Irvani, M. M., Lin, S.-T., Irifune, M., ki, M. K., Al-Barghouthy, G., et al. (2006). MPTP treatment of common marmosets impairs proteasomal enzyme activity and decreases expression of structural and regulatory elements of the 26S proteasome. *European Journal of Neuroscience*, 23(7), 1766–1774. doi:10.1111/j.1460-9568.2006.04718.x

Zhang, Y., Gao, J., Chung, K., Huang, H., Dawson, V. L., & Dawson, T. M. (2000). Parkin functions as an E2-dependent ubiquitin-protein ligase and promotes the degradation of the synaptic vesicle-associated protein, CDCrel-1. *PNAS*, 97(24), 13354–13359. doi:10.1073/pnas.240347797